UNIVERSIDAD DE JAÉN

FACULTAD DE CIENCIAS EXPERIMENTALES Y DE LA SALUD
DEPARTAMENTO DE QUÍMICA FÍSICA Y ANALÍTICA

TESIS DOCTORAL

ÚLTIMA GENERACIÓN DE SISTEMAS LUMINISCENTES MULTICONMUTADOS EN FLUJO CON APLICACIÓN EN LOS CAMPOS AGROALIMENTARIO Y FARMACOLÓGICO

PRESENTADA POR:
JULIA JIMÉNEZ LÓPEZ

DIRIGIDA POR:
DR. D. ANTONIO RUIZ MEDINA
DRA. DÑA. PILAR ORTEGA BARRALES
DR. D. EULOGIO JOSÉ LLORENT MARTÍNEZ

JAÉN, 26 DE NOVIEMBRE DE 2018

ISBN 978-84-9159-224-2

ÚLTIMA GENERACIÓN DE SISTEMAS LUMINISCENTES MULTICONMUTADOS EN FLUJO CON APLICACIÓN EN LOS CAMPOS AGROALIMENTARIO Y FARMACOLÓGICO

Los Directores:

Fdo. Dr. Antonio Ruiz Medina

Catedrático

Universidad de Jaén

Fdo. Dra. Pilar Ortega Barrales

Profesora Titular

Universidad de Jaén

Fdo. Dr. Eulogio J. Llorent Martínez

Profesor Ayudante Doctor

Universidad de Jaén

Memoria de Investigación presentada para aspirar al grado de Doctor en Química, con mención de Doctorado Internacional, por la Universidad de Jaén.

Fdo. Julia Jiménez López

Jaén, 2018

“No sería un gran
universo si no
fuera el hogar de
las personas que
amas”

Stephen Hawking (1942-2018)

Me gustaría aprovechar estas líneas para agradecer a todas aquellas personas que de alguna u otra forma han participado y contribuido para la realización de esta Tesis Doctoral, dedicando su tiempo y recursos de manera desinteresada y en pro de mi propio beneficio.

En primer lugar, quiero expresar mi profundo y sincero agradecimiento a mis directores Antonio Ruiz Medina, Pilar Ortega Barrales y Eulogio J. Llorent Martínez. Depositasteis vuestra confianza en mí desde el principio y desde aquel día, no habéis dejado de apoyarme. Sin duda, sin vuestra dedicación, enseñanza y confianza no hubiese posible la realización y elaboración de esta Tesis Doctoral. Habéis sido mi guía y mi inspiración para llegar hasta aquí.

Muchas gracias a los tres, porque, si hoy estoy aquí, a las puertas de esta oportunidad, es gracias a vosotros.

Muchas gracias al departamento de Química Física y Analítica de la Universidad de Jaén por su acogida y por poner a mi disposición lo que he necesitado en todo momento. He de hacer una mención especial a los maravillosos integrantes de mi grupo de investigación (FQM-363), Mª Luisa, Mª José, Ana, Lucía, Mª Paz, María y Paco, además de Marina, Cecilia, Paco y los miembros del área de Química Física. Habéis sido mis compañeros, pero realmente os habéis convertido en grandes amigos. He aprendido mucho de todos vosotros.

A mis amigos químicos Jaime e Irene. La Química forjó una gran amistad, que durará siempre.

Gracias a mis compañeros y compañeras de laboratorio y de sala. Con vosotros he compartido grandes momentos y muchas risas, además de siempre encontrar vuestro apoyo en esta complicada andadura.

También me gustaría dedicar un espacio a todas aquellas personas que en algún momento han formado parte del departamento o han estado de visita. A todos los amigos y compañeros que he ido dejando atrás durante las diferentes etapas que he recorrido hasta llegar aquí. Siempre es de gran ayuda poder contar con gente que te puede enseñar cosas nuevas o simplemente ofrecerte su amistad.

Por otro lado agradezco enormemente la cordialidad y hospitalidad brindada por el profesor Dr. D. João Luis Machado dos Santos, que hizo posible mi estancia de investigación en Oporto, ciudad que nunca olvidaré. En esta gran ciudad me hicisteis sentir como en casa. Especialmente dar las gracias a mis compañeras y amigas Sofia, Susana, Edite, Cláudia y a David. Fuisteis un pilar fundamental para mí estando a tantos kilómetros de casa y vuestra amistad la guardo como un tesoro. Muito obrigada a todos. Você é uma parte muito importante desta tese de doutorado.

En lo personal son muchas las personas a las que tengo que agradecer su cariño.

A mis padres, Lola y Manolo, que han sido mi referente en la vida. Soy lo que soy y he llegado hasta aquí gracias a vosotros. Siempre me habéis enseñado a mirar al frente sin temor, ya que con

constancia y esfuerzo todo es posible. Gracias por inculcarme unos valores, una forma de ser admirable y por enseñarme que la vida es un reto, un desafío y un regalo. Y vosotros sois ese gran regalo que me ha dado.

Gracias a mi hermana Lucía, mi otra mitad. Siempre has creído en mí y has sido mi "empujoncito" a superarme para conseguir lo mejor, como lo haces tú. Eres mi inspiración y mis alas para seguir volando.

A mi marido Fernando, mi compañero de viaje, de vida. Gracias por haber sido mi eterno apoyo, por ser mi sol en días de oscuridad, por conocerme y amarme, por enseñarme que una vida a tu lado nunca será suficiente. Gracias por ser único y estar a mi lado en todo momento. Contigo, siempre, "la vie en rose".

A mi hija Julia, que es la luz de mi vida. Posiblemente en este momento no entiendas mis palabras, pero para cuando seas capaz, quiero que te des cuenta de lo mucho que significas para mí. Eres la razón de que me levante cada día esforzándome por el presente y por el mañana, eres mi principal motivación. Como en todos mis logros, en este has estado presente, así que gracias a ti también mi cielo.

Gracias a mi cuñado, a mis tíos y a mi familia política, que es mi segunda familia. Siempre he encontrado en vosotros el apoyo y ánimo para continuar con este largo pero precioso camino.

Y por último y no menos importante, gracias a mis amigos y amigas, en especial a mi amiga Ana Belén. Los momentos difíciles a vuestro lado son cortos y bonitos porque siempre estáis ahí.

A todos, porque, de una manera u otra, formáis parte de este éxito. Os quiero muchísimo.

A mis padres

A mi hermana

A mi marido

A mi hija

Índice

Índice de contenido

Acrónimos y abreviaturas

Para la mayoría de los acrónimos se emplea la abreviatura o acrónimo anglosajón debido a su empleo más generalizado.

IUPAC	Unión Internacional de Química Pura y Aplicada
SFA	Análisis en flujo segmentado
CCFA	Análisis en flujo completamente continuo
CDFA	Análisis en flujo con dispersión controlada
FIA	Análisis por Inyección en Flujo
MCFIA	Análisis por inyección en flujo multiconmutado
MSFIA	Análisis por inyección en flujo multijeringa
MPFS	Sistemas en flujo multibomba
CIA	Análisis por inyección en flujo cruzado
SIA	Análisis por Inyección Secuencial
LOV	Lab-On-Valve
LSL	Luminiscencia Sensibilizada por Lantánido
ICP-OES	Espectroscopía de emisión óptica por plasma de acoplamiento inductivo
SERS	Espectroscopía Raman sensibilizada en superficie
FTIR	Espectroscopía infrarroja mediante transformada de Fourier
PTFE	Politetrafluoroetileno
EGM	Electrodo de Gotas de Mercurio
FIC	Culombimetría por inyección en flujo
RTPIF	Fluorescencia Inducida Fotoquímicamente a Temperatura Ambiente
PIF	Fluorescencia Inducida Fotoquímicamente
UV	Ultravioleta

SPS	Espectroscopía en Fase Sólida
QD	Quantum Dot
PET	Transferencia de Energía Fotoinducida
CB	Banda de conducción
VB	Banda de valencia
FRET	Transferencia de Energía de Resonancia de Fluorescencia
AuNP	Nanopartícula de oro
LMR	Límite Máximo de Residuos
BPA	Buena Práctica Agrícola
EFSA	Agencia Europea de Seguridad Alimentaria
HPLC	Cromatografía de líquidos de alta resolución
MS	Espectrometría de masas
GC	Cromatografía de gases
ECD	Detección de captura electrónica
IARC	Agencia Internacional para la Investigación sobre el Cáncer

Figuras y tablas

Figuras

Tablas

Resumen/Summary

1. Resumen

En esta Memoria de Investigación se proponen una serie de mejoras científico-técnicas relativas al desarrollo y aplicación de sistemas automatizados en flujo para el análisis de moléculas de diferente índole en los campos farmacológico y agroalimentario, plasmadas en las nueve publicaciones científicas que se presentan en esta Memoria.

Se ha puesto especial hincapié en incrementar el nivel de automatización de los sensores en flujo descritos hasta la fecha, perfeccionando el uso de los sistemas multiconmutados en flujo (MCFIA) en este tipo de sistemas analíticos. Se han empleado técnicas de detección luminiscentes, incidiendo especialmente en aquellas que han permitido un incremento en la selectividad y cuyo desarrollo hasta la fecha ha sido reducido, como es el caso de la Fluorescencia Inducida Fotoquímicamente, utilizada en cuatro de los cinco sensores espectroscópicos que se describen. Igualmente, se han utilizado nanopartículas fluorescentes para poder llevar a cabo la determinación luminescente de analitos que no presentan fluorescencia nativa; esta estrategia se ha usado en cuatro sistemas analíticos que se detallarán más adelante.

La principal característica de todos los métodos desarrollados es, en primer lugar, la automatización de los sistemas, lo cual conlleva ventajas tales como su rapidez, sencillez y bajo costo. Adicionalmente, en el caso de los sensores espectroscópicos, existe la posibilidad de determinar uno o varios analitos de forma selectiva y sensible en una gran variedad de muestras. Las características anteriormente descritas

hacen especialmente adecuado su uso en el análisis de rutina y control de calidad, como por ejemplo en los ensayos de contenido de compuestos de interés farmacológico y/o biológico en productos farmacéuticos y métodos de "screening" para determinar contaminantes en matrices agroalimentarias.

Los sensores espectroscópicos (también conocidos como optosensores) desarrollados en esta Memoria pueden clasificarse en función del número de analitos a determinar, pudiendo encontrar sensores monoparamétricos (si se realiza la detección de un solo analito) o multiparamétricos (si se trata de una detección de más de uno). En esta Memoria se recoge el desarrollo de cinco de este tipo de sensores, siendo cuatro de ellos sensores monoparámetro y el quinto biparámetro.

En el caso del sensor biparámetro, la estrategia a seguir para la separación de los analitos está basada en el empleo de una cierta cantidad adicional de soporte sólido en la célula de flujo, sin la necesidad de poner una minicolumna previa para su separación, ya que ésta se realiza justo por encima del área de detección. Uno de los analitos es retenido selectivamente en el soporte sólido mientras que el otro analito, que presenta una retención leve, atraviesa el soporte sólido debido a la distinta interacción entre los analitos y el soporte, permitiendo de esta manera su separación, la llegada a la zona de detección y su medida secuencial.

En todos los métodos se ha llevado a cabo un amplio estudio de las variables experimentales que hay que considerar en el desarrollo de este tipo de sensores como: características de los espectros y variables

instrumentales, variables de la unidad de retención-detección, variables químicas (pH, naturaleza del portador, etc.), separación de los analitos, variables del sistema de flujo, etc. Una vez optimizados los valores adecuados en cada método desarrollado, se procedió a la calibración de los métodos analíticos para cada analito y la obtención de los parámetros analíticos, evaluación de la selectividad mediante el estudio de interferentes y, finalmente, se procedió a la aplicación del método desarrollado a muestras reales o fortificadas.

De los resultados obtenidos se puede concluir que el acoplamiento de la espectroscopía en fase sólida con sistemas de flujo es de una gran utilidad para la resolución de un gran número de problemas analíticos en campos muy diversos, como el agroalimentario, principal campo en el que se aplican los optosensores desarrollados en esta Memoria de Investigación.

El otro gran aporte que se ha conseguido en esta Memoria de Investigación reside en la inserción, dentro de los sistemas multiconmutados, de partículas de última generación que permitan potenciar las propiedades físico/químicas de los sensores propuestos hasta la fecha, lo que se conoce como nanosensores químicos. Entre estas partículas cabe destacar los Quantum Dots (QDs), tanto por su aplicabilidad como por su potencialidad. La interacción del analito de interés con un ligando específico previamente unido a los QDs permite un cambio en las propiedades luminiscentes de estos últimos. Este cambio se puede poner de manifiesto en la célula de flujo, integrándose así de forma simultánea la reacción de las partículas sensoras y los analitos y la detección de estos últimos. Gracias a su uso, se han podido obtener sistemas sensores en flujo con una alta sensibilidad y

selectividad, que permitan un elevado número de análisis con un mínimo consumo de reactivos.

El uso de sistemas multiconmutados en todas las investigaciones que contribuyen en esta Memoria de Investigación permite lograr sistemas analíticos sencillos, de bajo coste, con disminución de consumo de muestra y reactivos y con una gran precisión y amplia versatilidad, además de permitir miniaturizar el montaje en flujo de estos sistemas analíticos, e incluso realizar análisis *in situ*. En general, estos sistemas ofrecen un mayor grado de automatización, aportando otras ventajas adicionales frente a los sistemas de análisis por inyección en flujo convencionales.

El empleo de este tipo de métodos analíticos es especialmente recomendable y ventajoso para controles de calidad o análisis de rutina aunque, como se ha demostrado en esta Memoria, se pueden abordar problemas analíticos más complejos, como puede ser el análisis de residuos de contaminantes en matrices agroalimentarias. Dichos métodos cumplen la normativa europea en cuanto a límite máximo de residuos (LMRs), ya que permiten detectar niveles de concentración más bajos que los que se establecen como máximos en dicha normativa.

Se ha de realizar, por tanto, una selección acertada de las moléculas que se quieren determinar para la aplicación de los sensores espectroscópicos o los nanosensores que se han presentado en esta Memoria, aportando un amplio rango de aplicaciones de alto interés debido al gran alcance que presentan dentro de cada uno de los campos entre los que se encuentran.

Debido a todo esto, en esta Memoria de Investigación se presentan nueve investigaciones, las cuales se pueden enmarcar en función del ámbito específico en el que se encuentran: cinco de ellas son optosensores en flujo continuo (mono- y biparamétricos) y cuatro de ellas son nanosensores que hacen uso de nanopartículas para la mejora de los sistemas en flujo, todos ellos aplicados a los campos agroalimentario y farmacológico. A continuación se especifican las muestras reales en donde se han llevado a cabo las aplicaciones de los sistemas desarrollados.

- Optosensores en flujo continuo:
  - Monoparamétricos:
    - ❖ Determinación de citrinina en arroz y en suplementos nutricionales.
    - ❖ Determinación de clotianidina en agua, arroz y miel.
    - ❖ Determinación de tiametoxam en verduras.
    - ❖ Determinación de nitenpiram en verduras crucíferas.
  - Biparamétrico:
    - ❖ Determinación de nitenpiram y piraclostrobina en uvas y vino.
- Nanosensores:
  - ❖ Determinación de rifamicinas en fármacos y orina.
  - ❖ Determinación de β-caroteno en zumos y suplementos nutricionales.

- Determinación de glifosato en agua y cereales.
- Determinación de tioles bioactivos gracias a la implementación del proceso de transferencia de energía de resonancia fluorescente (FRET).

Summary

In this Research Report, several scientific/technical improvements concerning the development and the application of automated flow systems are proposed. The systems developed were applied to the analysis of molecules of different nature in the pharmacological and agri-food fields. The research here described gave origin to nine scientific publications in scientific international journals.

Special emphasis was placed on increasing the level of automation of the flow sensors described to date, particularly improving the potential of multicommutated flow injection analysis (MCFIA) methods. The selection of luminescent detection techniques was performed by paying special attention to two aspects: a) increasing the selectivity of the analytical methods; b) the use of detection techniques that have been underused in flow systems, such as Photochemically Induced Fluorescence, which has been used in four of the five spectroscopic sensors described. Likewise, fluorescent nanoparticles have been used to carry out the luminescent determination of analytes that do not exhibit native fluorescence; this strategy has been used in four analytical systems that will be detailed later.

The main characteristic of all the developed methods is the automation of the systems, which provides advantages such as speed, simplicity, and low cost. Additionally, when making use of spectroscopic sensors, it was possible to determine one or several analytes selectively and sensitively in a large variety of samples. The characteristics described above make these systems particularly suitable

for their use in routine analysis and quality control, such as testing the content of compounds of pharmacological and / or biological interest in pharmaceutical products, and screening methods to determine contaminants in agri-food samples.

The spectroscopic sensors (also known as optosensors) developed in this Report can be classified according to the number of analytes that can be determined: monoparametric sensors if only one analyte is quantified, or multiparametric sensors if more than one analyte can be quantified. This Report includes the development of four monoparametric optosensors and one biparameter sensor.

In the case of the biparameter sensor, the strategy followed for the separation of the analytes was based on the use of an additional amount of solid support in the flow cell. These additional solid beads were placed just above the detection area. In this way, one of the analytes was selectively retained on the additional solid support while the other analyte passed through the solid support due to the different interaction between the analytes and the support (based on their different kinetics of retention/elution), thus allowing their separation and sequential arrival at the detection zone, where their analytical signals were recorded.

In all the flow sensors developed, an extensive study of the experimental variables required in the development of these analytical methods was performed: characteristics of the spectral and instrumental variables, variables of the retention-detection unit, chemical variables (pH, nature of the carrier, etc.), separation of the analytes, flow conditions, etcetera. Once the optimum conditions were selected for

each method, the analytical parameters were obtained for each analyte, the selectivity was evaluated by studying potential interferents, and the method was applied to the quantification of the analyte(s) in real or spiked samples.

Considering the results obtained, it can be concluded that the coupling of solid phase spectroscopy and flow systems is very useful for the resolution of a large number of analytical problems in several fields, such as the agri-food sector, the main target of most of the developed optosensors.

The other important contribution of this Research Report consists in the use of nanoparticles within the multicommutated systems to improve the analytical characteristics. These analytical methods, which allow enhancing the physical/chemical properties of the sensors by the use of last-generation nanoparticles, are known as chemical nanosensors. In this Report, Quantum Dots (QDs) have been selected due to their inherent properties. The interaction of the analyte of interest with a specific ligand previously bound to QDs produces changes in the luminescent properties of QDs and, consequently, in the analytical signal that is recorded. As a result, the analytical signal recorded on-line when the analyte-QDs reach the flow-cell allow integrating simultaneously the reaction of the sensor particles and analyte(s) with the detection of the latter. Due to these favourable characteristics, it was possible to develop flow systems with high sensitivity and selectivity, which allowed the quantification of different compounds with a minimum consumption of reagents.

The use of multicommutation methodology in all the systems here reported permitted to obtaining simple, precise, versatile, and low-cost analytical systems, minimizing sample and reagent consumption. In addition, the use of multicommutation also permits the miniaturization of the flow assembly of these systems, as well as carrying out on-site analysis. In general, these systems offer a high degree of automation, providing additional advantages to conventional flow injection analysis systems.

The use of the analytical methods mentioned above is especially recommended and advantageous for quality control or routine analysis. However, more complex analytical problems can also be addressed, such as the analysis of contaminant residues in agri-food samples, as the methods here described comply with European regulations regarding maximum residue limits (MRLs).

Taking into account all the previous information, it is clear that a careful selection of the analytes is required to take full advantage of the spectroscopic sensors or nanosensors that have been presented in this Report, so the methods can be applied to a wide range of samples within the corresponding research field.

The work detailed in this Research Report yielded nine analytical methods: five flow optosensors (mono- and biparametric) and four nanosensors that make use of nanoparticles for the improvement of the method characteristic. All the developed methods were applied to the agri-food and/or pharmacological fields. The classification of the analytical methods, specifying target compounds and analyzed samples, follows.

- Flow optosensors:
  - Monoparametric:
    - ❖ Determination of citrinin in rice and food supplements.
    - ❖ Determination of clothianidin in water, rice and honey.
    - ❖ Determination of thiamethoxam in vegetables.
    - ❖ Determination of nitenpyram in cruciferous vegetables.
  - Biparametric:
    - ❖ Determination of nitenpyram and pyraclostrobin in grapes and wine.
- Nanosensors:
  - ❖ Determination of rifamycins in pharmaceutical formulations and urine.
  - ❖ Determination of β-carotene in juices and food supplements.
  - ❖ Determination of glyphosate in water and cereals.
  - ❖ Determination of bioactive thiols thanks to the implementation of the fluorescent resonance energy transfer process (FRET).

Introducción

2. Introducción

La imparable demanda de análisis de control en los laboratorios de calidad y seguridad ha llevado a la búsqueda y desarrollo de nuevas metodologías analíticas que se adapten a los avances en ciencia y tecnología actuales. Esto se presenta como un reto para la Química Analítica, ya que han de desarrollarse nuevos métodos que sean eficaces, rápidos, selectivos, sensibles y respetuosos con el medioambiente.

La automatización de procedimientos analíticos en análisis químico permite la respuesta efectiva y rápida a los requisitos de los análisis que involucran la manipulación de muestras complejas o una gran cantidad de muestras en las que los analitos se determinarán a un nivel cada vez más bajo de concentración. De igual forma, se disminuye la participación humana y se reducen o eliminan numerosos factores que podrían afectar al rendimiento de los procedimientos analíticos, ya que se incrementa la velocidad de análisis, haciendo posible la realización de un mayor número de análisis en un menor tiempo.

El desarrollo de los métodos automáticos de análisis y su implementación en laboratorios analíticos se ha justificado por varias razones, entre las que destacan con una mayor importancia:

- el reemplazo parcial o completo de la participación humana en las tareas consideradas como peligrosas, dando lugar a una mayor seguridad y prevención de errores derivados de factores humanos.

- el rendimiento analítico se mejora, particularmente respecto a la precisión de los resultados.
- un uso más eficiente del potencial de la instrumentación analítica y mejor manejo de reactivos químicos.

Lógicamente, con la disminución en el consumo de reactivos y muestra se optimizan los costos analíticos y se mejora la seguridad de cara al medioambiente, debido a la disminución de la producción de desechos y la minimización de exposición del personal a productos químicos tóxicos. Más allá de la necesidad de reducir los costos, también existen razones que surgen de las demandas sociales para mejorar el nivel de salud humana, que involucran mayores controles de la contaminación existente, del agua potable y de la calidad de los alimentos y las bebidas destinadas al consumo, en donde es común recurrir a análisis de una gran cantidad de muestras en un corto espacio de tiempo.

En consecuencia, los métodos automáticos de análisis se han utilizado en muchas áreas, incluyendo, entre otras, las siguientes: análisis clínico y toxicológico, control de procesos industriales, análisis ambiental de rutina de aire, agua y control de suelos, y calidad de productos agroalimentarios y farmacológicos.

El creciente interés y la implementación de tales metodologías en diversos campos de aplicación han llevado al uso de nuevos conceptos y expresiones, lo que requiere un esfuerzo de la IUPAC (*Unión Internacional de Química Pura y Aplicada*) para estandarizar sus definiciones. La Comisión IUPAC para Nomenclatura Analítica estableció una serie de definiciones que distinguen y especifican las características esenciales de los métodos automáticos de análisis. Una

de las principales recomendaciones de la IUPAC se refiere a la clara distinción entre dispositivos automáticos y automatizados.

Los dispositivos automáticos se definen como "aquellos que llevan a cabo ciertas acciones requeridas para ser realizadas en puntos determinados en una operación, sin participación humana". Estos sistemas no presentan capacidad autónoma para decidir, ya que no tienen un sistema de retroalimentación, actuando con la misma secuencia de operaciones de la misma manera en todas las ocasiones.

Por el contrario, los dispositivos automatizados contienen un sistema de retroalimentación que les permite tomar decisiones sin participación humana. La secuencia en la que se realizan las operaciones depende de cada situación, siendo continuamente adaptada para cada muestra. Además, los sistemas son automonitorizados y autoajustables, con una mayor independencia de actuación.

2.1. Tipos de sistemas de análisis automáticos

En función de la estrategia de procesamiento de la muestra, los métodos automáticos de análisis pueden ser divididos en diferentes categorías: métodos de análisis discontinuos, métodos de análisis robotizados y métodos de análisis continuos o en flujo.

En los métodos automáticos de análisis discontinuos, las muestras se transportan mecánicamente hacia el detector. Cada muestra preserva su integridad física en recipientes separados a lo largo de cada operación de la unidad. Durante el transporte de las muestras, las diferentes etapas analíticas, como dilución, dosificación de reactivos, mezcla, o calentamiento, entre otros, se pueden ejecutar en una forma secuencial (**Figura 1**). En la zona de detección se obtiene una señal

analítica puntual para cada muestra, después de haber alcanzado el equilibrio químico (o estado estacionario).

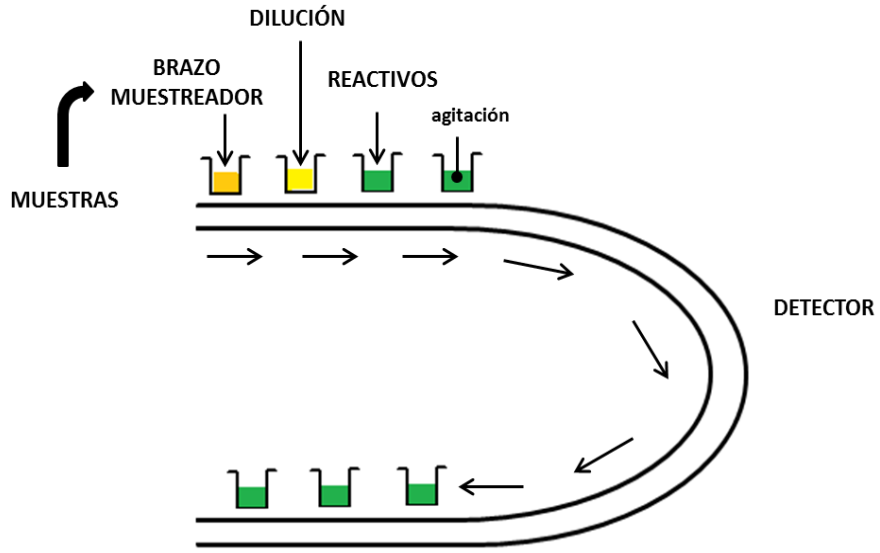

Figura 1. Esquema general de un sistema analítico automático discontinuo

Los métodos automáticos de análisis robotizados implican el uso de un mini robot controlado por un ordenador. Los movimientos del robot imitan las acciones de un operador humano en un procedimiento analítico. De manera general, el robot de laboratorio consiste en un brazo móvil equipado con una "mano" que proporciona los movimientos necesarios para transferir la muestra y los productos resultantes de las diferentes etapas de su procesamiento a una serie de aparatos e instrumentos. Un microprocesador controla los movimientos del robot y el funcionamiento de los diferentes instrumentos, de los cuales recibe las señales correspondientes con el fin de ser tratadas para obtener los resultados finales.

En los métodos automáticos de análisis en flujo (**Figura 2**), las soluciones de muestra se introducen sucesivamente en un canal en el

que circula un líquido o gas, generalmente conocido como flujo portador, encargado de transportar dichas muestras hacia el detector. Durante la propulsión de muestras desde el punto de inserción al detector, éstas pueden estar sujetas a una o más reacciones químicas (o cualquier otro tipo de operación analítica) para acondicionar debidamente las muestras antes de la determinación. Por lo tanto, los canales que llevan las muestras pueden confluir o no con otros canales que contienen reactivos, disoluciones tampón, agentes de enmascaramiento, etc. Al llegar al detector, la señal analítica es continuamente monitoreada a lo largo del tiempo y cada muestra o producto de reacción produce un efecto transitorio en la señal cuya altura o área podría estar relacionada con el parámetro que se evalúe en ese momento.

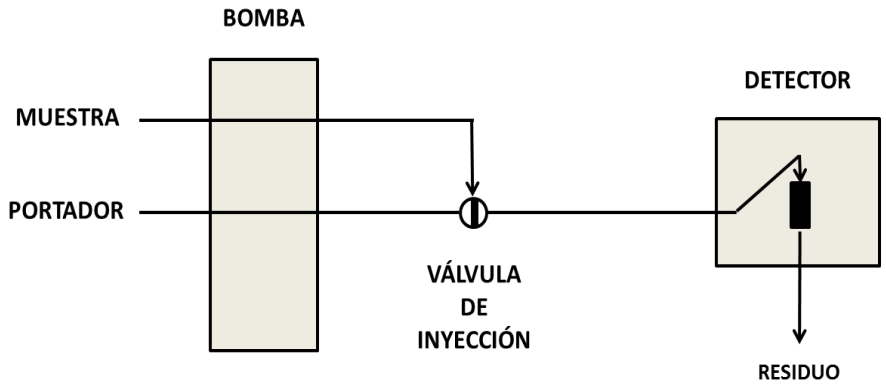

Figura 2. Esquema general de un sistema analítico continuo

2.2. Sistemas de análisis automáticos en flujo

De acuerdo con el tipo de flujo utilizado, los métodos de flujo se pueden clasificar como métodos de flujo segmentado y métodos de flujo no segmentado.

En los métodos de flujo segmentado, propuestos por Skeggs [1] en 1957, la corriente que fluye es segmentada por burbujas de aire que impiden la dispersión de la muestra y, en consecuencia, la identidad y la integridad de cada muestra se mantienen. Las burbujas insertadas se eliminan antes de su llegada al detector para eludir las interferencias en la señal analítica.

Los métodos de flujo no segmentado fueron introducidos por primera vez por J. Ruzicka y E. H. Hansen en 1975 [2]. En estas metodologías, pequeños volúmenes de muestra se insertan directamente en un flujo de portador no segmentado. Las muestras se van introduciendo directamente, a intervalos regulares de tiempo, en un canal por el que fluye un portador, que puede ser el propio reactivo en caso de ser necesaria una reacción química. El flujo atraviesa continuamente la célula de medida (cubeta de flujo) situada en la zona de detección de un determinado detector en donde se registra continuamente un cierto parámetro físico (absorbancia, fluorescencia, potencial del electrodo, etc.). El mayor interés científico de estos métodos ha sido debido, principalmente, a los menores costos de instalación y operación, mayor flexibilidad basada en una estructura modular que permite su reconfiguración simplificada a nuevas situaciones analíticas y, también, la mayor facilidad de operación y control. Además, estos métodos permiten minimizar el consumo de muestras y reactivos y disminuir el tiempo de análisis.

En la **Tabla 1** se muestra una clasificación de los métodos automáticos continuos basada en el modo en que se elimina la posible interferencia entre las muestras sucesivas [3].

Tabla 1. Métodos automáticos continuos

Flujo	Introducción de muestras		Naturaleza de flujo	Metodología
	Procedimiento	Tiempo		
Segmentado	Aspiración	Secuencial	Continuo	Análisis en flujo segmentado (SFA)
No segmentado	Inyección	Secuencial	Continuo	Análisis por inyección en Flujo (FIA)
	Aspiración	Secuencial	Discontinuo	Métodos cinéticos a flujo detenido
		Continua	Continuo	Análisis en flujo completamente continuo (CCFA)
		Secuencial	Continuo	
		Secuencial	Discontinuo	Análisis en flujo con dispersión controlada (CDFA)

2.2.1. Análisis por inyección en flujo (FIA)

La primera concepción de un sistema de análisis automático en flujo continuo es lo que conocemos como el sistema FIA (*Flow Injection Analysis*). El FIA es una modalidad de los sistemas en flujo continuo en la que el flujo no está segmentado por burbujas de aire. El término fue introducido en la década de los 70 por Ruzicka y Hansen [2] en Dinamarca y Stewart [4] en Estados Unidos. Las posibilidades y aplicaciones analíticas de esta modalidad son numerosas y ventajosas, ya que ofrece una gran sencillez en el manejo y requiere bajo costo en la inversión y mantenimiento en instrumentación, así como bajo costo de reactivos, proporcionando además resultados de una manera rápida y con alta exactitud y precisión [5]. Estas facilidades permitieron su rápida expansión en laboratorios de investigación o de control analítico, ya que, además presentar alta robustez, se puede emplear cualquier detector usual (siempre que se pueda introducir la muestra en flujo). Uno de los principales inconvenientes del FIA es que es una técnica esencialmente monoparamétrica, característica que ha sido superada por otros métodos de análisis en flujo que permiten la determinación simultánea de diferentes compuestos.

En la representación esquemática (**Figura 3**) pueden observarse los diferentes componentes que forman parte de este sistema de análisis que, en líneas generales, componen la mayoría de los sistemas en flujo continuo.

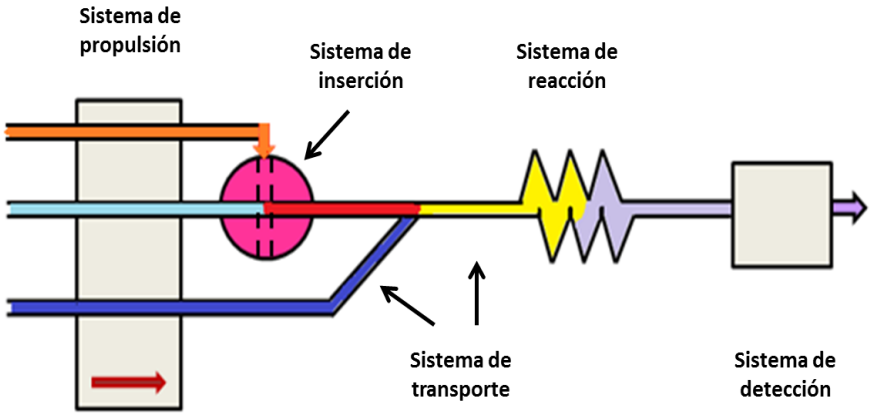

Figura 3. Componentes básicos de un sistema FIA

Los componentes básicos de un sistema FIA son los siguientes:

- Sistema de propulsión

  Establece un flujo de caudal lo más constante posible de una disolución (o de varias) que lleva disuelto un reactivo o hace de simple portador. Debe suministrar un flujo constante y regular en el sistema, ausente de pulsos y perfectamente reproducible.

  Como sistema de propulsión pueden utilizarse bombas, sistemas de presión o sistemas de gravedad. La bomba peristáltica es el sistema más usado para las metodologías en flujo (como en FIA o en análisis por inyección en flujo multiconmutado), el cual está basado en la presión ejercida por una serie de cilindros rotatorios sobre tubos de plástico flexibles. El diámetro interno de los tubos es, entre otros factores, el que determina el caudal suministrado por la bomba (**Figura 4**).

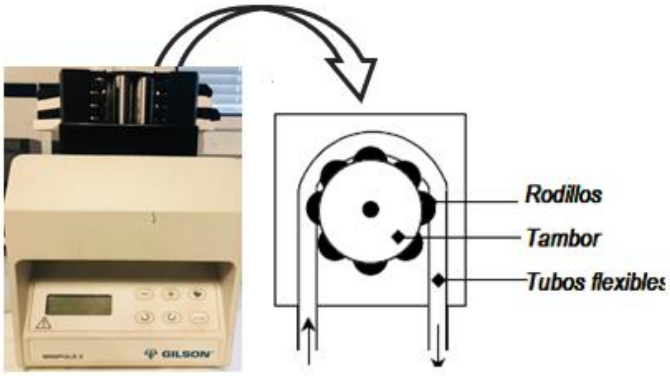

Figura 4. Bomba peristáltica y vista esquemática de la parte superior

- Sistemas de inserción

  Deben permitir la introducción o inserción de un volumen de muestra exactamente medido en la corriente portadora de forma completamente reproducible, sin crear perturbaciones en el flujo del portador. Estos dispositivos pueden controlarse eléctricamente y su uso debe ser, en cualquier caso, fácil, cómodo y rápido para que sea posible el aumento en la frecuencia de muestreo. El sistema de inserción habitual en FIA son las válvulas rotatorias, generalmente de seis vías, aunque los primeros sistemas de inserción utilizados fueron jeringas y agujas hipodérmicas (de ahí que se denominasen "sistemas de inyección").

- Sistema de transporte

  La misión fundamental de estos sistemas es conectar entre sí los diferentes elementos y conseguir en el transporte de los fluidos a su través un adecuado grado de dispersión de la

muestra con la corriente portadora. El flujo debe ser reproducible además de que la trayectoria de éste debe ser fácilmente programable para poder hacer una amplia variedad de ensayos. Para todos los sistemas de análisis en flujo, incluido el MCFIA, son utilizados tubos de pequeño diámetro, de entre 0.1 y 2 mm, de materiales químicamente inertes y termoestables, generalmente, Teflón (politetrafluoroetileno, PTFE) y propileno. La elección del material de los tubos usados (sobre todo en la bomba peristáltica) se realiza principalmente, en función del disolvente utilizado para las disoluciones que circularán por el sistema de flujo.

- Sistema de reacción

  En este sistema se puede desarrollar la reacción química o la fotodegradación de analito(s), en el caso de que fuese necesario. En el caso de reacción química, suelen ser utilizados tubos del mismo material que el sistema de transporte, enrollados en forma helicoidal, a los que se le puede poner baños termostatizados o mantas eléctricas. En el caso de la fotodegradación, se enrollan tubos del mismo material alrededor de una lámpara de mercurio que fotodegradará el analito. El fotorreactor se protege del medio exterior mediante papel de aluminio o una caja de aluminio. La fotodegradación es la base de los sistemas de fluorescencia inducida fotoquímicamente (*Photochemically Induced Fluorescence*, PIF), que se desarrollará más adelante.

- Sistema de detección

Estos sistemas deben permitir la medida continua de una propiedad del analito o de un producto de reacción del mismo, proporcionando información cuantitativa y cualitativa. La presencia de ciertos atributos en un detector es lo que lo hará adecuado como sistema de medida en la técnica de inyección, como son: bajo ruido, respuesta rápida y lineal en un amplio rango de concentraciones, y alta sensibilidad. Algunos tipos de detección (*apartado 2.3.)* también pueden proporcionar selectividad adicional.

Para medir las propiedades del analito en los sistemas de análisis en flujo es necesario el uso de una célula de flujo, que se introducirá en el instrumento donde se realizará esta medida y en el que desarrollará su señal analítica.

Como característica general de estas células, el camino óptico no debe ser superior a 2 mm para evitar que la intensidad relativa de luminiscencia de la línea base sea demasiado alta, lo que provocaría dificultades en la detección.

Además, es importante tener en cuenta el sistema de detección que se va a emplear en cada caso, lo que condicionará la estructura geométrica y el tipo de célula de flujo.

Para la detección espectrofotométrica, la célula de flujo usada es la que se muestra en la siguiente figura.

Tipo de detección	Quimioluminiscencia
Célula	Hellma 138 QS
Paso óptico	1.0 mm
Volumen interno	50 µl

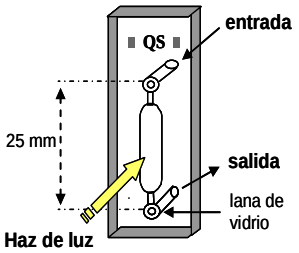

Figura 5. Célula empleada para detección espectrofotométrica y quimioluminiscente

Para los sensores con detección fluorescente o luminiscente sensibilizada con terbio la célula tendrá forma de prisma rectangular de base cuadrada, para posibilitar la emisión en un ángulo de 90º respecto a la excitación incidente (ver **Figura 6**).

Tipo de detección	Fluorescencia Luminiscencia sensibilizada por lantánido
Célula	Hellma 176.052 QS
Paso óptico	1.5 mm
Volumen interno	25 µl

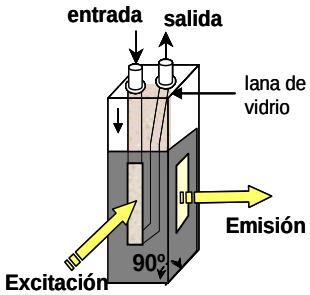

Figura 6. Célula empleada para detección fluorescente, fosforescente o luminiscente sensibilizada con lantánidos

Las principales características que presenta el FIA, y que de igual manera caracterizan a todos los métodos de análisis continuo, son:

- ✓ Elevada precisión
- ✓ Tiempos de análisis cortos o, lo que es igual, altas frecuencias de muestreo
- ✓ Simplicidad, sencillez

- ✓ Economía y versatilidad

Desde la concepción del FIA, una numerosa cantidad de instrumentos, configuraciones, tratamientos de muestras y técnicas de detección han sido diseñadas, implementadas y ejecutadas de manera incesante en busca de alternativas analíticas a este primer sistema analítico en flujo continuo. A pesar de que todas ellas siguen un mismo hilo conductor que es la esencia de ser metodologías analíticas en flujo, todas ellas presentan algunas diferencias que las caracterizan y que las hacen idóneas para diversos análisis.

La aparición de otras metodologías, como el análisis por inyección secuencial (SIA) y los sistemas de análisis por inyección en flujo multiconmutados, amplió el campo de investigación y aplicación de este tipo de sistemas analíticos, demostrando ser herramientas útiles para hacer frente a las demandas analíticas actuales con respecto al creciente número, diversidad y complejidad de las muestras analizadas. De igual forma, las nuevas metodologías permiten llevar a cabo análisis ambientales *in situ* y el acoplamiento con nuevos instrumentos, aumentando de esta forma su potencial analítico.

2.2.2. Análisis por inyección secuencial (SIA)

Fueron Ruzicka y Marshall en 1990 los que introdujeron otro tipo de sistemas de flujo no segmentado, considerado como la segunda generación de este tipo de sistemas: el SIA (*Sequential Injection Analysis*) [6]. Está basado en la aspiración secuencial de volúmenes precisos de muestra y reactivos que se conducen mediante un portador a un bucle de carga, desde donde son dispensados después dentro del

bucle de reacción por inversión del flujo, con lo que se logra un ahorro considerable de reactivos en comparación al FIA. La formación del producto de reacción permitirá la detección de la propiedad seleccionada, cuya señal analítica transitoria es en forma de pico y su altura o área está relacionada con la concentración del analito que se quiera determinar.

Las partes fundamentales de un sistema SIA (y que lo diferencia de un sistema FIA) son la válvula de selección multiposición, que es la encargada de controlar la dirección de las disoluciones en el sistema y la jeringa de pistón, que realiza la función de aspirar y propulsar las distintas disoluciones a través del sistema.

En la **Figura 7** se muestra una representación esquemática general de un sistema SIA.

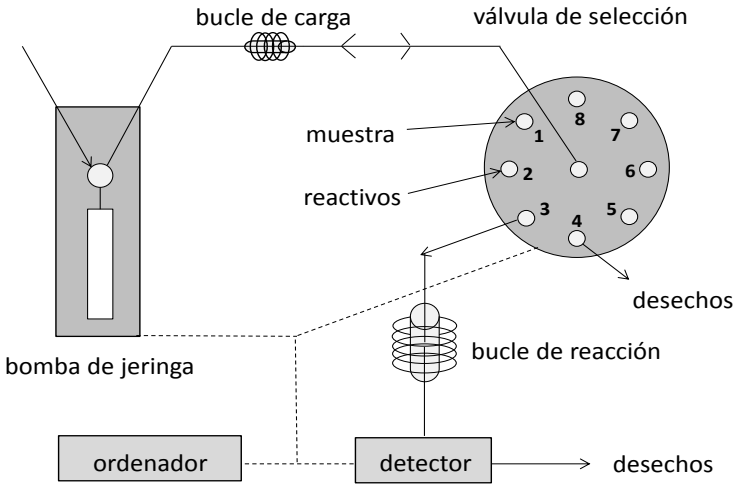

Figura 7. Representación esquemática general de un sistema SIA

Con respecto al FIA, las principales ventajas que presenta la metodología SIA son:

- Alta robustez y sencillez frente al FIA, debido al cambio de bombas peristálticas multicanal por bombas de jeringa.
- Menor consumo de muestra y reactivos, ya que la circulación de estas disoluciones puede ser controlada en el sistema, además de no ser modificado el bucle de muestra.
- Uso de la válvula multiposición como herramienta para realizar calibraciones automáticas, sin necesidad del cambio del bucle de muestra.
- Uso de un software adecuado para el control automático de todo el proceso.

Podrían considerarse como sus principales desventajas la disminución de la frecuencia de muestreo debido a la necesidad de aspirar las disoluciones antes de impulsarlas al detector (lo que aumenta el tiempo de análisis) y la dificultad que se puede presentar en la mezcla de muestra y reactivos al no poder llevar a cabo una confluencia directa de los mismos.

2.2.3. Análisis por inyección en flujo a través de sistemas multiconmutados

Dentro de las metodologías de análisis por inyección en flujo encontramos varias que hacen uso de sistemas multiconmutados. Estas metodologías presentan en común el uso de válvulas solenoides (y válvulas *pinch*) para la introducción de las disoluciones de muestra y reactivos en el sistema de flujo. Los sistemas multiconmutados pueden clasificarse en tres tipos: análisis por inyección en flujo

multiconmutado (MCFIA), análisis por inyección en flujo multijeringa (MSFIA) y sistemas en flujo multibomba (MPFS). Desarrollaré en extensión el MCFIA, ya que la investigación que se ha realizado para la elaboración de esta Memoria está centrada en el desarrollo de metodologías analíticas que hacen uso del mismo.

- Análisis por inyección en flujo multiconmutado (MCFIA)

  El análisis por inyección en flujo multiconmutado (*Multicommutated Flow Injection Analysis*) fue presentado como un nuevo enfoque de análisis en flujo por Reis y colaboradores en 1994 [7]. Está basado en el uso de válvulas solenoides de tres vías de conmutación rápida.

  La versatilidad y aplicabilidad del MCFIA aparecen como consecuencia de la mayor simplicidad y eficacia en el control de la dispersión de la muestra y reactivos en comparación con la metodología FIA. Esta metodología supone un nuevo concepto de análisis en flujo, que engloba y amplía al FIA, siendo una alternativa más versátil y con mayor potencial de miniaturización y automatización. Las características, las aplicaciones y las potencialidades de la técnica MCFIA han ido siendo revisadas por Rocha [8] y por Catalá [9] a lo largo de los años desde su aparición.

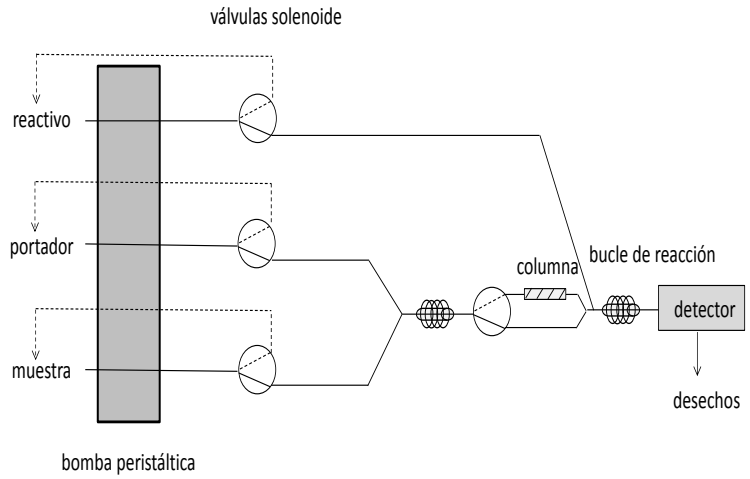

Figura 8. Representación esquemática general de un sistema MCFIA

En los inicios del MCFIA, este sistema utilizaba un sistema de conducción de líquidos que los aspiraba a través de las propias válvulas. Sin embargo, debido a que los sistemas de aspiración tienden a introducir burbujas de aire o producir la desgasificación de los líquidos dentro del sistema, se optó por la utilización de un sistema basado en la propulsión de los líquidos mediante bombas peristálticas. En este sentido, la configuración del sistema no difiere mucho del FIA convencional, ya que solo se diferencia en la introducción de las válvulas solenoides de tres vías en los canales de impulsión. Todos los demás componentes del sistema MCFIA son similares al del sistema FIA, como el sistema de propulsión donde es utilizada una bomba peristáltica, el sistema de transporte en el que siguen utilizándose los tubos adecuados (en función del disolvente utilizado), el sistema de reacción (si fuese necesario) y el sistema de detección, que variará dependiendo de la técnica analítica que se requiera.

❖ Válvulas de inserción

Las válvulas de inserción son el sistema de introducción/inserción de la muestra en los sistemas MCFIA. Estas válvulas deben permitir la introducción o inserción de un volumen de muestra exactamente medido en la corriente portadora de forma completamente reproducible, sin crear perturbaciones en el flujo del portador. Estos dispositivos pueden controlarse eléctricamente y su uso debe ser, en cualquier caso, fácil, cómodo y rápido para que sea posible el aumento en la frecuencia de muestreo. En el caso de los sistemas MCFIA, el sistema de inserción habitual son las válvulas solenoides.

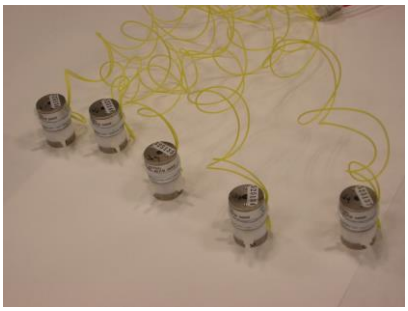

Figura 9. **Fotografía de válvulas solenoide de tres vías**

La introducción de las válvulas solenoide surge como mejora de las limitaciones que llegan a presentar las válvulas rotatorias de seis puertos (utilizadas en los sistemas FIA) respecto a la introducción de volúmenes de muestra. Con las válvulas solenoide [10], el volumen de muestra a introducir viene dado por el tiempo de inserción y el caudal. Por lo tanto, uno de los parámetros de medida clave de los sistemas FIA como es el volumen de inserción pasa a ser, para el

MCFIA, el tiempo de inserción. De esta manera, se permite el desarrollo de métodos de muestreo basados en el tiempo y se llega a lograr un sistema de flujo versátil y de fácil reconfiguración.

La versatilidad de las válvulas solenoide hace que no solo se llegue a hacer uso de éstas en los sistemas en flujo, sino que su uso se ha extendido a las técnicas cromatográficas. En cromatografía de líquidos, se han utilizado para la inserción de muestra y para la entrada y salida de disolventes y en cromatografía de gases para la entrada o salida de aire [11].

La implementación de una válvula de este tipo en los sistemas de flujo presenta una estructura funcional controlada por un ordenador, tal y como puede observarse en la **Figura 10**.

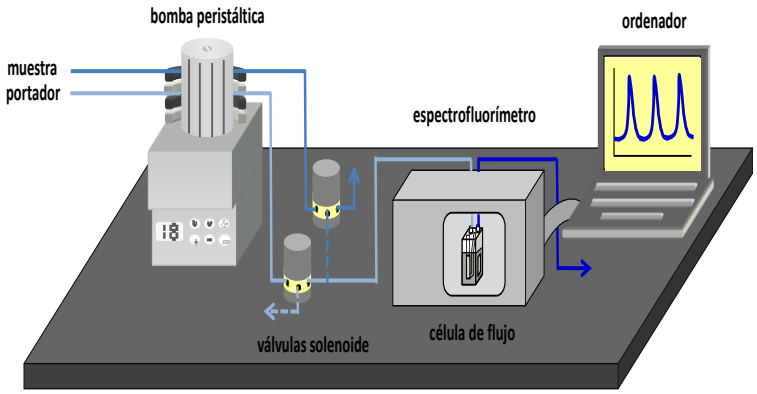

Figura 10. Esquema de un sistema MCFIA

En sistemas MCFIA que emplean válvulas solenoide, éstas actúan como un conmutador independiente controlado por un ordenador. Cada válvula se controla mediante dos posiciones distintas, OFF y ON, permaneciendo siempre dos

de los tres orificios de la válvula comunicados. Un esquema del funcionamiento de una válvula solenoide de tres vías se presenta en la **Figura 11**, para el caso en que la válvula controle el flujo del portador. Su explicación es la siguiente:

En posición OFF, el solenoide que está conectado al generador está relajado y la armadura se empuja hacia abajo, circulando el portador hacia el detector. Sin embargo, cuando se encuentra en posición ON, una cierta cantidad de energía proporcional al pulso eléctrico es transmitida al solenoide y la armadura (en forma de T invertida) es atraída hacia arriba; así, la salida del portador hacia el detector se bloquea siendo de esta forma recirculado al recipiente correspondiente.

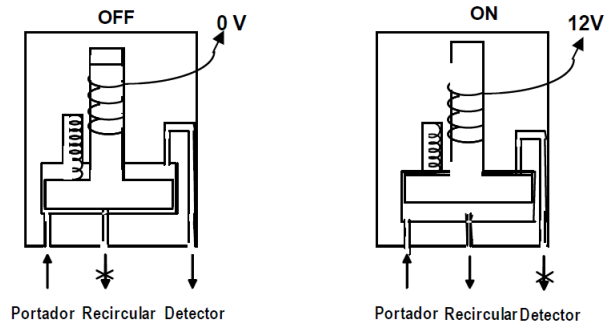

Figura 11. Esquema del funcionamiento de una válvula solenoide de tres vías

El volumen de muestra que se inserta es proporcional a la duración del pulso y puede ser modificado mediante la alteración del perfil de la secuencia de inserción, siendo posible la inserción de un solo segmento de muestra o varios segmentos idénticos o de distintas longitudes alternados con disolución portadora. La muestra se inserta en el sistema

durante el tiempo que la válvula permanece activa (ON) y no es necesario un consumo adicional en tareas de lavado.

Las microinserciones de pequeños segmentos de muestra "emparedados" entre microsegmentos de reactivo o portador ayudan a que ocurra un mezclado íntimo de las disoluciones de muestra, portador y reactivos incluso cuando el volumen de inserción es grande.

Se trata entonces de un sistema versátil que permite la inserción de volúmenes variables de muestra a través de un software y garantiza la inserción reproducible de volúmenes de muestra de unos pocos microlitros mediante el control electrónico de la duración de los pulsos.

Como es de esperar, al ser un sistema que presenta mejoras frente al FIA, el MCFIA tiene ciertas ventajas respecto a éste:

- ✓ La flexibilidad de la técnica MCFIA, que ha contribuido a aumentar las posibilidades del FIA al permitir la modificación del método analítico según la respuesta obtenida sin modificaciones físicas en el sistema.
- ✓ La versatilidad que presenta, ya que la multiconmutación permite alterar el tiempo de residencia en los reactores, los volúmenes de muestra insertados y, en definitiva, todas aquellas variables que inciden directamente en los perfiles de dispersión, sin necesidad de modificar físicamente el montaje. Para la reconfiguración del mismo, únicamente es necesario reprogramar la duración de los pulsos eléctricos que controlan la apertura y cierre

de las válvulas, o modificar la secuencia de conmutación de las mismas.

- ✓ La miniaturización de los montajes en flujo, ya que el reducido tamaño de las válvulas solenoide y de las interfaces electrónicas permite el desarrollo de equipos integrados de reducido tamaño y de instrumentación portátil para la realización de análisis *in situ*.
- ✓ La disminución del consumo de muestra y reactivos. Se consigue un ahorro considerable puesto que los reactivos sólo son insertados en el sistema en el momento necesario y no circulan continuamente a través del sistema.
- ✓ El aumento de la precisión, ya que la intervención del operador es mínima, que es la causa principal de los casos de falta de precisión. El proceso de inserción está controlado por un ordenador mediante un software adecuado y se favorece de esta manera el diseño de métodos analíticos completamente automáticos.
- ✓ La economía y la sencillez, ya que el precio global de la instrumentación del MCFIA es bastante inferior al del FIA.
- ✓ La ampliación de las modalidades de análisis en flujo, debido al "control electrónico" de la dispersión y la mayor versatilidad asociada al MCFIA, han permitido la implementación de modalidades de gradiente, de procedimientos automáticos para determinaciones multiparamétricas y de montajes multicanal complejos de manipulación sencilla y eficaz.

No obstante, los sistemas MCFIA presentan algunas desventajas:

- ✓ Las limitaciones en cuanto a volúmenes de inserción, ya que es necesario la sincronización de la unidad de bombeo y las microinserciones si los segmentos de muestra y reactivos introducidos son muy pequeños con el fin de evitar problemas de falta de precisión.
- ✓ La escasa comercialización de equipos, que causa la necesidad de *hardware* y *software* de fabricación propia, a pesar de la sencillez en su desarrollo.
- ✓ El mayor deterioro de las válvulas solenoide, ya que el calor disipado por el solenoide de las válvulas de conmutación cuando éstas se activan durante períodos de tiempo más o menos largos puede acortar el tiempo de vida útil de estos dispositivos. Para evitar el sobrecalentamiento de las válvulas, que puede llegar a deformar el teflón de las membranas internas, se recomienda incorporar algún tipo de sistema de protección electrónico del solenoide.

- Análisis por inyección en flujo multijeringa (MSFIA).

Esta nueva técnica, MSFIA (*Multi-Syringe Flow Injection Analysis*), fue propuesta a finales de los años 90 por el grupo de investigación del profesor Victor Cerdá [12]. Fue propuesta como una combinación del FIA, SIA y MCFIA.

El sistema está compuesto por una bureta multijeringa construida por adaptación de una bureta automática de jeringa usada para mover simultáneamente cuatro jeringas que van

conectadas al mismo motor. Cada jeringa está equipada con una válvula solenoide de tres vías, que funciona independientemente del desplazamiento del pistón y permite realizar los procesos de conmutación. De este modo, hay dos direcciones de flujo para el movimiento de impulsión y otras dos direcciones para la aspiración de disolución. Dado que una de las jeringas del módulo no se suele usar para inyectar la muestra, para evitar la contaminación entre distintas muestras inyectadas de forma consecutiva, es necesario un sistema de inyección adicional, tal como una válvula de inyección, de selección o de conmutación, conectada a la multijeringa para este fin y con el objetivo de automatizar el muestreo.

Una representación esquemática de este tipo de metodología puede observarse en la siguiente figura (**Figura 12**).

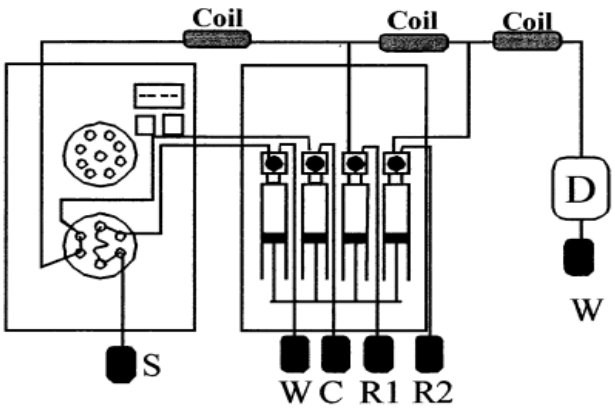

Figura 12. Representación esquemática de un sistema MSFIA. S: muestra, R1: reactivo 1, R2: reactivo 2, W: desecho, C: portador y D: detector. En esta imagen pueden observarse el módulo multijeringa (con jeringas y válvulas solenoides), la válvula rotatoria, los bucles de reacción y la zona de detección. Reeditada de [12]. Copyright (2018), con permiso de Elsevier

La principal desventaja de esta técnica deriva de la necesidad de recargar las jeringas, lo cual puede repercutir en una disminución de la frecuencia de muestreo en el análisis, además de la limitación que se presenta en cuanto al movimiento en bloque de las cuatro jeringas.

- Sistemas en flujo multibomba (MPFS)

Los sistemas MPFS (*MultiPumping Flow Systems*) los describieron Lapa y colaboradores en 2002 [13]. Estos sistemas están basados en el uso de microbombas solenoides (**Figura 13**) para impulsar los líquidos dentro del sistema de flujo. Estos pequeños dispositivos, de bajo coste, garantizan el consumo mínimo de reactivos, ya que cada microbomba puede ser operada individualmente.

Figura 13. Fotografía de una microbomba solenoide de un sistema MPFS

La simplicidad y bajo coste del circuito de control, la portabilidad y el tamaño miniaturizado del analizador construido son las características más destacadas de este sistema. Estos sistemas presentan algunas desventajas como la posibilidad de

bloqueo con pequeñas partículas, así como el posible descalibrado debido a la sobrepresión en el sistema de flujo.

2.2.4. Lab-on-Valve (LOV)-µSIA

Considerada como una metodología de análisis por inyección en flujo de tercera generación, el sistema Lab-on-Valve fue propuesto por Ruzicka en el año 2000 [14], constituyendo una alternativa para la miniaturización de los ensayos (a nivel de microlitro o sub-microlitro). Se trata de una modificación del sistema SIA, miniaturizando el mismo, por lo que se denomina micro-SIA, acoplado al LOV. El método está basado en un sistema de canales integrado a una celda de flujo multipropósito, montado sobre una válvula multiposición convencional (**Figura 14**). Entre las ventajas del LOV, se encuentran su compactibilidad y la posición rígida permanente del canal que procesa la muestra, que asegura la repetitividad de la manipulación de los microfluidos.

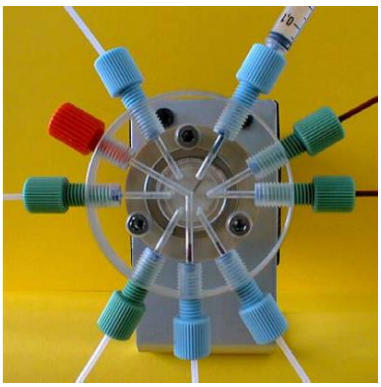

Figura 14. Fotografía de un cabezal de un sistema LOV

2.2.5. Análisis por inyección en flujo cruzado (CIA)

El análisis por inyección en flujo cruzado (*Cross Injection Analysis*) fue presentado como una nueva estrategia de análisis en flujo por Nacapricha y colaboradores en 2013 [15]. La plataforma del CIA tiene un canal como ruta de flujo analítico (canal del eje X) y cuatro canales (canales del eje Y) perpendiculares a este canal. Estos canales se encuentran perforados en un bloque rectangular acrílico. Ambos extremos del eje Y están conectados con tubos al mismo conjunto de rodillos de una bomba peristáltica para formar cuatro líneas de flujo (**Figura 15**). En el CIA, la muestra y los reactivos se introducen en la corriente de flujo analítico de la plataforma (canal del eje X) a través de un tubo de bomba individual conectado a los canales Y de la plataforma. A diferencia del SIA y de las técnicas de multiconmutación, la introducción de los líquidos en esta metodología es simultánea. El empleo del modo de flujo cruzado se ha realizado para la mejora del mezclado logrando así una alta sensibilidad.

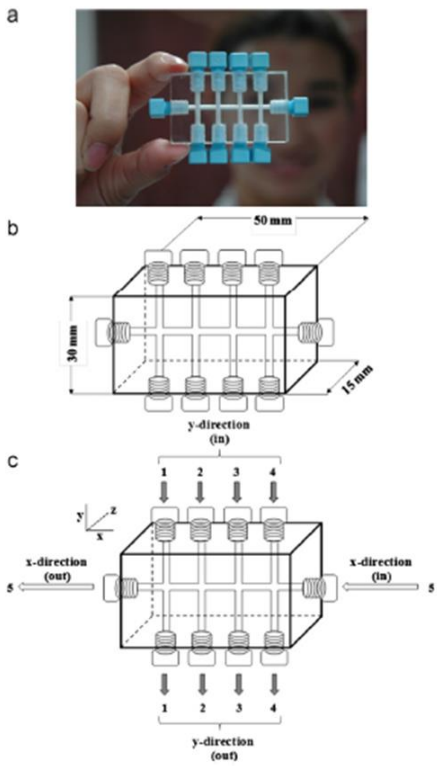

Figura 15. (a) Fotografía de la plataforma de un sistema CIA; (b) diagrama esquemático de la plataforma CIA con dimensión externa; (c) direcciones de flujo de los líquidos. Reeditada de [15]. Copyright (2018), con permiso de Elsevier

2.3. Técnicas de detección

Las técnicas de detección que se usan en los sistemas de inyección en flujo pueden clasificarse en dos tipos según que se mida directamente una propiedad de la especie disuelta en la muestra insertada o, de lo contrario, que sea necesaria una reacción adicional que origine un producto de reacción detectable.

Las técnicas de detección más usadas en los sistemas en flujo comprenden diferentes tipos dentro de los métodos analíticos, como

son los detectores ópticos y los electroanalíticos, que se explicarán a continuación.

2.3.1. Técnicas de detección ópticas

Este tipo de técnicas son las más usada en los sistemas de flujo, ya que un gran número de especies pueden determinarse bien por las propiedades intrínsecas que presenta dicha(s) especie(s) o por las de un producto de reacción con un reactivo o proceso determinado. Su clasificación se realiza en función de la técnica de análisis que sirve de base a la detección.

2.3.1.1. Espectrofotometría de absorción molecular UV-Visible

Constituye una de las técnicas de detección más empleadas, ya que existe una numerosa cantidad de especies que absorben en la región UV-Visible [16, 17] del espectro o que pueden ser derivatizadas para la generación de un producto absorbente a través de métodos basados en reacciones selectivas coloreadas [18-20].

Para el uso de este tipo de detección en sistemas de flujo, es necesario el empleo de una célula de flujo, generalmente fabricada con cuarzo o vidrio óptico, para realizar la medida de la señal analítica dependiendo de la zona de la región donde ésta se realice. Para esta técnica de detección, se utiliza la célula de flujo que puede observarse en la **Figura 5**.

2.3.1.2. Luminiscencia molecular

Otra de las técnicas más empleadas para el desarrollo de método de análisis en flujo continuo es la espectroscopía de luminiscencia molecular. El fenómeno de la luminiscencia está basado en la emisión de energía en forma de radiación electromagnética (UV, visible o infrarroja cercana) por parte de moléculas, átomos o iones, como resultado de la transición desde un estado electrónicamente que ha sido excitado previamente con radiación electromagnética a un estado de menor energía, generalmente el estado fundamental [21].

La fluorescencia y la fosforescencia [22, 23] son las dos manifestaciones más conocidas de la luminiscencia producida por especies moleculares de utilidad analítica. La quimioluminiscencia [24] es otra de las manifestaciones que está adquiriendo mayor importancia en los últimos años, al igual que es destacable el uso de la luminiscencia sensibilizada por lantánidos.

- Fluorescencia molecular

  La fluorescencia molecular es la fotoluminiscencia de tiempo de vida corto procedente de un singlete excitado. Las especies excitadas se relajan al estado fundamental, liberando su exceso de energía en forma de fotones.

  Este tipo de detección presenta numerosas ventajas, como alta selectividad, bajos límites de detección, capacidad para la miniaturización y bajo coste, por lo que su uso es bastante extendido. Uno de los principales inconvenientes que presenta esta técnica es el escaso número de especies que presentan fluorescencia nativa, aunque el campo de aplicación

puede ampliarse gracias al uso de reacciones químicas sencillas derivatizadoras [25] o bien de la fluorescencia inducida fotoquímicamente [26]. Debido a que la fluorescencia fotoinducida abarca gran parte de esta Memoria de Investigación, se desarrollará ampliamente más adelante, en el *apartado 2.3.3*.

Las células fluorimétricas de flujo, al igual que las fotométricas, responden a las características y materiales adecuados para el sistema de análisis en flujo, además de estar disponibles en el mercado. A diferencia de las fotométricas, estas células presentan tres ventanas en tres de las caras de la célula, mientras que la cuarta cara es opaca.

Para esta técnica de detección, la célula de flujo empleada en el sistema es del tipo que se observa en la **Figura 6**.

Esta técnica de detección ha sido empleada en todos los estudios que se han realizado para esta Memoria, a través de fluorescencia directa o fluorescencia fotoinducida, remarcando la versatilidad y la importancia de la técnica para el desarrollo de metodologías analíticas.

- Fosforescencia

Otra de las técnicas espectroscópicas de emisión molecular usadas en sistemas en flujo es la fosforescencia [27, 28]. Se caracteriza por ser una fotoluminiscencia de tiempo de vida largo procedente de un triplete excitado, formado por la absorción de radiación ultravioleta, visible o infrarroja cercana. Debido a que esta técnica requiere algunas características

determinadas para que se registre una señal fosforescente razonable como soportes sólidos, medios organizados, etc., su uso no está tan generalizado como la fluorescencia o quimioluminiscencia para su aplicación en los sistemas de análisis en flujo continuo.

La célula de flujo utilizada para la fosforescencia es la que se aprecia en la **Figura 6**, que se introducirá en el espectrofluorímetro, instrumento utilizado para las medidas de luminiscencia retardada.

- Quimioluminiscencia

Es definida como la producción de radiación electromagnética como resultado de una reacción química, de forma que alguno de los productos de reacción se obtiene en el estado excitado y emite luz al volver a su estado fundamental. El que se produzca este fenómeno es algo poco común, ya que si la energía liberada en la reacción química no es lo suficientemente elevada para provocar la excitación, es disipada en forma de calor u ocurre la combinación de ambos. El proceso por el que se produce la quimioluminiscencia es el mismo que para la fluorescencia o la fosforescencia excepto que no es necesaria ninguna fuente de excitación. Las aplicaciones de la quimioluminiscencia como detección en sistemas de flujo continuo son elevadas [29-31], empleadas para el análisis clínico [32], medioambiental[33-35] y farmacéutico[36, 37].

En la quimioluminiscencia se emplea normalmente un tipo de célula de flujo de metacrilato, con un interior helicoidal para una mayor superficie de exposición del analito que circula

por ella hacia el tubo fotomultiplicador. Sin embargo, si se requiere el uso de un soporte sólido en la célula, debido a la dificultad de inserción en el tipo de célula anterior, además del aumento de cantidad de soporte sólido necesario, se utiliza la célula que se observa en la **Figura 5**, con un volumen interno mayor que las usadas para espectrofotometría.

- Luminiscencia sensibilizada por lantánidos (LSL)

  La formación de quelatos o complejos entre el europio, y en especial el terbio, con ligandos orgánicos, y la capacidad de producir transferencia de energía intramolecular (o intermolecular en ocasiones) a través del estado triplete del ligando a niveles de emisión del ion lantánido es lo que caracteriza este tipo de luminiscencia. La excitación se produce a la longitud de onda característica del compuesto orgánico (el analito en cuestión, que debe ser fluorescente) y la emisión se produce a la longitud de onda característica del lantánido [38-40]. Entre las principales ventajas que presenta esta técnica está el gran desplazamiento de Stokes, bandas de emisión muy estrechas y elevado tiempo de vida media de la luminiscencia, gracias a lo cual se consigue una alta selectividad en las medidas que se realizan (puesto que se evita la posible interferencia de otros compuestos fluorescentes que puedan estar presentes en la muestra). El principal inconveniente es el escaso número de compuestos que pueden complejarse con los iones lantánidos para el uso de esta técnica, demostrándose así de nuevo su alta selectividad.

La célula de flujo utilizada para este tipo de detección es la misma que en el caso de la fluorescencia y la fosforescencia, y que puede observarse en la **Figura 6**.

2.3.1.3. Espectroscopía vibracional

Dentro de la espectroscopía vibracional, podemos distinguir el uso de la espectroscopía infrarroja y la espectroscopía Raman.

- Espectroscopía Infrarroja

El acoplamiento de la espectroscopía infrarroja con las técnicas de inyección en flujo hizo que el análisis cuantitativo de líquidos por esta técnica fuese ocupando un lugar cada día más importante en la literatura científica [41-43], a pesar de que la sensibilidad obtenida no ha sido muy elevada. La espectroscopía infrarroja mediante transformada de Fourier (FTIR) [44] es la que mayor uso presenta debido a su alta velocidad de barrido.

Las principales desventajas de esta técnica de detección se centran en la falta de transparencia de los disolventes empleados en la región del espectro correspondiente al infrarrojo y la dificultad de montaje y limpieza de las células.

- Espectroscopía Raman

Este tipo de espectroscopía también puede aplicarse como sistema de detección en los métodos de análisis en flujo continuo, tanto para especies orgánicas como inorgánicas. Además de la ventaja que presenta el uso de la instrumentación de esta técnica (ya que requiere pequeños volúmenes de muestra

y no está sujeta a la influencia negativa de la humedad), también supone una menor probabilidad en la superposición parcial de mezclas y además, las medidas cuantitativas son más simples [45].

A pesar de dichas ventajas, la sensibilidad de esta técnica no es muy elevada, pudiéndose mejorar con otras variantes de la espectroscopía Raman como la espectroscopía Raman sensibilizada en superficie (SERS) [46-48].

2.3.1.4. Espectroscopía atómica

La implementación de esta técnica en las metodologías analíticas de análisis en flujo [49] solventa el problema del consumo excesivo de muestra en algunos tipos de estas técnicas. Una característica fundamental de su uso es el hecho de no precisar célula de flujo, además de la baja dispersión, factor adicional que da lugar a una mayor sensibilidad. A pesar de que son utilizadas técnicas como la absorción atómica [50, 51], fotometría de llama [52] y fluorescencia atómica [53], es destacable en particular el uso de la espectroscopía de emisión óptica por plasma de acoplamiento inductivo (ICP-OES) como sistema de detección, ya que proporciona una alta sensibilidad, frecuencia de muestreo y versatilidad [54].

2.3.2. Técnicas de detección electroquímicas

Los detectores electroquímicos son de gran utilidad en sistemas hidrodinámicos debido a su selectividad, sensibilidad y linealidad de respuesta en un amplio rango de concentración. La propia naturaleza de

los procesos electroquímicos, que generalmente ocurren en una superficie, los hace muy atractivos y convenientes para la detección miniaturizada. El material que presenta el electrodo es el principal inconveniente de este tipo de detectores. El envenenamiento de la superficie en el caso de electrodos sólidos debido a la adsorción se manifiesta en una pérdida de estabilidad a causa de la pasivación y consecuente disminución de la señal.

Su clasificación puede realizarse en función de algunos criterios como la base de la medida, la situación de la superficie activa o sensor responsable de la señal analítica o bien de la posición del electrodo de referencia.

A continuación se comentan las técnicas electroanalíticas más utilizadas como sistemas de detección para metodologías de análisis por inyección en flujo continuo.

- Técnicas potenciométricas

  La detección potenciométrica [55-58] tiene grandes ventajas como la simplicidad del dispositivo experimental, sensibilidad, selectividad, rápida respuesta y química relativamente simple. Los principales inconvenientes que presentan son la difícil interpretación de la medida si el ion a determinar está prácticamente complejado, y el hecho de que son sensibles a la actividad iónica solo en la inmediata vecindad de la membrana.

- Técnicas amperométricas

  Dentro de estas técnicas hay que distinguir aquellos diseños que implican electrodos sólidos y los que utilizan gotas

de mercurio (EGM), los cuales [59] presentan la ventaja de poseer una superficie continuamente renovada que asegura una sensibilidad y un nivel de la línea base estable. El campo de aplicación de los detectores amperométricos abarca, fundamentalmente, la determinación a muy bajas concentraciones de compuestos fisiológicamente activos [60], incluidos neurotransmisores y sus precursores y metabolitos [61].

- Técnicas coulombimétricas

  Este tipo de técnica de detección ha sido integrada en los sistemas en flujo a través de la culombimetría por inyección en flujo (FIC), basada en la medida de la integral del pico corriente-tiempo (i-t) obtenido en la inyección de un pequeño volumen de disolución que contiene especies electroactivas, en un flujo de electrolito-soporte que pasa a través de un detector que opera en condiciones de transporte de masa limitado [62-64]. Esta técnica resulta ser más efectiva cuando el electrodo tiene una gran superficie y pequeño volumen interno, denominándose entonces "electrodo coulométrico".

- Técnicas conductimétricas

  La asociación de la conductimetría con métodos de análisis por inyección en flujo [65, 66] ha dado lugar a un nuevo método de inyección en flujo, donde las muestran son eluidas a través de una célula de conductividad miniaturizada. Una columna de cambio iónico reduce la contribución a la conductividad del ácido o la base por neutralización. La

conductividad diferencial es, por tanto, proporcional al contenido de ácido o base, no teniendo en cuenta la sal.

2.3.3. Fluorescencia inducida fotoquímicamente (PIF)

Debido a que gran parte de las investigaciones recogidas en esta Memoria están basadas en el uso de esta técnica, voy a extenderme con detalle en su explicación.

- Fundamento teórico de la fluorescencia inducida fotoquímicamente

  La fluorescencia molecular es un potente método de análisis ya que presenta alta sensibilidad y selectividad bajo las condiciones adecuadas. Sin embargo, muchos analitos presentan una nula o muy débil fluorescencia, lo que hace que su determinación analítica mediante la técnica de fluorescencia sea inviable o de muy baja sensibilidad.

  En ciertas ocasiones, la radiación UV produce fotoconversiones en la estructura del analito originándose cambios en su fluorescencia. Este fenómeno ha dado lugar a que se hayan puesto a punto multitud de métodos [67-69] que mediante el uso de reacciones fotoquímicas aumenten la sensibilidad, selectividad y precisión de la detección fluorimétrica. A este método se le conoce como "Fluorescencia Inducida Fotoquímicamente a Temperatura Ambiente (*Room Temperature Photochemically Induced Fluorescence*, RTPIF) o simplemente Fluorescencia Inducida Fotoquímicamente" (*Photochemically Induced Fluorescence*, PIF).

En muchos compuestos, la reacción fotoquímica conlleva un aumento del coeficiente de absorción y del rendimiento cuántico de fluorescencia con relación a los del analito. Por tanto, el aumento de la señal de fluorescencia del fotoproducto origina un aumento de la sensibilidad de la detección fluorimétrica.

Los fundamentos teóricos de la técnica PIF han sido descritos a lo largo de los años por diferentes autores [70, 71], por lo que aquí se recogerá un breve resumen de estos.

Si se parte de la premisa de que una disolución suficientemente diluida como para que la absorbancia sea menor de 10^{-2}, la velocidad de fotorreacción viene dada por la siguiente expresión:

$$v = -\frac{dC_A}{dT} = \frac{dC_B}{dt} = \sum_{\lambda P} \emptyset_{\lambda P}\, I_{0,\lambda P} a_{\lambda P}$$

en la que el sumatorio afecta a aquellas longitudes de onda incidentes (λ_P) que producen fotorreacción. El resto de variables que entran en juego son las siguientes:

$\varphi_{\Lambda p}$: Rendimiento cuántico de fluorescencia

$I_{0,\ \Lambda p}$: Intensidad de radiación incidente a cada longitud de onda

$a_{\lambda P}$: 2.303x ε_A, donde ε_A es la absortividad molar a cada λ

b: Paso óptico

C_A: Concentración del analito

C_B: Concentración del fotoproducto

Si se admite que I_{0,λ_P} es constante y mucho mayor que C_A, la expresión anterior puede llegar a convertirse en la ecuación de primer orden:

$$(C_A)_t = (C_A)_0\, 10^{[-\sum_{\lambda P} \emptyset_{\lambda P} I_{0,\lambda P} a_{\lambda P} bt]}$$

donde $(C_A)_t$ es la concentración del analito a un tiempo t y $(C_A)_0$ su concentración inicial.

Por lo tanto, hay que tener en cuenta dos consideraciones tras lo expuesto: que el analito sea fluorescente y el fotoproducto no, por lo que tendría lugar una disminución de la fluorescencia y se mediría el decrecimiento de ésta (que no es lo común), o bien que el analito sea débilmente fluorescente (o no fluorescente) y el fotoproducto fuertemente fluorescente, en cuyo caso se observaría un aumento de la fluorescencia y la medición se basaría en el aumento de ésta, todo ello basado en la relación entre la concentración inicial del analito y la señal fluorescente final.

- Características de las fotorreacciones PIF

Han de cumplirse una serie de requisitos para que llegue a producirse una fotorreacción en la que se generen compuestos fluorescentes a partir de otros que no lo son o lo son débilmente:

- ✓ El analito debe absorber fuertemente en la región UV para iniciar la reacción fotoquímica.
- ✓ La radiación absorbida debe ser de una longitud de onda que no sea absorbida significativamente por el(los) fotoproducto(s).
- ✓ Deberá haber un aumento de la rigidez estructural o de la aromaticidad de los fotoproductos que dé lugar a un aumento del coeficiente de absorción y a un rendimiento cuántico de fluorescencia mayor que el del analito.

- ✓ Estabilidad química y térmica (en los casos en los que se lleve a cabo a una temperatura mayor que la temperatura ambiente) de los fotoproductos, al menos en el intervalo de tiempo necesario para su medida.
- ✓ El proceso de fotoconversión deber ser eficiente y tener un alto rendimiento fotoquímico.

- Componentes esenciales de la técnica PIF

La técnica PIF se basa en la radiación con luz UV de la disolución que contiene los analitos, produciéndose la fotoconversión de los analitos no fluorescentes o débilmente fluorescentes en fotoproductos fluorescentes. Por lo tanto, el núcleo central de esta técnica es el fotorreactor donde se produce dicha reacción. El fotorreactor se construye mediante una lámpara de UV alrededor de la cual se encuentra enrollado un reactor de PTFE.

En los sistemas estáticos, las fotorreacciones se llevan a cabo irradiando un recipiente (normalmente hecho de cuarzo), donde se ubica el analito, con una lámpara de elevada potencia (200 W) [69] y posteriormente se procede a la medida del fotoproducto una vez generado.

Sin embargo, en los sistemas en flujo, como ocurre en los estudios desarrollados en esta Memoria, la fotorreacción se realiza on-line con lámparas de baja intensidad (que depende de la intensidad que necesite el analito a determinar) [72]. Aunque se han desarrollado fotorreactores de cuarzo acoplados a los sistemas en flujo, éstos resultan ser caros, frágiles y difíciles de integrar en este tipo de metodología analítica. Por ello, la

lámpara se ubica en el interior de una caja de material reflectante como el aluminio para así conformar el fotorreactor.

Además, el uso de tubos de PTFE supera ampliamente al uso de reactores de cuarzo gracias a la alta transparencia en la zona espectral, además de las múltiples ventajas que posee su uso para los sistemas de análisis en flujo (bajo coste, facilidad de incorporación en el sistema, variedad de medidas disponibles, etc.).

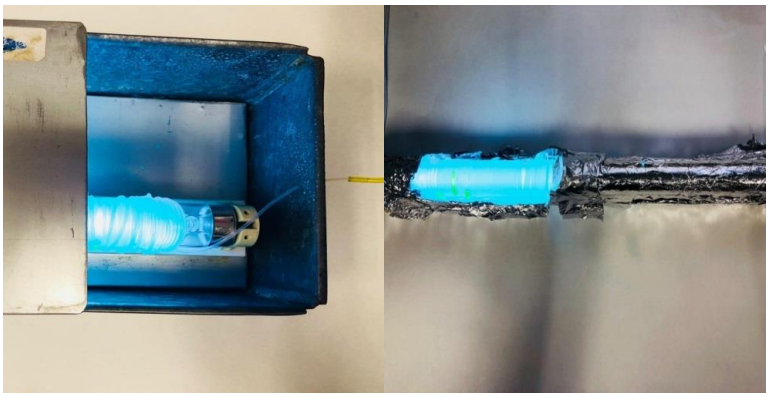

Figura 16. Fotografía de los fotorreactores construidos en nuestro laboratorio de investigación

Para construir el fotorreactor, por tanto, se enrolla tubo de PTFE de forma helicoidal sobre la lámpara. En algunos casos, es necesario un sistema de refrigeración dentro del fotorreactor, como por ejemplo un baño termostatizado o un ventilador, evitando de esta forma pérdidas de señal por desactivación térmica, aunque generalmente no es necesario este componente adicional en el fotorreactor.

La Fluorescencia Inducida Fotoquímicamente también ha sido usada en metodologías cromatográficas a través de la derivatización post-columna [73-75], en la que un parámetro clave para optimizar es la dispersión debido a que puede

provocar ensanchamientos de bandas, disminuyendo la eficiencia de la separación cromatográfica. Existe la posibilidad, descrita en algunos estudios, de que el fotorreactor sea eliminado y la irradiación del analito se produzca directamente en el área de detección mediante irradiación de la lámpara del espectrofluorímetro, moviéndose continuamente el monocromador durante las fases de irradiación y de medida [76]. Además de la complejidad que presenta (frente a la simplicidad que supone situar el fotorreactor previamente), posee desventajas notables como la detención del flujo durante el tiempo de irradiación/medida (por lo que habría una menor frecuencia de muestreo) y un excesivo movimiento mecánico del equipo, con su consecuente desgaste.

- Tiempo de irradiación

El tiempo de irradiación es un factor crucial que viene determinado por la longitud del fotorreactor y el caudal en sistemas de flujo continuo. Debido a que se busca obtener la máxima cantidad de fotoproducto para así obtener la máxima señal analítica, se ha de optimizar el tiempo de irradiación del analito dentro del fotorreactor. Si el analito es irradiado un tiempo inferior al óptimo, existirá una cierta cantidad de analito inicial susceptible de fotoconversión, mientras que si es irradiado a valores de tiempo superiores al óptimo, la intensidad de señal disminuirá debido a que el fotoproducto generado puede ser a su vez fotodegradado en el medio de reacción que se encuentre, además de originarse dispersiones en el sistema de flujo.

- Integración del PIF en los sistemas en flujo

Las aplicaciones de esta técnica en la determinación de analitos en sistemas en flujo son sensiblemente menores que en el caso de metodologías como la cromatografía de líquidos. La primera descripción de un acoplamiento de este tipo fue en 1991, mediante el uso del FIA, fecha en la que Chen y colaboradores [77, 78] analizaron tres fenotiazinas en fármacos haciendo el uso de PIF.

Las aplicaciones están centradas principalmente en compuestos de interés farmacológico [79-83], ampliándose su aplicación en los últimos años a la determinación de pesticidas en el ámbito agroalimentario [84-87], campo en el que se ha basado gran parte de esta Memoria de Investigación.

2.4. Implementación de la espectroscopía en fase sólida (SPS) en los sistemas de análisis por inyección en flujo: Optosensores en flujo continuo

La Espectroscopía en Fase Sólida (*Solid Phase Spectroscopy*, SPS) surge como intento de aplicación al análisis cuantitativo del fundamento de los "*resin spot tests*" (ensayos a la gota sobre resinas intercambiadoras de iones). Esta técnica consiste en ensayos cualitativos de observación visual basados en la aparición de coloración en unos granos de resina de cambio iónico debido a la fijación en ella del producto de reacción del analito (especie cargada eléctricamente) con los reactivos. A pesar de los numerosos trabajos sobre "*resin spot tests*" publicados desde que en 1954 Fujimoto [88, 89] propusiera la referida técnica de microanálisis cualitativo, en ninguno de ellos se hizo

un intento de cuantificación del analito y tuvieron que pasar más de dos décadas hasta que, en 1976, Yoshimura [90] diera a conocer los primeros métodos de determinación cuantitativa basados en la medida directa de la absorbancia de la especie coloreada retenida en la resina, que fue llamada "*Colorimetría de Cambio Iónico*" y que actualmente suele denominarse espectroscopía en fase sólida (SPS).

La SPS está basada en el uso combinado de un soporte sólido para que tenga lugar la preconcentración del analito (o de su producto de reacción) con la medida directa de la absorción de radiación de la especie de interés retenida sobre el mencionado soporte sólido. Una vez retenida la especie de interés sobre la fase sólida, ésta es separada del resto de la disolución por filtración y trasvasada a una cubeta (generalmente de 1 mm de paso óptico) donde se lleva a cabo la detección espectroscópica.

Una gran ventaja de la SPS es la elevada sensibilidad que se consigue, pudiendo aplicarse al análisis de elementos traza sin la necesidad de realizar pasos previos de preconcentración, como en el caso de la espectroscopía convencional. Por otra parte, es interesante destacar la elevada selectividad obtenida con esta metodología, debido a la retención selectiva del analito (o su producto de reacción) sobre el soporte sólido, así como la sencillez de la técnica y el bajo coste de la instrumentación que requiere.

Inicialmente la técnica se aplicó a un amplio conjunto de iones y compuestos [91-94], y más tarde se expandió el abanico de posibilidades que presenta dicha técnica cuando se introdujo la espectrofluorimetría como método de detección [95, 96]. Posteriormente, la SPS se combinó con el FIA incorporando el soporte sólido a una célula de flujo. Una superficie sólida activa rodeada por

una corriente que fluye a su través, combinada con la monitorización de la interacción entre dicho flujo y la superficie fue llamada por primera vez sensor óptico en flujo (*flow-through sensor*) por Ruzicka y Hansen [97]. Estos sistemas, también denominados optosensores en flujo, pueden realizar simultáneamente la reacción, separación, preconcentración y detección en la misma célula de medida. En la **Figura 17** se muestra un esquema de la implementación de ambas metodologías.

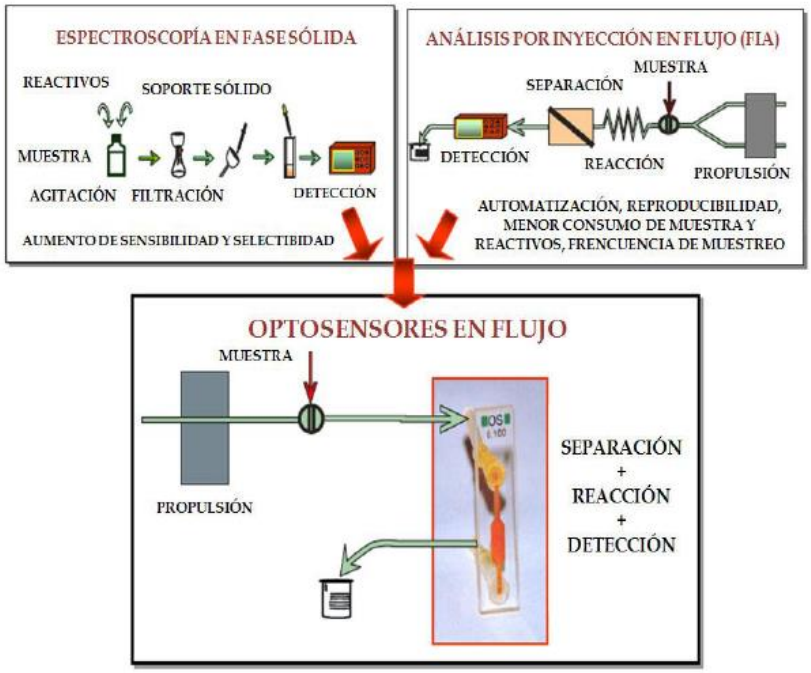

Figura 17. Integración de la SPS con el FIA: Sensores espectroscópicos en flujo

2.4.1. Fundamento de los optosensores en flujo continuo

Un sensor químico (o bioquímico) ideal puede definirse como un dispositivo analítico (miniaturizado) que responde de manera directa, reversible, continua, rápida, exacta y precisa a los cambios de

concentración de una (o más) especie(s) de una muestra [98]. Consta de una microzona sensora, donde tiene lugar una reacción química (o bioquímica) y/o un proceso de separación, que está conectada con (o integrada en) un transductor, que en el caso de los optosensores se trata de un transductor óptico. La amplia variedad existente de sensores hace difícil describir su comportamiento en términos generales; no obstante, establecer sus propiedades genéricas, indispensables unas, deseables otras, resulta mucho más fácil. Algunas de ellas coinciden con características esenciales de la metodología FIA, SIA o MCFIA, como son exactitud y precisión; otras se refieren al tipo de funcionamiento (reversibilidad y reutilizabilidad en procesos regenerables), además de la sensibilidad y la selectividad que aporta la espectroscopía en fase sólida. Otras características básicas son aquellas relacionadas con el tiempo: respuesta lo más próxima posible a tiempo real y rapidez en los procesos reversibles y en los de regeneración y estabilidad (duración y tiempo de vida operacional). Finalmente, también es de destacar: simplicidad de construcción y operación, robustez, bajo costo, posibilidad de utilización con muestras complejas o sistemas en evolución y, por último, necesidad de no interpretación por parte del operador.

Los optosensores en flujo continuo son compatibles con detectores espectroscópicos moleculares no destructivos. El bolo de muestra es insertado en la corriente de portador y la radiación interacciona directamente con la zona sensora integrada en el área de detección. Estos dispositivos proporcionan una respuesta rápida, reversible y continua que es transducida a través del detector.

2.4.2. Componentes de los optosensores en flujo continuo

Como se ha mencionado anteriormente, los optosensores en flujo surgen de la combinación del FIA con la SPS; por tanto, los elementos de estos dispositivos son los propios de un sistema de inyección en flujo (sistemas de propulsión, transporte, inyección y detección). La única diferencia, en principio, con respecto a un sistema en flujo, es la presencia de soporte sólido en la célula de flujo, donde se llevan a cabo las medidas espectroscópicas. Se desarrolla a continuación los distintos tipos de soportes sólidos utilizados, así como la célula de flujo empleada para el desarrollo de los sistemas propuestos en esta Memoria.

El soporte sólido es el elemento más importante en este tipo de sensores. La elección del soporte, entre la gran variedad de materiales sintéticos y naturales que pueden emplearse, constituye una parte esencial del diseño del sensor, ya que sobre la superficie del mismo se va a producir la integración de reacción y/o retención y la detección espectroscópica. El soporte sólido empleado debe reunir ciertos requisitos:

- ✓ El tamaño de las partículas debe ser adecuado (entre 40 y 120 μm generalmente), ya que tamaños de partícula menores podrían generar sobrepresiones en el sistema.
- ✓ El material escogido debe ser químicamente inerte a los componentes de las soluciones del flujo y resistente al flujo continuo, garantizando reproducibilidad en la respuesta del sensor.
- ✓ Debe ser compatible con el sistema de detección usado (por ejemplo, en los sensores fotométricos, la absorción de fondo

debe ser suficientemente baja para permitir realizar las medidas sin saturar el detector).

Dos son los grupos principales de soportes que han sido empleados: los polímeros de intercambio iónico y los sólidos adsorbentes no polares.

Dentro de los polímeros de intercambio iónico han sido utilizados polímeros de polidextrano, en concreto los geles Sephadex QAE A-25 y SPC-25 (**Figura 18**). El proceso de retención se produce gracias al intercambio iónico.

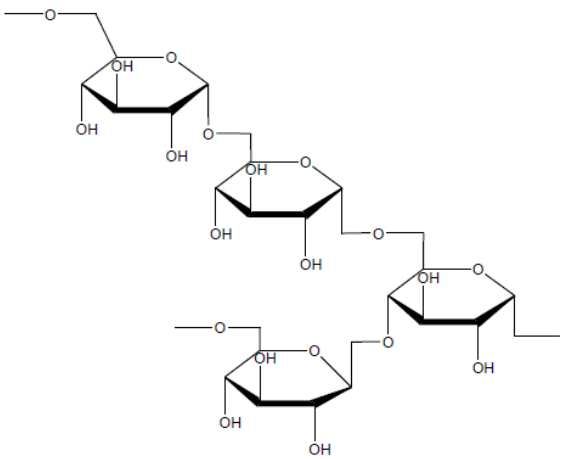

Figura 18. Esquema del esqueleto de polisacárido de los polímeros de dextrano

Dentro de los sólidos adsorbentes no polares se ha empleado como soporte sólido el gel de sílice C_{18}, de naturaleza hidrófoba, que presenta un mecanismo de naturaleza adsortiva. Su estructura se muestra en la **Figura 19**.

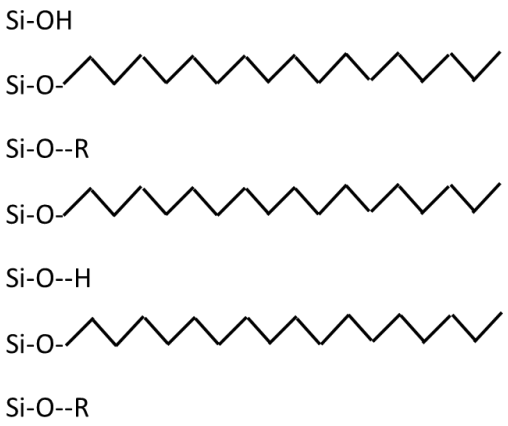

Figura 19. Estructura general de un gel de sílice C_{18}

Las células de flujo son otro elemento clave en el diseño de optosensores en flujo. Una célula de flujo ideal para un sensor en flujo debe reunir dos requisitos:

- ✓ Conseguir la concentración del producto de interés sobre el soporte en un área de la célula tan pequeña como sea posible.
- ✓ El haz de radiación debe incidir sobre esta área (sin irradiar las proximidades de la zona citada).

El nivel de sólido en la célula es una variable clave: debe llenarse hasta una altura tal que el haz de luz incida completamente sobre el soporte sólido y sin que éste apenas llegue a exceder el límite superior del haz de luz, pues alturas crecientes a partir de este límite originan la fijación de la especie de interés por encima del haz (fuera de la zona de detección) o bien una dispersión del bolo de muestra a lo largo de una mayor cantidad de sólido, con pérdida de sensibilidad y disminución de frecuencia de muestreo. Niveles más bajos del indicado producen, por su parte, una disminución de la señal, pues la luz pasa total o parcialmente a través del flujo de solución. En definitiva, la

parte superior del sólido debe mantenerse tan próxima al límite superior del haz como sea posible, pero por encima de él.

En la **Figura 6**, que se puede observar en el apartado "*3.2.1. Análisis por inyección en flujo (FIA)*", se muestra una representación esquemática de la célula de flujo Hellma 176.752-QS, de la cual se hizo uso para el desarrollo de los optosensores recogidos en esta Memoria de Investigación.

2.4.3. Desarrollo de optosensores en flujo continuo: optimización de variables experimentales

En este apartado se describirán las distintas etapas y los distintos factores y variables que se tienen en cuenta a la hora de estudiar y desarrollar un optosensor en flujo continuo.

2.4.3.1. Variables de la unidad de retención/detección

El punto de partida en SPS es la elección de un soporte sólido adecuado donde fijar el/los compuesto/s de interés. La elección del soporte entre la gran variedad de materiales sintéticos y naturales que pueden emplearse constituye una parte esencial del diseño del sensor. Para la elección de este soporte hay que considerar la naturaleza, estructura y propiedades físicas y químicas de los analitos, reactivos o productos de reacción que vayamos a fijar en él, además de la transparencia del mismo en la zona del espectro en la que se trabaje, ya que no debe originarse una línea base demasiado alta.

En general, se suelen usar resinas de intercambio iónico cuando el analito (o producto de reacción) presenta un equilibrio ácido-base

que permita que pueda estar cargado en un intervalo de pH determinado en función del valor de su pKa. En el caso de que la molécula sea apolar o no presente grupos funcionales que permitan su retención en un intercambiador de iones, se usan soportes sólidos sin grupos funcionales donde la retención de la especie de interés se lleva a cabo mediante un mecanismo principalmente de adsorción. Por tanto, a la hora de seleccionar el soporte sólido es necesario prestar especial atención a variables químicas tales como el pH de la muestra o del portador, ya que pueden tener gran influencia en el comportamiento del analito en la fase sólida. A la hora de seleccionar un soporte sólido de entre varios que permiten la retención del analito (o especie de interés) se elegirá aquel que proporcione una mayor señal analítica y una fácil regeneración del mismo.

En el caso de los sensores monoparámetro, sólo interesa la retención de un analito, por lo que se elegirá un soporte sólido de acuerdo con la naturaleza del mismo. Sin embargo, en los sensores multiparámetro será necesario seleccionar un soporte sólido que permita la retención de todos los analitos que entren en juego.

Una vez seleccionado el soporte sólido se procede a la realización de los espectros de luminiscencia correspondientes al/los analito/s, debiéndose obtener estos tanto en disolución como en fase sólida. En un estudio preliminar, se realizan dichos espectros en disolución para conocer las longitudes de onda del analito, que posteriormente se contrastarán en fase sólida, debido a que el efecto hipso/batocrómico que ocurre al utilizar la fase sólida en el medio puede desplazar ligeramente estas longitudes de onda. De esta forma se pueden establecer sus características espectrales y seleccionar las longitudes de onda de excitación y emisión óptimas para la medida.

2.4.3.2. Variables instrumentales

Debido a la presencia del soporte sólido en el detector, la señal de fondo en los optosensores en flujo es generalmente alta, por lo que la optimización de las variables instrumentales es fundamental para la medición del analito en un amplio rango de concentraciones. En optosensores con detección luminiscente, las variables instrumentales a optimizar son la anchura de las rendijas de excitación y emisión y el voltaje del tubo fotomultiplicador. En el caso de detección empleando LSL, es necesario optimizar el tiempo de retardo (*delay time*) y tiempo de medida (*gate time*). El tiempo de retardo es el tiempo que tarda el detector en comenzar a adquirir la señal de emisión tras producirse la excitación; esta variable nos proporciona la condición necesaria para que no se adquiera señal de fluorescencia, sino sólo señal de luminiscencia retardada. Por otra parte, el tiempo de medida es el tiempo durante el cual el detector está adquiriendo la señal analítica.

2.4.3.3. Variables químicas

Entre las variables químicas a estudiar se incluyen: la naturaleza, concentración y pH de la disolución de muestra, la naturaleza, concentración y pH del portador y eluyente (si lo hay) y la concentración y volumen de reactivos (en los casos donde sea necesaria una reacción derivatizadora). Todas ellas influyen, en mayor o menor medida, en la retención/elución de los analitos y, por lo tanto, en la señal analítica y en la separación de los diferentes componentes en el caso de mezclas de dos o más especies.

La naturaleza, concentración y pH de la muestra es una variable crítica cuando se trabaja con soportes sólidos, ya que determinará su

elección. El pH tiene influencia especialmente en las especies que poseen comportamiento ácido–base, provocando su ionización y permitiendo así la fijación o no de éstas en un determinado soporte. Sin embargo, generalmente carece de efecto significativo cuando el analito no sufre equilibrios protolíticos.

El pH y la naturaleza de la disolución portadora también deben ser estudiados, ya que pueden influir en la señal en sentido similar al de la muestra. Cuando el soporte sólido utilizado sea una resina de intercambio iónico, lo más apropiado es utilizar disoluciones de portador acuosas, mientras que cuando el soporte sólido utilizado sea un gel adsorbente no polar, los portadores más adecuados son de naturaleza alcohólica.

Tras la medida, la zona sensora tiene que ser regenerada para la siguiente determinación, haciendo así que el sensor sea reutilizable. Llevar a cabo este paso de regeneración es un requisito clave, ya que va a determinar la rapidez, sencillez del montaje, repetitividad, vida media del soporte sólido, etc. Dependiendo del tipo de analito y de sus propiedades físicas y químicas (polaridad, equilibrios ácido-base, grupos funcionales característicos, mecanismo de retención del soporte sólido elegido, etc.) se optará por una determinada estrategia para llevar a cabo la elución del analito y proceder a otra nueva determinación. Las estrategias a seguir son:

- ✓ Si la propia disolución portadora actúa como eluyente (caso más simple para la regeneración), el proceso de regeneración comienza justo en el momento en el que el extremo posterior del bolo de muestra alcanza el soporte sólido. La concentración creciente de la solución portador/eluyente suele actuar disminuyendo la respuesta analítica del sensor en el caso de cambiadores iónicos, pues los

iones del eluyente compiten con la especie de interés por su fijación en la zona sensora. Es el procedimiento más sencillo y permite frecuencias de muestreo altas y asegura una mayor duración del soporte cuando éste es una resina de intercambio iónico. En el caso de fases sólidas que no sean de intercambio iónico, como es el gel de sílice C_{18}, también es posible la regeneración total a través de la disolución portadora mediante la modificación de las cantidades de metanol:agua que haya en ésta.

- ✓ En los casos en los que no es posible la regeneración del sensor con el propio portador se emplea una solución eluyente adicional, que se hace llegar a la zona sensora mediante la inserción de un volumen definido en el sistema. Se consigue una mayor sensibilidad al no haber elución simultánea al proceso de retención, siendo la preconcentración más efectiva. No obstante, el uso de un eluyente da lugar a una menor frecuencia de muestreo y acorta la vida del sensor si el soporte es una resina de intercambio iónico. Los agentes utilizados en la regeneración de sensores varían en función de la naturaleza de las especies retenidas y del tipo de interacción entre dichas especies y el soporte sólido. Pueden utilizarse, entre otros, agentes oxidantes o reductores, tensioactivos, agentes complejantes y disoluciones ácidas, básicas y salinas (las más usadas generalmente). En el caso de utilizar gel de sílice C_{18} como soporte sólido suelen emplearse soluciones metanólicas de diferente concentración.

2.4.3.4. Variables del sistema de flujo

En este caso cabe distinguir entre el volumen de muestra, el caudal y el tiempo de irradiación (para detección por PIF).

Una de las características más destacables de los sensores en flujo continuo es la posibilidad de incrementar sustancialmente la sensibilidad aumentando el volumen de muestra insertado, lo que conlleva el incremento de la cantidad de analito retenido en la zona de detección. Cuando el coeficiente de distribución es alto, la dependencia de la señal con el volumen de muestra es lineal. Esto dota a estos sensores de una gran versatilidad para trabajar en un amplio rango de concentraciones, simplemente cambiando el volumen de muestra insertado. Es necesario tener en cuenta que en los sensores basados en las metodologías FIA y SIA se habla de volumen de muestra, mientras que en los sensores basados en MCFIA hay que hablar de tiempo de inserción de muestra (conocido el tiempo de inserción y el caudal, se puede calcular el volumen insertado). Como el desarrollo de nuestros estudios está basado en sistemas MCFIA, este último caso es el que nos ocupa.

La influencia del caudal depende de la rapidez del proceso de retención en la zona sensora. Cuando la cinética de retención del analito es muy rápida se originan señales apenas afectadas por el caudal, dentro de los valores permitidos para éste. En cambio, cuando la cinética de retención es lenta se obtienen señales analíticas que decrecen al aumentar el caudal, lo que conlleva una disminución en la sensibilidad, aunque por otro lado aumenta la frecuencia de muestreo. Por lo tanto, hay que adoptar una solución de compromiso entre sensibilidad y rapidez de análisis.

Como ya fue mencionado, el tiempo de irradiación es un factor crucial en aquellos optosensores que están basados en PIF y viene determinado por la longitud del fotorreactor y el caudal.

2.5. Implementación del uso de nanomateriales en los sistemas de análisis por inyección en flujo

Recientemente, la nanociencia y la nanotecnología se han convertido en temas ampliamente discutidos dentro de los campos científico e industrial, que tienen y tendrán una influencia en la tecnología y en la calidad de vida del ser humano ya que a medida que pasan los años la nanotecnología está cada vez más presente en nuestro día a día. En consecuencia, la necesidad de información y el número de artículos científicos sobre estas áreas emergentes crece exponencialmente, por lo que también está en aumento el número de nanoproductos y nanopartículas que han sido introducidos en el mercado.

La química analítica puede relacionarse con el creciente aumento de nanomateriales de diversas formas:

- Mediante la caracterización y/o determinación de nanomateriales en una amplia variedad de muestras como cosméticos, alimentos, fármacos y matrices ambientales. La valiosa información (bio)química de la química analítica proporciona un importante apoyo al desarrollo integral de la nanociencia y la nanotecnología. A pesar de su importancia estratégica, el número de estudios analíticos sobre nanociencia y nanotecnología solo representa el 30-35% en este campo.
- Mediante el desarrollo de nanomateriales como sorbentes, fases estacionarias y pseudoestacionarias, soportes inertes y activos, que tienen como último fin la mejora y el desarrollo de nuevos procesos analíticos. Alrededor del 65-70% de los artículos publicados en la literatura científica están relacionados con este uso para los nanomateriales.

- Mediante la considerada "tercera vía" [99], que se describe como una alternativa complementaria a las dos facetas clásicas que se han descrito anteriormente. En la **Figura 20**, se describe este concepto como una combinación de esas facetas. Las nanopartículas pueden actuar simultáneamente como un objeto (analito) en la muestra y una herramienta que puede usarse en diferentes pasos del mismo proceso analítico (preparación de muestra, separación y detección). A pesar de su importancia estratégica, en la literatura científica existen poco estudios sobre este tema.

Figura 20. Combinación de las facetas clásicas para dar lugar a la "tercera vía"

Las metodologías analíticas basadas en el uso de nanopartículas que se han desarrollado en esta Memoria están basadas principalmente en el uso de la segunda faceta, ya que se hace uso de las nanopartículas para la determinación de compuestos no fluorescentes, mejorando y desarrollando nuevas estrategias en los métodos de análisis en flujo.

2.5.1. Empleo de nanopartículas como nanosensores químicos para la mejora de métodos de análisis en flujo

Los puntos cuánticos (*quantum dots*, QDs) son nanopartículas cristalinas de materiales semiconductores tridimensionales descubiertas en 1981 [100]. La primera aplicación más significativa de los QDs fue desarrollada y publicada en 1998 en la revista *Science* por los grupos de Alivisatos y Nie, que consistía en la visualización de tejidos vivos gracias a las características fluorescentes de estos nanocristales [101, 102]. Los QDs están compuestos de cientos o miles de átomos de una mezcla de elementos de los grupos de la tabla periódica II-VI (CdSe, CdTe), III-V (GaN, InAs) o IV-VI (PbSe, PbS) [103, 104]. La estructura básica de un QD consiste en un *core* o núcleo, formado por dicha mezcla de elementos semiconductores (como CdTe, CdSe, PbS,…), que bien puede ser recubierto con un *shell* o cáscara y con un *capping*, que servirá para funcionalizar la superficie del QD o directamente con ese *capping* (**Figura 21**). Generalmente presentan una geometría quasiesférica con un tamaño que abarca desde 1 a 10 nm y que proporciona propiedades optoelectrónicas únicas debido al efecto de confinamiento cuántico. Este efecto está basado en el confinamiento de los electrones y huecos de los QDs en las tres dimensiones del espacio cuando el tamaño de la nanopartícula es menor al radio del excitón de Bohr [105]. Por lo tanto, los estados electrónicos y los perfiles de emisión luminiscente, varían con el tamaño del QD, siguiendo de manera general, el comportamiento esperado para una partícula atrapada en una caja 3D. De hecho, los niveles energéticos de los QDs se comportan de manera más parecida a átomos o moléculas (niveles discretos cuantizados) que a un material macroscópico y en ocasiones son llamados "*átomos artificiales*". Además, los QDs de

diferentes materiales o del mismo material con distintos tamaños, debido al confinamiento, presentan un *bandgap* con diferente energía. Este hecho permite generar fotoluminiscencia con bandas estrechas de emisión y ajustable según el tamaño y material de las nanopartículas [106, 107].

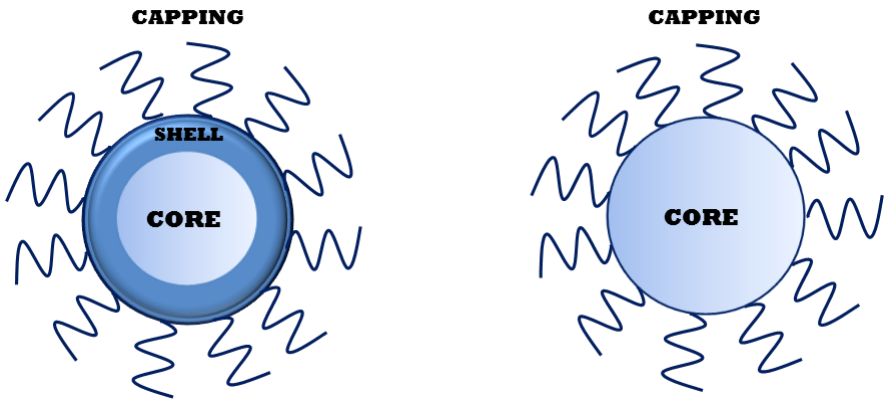

Figura 21. Estructura básica de los QDs

La fotoluminiscencia puede ocurrir mediante la absorción de fotones de energía superiores al *bandgap*, que crea un excitón (par electrón-hueco) y su posterior relajación vía fonones (relajación vibracional) al estado excitado de menor energía, produciéndose la emisión desde el nivel más bajo del estado excitado hasta el estado fundamental. El efecto de confinamiento cuántico proporciona a los QDs algunas propiedades ópticas como un amplio espectro de excitación, un espectro de emisión estrecho y ajustable (que depende del tamaño y material del QD), alta fotoestabilidad (capacidad de mantener su fluorescencia durante un elevado tiempo) y un tiempo de vida del estado excitado alto (30-200 ns), que les ofrecen numerosas ventajas frente a los fluoróforos moleculares más utilizados.

Debido a las excepcionales propiedades ópticas, químicas y electrónicas que se comentan, ha surgido un extraordinario interés por los QDs en numerosas y diversas áreas científicas y tecnológicas, demostrando ser altamente útiles para el desarrollo de nanosensores químicos, además de su uso en nanoelectrónica, celdas solares, fotocatálisis, marcado celular, etc.

En los últimos años se ha incrementado el uso de estos nanocristales semiconductores como sensores luminiscentes en el campo de la Química Analítica para la detección de una variedad de analitos, incluidos compuestos orgánicos, inorgánicos y biológicos [108-111]. En su aplicabilidad, el control de tamaño, la morfología y los ligandos de superficie del QD son esenciales ya que determinarán sus propiedades ópticas y su respuesta de fotoluminiscencia.

Otra consideración a tener en cuenta es el *capping* de los QDs (moléculas que recubren su superficie), ya que esto podrá influir críticamente en la sensibilidad y selectividad de los sistemas que utilizan estas nanopartículas. La funcionalización de los QDs tiene como objetivo modificar su solubilidad en distintos disolventes, ayudar al reconocimiento molecular y celular, alterar la permeabilidad en las membranas y mejorar la capacidad de interacción con determinados analitos. Existen numerosos compuestos que pueden servir de *capping* en los QDs, siendo los compuestos con grupos tiol uno de los más utilizados (ácidos mercaptopropiónico, L-cisteína, glutationa, tioglicerol, etc.) [112]. La modulación de la fotoluminiscencia de los QDs como una respuesta selectiva al reconocimiento de un determinado analito se puede observar a través de la intensificación (*enhancing*) de la intensidad de la fluorescencia o el decrecimiento (*quenching*) de ésta [113].

El conocimiento y comprensión del mecanismo de interacción entre el analito y las nanopartículas nos permite diseñar nuevos sensores basados en QDs. Ambos comportamientos se han descrito en diversas metodologías analíticas, pero el proceso más común es, indudablemente, el efecto *quenching* (**Figura 22**), donde la interacción entre un determinado analito y el *capping* de los QDs atenúan la intensidad de la fluorescencia de los QDs.

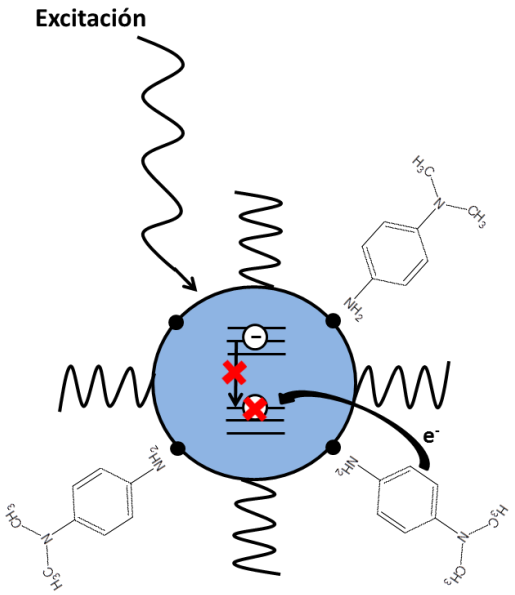

Figura 22. Diagrama del proceso *quenching* para los QDs

Los estudios realizados hasta la fecha con estas nanopartículas están principalmente centrados en la determinación de diferentes analitos de interés farmacológico, agroalimentario o ambiental. En general, los analitos no presentan fluorescencia (o ésta es débil) y originan un fenómeno *quenching* sobre la fluorescencia de QDs, mecanismo que se denomina transferencia de energía fotoinducida (*Photo-induced Energy Transfer*, PET) y que se describe a continuación. Se crea un estado excitado del QD absorbiendo un fotón

de luz. Su fotoexcitación genera un par electrón-hueco (excitón) en la banda de conducción (CB) y la banda de valencia (VB). Los excitones son buenos reductores (transfieren electrones desde un orbital molecular de alta energía a un aceptor de electrones) y buenos oxidantes (transfieren electrones desde un electrón donante a un hueco en el orbital molecular originalmente lleno) y pueden revertir la transferencia de electrones y agujeros [114]. En presencia de un aceptor de electrones, con el potencial redox del nivel de energía LUMO menos negativo que el potencial de la banda de conducción del QD, tiene lugar la transferencia de electrones a la especie aceptora. De la misma manera, en presencia de un donador de electrones, con un potencial del nivel HOMO más negativo que la banda de valencia del QD, el proceso de transferencia de electrones ocurre desde el donante hasta los agujeros de la banda de valencia que hay en el QD [115, 116] (**Figura 23**). Por lo tanto, cualquiera de las reacciones competitivas de transferencia de electrones conduce a la disminución de la intensidad de emisión de los QDs debido a la aniquilación de la recombinación de electrones en los QDs excitados.

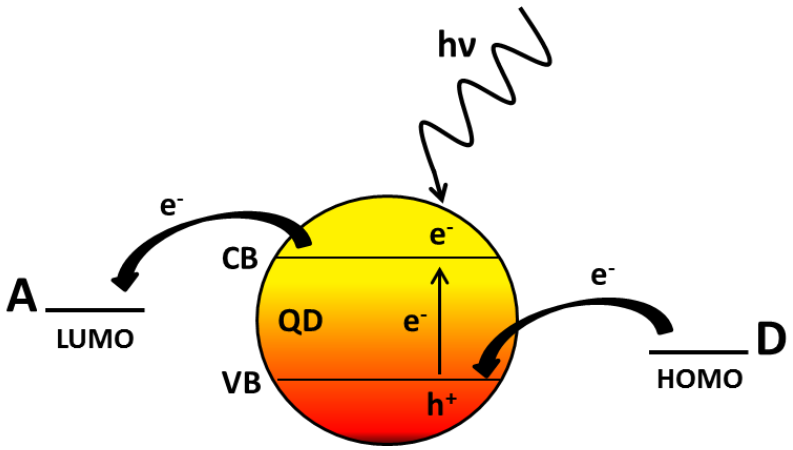

Figura 23. Caminos de extinción de transferencia de electrones de partículas QD por aceptor de electrones (A) o unidades de donadores de electrones (D)

Se han publicado varios trabajos en los que se aplicaron mecanismos de PET para detección de una variedad de analitos utilizando CdTe-QDs como quimio-sensores fluorescentes, entre los que cabe destacar algunos estudios realizados por Joao L.M. Santos y colaboradores [108, 117-120] y los desarrollados en el grupo de investigación en el que se ha realizado esta Memoria [121, 122].

Además de las clásicas interacciones entre QDs y las especies que se desee determinar, existen otros tipos de mecanismos para su determinación, entra las que se va a mencionar la transferencia de energía de resonancia de fluorescencia (*Fluorescence resonance energy transfer*, FRET), temática principal de la estancia predoctoral que he realizado en el grupo de investigación del profesor João L.M. Santos (Universidad de Oporto, Portugal).

La FRET es la transferencia de energía no-radiante entre un luminóforo donador de estado electrónicamente excitado (D) y un aceptor (A) a través de interacciones dipolo-dipolo de largo alcance [123]. La eficiencia del sistema FRET depende de la orientación de los

momentos dipolares del donador y del aceptor, el grado de superposición espectral entre espectros de excitación-emisión de donador y aceptor y la distancia entre el par entre los que se produce FRET (1-10 nm) [124].

En este sentido, diversos trabajos han explotado el uso de los QDs en los sistemas FRET, debido a las características fotoluminiscentes dependientes del tamaño de QD que los hacen excelentes donadores [113, 124], teniendo en cuenta las numerosas ventajas que presenta su uso para el desarrollo de sensores. De hecho, cuando los QDs se usan como donadores en un proceso FRET, el ajuste de tamaño obtenido durante su síntesis permite variar la distancia entre el par donador/aceptor y hacer coincidir la emisión del QD con la banda de absorción del aceptor, generando sistemas de detección con una sensibilidad bastante elevada [113, 125]. Sin embargo, debido a que las amplias bandas de absorción del QD favorecen la diafonía de excitación, no ha sido estudiado en profundidad la selección de QD como aceptor [125].

Como se ha comentado anteriormente, el *capping* superficial de los QDs es un parámetro importante en el desarrollo de metodologías analíticas que involucren su uso, por lo que para este tipo de interacciones también ha de tenerse en cuenta, ya que puede afectar a la distancia entre el par donador-aceptor y la capacidad del semiconductor de unirse a otra molécula, comprometiendo la efectividad del FRET [125, 126]. En consecuencia, la optimización del volumen de los ligandos de las nanopartículas es un paso crucial para el desarrollo de estos sistemas [127]. Las moléculas de tiol de cadena corta, generalmente utilizadas como ligandos de superficie en QDs, además de controlar la estabilidad de las nanopartículas y determinar su carga

superficial, también proporcionan plataformas para la funcionalización posterior [128-130]. De hecho, la funcionalización de los QDs con moléculas o ligandos apropiados es muy importante para aumentar las posibilidades de interacción, la selectividad y la eficiencia del proceso de FRET [129].

En los últimos años, las nanopartículas de oro (AuNPs) se han posicionado como excelentes aceptores de fluorescencia, reemplazando los inhibidores orgánicos tradicionales que eran los más utilizados en los sistemas FRET y abriendo nuevas perspectivas para la determinación de diferentes (bio) moléculas y compuestos. Las AuNPs poseen altos coeficientes de extinción molar y amplio ancho de banda de energía dentro de la región de luz visible que se superpone a las longitudes de onda de emisión de los donadores FRET comunes [131, 132].

Los sistemas de detección basados en la pareja QDs-AuNPs como donadores-aceptores son muy atractivos para aplicaciones químicas y biológicas y han dado lugar a varias publicaciones científicas [133-136]. Basándose en esta interacción, se ha desarrollado un estudio de diferentes compuestos de alto interés biológico para esta Memoria.

2.6. Los analitos y su determinación

Los analitos que han sido seleccionados para el desarrollo de esta Tesis Doctoral se han clasificado en dos grandes grupos: contaminantes y compuestos de interés farmacológico y/o biológico. Ambos grupos se pueden enmarcar en los campos agroalimentario y farmacológico, respectivamente. A continuación se realizará una breve

introducción de cada uno de estos analitos así como las técnicas de análisis descritas en bibliografía que han sido utilizadas para su determinación.

2.6.1. Contaminantes

Los contaminantes son sustancias que no se han agregado intencionalmente a los alimentos y pueden estar presentes en los mismos como resultado de las diversas etapas de su producción, envasado, transporte o mantenimiento, además de ser el resultado de la contaminación ambiental. Debido a que la contaminación generalmente tiene un impacto negativo en la calidad de los alimentos y puede implicar un riesgo para la salud humana, todos los alimentos que se destinan al consumo humano o animal en la Unión Europea (UE) están sujetos a un límite máximo de residuos (LMR) de contaminantes en su composición con el fin de proteger la salud humana y animal.

El Codex Alimentarius [137] define el LMR como la concentración máxima de residuos de un contaminante (expresada en mg kg^{-1}) permitida legalmente para su uso en la superficie o la parte interna de los productos alimenticios. Los LMRs están basados en datos de BPA (Buena Práctica Agrícola) y su objetivo es lograr que los alimentos derivados de productos básicos que se ajustan a los respectivos LMRs sean toxicológicamente aceptables.

Las autoridades competentes nacionales de los Estados Miembros son los responsables de la evaluación del riesgo para el consumidor (Agencia Española de Seguridad Alimentaria y Nutrición) y del registro del uso del producto fitosanitario (Ministerio de Agricultura y Pesca, Alimentación y Medio Ambiente). Asimismo, las

Comunidades Autónomas están encargadas del control y de la aplicación de estos LMRs.

Los LMRs que se han seleccionado para los contaminantes estudiados han sido fijados por el Codex Alimentarius y/o la Unión Europea.

En esta Memoria se han estudiado diferentes familias de contaminantes, como son las micotoxinas y los pesticidas, dos de los principales contaminantes presentes en nuestro día a día y que mayor impacto causan en el medioambiente y en la salud humana y animal.

2.6.1.1. Micotoxinas

Las toxinas fúngicas o micotoxinas son compuestos químicos producidos de forma natural (no antropogénicos) en el metabolismo secundario de algunos géneros de hongos.

Existe una amplia variedad de micotoxinas que pueden afectar a la salud humana y animal (como la del ganado), dependiendo del hongo que las produce, y cuya presencia depende de muchos factores como el tipo de alimento, la humedad y la temperatura. Entre ellas, se pueden destacar las aflatoxinas (B1, B2, G1, G2, M1), la ocratoxina A, la patulina y la citrinina.

Estas micotoxinas, que entran en la cadena alimentaria normalmente a través de cultivos contaminados (principalmente cereales), pueden afectar a la salud humana y animal. Algunas de las micotoxinas más importantes desde el punto de vista agrícola conocidas en la actualidad pueden causar diversos efectos adversos como la inducción del cáncer y mutagenicidad, así como problemas en el metabolismo de los estrógenos, problemas gastrointestinales o

problemas en el riñón. En particular, se ha vinculado el desarrollo de cáncer de hígado, el deterioro del crecimiento infantil y toxicosis aguda a las aflatoxinas, así como la aparición de enfermedades renales a la ocratoxina A [138].

Algunas micotoxinas son también inmunodepresoras, reduciendo de esta forma la resistencia a enfermedades infecciosas. Hay micotoxinas que producen estos efectos toxicológicos por exposición a las mismas a largo plazo y otras que presentan, además, efectos agudos (principalmente gastrointestinales).

- **Citrinina**

  La citrinina (**Figura 24**) es una micotoxina producida por varias cepas fúngicas pertenecientes a los géneros *Penicillium*, *Aspergillus* y *Monascus*. Es una conocida hepatonefrotoxina que puede ocasionar daños funcionales y estructurales renales y alteraciones en el metabolismo hepático [139, 140]. El mecanismo de toxicidad de la citrinina no se conoce completamente, ya que no se sabe si la toxicidad de la citrinina y su genotoxicidad son consecuencia del estrés oxidativo o del aumento de la permeabilidad de las membranas mitocondriales.

  La citrinina ha sido encontrada como contaminante en cereales, especias, arroz y productos afines, productos cárnicos fermentados y piensos de animales.

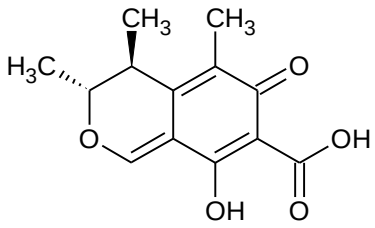

Figura 24. Estructura de la citrinina

En los últimos años se han desarrollado métodos de análisis en diversas matrices. Debido a que presenta fluorescencia nativa, su determinación ha sido posible mediante el empleo de detección fluorescente [141-143]. Además, se han desarrollado métodos basados en immunoensayos [144-146], sensores electroquímicos [147] o cromatografía de líquidos acoplada a espectrometría de masas (HPLC-MS) [148-151].

2.6.1.2. Pesticidas

La Comisión Europea [152] define un pesticida como "*algo que previene, destruye o controla un organismo dañino ('plaga') o enfermedad, o protege las plantas o los productos vegetales durante la producción, el almacenamiento y el transporte*".

El término pesticida incluye, entre otros: herbicidas, fungicidas, insecticidas, acaricidas, nematicidas, molusquicidas, rodenticidas, reguladores del crecimiento, repelentes, etc., entre los que se encuentran los analitos que describimos en esta Memoria.

- **Neonicotinoides**

Los neonicotinoides son una familia de insecticidas que actúan en el sistema nervioso central de los insectos y, con menor toxicidad, en vertebrados. Actúan de modo selectivo e irreversible sobre los receptores nicotínicos de la acetilcolina en las células nerviosas de los insectos, paralizándolos y provocando su muerte [153].

Los neonicotinoides están entre los insecticidas más usados a nivel mundial, pero recientemente el uso de ciertos productos químicos de esta familia está siendo restringido en varios países debido a una posible conexión con el conocido como "*desorden del colapso de colonias apícolas*". La Agencia Europea de Seguridad Alimentaria (EFSA) ha reiterado que la mayoría de los usos de estos productos perjudican a los polinizadores silvestres y las abejas. De hecho, un estudio publicado por la EFSA el 28 de febrero de 2018, actualiza los resultados ya publicados en 2013 después de que la Comisión Europea impusiera el control sobre el uso de estas sustancias.

- **Clotianidina**

La clotianidina (**Figura 25**) es un insecticida que es absorbido por las plantas y luego liberado a través del polen y el néctar. Debido a su uso en control de plagas, el tratamiento de plantas con este insecticida resulta peligroso para los insectos que se alimentan de estos productos de la planta.

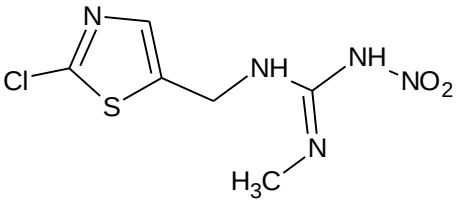

Figura 25. Estructura de la clotianidina

En 2013, la Comunidad Europea publicó un Reglamento que restringía el uso de las sustancias activas insecticidas clotianidina, tiametoxam e imidacloprid y prohibía el uso y la venta de semillas tratadas con fitosanitarios que las contuvieran [154]. Este Reglamento tenía por objetivo la protección de las poblaciones de abejas, de acuerdo a nueva información científica sobre los efectos subletales de los neonicotinoides en las abejas.

Cuando las abejas entran en contacto con este compuesto, éste puede ser transmitido entre ellas dentro de la colmena y sus residuos pueden encontrarse en los productos alimentarios provenientes de las abejas, como la miel [155].

Además, en enero de 2016, el laboratorio de referencia de la Unión Europea para Health of Bees publicó los resultados del primer programa para monitorear la despoblación de colmenas en 17 países europeos. Los datos mostraron una tasa muy variable de mortalidad invernal entre los países entre los años 2012-2014, que van desde el 2.4 hasta el 15.4 %, siendo aún mayor en años anteriores [156]. En general, la situación es más leve en países mediterráneos que en el norte de Europa.

Los métodos de análisis actuales usados para la determinación de clotianidina se basan principalmente en HPLC-MS o HPLC con detección UV [157-160], immnoensayos [161], GC-ECD (cromatografía de gases con detección de captura electrónica) [162] y métodos voltamperométricos [163].

- **Tiametoxam**

El tiametoxam (**Figura 26**) es un insecticida sistémico cuya estructura química lo hace altamente soluble en agua, por lo cual posee una alta movilidad dentro de la planta. El tiametoxam es absorbido rápidamente y transportado a toda la planta donde actúa como un impedimento a la alimentación de insectos sobre la planta. Es activo en el estómago de los insectos y también por contacto directo. En los insectos actúa, al igual que otros neonicotinoides, interfiriendo la transmisión nerviosa entre neuronas al unirse a receptores nicotínicos de acetilcolina. Posee un amplio espectro de actividad como insecticida y un gran efecto residual.

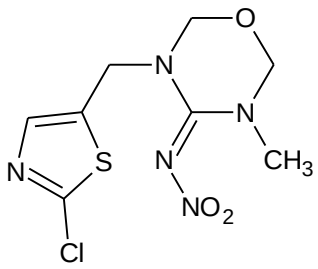

Figura 26. Estructura del tiametoxam

Al igual que la clotianidina, el uso del tiametoxam está restringido por la Unión Europea desde 2013. En la actualidad, los principales métodos de análisis de este insecticida están basados en HPLC-MS [164-167], GC-MS [168, 169] y voltamperometría [170].

- **Nitenpiram**

El nitenpiram actúa como neurotoxina, uniéndose e inhibiendo los receptores nicotínicos de acetilcolina específicos de los insectos, provocando la muerte rápida de estos. Es utilizado en agricultura además de en veterinaria para matar parásitos externos del ganado y de los animales domésticos.

El nitenpiram (**Figura 27**) es utilizado por vía oral en animales domésticos para controlar las pulgas, pero no es capaz de matar los huevos del insecto y no tiene actividad a largo plazo. Por lo tanto, no es eficaz como preventivo de pulgas a largo plazo.

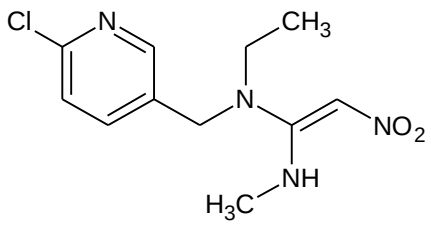

Figura 27. Estructura del nitenpiram

No es uno de los tres insecticidas de la familia de los neonicotinoides que están directamente relacionados con el

"desorden del colapso de colonias apícolas", pero es considerado como uno de los insecticidas más utilizados a nivel mundial. Su uso ha sido restringido en diversos lugares aunque no en países occidentales de la Unión Europea.

Hasta la fecha, los métodos de análisis usados para la determinación del nitenpiram están basados en HPLC-MS [155, 158, 171], GC-ECD [172] y métodos electroquímicos [173, 174].

- **Piraclostrobina**

La piraclostrobina (N-{2-[1-(4-clorofenil)-1H-pirazol-3-iloximetil]fenil}-(N- metoxi)carbamato de metilo) (**Figura 28**) es una estrobilurina de última generación que posee rapidez de acción, eficacia y amplio espectro de control sobre patógenos. Como otras estrobilurinas, es relevante por poseer, además de actividades antifúngicas, distintas actividades biológicas, antivirales y antitumorales. Respecto a su modo de acción, este fungicida actúa a través de la inhibición de la respiración mitocondrial bloqueando la transferencia de electrones dentro de la cadena respiratoria [175].

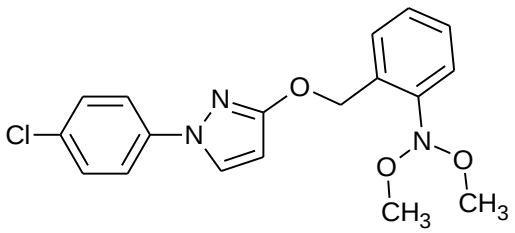

Figura 28. Estructura del piraclostrobina

Se utiliza en una amplia gama de cultivos como cereales, vid, frutas de pepita, cucurbitáceas, tomates y patatas. En la vid es utilizado contra la *Plasmopara viticola*, responsable del *mildiu* o del *oídium*.

Se han desarrollado diversos métodos para la determinación de este analito, principalmente métodos HPLC-MS [176-179] y voltamperométricos [180].

- **Glifosato**

El glifosato (N-fosfonometilglicina), herbicida organofosforado más ampliamente utilizado en todo el mundo, fue introducido por primera vez en el mercado en 1974 [181]. La introducción de cultivos tolerantes a herbicidas genéticamente modificados en 1996 aumentó considerablemente las aplicaciones de este pesticida [181, 182]. Hoy en día, el glifosato (**Figura 29**) se usa para controlar malezas en la agricultura, control de vegetación en áreas no agrícolas y además puede ayudar a la cosecha como desecante de cultivos [182]. Considerado como un herbicida de amplio espectro, actúa interfiriendo en la síntesis de los aminoácidos fenilalanina, tirosina y triptófano. Al igual que otros compuestos organofosforados, sus características principales son su alta toxicidad, su baja estabilidad química y su nula acumulación en los tejidos, característica que lo posiciona en ventaja con respecto a los organoclorados de baja degradabilidad y gran bioacumulación.

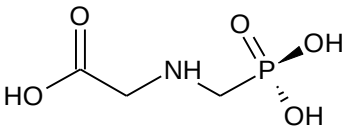

Figura 29. Estructura del glifosato

En los últimos años, el extendido uso del glifosato se ha vuelto alarmante. Aunque la potencial toxicidad del glifosato para los mamíferos es normalmente descrita como de rango bajo, la Agencia Internacional para la Investigación sobre el Cáncer (IARC) evaluó el glifosato como "probablemente cancerígeno para los humanos (Grupo 2A)" en 2015 [183]. Esta evaluación ha generado controversia, ya que ni la Unión Europea [182] ni varios paneles de expertos independientes [184] confirmaron estas conclusiones de la IARC. Sin embargo, debido a las altas cantidades de glifosato utilizadas actualmente, así como su alta solubilidad en agua (12 g L^{-1}), hacen que este herbicida puede propagarse fácilmente y convertirse en un riesgo para el medio ambiente y la salud humana.

Para la determinación del glifosato se han desarrollado métodos de análisis basados en HPLC-MS [185-187] o HPLC-UV a través de una derivatización previa [188, 189]. Además, otros métodos basados en espectrofotometría [190, 191], espectroscopía Raman [192] y voltamperometría [193-195] han sido igualmente utilizados para su análisis.

2.6.2. Compuestos de interés farmacológico y/o biológico

- **β-caroteno**

El β-caroteno (**Figura 30**) es el carotenoide más abundante en la naturaleza y el más importante para la dieta humana. Su estructura fue determinada en el año de 1930 por Paul Karrer, trabajo que le valió el Premio Nobel de Química. Éste describió por primera vez en la historia la estructura de una vitamina o pro-vitamina.

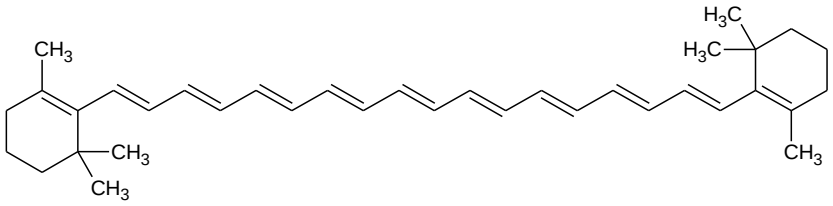

Figura 30. Estructura del β-caroteno

El β-caroteno es un compuesto orgánico fuertemente coloreado que está presente en diversos alimentos, como zanahorias, espinacas, calabazas o frutas como papaya, naranja, mandarina y melocotón. El β-caroteno, al ser una fuente de vitamina A e indispensable para la dieta humana, debe ingerirse mediante la alimentación diaria o bien a través de suplementos alimenticios que lo contengan. Presenta grandes propiedades antioxidantes, ayudando por tanto a neutralizar los radicales libres que dañan los lípidos de las membranas celulares y el material genético. Por ello, es utilizado para tratar diversos trastornos y reducir el riesgo de algunos tipos de cáncer y degeneración ocular relacionada con la edad [196-198].

Se han utilizado diferentes métodos de análisis para la determinación del β-caroteno. Principalmente, son métodos basados en HPLC-UV [199-202] y espectroscopía de infrarrojo cercano o Raman [203-205].

- **Rifaximina y Rifampicina**

La rifampicina y la rifaximina son dos derivados semisintéticos de las rifamicinas. Son los más conocidos y útiles dentro de este grupo de antibióticos. Las rifamicinas se obtienen de la bacteria *Actinomycete*, cuyo papel es la inhibición de la síntesis del ácido ribonucleico en una amplia gama de microbios patógenos. Juegan un papel preponderante como antibióticos en la terapia contra la tuberculosis y en enfermedades de tipo hepático e intestinal, además de actuar en quemaduras, piodermitis, heridas infectadas, impétigo y úlceras varicosas.

La rifampicina (**Figura 31**) tiene acción bactericida y ejerce un potente efecto de esterilización contra los bacilos tuberculosos tanto en localizaciones celulares como extracelulares, por lo que es usado en el tratamiento de la tuberculosis [206, 207]. Además, debido a su demostrado efecto inhibidor sobre el crecimiento de una variedad de células cancerosas humanas, se considera que tiene potentes propiedades antiangiogénicas, especialmente sobre tumores hepatobiliares.

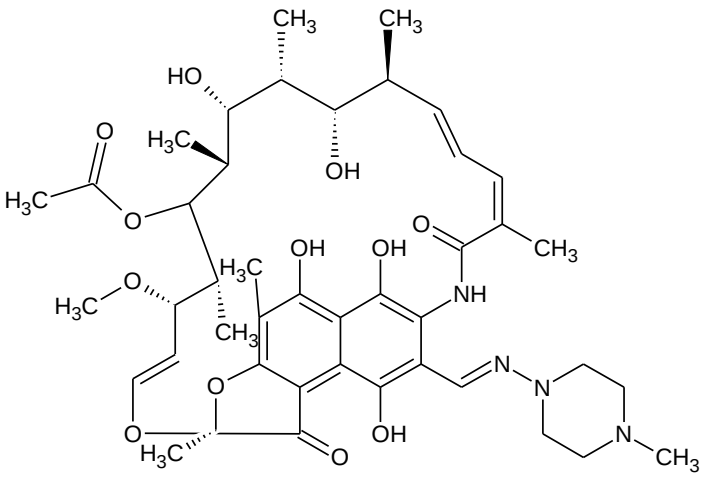

Figura 31. Estructura de la rifampicina

La rifaximina (**Figura 32**) se emplea en medicina para el tratamiento de enfermedades intestinales como la afectación de enterobacterias, incluida la encefalopatía hepática [208] e infecciones intestinales tales como el síndrome del intestino irritable, colitis ulcerosa, enfermedad diverticular, diverticulitis aguda y la colitis pseudomembranosa.

Su mecanismo de acción consiste en inhibir la síntesis del ARN bacteriano, dificultando de esta forma la multiplicación del agente infeccioso.

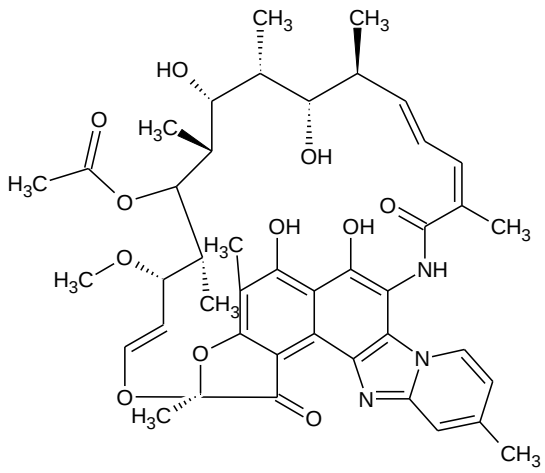

Figura 32. Estructura de la rifaximina

Los métodos de análisis descritos hasta la fecha para la determinación de estas rifamicinas están basados en espectrofotometría [209-211], HPCL-MS, HPLC-UV y HPLC con detector de radionucleidos [212-214], voltamperometría [215] y espectroscopía Raman [216].

- **Tioles o mercaptanos**

Los tioles o mercaptanos (nombre que se les daba tradicionalmente) son compuestos que presentan un grupo funcional común: el grupo tiol, formado por un átomo de azufre y un átomo de hidrógeno (-SH). El grupo tiol es el análogo del azufre al grupo hidroxilo (-OH) que se encuentran en los alcoholes. Debido a que el azufre y el oxígeno pertenecen al mismo grupo de la tabla periódica, comparten algunas propiedades de enlace similares.

La elección de un grupo de analitos que presentasen un grupo tiol se realizó de acuerdo a la unión que se producía entre ellos, las AuNPs y los QDs, para su posterior estudio del proceso FRET. Se escogieron un total de cinco analitos que presentaban variadas estructuras y usos, pero con el grupo tiol en común. Los tioles seleccionados fueron:

- **Captopril**:

  El captopril (**Figura 33**) es un inhibidor de la enzima convertidora de angiotensina que actúa bloqueando la proteína peptidasa del centro activo de la misma. Es usado en medicina para tratar la hipertensión, además de ayudar a retrasar el mayor debilitamiento del corazón en algunos pacientes después de insuficiencias cardiacas, para tratar fallos congestivos del corazón y para el tratamiento de la nefropatía diabética en pacientes afectados.

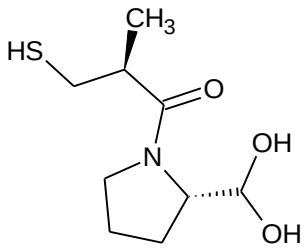

Figura 33. Estructura del captopril

- **Glutationa**:

  La glutationa (**Figura 34**) es un tripéptido no proteínico constituido por tres aminoácidos: glutamato, cisteína y glicina. Es el principal antioxidante de las células y su función principal es proteger las células y las mitocondrias del cuerpo humano del daño oxidativo y

peroxidación. Es esencial para que el sistema inmunológico pueda ejercer todo su potencial y desempeña un papel fundamental en numerosas reacciones metabólicas y bioquímicas tales como la síntesis y reparación del ADN, la síntesis de proteínas, la síntesis de prostaglandinas, el transporte de aminoácidos y la activación de enzimas.

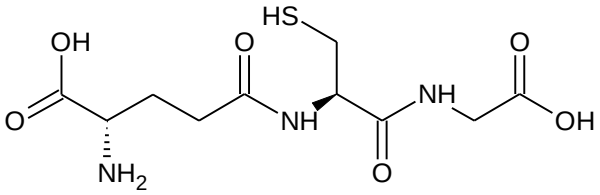

Figura 34. Estructura de la glutationa

❖ **L-cisteína**:

La L-cisteína (**Figura 35**) es un aminoácido no esencial (ya que lo pueden sintetizar los seres humanos por sí mismos), componente importante de la piel, el cabello y las uñas. Se trata de un nutriente que actúa como antioxidante, protegiendo a nuestro organismo contra el daño por radiación y protegiendo a su vez tanto al hígado como al cerebro de daños causados por determinadas toxinas. Su uso está destinado principalmente para retrasar el envejecimiento, para controlar la salud del sistema inmune y del cabello.

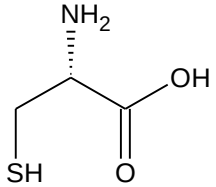

Figura 35. Estructura de la L-cisteína

❖ **Ácido mercaptosuccínico o tiomálico**:

El ácido mercaptosuccínico (**Figura 36**) es un ácido dicarboxílico utilizado en la investigación bioquímica, en la elaboración de antídotos de metales pesados y en la industria del caucho.

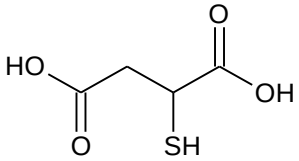

Figura 36. Estructura del ácido mercaptosuccínico

❖ **Sodio 2-mercaptoetanosulfonato**:

El 2-mercaptoetanosulfonato sódico (**Figura 37**) es un agente uroprotector soluble en agua. Reduce la incidencia de cistitis hemorrágica y hematuria en la quimioterapia contra el cáncer.

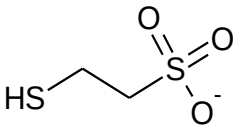

Figura 37. Estructura del sodio 2-mercaptoetanosulfonato

Los tioles, en general, han sido determinados mediante una gran variedad de métodos de análisis, basados en HPLC-MS [217-220] y fluorescencia [221-224], entre otros.

Objetivos

3. Objetivos

El objetivo general de esta Memoria de Investigación es el avance en el desarrollo y la aplicación de nuevos enfoques y estrategias en los sistemas multiconmutados en flujo que demuestren la versatilidad, aplicabilidad y el alto potencial de este tipo de sistemas analíticos, gracias al uso de optosensores en flujo y de nanomateriales que funcionan como nanosensores químicos en la mejora de dichos sistemas.

Se prestará especial atención a los siguientes aspectos:

- Implementación de la multiconmutación en el campo de los optosensores espectroscópicos, con el objeto de aportar una mayor automatización, reproducibilidad y menor consumo de reactivos y muestra en dichos sistemas.

- Posibilidad de determinar analitos no fluorescentes (o cuya fluorescencia es débil) mediante el uso de fluorescencia inducida fotoquímicamente (PIF). Se ha podido así desarrollar métodos con elevada velocidad de reacción, más sensibles y más selectivos.

- Empleo de nanopartículas que funcionan como nanosensores químicos, proporcionando sistemas analíticos de última generación sensibles y selectivos, con grandes perspectivas en sus campos de aplicación.

- Aplicación de los sensores desarrollados a diferentes matrices que abarquen diversos campos de interés como son el agroalimentario y el farmacológico (análisis de contaminantes y

principios activos, respectivamente). Muchas de las matrices con las que se trabaja son de alta complejidad, por lo que, en cada caso, se ha llevado a cabo el tratamiento de muestra más adecuado.

Se pretende por tanto, presentar nuevos enfoques para el desarrollo de métodos analíticos sencillos, que ofrezcan características analíticas atractivas en términos de sensibilidad, selectividad, rapidez, bajo coste y versatilidad, mostrando su aplicabilidad a muestras reales en los campos agroalimentario y farmacológico que puedan ser una alternativa real a los bien establecidos métodos cromatográficos.

La ejecución de esta Memoria se ha realizado gracias a un contrato predoctoral concedido por el Ministerio de Educación, Cultura y Deporte a través de sus "*Ayudas para la formación de profesorado universitario (FPU)*" (FPU2013/03869).

Parte del trabajo de esta Memoria se enmarca además dentro del proyecto de investigación financiado por el Ministerio de Economía, Industria y Competitividad *"Última generación de sensores luminiscentes multiconmutados aplicados al análisis de contaminantes en alimentos"* (CTQ2016-75011-R).

Resultados y discusión

4. Resultados y discusión

Los estudios desarrollados a lo largo de estos años han dado lugar a una Tesis Doctoral que abarca fundamentalmente dos ámbitos de aplicación: (1) optosensores en flujo continuo y (2) sistemas analíticos automáticos que hacen uso de nanomateriales para la mejora de sistemas analíticos en flujo. En ambos casos se lleva a cabo detección luminiscente.

Se discuten a continuación los estudios que se han llevado a cabo para la elaboración de esta Memoria, estando todos ellos publicados o en proceso de publicación en revistas internacionales recogidas en el Journal Citation Report.

PARTE I. DESARROLLO DE METODOLOGÍAS ANALÍTICAS QUE HACEN USO DE SENSORES EN FASE SÓLIDA

1. Optosensor fluorimétrico multiconmutado para la determinación de citrinina en arroz y suplementos de levadura roja de arroz / Multi-commutated fluorometric optosensor for the determination of citrinin in rice and red yeast rice supplements.

2. Determinación de clotianidina en productos alimenticios mediante el uso de un sistema automatizado con detección por fluorescencia inducida fotoquímicamente / Determination of clothianidin in food products by using an automated system with photochemically induced fluorescence detection.

3. Desarrollo de un sensor de fluorescencia inducida fotoquímicamente sensible y semiautomático para la determinación de

tiametoxam en vegetales / Development of an semi-automatic and sensitive photochemically induced fluorescence sensor for the determination of thiamethoxam in vegetables.

4. Optosensor en flujo a través de fluorescencia inducida fotoquímicamente para el cribado de residuos de nitenpiram en vegetales de familia crucífera / A photochemically induced fluorescence based flow-through optosensor for screening of nitenpyram residues in cruciferous vegetables.

5. Sensor sensible que hace uso de fluorescencia inducida fotoquímicamente para la determinación de nitenpiram y piraclostrobina en muestras de uvas y vino / Sensitive photochemically induced fluorescence sensor for the determination of nitenpyram and pyraclostrobin in grapes and wines.

PARTE II. DESARROLLO DE METODOLOGÍAS ANALÍTICAS QUE HACEN USO DE NANOMATERIALES

6. Determinación automatizada de rifamicinas hacienda uso de quantum dots de MPA-CdTe / Automated determination of rifamycins making use of MPA–CdTe quantum dots.

7. Nuevas perspectivas del uso de quantum dots en el campo agroalimentario: Determinación de β- caroteno en zumos de fruta tropicales y suplementos alimenticios / New perspectives of quantum dots in the food field: determination of β-carotene in tropical fruit juices and food supplements.

8. Sistema multiconmutado en flujo para la determinación de glifosato basado en el efecto de extinción de la fluorecencia de los quantum dots de CdTe / Multicommutated flow system for the determination of glyphosate based on its quenching effect on CdTe-quantum dots fluorescence.

9. Aprovechamiento del potencial de la transferencia de energía de resonancia de fluorescencia (FRET) entre los puntos cuánticos CdTe y las nanopartículas de Au para la determinación de tioles bioactivos / Exploiting the fluorescence resonance energy transfer (FRET) between CdTe quantum dots and Au nanoparticles for the determination of bioactive thiols.

Parte I

Multi-commutated fluorometric optosensor for the determination of citrinin in rice and red yeast rice supplements

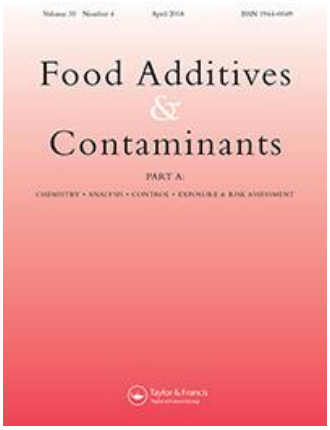

1. "Multi-commutated fluorometric optosensor for the determination of citrinin in rice and red yeast rice supplements"

J. Jiménez-López, E. J. Llorent-Martínez, P. Ortega-Barrales, A. Ruiz-Medina*

Publicado en Food Additives & Contaminants: Part A, en Septiembre de 2014, volumen 31:10, páginas 1744-1750.

Resumen

La citrinina es un metabolito secundario tóxico, que se aísla del *Penicillium citrinum*, aunque también puede ser producido por otras especies de *Penicillium* y *Aspergillus*. Presenta propiedades altamente tóxicas, mutagénicas, teratogénicas y cancerígenas y se encuentra a menudo en cultivos, vegetales y frutas. Cuando se desarrolló este método de análisis para la determinación de la citrinina, no existía una legislación específica sobre los niveles máximos permitidos para ésta, por lo que no existía ningún método analítico oficial para su determinación.

Se desarrolló un optosensor en flujo continuo con detección luminiscente usando Sephadex SPC-25 como fase sólida. Se utilizó el análisis por inyección de flujo multiconmutado como sistema automatizado de análisis. De esta manera, se minimizó la generación de

residuos y la intervención humana en el análisis, que son aspectos críticos cuando se trata de compuestos altamente tóxicos como la citrinina. Las longitudes de onda de excitación / emisión óptimas fueron 330/494 nm y se obtuvoun rango dinámico lineal de 35- 900 ng mL^{-1}. Se obtuvo un límite de detección de 10.5 ng mL^{-1} y desviaciones estándar relativas inferiores al 3%. El optosensor desarrollado se aplicó a la determinación de citrinina en arroz y suplementos dietéticos que contenían arroz de levadura roja.

Las principales ventajas del método propuesto consistían en una alta frecuencia de muestreo, una baja generación de residuos y la gran versatilidad de los sistemas multiconmutados, lo que permitiría adaptar el método en caso necesario para otros compuestos o para incluir un proceso adicional on-line. Por lo tanto, este método representa una alternativa para la determinación de citrinina en matrices alimentarias para su uso en laboratorios de control de calidad, ya que se trata de una micotoxina de gran actualidad debido a su toxicidad.

1. "Multi-commutated fluorometric optosensor for the determination of citrinin in rice and red yeast rice supplements"

Abstract

Citrinin is a toxic secondary metabolite, first isolated from *Penicillium citrinum*, although is also produced by other species of *Penicillium* and *Aspergillus*. It presents highly toxic, mutagenic, teratogenic and carcinogenic properties, and is often found in crops, vegetables, and fruits. To our knowledge, there is no specific legislation on maximum levels permitted for citrinin, so no official analytical method is currently available for its determination.

In our laboratory, we have developed a fluorometric flow-through optosensor using Sephadex SPC-25 as solid support. Multicommutated Flow Injection Analysis was used for the construction of the manifold and for the handling of solutions. In this way, we minimized wastes generation and human intervention, critical aspects when dealing with highly toxic compounds such as citrinin. The optimum excitation/emission wavelengths were set at 330/494 nm/nm, and the calibration curve was linear in the concentration range from 35 to 900 ng mL^{-1}. A detection limit of 10.5 ng mL^{-1} and RSDs lower than 3% were obtained. The developed optosensor was applied to the determination of citrinin in rice and dietary supplements containing red yeast rice.

Keywords: Mycotoxin; solid-phase spectroscopy; multicommutation; food; luminescence; rice

Introduction

Mycotoxins are a group of structurally diverse secondary metabolites produced by various fungal species. They are naturally occurring contaminants whose presence in food- and feedstuffs cannot be completely avoided. The ingestion of these compounds may cause serious health problems to humans, including liver, kidney or nervous system damage, and carcinogenesis (Bennett & Klich 2003; Xu et al. 2006). As a result, it is important to establish maximum permitted levels of mycotoxins in different foods and feeds, and to develop reliable analytical methods for quality control purposes.

The mycotoxin citrinin (CIT) is a toxic secondary metabolite, first isolated from filamentous fungus *Penicillium citrinum*, but also produced by other species of *Penicillium*, *Aspergillus*, and *Monascus* (Xu et al. 2006). It is a known hepato-nephrotoxin that causes functional and structural kidney damage and alterations in liver metabolism (Nigović et al. 2013; Xu et al. 2006). CIT has been found to contaminate breakfast cereals (Molinié et al. 2005), spices (Yogendrarajah et al. 2013), rice (Nguyen et al. 2007) and related products (Li et al. 2012), fermented meat products (Markov et al. 2013), and feedstuffs (Kononenko & Burkin 2008), among others. At the present, there is not any legislation on CIT maximum permitted level, mainly due to the lack of an official analytical method and its instability in food as a result of structural changes that CIT suffers by

its chelating ability, the effect of pH and the effect of temperature (Arévalo et al. 2011).

Different analytical methods have been developed for the determination of CIT in a variety of samples in the last few years. Most of them are based on immunoassays (Abramson et al. 1996; Arévalo et al. 2011; Kononenko & Burkin 2008; Li et al. 2012), or make use of HPLC with fluorescence (Abramson et al. 1999; Dohnal et al. 2010; Markov et al. 2013; Mornar et al. 2013) or mass spectrometry (Arroyo-Manzanares et al. 2013; Mornar et al. 2013; Yogendrarajah et al. 2013) detections. Here we propose the use of flow-through optosensing as an alternative for the determination of CIT in rice and rice-related products. This methodology consists in the implementation of solid phase spectroscopy (SPS) in flow analysis. A solid support is used to retain and pre-concentrate the target species in the detection area, followed by spectroscopic measurements on the same solid-phase, being all the steps carried out on-line. In this way, sensitivity and selectivity are highly increased when compared to the determination in homogeneous solution (Llorent-Martínez et al. 2011).

Among the different flow methods of analysis currently available, we have made used of Multicommutated Flow Injection Analysis (MCFIA), due to its favourable characteristics such as its simplicity, versatility, low consumption of reagents, and low-cost (Llorent-Martínez et al. 2010). In general, multicommutation refers to the use of solenoid valves automatically controlled by appropriate software, being the valves individually switched on/off by means of an electric pulse. The potentiality of the implementation of SPS in MCFIA has been previously demonstrated with applications in clinical and food

analysis (Llorent-Martínez et al. 2007; Llorent-Martínez et al. 2009; Llorent-Martínez et al. 2005).

In this paper, the fluorometric quantitation of CIT has been carried out using two different extraction procedures: liquid-liquid extraction (LLE) and QuEChERS. The multicommutated optosensor was applied to the quantitation of the analyte in rice and supplements containing red yeast rice. This yeast rice, traditional in China, is the fermented product from steamed rice by *Monascus purpureus,* and has been served as a natural dietary supplement for thousands of years in some Asian countries. Efforts to decrease CIT content should be made to avoid contamination in rice, red yeast rice, and related products. The proposed system is a rapid and easy way to evaluate the concentration of this analyte in the selected samples.

Materials and methods

Instrumentation

Luminescence measurements were performed with a Cary-Eclipse Luminescence Spectrometer (Varian Inc., Mulgrave, Australia). The spectrometer was connected to a computer with a Cary-Eclipse (Varian) software package for data collection and treatment.

A Hellma flow cell 176.752-QS (25 μL of inner volume and a light path length of 1.5 mm) was used. The cell was filled with Sephadex SP C-25 solid phase microbeads, and was blocked at the outlet with glass wool to prevent displacement of the support particles.

The manifold is illustrated in **Fig. 1**. A four-channel Gilson Minipuls-3 (Villiers Le Bel, France) peristaltic pump with rate selector and methanol-resistant pump tubes type Solvflex (Elkay Products,

Shrewsbury, MA, USA) were used. An electronic interface based on ULN 2803 integrate circuit was employed to generate the electric potential (12V) and current (100 mA) required to control the four 161T031 NResearch three-way solenoid valves (Neptune Research, MA, USA). The software for controlling the system was written in Java. Flow lines of 0.8 mm internal diameter PTFE tubing and methacrylate connections were also used.

The level of the resin packed in the flow cell had to be carefully selected in order to ensure that the upper part of the resin was just in the light path. In this way, the best sensitivity was obtained. Before starting the measuring process, the carrier solution was passed through the sensing zone for five minutes to condition it.

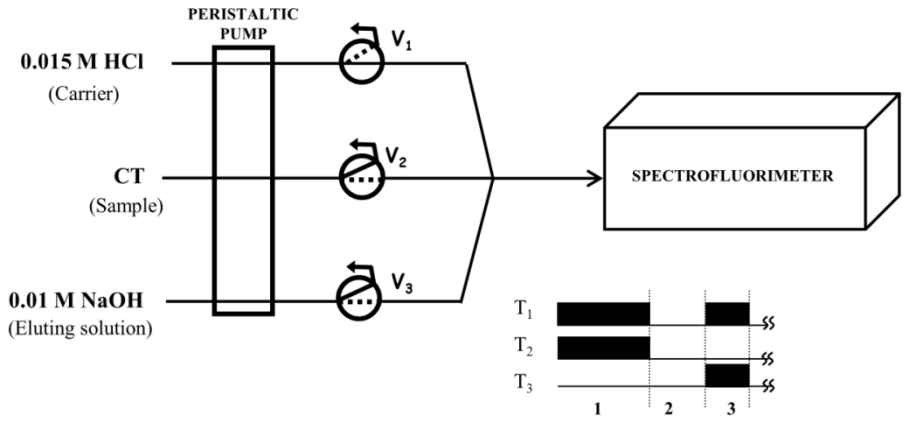

Fig. 1. Upper part: manifold, in which V_n=3-way solenoid valve n. Bottom part: valves scheme. T_n corresponds to the time procedure of V_n. The filled rectangles above the time lines for each valve indicate the times at which the corresponding valve was switched on. The steps were as follows: 1) sample introduction; 2) CIT signal recording; 3) CIT elution.

A Selecta Ultrasons ultrasonic bath (Barcelona, Spain), a Crison Model 2012 pH-meter with a glass/saturated calomel combination electrode (Barcelona, Spain), and a Selecta Mixtasel-BL (Barcelona, Spain) centrifuge were also used.

Reagents and solutions

CIT (≥ 98%) was purchased from Acros Organics (Thermo Fisher Scientific, Madrid, Spain). Stock solution of 100 μg mL^{-1} CIT was prepared in methanol (MeOH; Sigma, Madrid, Spain). It was stable for at least 1 month when stored in the freezer at -18ºC. Working solutions were prepared daily by suitable dilution with deionized water.

MeOH, ethanol, acetonitrile, acetic acid, hydrochloric acid (HCl), anhydrous sodium acetate, sodium hydroxide (NaOH), and anhydrous magnesium sulphate ($MgSO_4$) were obtained from Sigma. Siliceous earth purified and calcined was purchased from Panreac (Barcelona, Spain). All of them were analytical reagent grade.

Sephadex-QAE A-25, Sephadex-CM C-25, and Sephadex-SP C-25 resins, all of them 40–120 μm average particle size, were bought from Sigma. C_{18} bonded phase silica gel beads, 55-105 μm average particle size, were obtained from Waters (Milford, USA). Chelex-100 in sodium form, 200-400 mesh, was purchased from Fluka (Buchs, Switzerland).

Sample treatment

We analysed CIT in four rice samples (white rice and brown rice), and three dietary supplements (two in tablets and one in capsules presentation) containing red yeast rice. All samples were obtained from local markets or from a community pharmacy, and were thoroughly ground and homogenized before the extraction. In the case of tables, ten tablets were previously weighed, and the average weight of one tablet was analyzed. Likewise, the content of 10 capsules was pooled, and the average weight of one capsule was used for CIT quantitation. Two different extraction procedures were tested and its comparison was performed. The first one consisted in a conventional LLE, similar to the procedure developed by Nigović et al. (Nigović et al. 2013): 2 g of sample were weighed in a PTFE centrifuge tube and 20 mL of MeOH:H_2O (80:20, v:v) were added. The screw cap was closed and the tube was vigorously shaken for 5 min. The tube was left in an ultrasonic bath for 1 h (room temperature). Then, it was centrifuged for 5 min at 3000 rpm and the supernatant was collected.

The second extraction procedure was a modified QuEChERS procedure (Anastassiades et al. 2003). The QuEChERS extraction method was designed for samples with high moisture percentage, and it has to be adapted to dry samples, like rice, usually reducing sample weight and/or adding water. In this case, 10 g of sample were weighed in a 50 mL PTFE centrifuge tube and 20 mL of 1% (v:v) acetic acid in acetonitrile were added. The screw cap was closed and the tube was centrifuged at 2000 rpm for 10 min. Then, 0.85 g of anhydrous sodium acetate and 1.5 g of anhydrous $MgSO_4$ were added, repeating the centrifugation at 2000 rpm for 8 min. 10 mL of the supernatant (acetonitrile phase) were taken with a pipette and transferred to a 15

mL centrifuge tube. After adding 300 mg anhydrous $MgSO_4$ and 200 mg siliceous earth purified and calcined, the tube was energetically shaken for 1 min by hand and centrifuged again for 8 min at 3000 rpm. Finally, the supernatant was collected.

For both sample treatments, suitable dilutions of the supernatants were made with 0.015 mol L^{-1} HCl solution before recording the analytical signal.

General procedure

The manifold and flow procedure are shown in Figure 1. The MCFIA system consisted of a peristaltic pump and a set of 3 three-way solenoid valves, automatically controlled by appropriate software. Each valve can adopt two positions, "on" and "off", being the whole system assimilated to an electronic circuit with a variable number of active nodes.

A flow-rate of 1.7 mL min^{-1} was used in all experiments. In the initial status, all valves were switched off and the carrier (0.015 mol L^{-1} HCl) was flowing through the flow-through cell while all other solutions were being recycled to their respective vessels. The sample was introduced by simultaneously switching on valves V_1 and V_2 for 85 s (step 1). CIT was carried towards the flow-through cell by the carrier solution, and its analytical signal was recorded (step 2). Then, CIT was completely eluted from the solid support using an eluting solution of 0.01 mol L^{-1} NaOH; this was achieved by switching on valves V_1 and V_3 for 40 s (step 3). In this way, the system remained ready for the next sample insertion.

Calibration standards and samples were analyzed by triplicate. Luminescence measurements were made at excitation/emission wavelengths of 330/494 nm/nm. The analytical signal was expressed as peak height mean values.

Results and discussion

Extraction Procedure Optimization

Many approaches have been utilised to purify samples containing mycotoxins. Both LLE and solid-phase extraction (SPE) are the typically applied clean-up methods. SPE has commonly been used because of its superior precision and recoveries, with C_8, polyamide columns, molecularly imprinted polymers, etc. In the proposed method, to obtain a quantitative extraction yield from the selected complex samples, two different extraction procedures were evaluated: LLE and QuEChERS (this last one as alternative to SPE). To optimize both extraction processes, a representative specimen of each sample type was used to get better insight.

When LLE was evaluated, organic solvents of different polarities (MeOH, ethanol, and acetonitrile) were used to assess their extraction efficiency. As the best recoveries were obtained using MeOH, further investigations were performed using this solvent with different proportions of deionized water (50, 40, 30, 20, and 10%). The use of 80% (v:v) MeOH provided the maximum CIT recoveries. In addition, as an ideal extraction procedure should yield the highest amount of the analyte in the shortest possible time, the influence of the extraction time in the range from 15 to 90 min was investigated. The maximum amount of CIT was extracted from all sample types using 60

min, and further increases of the extraction time did not increase the extraction efficacy. Finally, heat is usually used to accelerate the extraction process and to obtain higher analyte recoveries; however, to avoid the degradation of CIT, the extraction procedure was performed only at room temperature.

QuEChERS, used as an alternative second extraction procedure, presents some advantages, such as its simplicity, minimum steps, and effectiveness for cleaning-up complex samples. It involves two steps: the first one is an extraction step based on partitioning via salting-out extraction involving the equilibrium between an aqueous and an organic layer, and the second one is a dispersive SPE step that involves further clean-up using combinations of $MgSO_4$ and different sorbents. In this case, siliceous earth purified and calcined has been selected as sorbent to remove interfering substances as alternative to C_{18} or primary and secondary amine (PSA), used in other cases.

Spectral characteristics and solid support

The structure of CIT is shown in Figure 2. We tested its potential retention on three different types of solid supports: a) non-ionic C_{18} silica gel beads; b) anion-exchanger Sephadex-QAE A-25; c) cation-exchangers Sephadex-SP C-25, Sephadex-C CM-25, and Chelex-100. Experiments with all solid supports were performed in the pH range of 1-12. It was observed that the best analytical signal was obtained with the cation-exchanger solid supports using acidic medium. Of these, SPC-25 resin was selected for further experiments, due to the highest analytical signal achieved. The spectral features of CIT were

recorded with the analyte retained on the solid support, being the maxima excitation/emission wavelengths 330/494 nm/nm. Comparing spectra on beads and homogeneous solution (331/500 nm/nm), working in the same conditions and in the same flow cell, a hypsochromic shift in both maxima excitation and emission wavelengths was found. This can be attributed to the modification of the surrounding environment of the analyte on the solid phase with respect to the solution medium.

In addition, as a result of the retention of CIT on the sensing support, the obtained signal was 7 times higher than that obtained in aqueous solution, as the result of the preconcentration of the analyte on the active solid support in the detection area of the spectrofluorimeter.

Instrumental variables

Luminescence measurements carried out in solid-phase media are usually affected by background signal levels higher than those ones found in homogeneous solution, obviously due to the presence of the solid support in the irradiated zone. Therefore, instrumental parameters have to be carefully investigated in order to achieve the best possible signal-to-background ratio. For this reason, the influence of the voltage of the photomultiplier tube (400-800 V) and the instrument excitation and emission slit widths (5-20 nm) on the analytical signal had to be studied. The photomultiplier tube voltage was set at 620 V and the excitation/emission slit widths were fixed at 10/10 nm/nm.

Chemical variables

The first variable under study was the pH of the sample solution. The maximum analytical signal was obtained for a pH value in the range 1.5-2.5, in which the analyte could present positive charge and be retained on the cation-exchanger resin. This is in accordance with the pK_a value of CIT, 2.3. Higher pH values produced a decrease in the analytical signal because the analyte was not properly retained on the solid support, whereas lower pH values decreased the signal due to the high ionic strength of the solution, which caused a slight desorption of CIT from the solid support microbeads. Due to the relatively high volume of sample introduced in the system, the carrier solution was not enough to provide the required acidic medium to the sample solution, so both sample and carrier solutions were adjusted at a pH value of 1.8. Hence, a carrier solution of 0.015 mol L^{-1} HCl was selected, and all dilutions of sample solution were also carried out with 0.015 mol L^{-1} HCl.

After CIT was retained on the solid support microbeads and its analytical signal was recorded, it was partially eluted by the carrier solution, but not completely. An increase in the ionic strength of the carrier solution was useful for the elution of CIT. However, overpressures appeared in the system due to the compaction of the solid support, and the analytical signal was also lower. Hence, an eluting solution (0.01 mol L^{-1} NaOH) was used after the recording of the analytical signal. In this way, CIT was deprotonated and desorbed from the solid support, remaining the system ready for the next sample insertion again.

Flow variables

The sample introduction time and the flow-rate of the peristaltic pump were the studied variables in this section. The flow-rate was studied from 1.0 up to 2.0 ml min^{-1}. When increasing the flow-rate, the sample frequency was also increased. As a result, the highest possible flow-rate was selected. For flow-rates higher than 1.7 ml min^{-1} a lower repeatability was observed and overpressures on the solid support in the flow cell were produced, so 1.7 ml min^{-1} was chosen as the optimum flow rate.

Using the optimized flow-rate, the sample introduction time was studied ranging from 15 to 110 s (see **Fig. 2**). When increasing the sampling time, the signal increased due to a higher amount of analyte being introduced into the flow system, so the amount of analyte sorbed on the solid support is higher. Hence, sensitivity was improved, although the sampling frequency diminished. The analytical signal increased up to 85 s and then remained constant, so 85 s was selected as the optimum sample time.

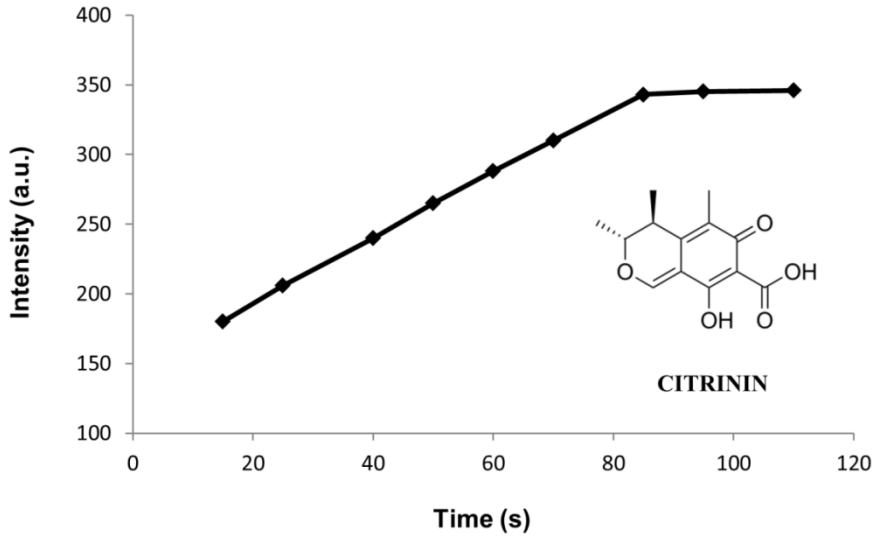

Fig. 2. Effect of the sample insertion time on the analytical signal. The study was performed with a standard solution of 400 ng mL^{-1} CIT.

Analytical parameters

The analytical parameters of the systems were studied using the optimized working conditions previously discussed. The data were fitted by standard least-squares treatment (univariate method) and the calibration is shown in **Table 1**. The limit of detection was estimated as the CIT concentration that produced an analytical signal equal to three times the standard deviation of background luminescence. The repeatability was studied at two different levels (150 and 750 ng mL^{-1} of CIT); it was established for ten independent analyses of CIT standard solutions containing.

Table 1. Analytical parameters.

Parameter	
Linear dynamic range / ng mL^{-1}	35-900
Calibration Graph	
Intercept	15.64
Slope (mL ng^{-1})	0.8441
Correlation coefficient	0.9950
Detection limit / ng mL^{-1}	10.5
Quantitation limit / ng mL^{-1}	35
Intra-day RSD (%, n=10)	
150 ng mL^{-1}	1.5
750 ng mL^{-1}	1.8
Excitation/emission slits (nm/nm)	10/10
Photomultiplier tube voltage (V)	620 V
Sampling frequency (h^{-1})	18

The ruggedness and robustness of the system were also studied. The first one was assessed by comparison of the intra- and inter-day assay results undertaken by two analysts. The RSD values (%) for intra- and inter-day assays did not exceed 4 and 7%, respectively, indicating the ruggedness of the sensor. In addition, the robustness was

investigated under a variety of conditions such as small changes in sample and carrier solutions (0.014-0.016 mol L^{-1} HCl), flow-rate (1.6-1.8 mL min^{-1}), and excitation/emission wavelengths (± 2 nm). CIT recoveries were in the 95.0-105.0 % range in all cases (considering 100% the value obtained under the optimum conditions), therefore demonstrating the robustness of the proposed system.

Applications

The proposed method was applied to the determination of CIT in real samples. In all cases, both LLE and QuEChERS extraction procedures were used, and the results compared. Considering that CIT concentration was below the detection limit of the method in all the rice samples and dietary supplements, we performed recovery experiments, spiking each sample at three different CIT concentration levels. CIT concentration was determined using the previously indicated procedure. We decided to perform recovery studies over the selected samples at levels in the range 20-150 μg g^{-1} (CIT is not regulated). The results are shown in **Tables 2 & 3**.

Table 2. Recovery experiments in rice.

Sample	LLE		QuEChERS	
	Added (μg g^{-1})	[a]Recovery ± RSD (%)	Added (μg g^{-1})	[a]Recovery ± RSD (%)
White rice 1	20	101 ± 2	5	107 ± 1
	40	102 ± 1	10	108 ± 1
	80	98 ± 1	20	104 ± 2

White rice 2	50	96 ± 2	15	107 ± 1
	100	98 ± 2	25	103 ± 1
	150	97 ± 1	50	104 ± 2
Brown rice 1	20	98 ± 1	5	105 ± 2
	40	95 ± 1	10	105 ± 1
	80	99 ± 2	20	102 ± 2
Brown rice 2	50	97 ± 2	15	107 ± 2
	100	101 ± 2	25	104 ± 1
	150	97 ± 1	50	102 ± 2

[a] n=3

Table 3. Recovery experiments in dietary supplements.

Sample	LLE		QuEChERS	
	Added ($\mu g\ g^{-1}$)	[a]Recovery ± RSD (%)	Added ($\mu g\ g^{-1}$)	[a]Recovery ± RSD (%)
Supplement 1 (*Tablets*)[a]	20	97 ± 2	5	62 ± 1
	40	101 ± 2	10	65 ± 1
	80	97 ± 1	20	64 ± 2
Supplement 2 (*Tablets*)[a]	50	98 ± 1	15	68 ± 1
	100	103 ± 2	25	66 ± 2
	150	97 ± 1	50	65 ± 2
Supplement 2 (*Capsules*)[a]	50	98 ± 1	5	67 ± 2
	100	102 ± 2	10	67 ± 1
	150	102 ± 2	20	65 ± 2

[a] 600 mg red yeast rice per tablet/capsule.

For the analysis of rice samples (white and brown types), satisfactory recoveries were obtained with both extraction procedures, observing similar results in terms of recovery percentages (95-108%) and relative standard deviations (lower than 3% in all cases). However, a higher dilution was required when using the QuEChERS extraction procedure in order to eliminate the signal of the blank solution. On the other hand, different results were observed when determining CIT in dietary supplements. In this case, good percentage recoveries were obtained using LLE, but recoveries lower than 70% were obtained with the QuEChERS method.

To summon up, QuEChERS procedure could be applied only to rice samples while LLE procedure was satisfactory applied to rice and dietary supplements. In both cases the sensitivity obtained with the proposed method was high enough to allow determining CIT in rice and supplements containing red yeast rice, so demonstrating that this analytical method fulfills the requirements for its application in quality control analyses.

Conclusions

Standardized manufacturing practices should be established for rice or red rice dietary supplements in order to ensure efficiency and safety of these products, equivalence of active ingredient content in preparations being sold to the public, and to limit the production of unwanted by-products of fermentation such as CIT. Usually chromatographic techniques are used for the quantitation of CIT in food samples. In this work we present a flow-through optosensor with fluorescence detection as an interesting alternative. Two sample

treatments were tested, LLE and QuEChERS, and it was observed that LLE presented superior advantages in terms of simplicity and obtained recoveries. Considering the high sample throughput, low wastes generation, and versatility of multicommutated systems, in our opinion the proposed system could be useful for the analysis of CIT in rice and rice-derived products.

References

Abramson, D., Usleber, E., & Märtlbauer, E. 1996. Determination of Citrinin in Barley by Indirect and Direct Enzyme Immunoassay. J AOAC Int. 79:1325-1329.

Abramson, D., Usleber, E., & Märtlbauer, E. 1999. Rapid determination of citrinin in corn by fluorescence liquid chromatography and enzyme immunoassay. J AOAC Int. 82:1353-1356.

Anastassiades, M., Lehotay, S. J., Štajnbaher, D., & Schenck, F. J. 2003. Fast and easy multiresidue method employing acetonitrile extraction/partitioning and "dispersive solid-phase extraction" for the determination of pesticide residues in produce. J AOAC Int. 86:412-431.

Arévalo, F. J., Granero, A. M., Fernández, H., Raba, J., & Zón, M. A. 2011. Citrinin (CIT) determination in rice samples using a micro fluidic electrochemical immunosensor. Talanta. 83:966-973.

Arroyo-Manzanares, N., Huertas-Pérez, J. F., Gámiz-Gracia, L., & García-Campaña, A. M. 2013. A new approach in sample treatment combined with UHPLC-MS/MS for the determination of multiclass mycotoxins in edible nuts and seeds. Talanta. 115:61-67.

Bennett, J. W., & Klich, M. 2003. Mycotoxins. Clin Microbiol Rev, 16:497-516.

Dohnal, V., Pavlíková, L., & Kuča, K. 2010. Rapid and sensitive method for citrinin determination using high-performance liquid chromatography with fluorescence detection. Anal Lett. 43:786-792.

Kononenko, G. P., & Burkin, A. A. 2008. A survey on the occurrence of citrinin in feeds and their ingredients in Russia. Mycotoxin Res. 24:3-6.

Li, Y., Wu, H., Guo, L., Zheng, Y., & Guo, Y. 2012. Microsphere-based flow cytometric immunoassay for the determination of citrinin in red yeast rice. Food Chem. 134:2540-2545.

Li, Y., Zhou, Y. C., Yang, M. H., & Ou-Yang, Z. 2012. Natural occurrence of citrinin in widely consumed traditional Chinese food red yeast rice, medicinal plants and their related products. Food Chem. 132:1040-1045.

Llorent-Martínez, E. J., Barrales, P. O., Luisa Fernández-de Córdova, M., & Ruiz-Medina, A. 2010. Multicommutation in flow systems: A useful tool for pharmaceutical and clinical analysis. Curr Pharm Anal. 6:53-65.

Llorent-Martínez, E. J., García-Reyes, J. F., Ortega-Barrales, P., & Molina-Díaz, A. 2007. Multicommuted fluorescence based optosensor for the screening of bitertanol residues in banana samples. Food Chem. 102:676-682.

Llorent-Martínez, E. J., Ortega-Barrales, P., Fernández-De Córdova, M. L., & Ruiz-Medina, A. 2011. Contribution to automation for determination of drugs based on flow-through optosensors. Appl Spectrosc Rev. 46:339-367.

Llorent-Martínez, E. J., Ortega-Barrales, P., Fernández De Córdova, M. L., & Ruiz-Medina, A. 2009. Development of an automated chemiluminescence flow-through sensor for the determination of 5-aminosalicylic acid in pharmaceuticals: A comparative study between sequential and multicommutated flow techniques. Anal Bioanal Chem. 394:845-853.

Llorent-Martínez, E. J., Ortega-Barrales, P., & Molina-Díaz, A. 2005. Multicommuted optosensor for the determination of pipemidic acid in biological fluids. Anal Biochem. 347:330-332.

Markov, K., Pleadin, J., Bevardi, M., Vahčić, N., Sokolić-Mihalak, D., & Frece, J. 2013. Natural occurrence of aflatoxin B1, ochratoxin A and citrinin in Croatian fermented meat products. Food Control. 34:312-317.

Molinié, A., Faucet, V., Castegnaro, M., & Pfohl-Leszkowicz, A. 2005. Analysis of some breakfast cereals on the French market for their contents of ochratoxin A, citrinin and fumonisin B1: Development of a method for simultaneous extraction of ochratoxin A and citrinin. Food Chem. 92:391-400.

Mornar, A., Sertić, M., & Nigović, B. 2013. Development of a rapid LC/DAD/FLD/MSn method for the simultaneous determination of monacolins and citrinin in red fermented rice products. J Agri Food Chem. 61:1072-1080.

Nguyen, M. T., Tozlovanu, M., Tran, T. L., & Pfohl-Leszkowicz, A. 2007. Occurrence of aflatoxin B1, citrinin and ochratoxin A in rice in five provinces of the central region of Vietnam. Food Chem. 105:42-47.

Nigović, B., Sertić, M., & Mornar, A. 2013. Simultaneous determination of lovastatin and citrinin in red yeast rice supplements by micellar electrokinetic capillary chromatography. Food Chem. 138:531-538.

Rocha, F. R. P., Reis, B. F., Zagatto, E. A. G., Lima, J. L. F. C., Lapa, R. A. S., & Santos, J. L. M. 2002. Multicommutation in flow analysis: Concepts, applications and trends. Anal Chim Acta. 468:119-131.

Xu, B. J., Jia, X. Q., Gu, L. J., & Sung, C. K. 2006. Review on the qualitative and quantitative analysis of the mycotoxin citrinin. Food Control. 17:271-285.

Yogendrarajah, P., Van Poucke, C., De Meulenaer, B., & De Saeger, S. 2013. Development and validation of a QuEChERS based liquid chromatography tandem mass spectrometry method for the determination of multiple mycotoxins in spices. J Chromatogr A. 1297:1-11.

Determination of clothianidin in food products by using an automated system with photochemically induced fluorescence detection

2. "Determination of clothianidin in food products by using an automated system with photochemically induced fluorescence detection"

J. Jiménez-López, P. Ortega-Barrales, A. Ruiz-Medina*

Publicado en Journal of Food Composition and Analysis, en Abril de 2016, volumen 49, páginas 49–56.

Resumen

En este trabajo se ha propuesto un sistema de flujo continuo usando como técnica de detección la fluorescencia inducida fotoquímicamente (PIF) integrada en la espectroscopía en fase sólida. Dicho sistema se ha desarrollado empleando multiconmutación, y se ha aplicado a la determinación de la clotianidina (un insecticida neonicotinoide no fluorescente).

El pesticida es insertado en la corriente portadora (0.015 mol L^{-1} ácido acético/acetato de sodio, pH = 5.0) y fluye a través de un fotorreactor consistente en un tubo de PTFE enrollado alrededor de una lámpara de mercurio de baja presión (15W). En dicho fotorreactor, se produce la reacción fotoquímica de la clotianidina, y el fotoproducto fluorescente que se genera se transporta a una celda de flujo llena con el soporte sólido Sephadex-SP C-25, donde se retiene y monitoriza (λ_{ex}

= 357 nm / λ_{em} = 418 nm). El método presenta un límite de detección de 1.5 ng mL^{-1}, una frecuencia de muestreo de 23 muestras por hora y una repetitividad inferior al 3%.

El sistema que se describe ha sido aplicado con éxito a la determinación de clotianidina en muestras de agua potable, arroz y miel. Teniendo en cuenta que el límite máximo de residuos especificado por el Codex Alimentarius para granos de arroz es de 0.5 mg kg^{-1}, se han llevado a cabo estudios de recuperación para concentraciones de clotianidina en el rango de 0.3-10.0 mg kg^{-1}, obteniendo recuperaciones cercanas al 100%.

Con este estudio, se han alcanzado los dos objetivos propuestos: por un lado, desarrollar un método multiconmutado sensible y selectivo para la detección de trazas de residuos de clotianidina a través de la medida de la fluorescencia de uno de los fotoproductos generados, siendo de esta manera una buena alternativa a los métodos cromatográficos; por otro lado, validar este método usando diferentes tipos de muestras que pueden encontrarse en el medioambiente y en el sector agroalimentario como son el agua, los cereales y la miel.

2. "Determination of clothianidin in food products by using an automated system with photochemically induced fluorescence detection"

Abstract

A flow-through system based on the integration of solid-phase spectroscopic detection implemented with photochemically induced fluorescence (PIF) is proposed for the determination of clothianidin (a non-fluorescent neonicotinoid insecticide) through a multicommutated method. The pesticide is injected into the carrier stream (0.015 mol L^{-1} $C_2H_4O_2/NaC_2H_3O_2$, pH=5.0) and flows towards a homemade photoreactor, which consists of a PTFE tubing loosely coiled around a low pressure mercury lamp (15W). After the photochemical reaction of clothianidin, the generated fluorescent photoproduct is transported to a flow cell packed with Sephadex-SP C-25 where it is retained and monitored (λ_{ex}= 357 nm / λ_{em}= 418 nm). The method presents a detection limit of 1.5 ng mL^{-1}, a sample throughput of 23 h^{-1} and inter-day relative standard deviation lower than 3%. The described system has been satisfactorily applied to the determination of clothianidin in samples of drinking water, rice and honey. Taking into account that the maximum residue limit specified in the Codex Alimentarius Commission for rice grains is 0.5 mg kg^{-1}, recovery experiments have been carried out for clothianidin concentrations in the 0.3-10.0 mg kg^{-1} range.

Keywords: Clothianidin; Solid-phase spectroscopy; Multicommutation; Food analysis; Photochemically induced fluorescence; Neonicotinoids; Food safety; Pesticide residue; Food composition

1. Introduction

Neonicotinoids are a class of insecticides deriving from the nicotine moiety. Their use has increased considerably in the last few decades, and they represent one of the fastest growing types of insecticides. Both food quality and safety are affected by their application to crops at various stages of cultivation and during the post-harvest storage, thus causing damage to the final link in the food chain, namely, the consumer.

Clothianidin (**Fig. 1**), a member of this family, has been widely used for long-term control of a wide variety of pests (Tomizawa and Casida, 2005; Uneme, 2011); it is also used in seed dressings and added to the soil (Sánchez-Bayo, 2013). Clothianidin is receiving increased scrutiny since it has been implicated in adversely affecting pollinators and linked to colony collapse disorder in insects such as bees. Therefore, studying its use on different types of food crops is gaining much interest.

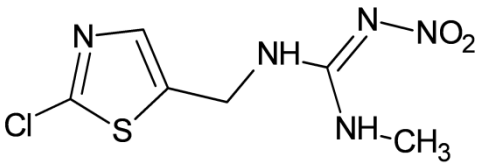

Fig. 1. Structure of clothianidin.

The Codex Alimentarius Commission (CAC) has stipulated that the Maximum Residue Limits (MRLs) of clothianidin remain within the range 0.02–2.0mg kg^{-1}, depending on type of food (cereals, vegetables or fruits) (2015). For this reason, it is necessary to detect clothianidin residues by sensitive and rapid methods in order to protect non-target organisms and environment from damage. Specifically, the European Commission banned its use in December 2013, finding that this chemical is harmful to bees. When honeybees come into contact with this compound, it may be taken along with the bees into the beehive, and their residues may then be found in bee products such as honey (Jovanov et al., 2013). In April 2014, the Reference Laboratory of the European Union for Health of Bees published the results of the first program to monitor the depopulation of hives in 17 European countries. The data show a highly variable rate of winter mortality between countries, ranging from 3.5 to 33.6%. In general, the situation is milder in the Mediterranean countries than in northern Europe. Restricting the use of clothianidin in agriculture will be reviewed within a maximum term of two years.

Currently available methods for the determination of clothianidin are based mainly on high performance liquid chromatography (HPLC) (Chen et al., 2013; Chen et al., 2005; Hou YY, 2011; Kim et al., 2012;

Vichapong et al., 2013; Vichapong et al., 2015) and gas chromatography (GC) (Li et al., 2012). Although these methods are very sensitive and precise, they are not suitable for high-throughput and rapid screening of large numbers of samples. Thus there is much interest in exploiting less-expensive yet reliable methods for the determination of this compound. Among these methods, fluorescence methods are generally rapid and reliable, but their application rather limited by the fact that neonicotinoids (including clothianidin) are not naturally fluorescent, and must therefore be converted into fluorescent species.

An alternative method, so-called photo-induced fluorescence (PIF), is based on the photochemical transformation of a non-fluorescent or weakly fluorescent analyte into strongly fluorescent photoproduct(s) by using UV irradiation (Icardo and Calatayud, 2008; Mbaye et al., 2009). Sensitivity and selectivity can be increased by coupling PIF and solid-phase spectrometry (SPS) (Molina-García et al., 2011b). Beads of an active surface (solid support) can be placed into an appropriate flow-cell, thus obtaining a continuous sensing device that allows on-line species monitoring (Ayora Cañada et al., 2002; Ruiz-Medina et al., 2001). The solid support has to be regenerated after measurements to allow the sensing system to be reused. In these systems, called flow-through sensors, separation and preconcentration steps occur simultaneously with the detection step (Llorent-Martínez et al., 2013; Ruedas Rama et al., 2004).

Automation in the method can be achieved in various ways. In 1996, Aaron et al. (Garcia et al., 1996) were the first to determine pesticides by combining the PIF technique with flow-injection analysis (FIA). As

alternative to FIA, new and modern flow methodologies such as multicommutated approaches can be used (Feres et al., 2008; Llorent-Martínez et al., 2011). Multicommutated flow injection analysis (MCFIA) (Cerda and Pons, 2006; Chailapakul et al., 2006; Jiménez-López et al., 2014) has been selected as automatic methodology due to its low-cost components, low consumption of reagents, high repeatability and sample throughput, robustness and simplicity of the system, which was designed to make use of three-way solenoid valves automatically controlled by a computer with homemade software.

The objective of this paper is twofold: (i) to develop a sensitive and selective multicommutated flow method for detecting trace clothianidin residues by measuring the fluorescence of one of its photodegradation products generated, so providing an alternative to the existing chromatographic methods; and (ii) to validate the method using different types of samples from the environment and found in the agro-food sector: water, cereals and honey. QuEChERS (quick, easy, cheap, effective, rugged and safe) method (Anastassiades et al., 2003) was applied as sample pre-treatment to extract and separate the analyte from some interfering substances present in the matrix. To the best of our knowledge, a fluorimetric system is being proposed for the first time for the analysis of clothianidin in these products.

2. Materials and methods

2.1. Instrumentation

A four-channel Gilson Minipuls-3 (Villiers Le Bel, France) peristaltic pump with rate selector and methanol-resistant pump tubes, type

Solvaflex (Elkay Products, Shrewsbury, MA, USA) were used. An electronic interface based on ULN 2803 integrated circuit was employed to generate the electric potential (12V) and current (100 mA) required to control the four 161T031 NResearch three-way solenoid valves (Neptune Research, MA, USA). The software for controlling the system was written in Java. Flow lines of 0.8 mm internal diameter PTFE tubing and methacrylate connections were also used.

A homemade continuous photochemical reactor was constructed by coiling a PTFE tubing (180 cm) around a low-pressure mercury lamp (15 W, 254 nm). This reactor has already been used in other systems proposed by the authors (Jiménez-López et al., 2016; Molina-García et al., 2011a; Molina-García et al., 2011c). It was placed inside an aluminum box to permit the maximum reflectance of UV light. Since the aluminum foil allowed heat dissipation, no cooling device was needed, and all the experiments were carried out at room temperature.

A Varian Cary-Eclipse spectrofluorimeter (Varian, Mulgrave, Melbourne, VIC, Australia) was used for recording spectra and making fluorescence measurements. It was controlled by a microprocessor fitted with the Cary Eclipse software package. The instrumental variables established were as follows: 357 and 418 nm for excitation and emission wavelengths, respectively; 5 and 10 nm for excitation and emission slits, respectively; and 750 V for photomultiplier tube voltage. A Hellma flow cell 176.752-QS (25 μL of inner volume and a light path length of 1.5 mm) was used inside the spectrofluorimeter. The cell was filled with Sephadex SP C-25 solid phase microbeads, and was blocked at the outlet with glass wool to prevent displacement of the support particles. The level of the resin packed in the flow cell had to

be carefully selected in order to ensure that the upper part of the resin fell precisely in the light path. In this way, the best sensitivity was obtained. Before starting the measuring process, the carrier solution was passed through the sensing zone for 5 min to condition it.

A Selecta Ultrasons ultrasonic bath (Barcelona, Spain), a Crison Model 2012 pH-meter with a glass/saturated calomel combination electrode (Crison, Barcelona, Spain), and a centrifuge (Selecta, Barcelona, Spain) were also used.

2.2. Reagents and solutions

Clothianidin (≥ 99.9%) was purchased from Fluka (Sigma-Aldrich, Madrid, Spain). Stock solution of 100 μg mL^{-1} clothianidin was prepared in Mili-Q water (Sigma, Madrid, Spain). It was stable for at least 1 month when stored in the refrigerator at +4ºC. Working solutions were prepared daily by suitable dilution with Milli-Q water.

Acetonitrile (C_2H_3N), acetic acid ($C_2H_4O_2$), hydrochloric acid (HCl), anhydrous sodium acetate ($NaC_2H_3O_2$), sodium hydroxide (NaOH), and anhydrous magnesium sulfate ($MgSO_4$) were obtained from Sigma. Sodium dodecyl sulfate (SDS), Triton X-100 and purified and calcined siliceous earth were purchased from Panreac (Barcelona, Spain). Formic acid (CH_2O_2), sodium formate ($NaCHO_2$), citric acid ($C_6H_8O_7$), sodium citrate ($C_6H_7NaO_7$) and succinic acid ($C_4H_6O_4$) were purchased from Sigma (Madrid, Spain). All of them were analytical reagent grade.

The carrier stream consisted of 0.015 mol L^{-1} $C_2H_4O_2/NaC_2H_3O_2$ (pH 5.0) buffer solution. Stock solution (0.2 mol L^{-1}) was prepared by dissolving 1.8915 g of $NaC_2H_3O_2$ with deionized water and adjusting

the pH to 5.0 with the appropriate amount of 0.1 mol L^{-1} $C_2H_4O_2$ to 100 ml of final volume. The eluent used to fully regenerate the solid support in the analysis of real samples was 0.005 mol L^{-1} NaOH solution.

Sephadex-QAE A-25, Sephadex-CM C-25, and Sephadex-SP C-25 resins, all of them 40–120 μm average particle size, were bought from Sigma. C_{18} bonded-phase silica gel beads, 55–105 μm average particle size, were obtained from Waters (Milford, MA, USA). Chelex-100 in sodium form, 200–400 mesh, was purchased from Fluka (Buchs, Switzerland).

2.3. Sample treatment

Clothianidin was determined in 5 water samples (tap and mineral water), 4 rice samples (white and brown), and 6 honey samples (rosemary, orange blossom and thyme). All of these samples, except tap water, were obtained from local markets located in Jaén, a province of Spain. Tap water was collected from the local water supplier.

Sample treatment was applied in the case of rice and honey samples. No treatment was necessary in the case of water samples. Rice samples were thoroughly ground and homogenized before the extraction. Honey samples were homogenized. QuEChERS was used as the extraction procedure. Nevertheless, this procedure was designed for samples with high moisture percentage, so it needed to be adapted to dry samples or those with low moisture percentage, such as rice, in order to reduce sample weight and/or to add water (Jiménez-López et al., 2014). Thus 10 g of sample (rice or honey) were weighed in a 50 mL PTFE centrifuge tube. Next, 20 mL of water and 20 mL of 1% (v:v) $C_2H_4O_2$ in acetonitrile were added. The screw cap was closed and the tube was

shaken for 1 min and then the sample was centrifuged at 2000 rpm for 10 min. Then, 0.85 g of anhydrous sodium acetate and 1.5 g of anhydrous $MgSO_4$ were added and the mixture was shaken and centrifuged again for 8 min. Then 10 mL of the supernatant (acetonitrile phase) were taken and transferred to a 15 mL centrifuge tube. After adding 300 mg anhydrous $MgSO_4$ and 200 mg purified and calcined siliceous earth, the tube was manually shaken for 1 min and centrifuged again for 8 min at 3000 rpm. Finally, the supernatant was collected.

In the case of honey samples, 0.20 μm filters were also used for improving the purity of the obtained extract.

Suitable dilutions of the supernatants were made with 0.015 mol L^{-1} $C_2H_4O_2/NaC_2H_3O_2$ buffer solution before recording the analytical signal.

2.4. General procedure

Manifold and flow procedure is shown in **Fig. 2**. The MCFIA system consisted of a peristaltic pump and a set of 3 three-way solenoid valves, automatically controlled by appropriate software. Each valve can adopt two positions, "on" and "off", and the whole system can be assimilated to an electronic circuit with a variable number of active nodes.

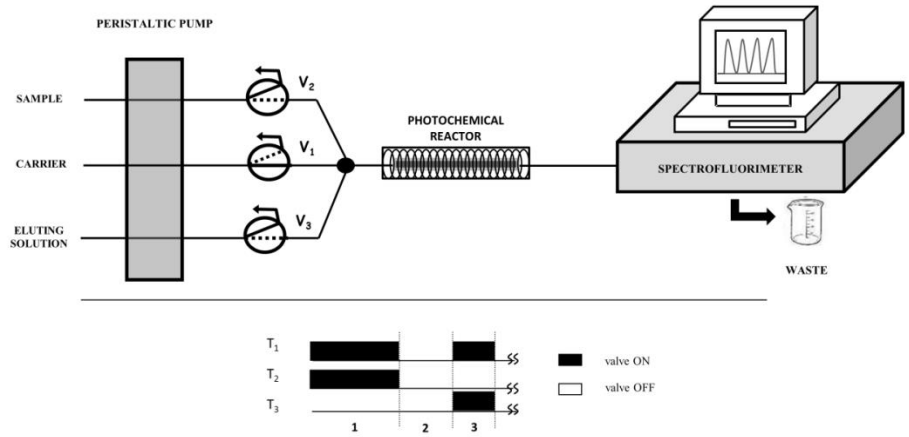

Fig. 2. Upper part: manifold, in which Vn=3-way solenoid valve n. Bottom part: valves scheme. Tn corresponds to the timing course of Vn. The filled rectangles above the time lines for each valve indicate the times at which the corresponding valve was switched on. The steps were as follows: 1) sample introduction; 2) signal recording; 3) elution.

A flow-rate of 1.5 mL min^{-1} was used in all experiments. In the initial status, all valves were switched off and the carrier (0.015 mol L^{-1} $C_2H_4O_2$/ $NaC_2H_3O_2$ buffer solution, pH 5.0) was flowing through the flow-through cell while all other solutions were being recycled to their respective vessels. The sample was introduced by simultaneously switching on valves V_1 and V_2 for 70 s (step 1). The sample solution was carried towards the photoreactor where the photoconversion of clothianidin into a fluorescent compound took place. Afterwards, the fluorescent photoproduct reached the solid support (Sephadex-SP C-25) filling the flow-cell, was transitorily retained and its relative fluorescence intensity was recorded operating at 357 and 418 nm for excitation and emission wavelengths, respectively (step 2). Finally, the photoproduct was completely eluted from the solid support using an

eluting solution of 0.005 mol L^{-1} NaOH; this was achieved by switching on valves V_1 and V_3 for 20 s (step 3). In this way, the system remained ready for the next sample insertion.

Calibration standards and samples were analyzed in triplicate. The analytical signal was expressed as peak height mean values.

3. Results and discussion

3.1. Spectral characteristics and solid support

The potential retention of clothianidin photoproduct on three different types of solid supports was evaluated: a) anion-exchanger Sephadex-QAE A-25; b) cation-exchangers Sephadex-SP C-25, Sephadex-CM C-25, and Chelex-100; and c) non-ionic C_{18} silica gel beads. Experiments with all solid supports were performed in the pH range of 1-12. Under an acidic medium, it was observed that the best analytical signal was obtained with cation-exchanger solid supports. Sephadex-SP C-25 resin was selected for further experiments, due to the highest analytical signal achieved (20% higher than Sephadex-CM C-25 or Chelex-100).

The excitation and emission spectra were recorded once the photoproduct generated in acid medium was retained on Sephadex-SP C-25 resin and 357 and 418 nm wavelengths were chosen ($\lambda_{ex}/\lambda_{em}$). Comparing wavelengths on beads and homogeneous solution (360/421 nm/nm, $\lambda_{ex}/\lambda_{em}$), working in the same conditions and in the same flow cell, a hypsochromic shift in both maxima excitation and emission wavelengths was found (**Fig. 3**). This can be attributed to the

modification of the surrounding environment of the analyte on the solid phase with respect to the solution medium.

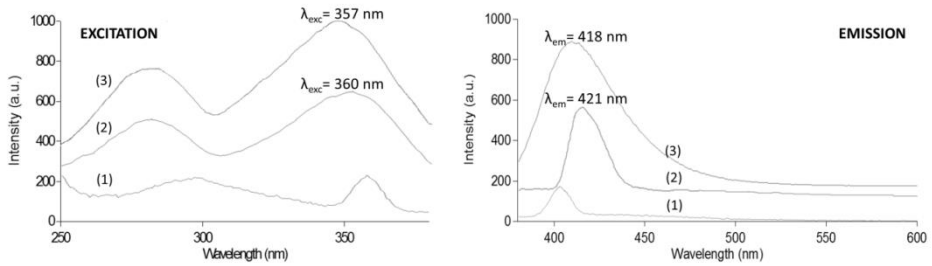

Fig. 3. Fluorescence spectra of clothianidin and its photoproduct. (1) Clothianidin in homogeneous solution (5 μg mL-1). (2) Photoproduct of clothianidin in homogeneous solution (5 μg mL-1 of clothianidin). (3) Photoproduct of clothianidin retained on Sephadex-SP C-25 (0.5 μg mL-1 of clothianidin). Irradiation time: 55 s.

In addition, as a result of the preconcentration of the analyte on the active solid support in the detection area of the spectrofluorimeter, the obtained signal was 15 times higher than the one obtained in aqueous solution.

3.2. Instrumental variables

Due to the presence of the solid support in the irradiated zone, luminescence measurements carried out in solid-phase media are usually affected by background signal levels higher than those found in homogeneous solution. Therefore, instrumental parameters have to be carefully investigated in order to obtain the best possible signal-to-background ratio. For this reason, the influence of the voltage of the photomultiplier tube (400-800 V) and the instrument excitation and

emission slit widths (5-20 nm) on the analytical signal had to be examined. The excitation and emission slits were established in 5 and 10 nm, respectively, because this combination caused the best photoproduct/background signal ratio.

For the photomultiplier tube voltage, when increasing the voltage, the sensitivity improves, but the background signal is also increased (so diminishing the linearity range of the method). Therefore a compromise between sensitivity and linear dynamic range had to be achieved, and 750 V was finally established.

3.3. Chemical variables

The influence of pH on the fluorescence intensity was studied, by inserting into a water carrier stream, different clothianidin solutions adjusted to a pH value ranging from 1.0 to 13.0 (with HCl or NaOH) before irradiation. A significant fluorescence intensity of clothianidin photoproduct signal was obtained for pH values below 6.0, reaching its maximum in the pH range 4.0–5.0. It was observed that pH values higher than 6 caused a 70% decrease in the analytical signal, because the photoproduct was not properly retained on the solid support, whereas pH values lower than 4 decreased the signal around 30% due to the high ionic strength of the solution, which caused a slight desorption of clothianidin photoproduct from the solid support microbeads.

Among several buffer solutions tested to adjust the optimum sample pH (formic acid/sodium formate, acetic acid/anhydrous sodium acetate, citric acid/sodium citrate, succinic acid/NaOH), the best results were obtained with $C_2H_4O_2$/$NaC_2H_3O_2$ buffer solution. Thus pH 5.0 was

selected for subsequent use in order to adjust sample pH. Changes in the buffer concentration resulted in few variations in the fluorescence signal obtained, so different buffer concentrations were tested ($5x10^{-3}$-$5x10^{-2}$ mol L^{-1}); 0.015 mol L^{-1} was chosen as the optimum concentration.

The use of the same 0.015 mol L^{-1} $C_2H_4O_2/NaC_2H_3O_2$ buffer solution (pH 5.0) as carrier stream instead of water produced a remarkable improvement in the stability of the baseline, but only a modest increase in the fluorescence signal. Obviously, the identical nature of the carrier and sample buffer solutions causes minimum changes in the compaction of the solid support after each insertion of sample.

After clothianidin photoproduct was retained on the solid support, it was partially eluted by the carrier solution in the case of real samples. An increase in the ionic strength of the carrier solution at the same pH was useful for the complete elution of the photoproduct. However, overpressures appeared in the system due to the compaction of the solid support, and the analytical signal was also lower. Hence, an eluting solution (0.005 mol L^{-1} NaOH) was used after recording the analytical signal. Lower concentrations did not allow complete elution of the photoproduct. In this way, clothianidin photoproduct was desorbed from the solid support, and the system was ready for the next sample insertion.

Taking into account other PIF systems, the use of a surfactant into the sample was studied to check the increase in the analytical signal. SDS and Triton X-100 were tested. SDS provided better analytical signals for the same level of concentration. For this reason its concentration

was optimized by injecting clothianidin solutions into the system with increasing amounts of SDS (10^{-3}-10^{-2} mol L^{-1}). Finally, $8x10^{-3}$ mol L^{-1} SDS solution was selected since it provided the highest analytical signal. Higher and lower SDS concentrations caused a decrease in the fluorescence signal. Nevertheless, with the optimal concentration, the signal increased only by 5–7%. For this reason, and because SDS is a harmful product, its use was not justified for routine analysis.

3.4. Flow system variables

The residence time of clothianidin in the photochemical reactor, and consequently the irradiation time, is a critical variable. It is determined by both the flow-rate and the length of the photoreactor. To determine the optimum residence time, 200 ng mL^{-1} pesticide solution at a flow rate of 1.5 mL min^{-1} was inserted in the system, and the flow was stopped just when the sample plug was inside the photoreactor and the UV lamp was turned on for increasing periods of time each time (20–100 s). After turning off the lamp and re-establishing the flow, the PIF signal was recorded. The shape of the curve obtained (**Fig. 4**) suggests a two-step photolysis mechanism: a first step in which the concentration of fluorescent photoproduct increases with increasing irradiation periods, and a second step after reaching the maximum in which the fluorescent photoproduct is degraded by the UV irradiation. The optimum irradiation time was 55 s. Thus, shorter irradiation times resulted in low conversion into fluorescent products, whereas long times decreased the fluorescence through subsequent reaction of the photoproducts.

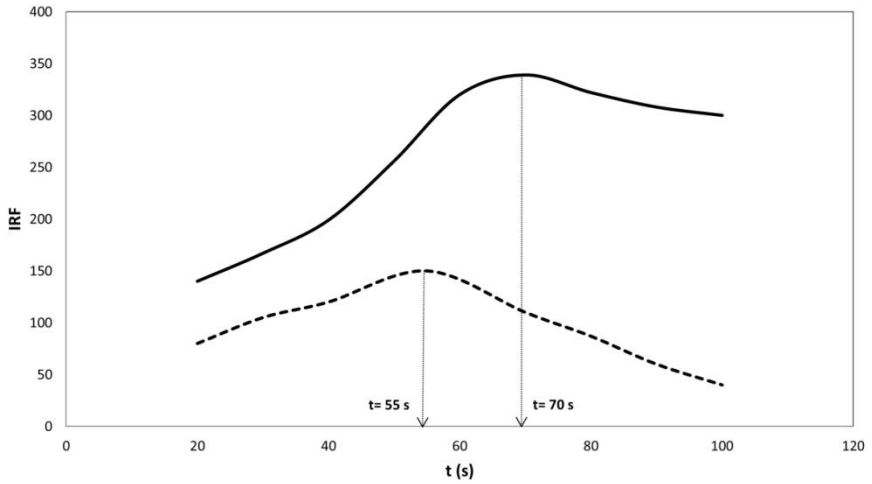

Fig. 4. Effect of both sample insertion time (solid line) and sample irradiation time (dotted line) on the analytical signal; 400 and 200 ng mL^{-1} of clothianidin, respectively.

The use of higher flow rates combined with longer photoreactors originated overpressure problems, so the flow-rate was studied from 1.0 up to 2.0 mL min^{-1}. When increasing the flow-rate, the sample frequency is also increased but a lower repeatability was observed for flow-rate higher than 1.5 mL min^{-1}. Therefore 1.5 mL min^{-1} was chosen as the optimum flow rate.

The effect of the temperature on the fluorescence intensity was also examined. Such an effect is of great theoretical significance and practical benefit. Increasing the temperature increases molecular thermal motion, thereby also increasing the probability of radiationless transitions and reducing the fluorescence quantum yield as a result. The influence of temperature was studied over the range 15−45 °C. As expected, the fluorescence intensity decreased as the temperature was raised. But it happened only when temperature was higher than 35 ºC.

Because no significant heating is observed, the procedure was developed at room temperature.

The sample insertion time is another variable studied in this section. Using the optimized flow-rate, the sample introduction time was studied ranging from 40 to 100 s for a 400 ng mL^{-1} sample solution (see **Fig. 4**). When the sampling time increases, the signal increases due to a higher amount of analyte introduced into the flow system; so the amount of photoproduct sorbed on the solid support is higher. The analytical signal increased up to 70 s and then remained constant. Taking into account this result, 70 s was selected as the optimum sample time in order to obtain maximum sensitivity.

3.5. Analytical parameters

In order to evaluate the analytical usefulness of the PIF approach, the analytical parameters of the systems were studied using the optimized working conditions previously discussed. The data were fitted by standard least-squares treatment (univariate method) and the calibration is shown in **Table 1**. Eventual matrix effect was evaluated by comparing the slopes of aqueous standards and standard addition calibration graphs for different types of samples. No matrix effect was detected. The limit of detection and quantitation were estimated as the clothianidin concentrations that produced analytical signals equal to 3 and 10 times, respectively, the standard deviation of background luminescence. The detection limit was determined to be 1.5 ng mL^{-1}, thus demonstrating that the sensitivity of the method was good enough to ensure a reliable determination level lower than the MRL. This value is comparable or lower than those obtained by other analytical methods

(Jovanov et al., 2013; Kim et al., 2012; Li et al., 2014a; Li et al., 2014b; Wang et al., 2012; Xie et al., 2011) (**Table 2**). When comparing with immunoanalytical methods (Li et al., 2014a; Li et al., 2014b; Uchigashima et al., 2012), the greatest advantage introduced by the proposed system is high throughput and a lower cost of the reagents.

Table 1

Analytical parameters.

Parameter	
Excitation/ emission slits (nm/nm)	5/10
Photomultiplier tube voltage (V)	750
Analytical curve	
Intercept ± SD (n=3)	29.74 ± 0.04
Slope (mL ng^{-1}) ± SD (n=3)	0.7313 ± 0.007
Regression coefficient	0.9989
Linear dynamic range (ng mL^{-1})	5-500
Detection limit (ng mL^{-1})	1.5
Quantitation limit (ng mL^{-1})	5
Intra-day RSD (%) (n=7)	
50 ng mL^{-1}	2.6
250 ng mL^{-1}	1.9
Inter-day RSD (%) (n=7)	
100 ng mL^{-1}	3.8
400 ng mL^{-1}	4.9
Sample throughput, h^{-1}	23

Table 2

Comparison with previous methods.

Technique	**Detection**	**Sample pretreatment**	**LOD**	**RSD (%)**	**Ref.**
LC	MS/MS	QuEChERS	10-20 ng mL^{-1}	< 10	Kim et al. 2012

HPLC	DAD[a]	d-SPE[b] and DLLME[c]	2 ng mL^{-1}	0.9-12.6	Wang et al. 2012
FPIA[d]	Fluoresc.	Solid-liquid extraction	5.5 ng mL^{-1}	< 12.9	Li, Liu et al. 2014
LC	MS/MS	DLLME	0.5-1.0 μg kg^{-1}	2.74–11.8	Jovanov et al. 2013
LC	MS/MS	HLB[e] solid phase extraction	10-20 ng mL^{-1}	≤ 8.6	Xie et al. 2011
HPLC	DAD	octanol–water microextraction	0.25–0.5 ng kg^{-1}	0.1-4.73	Vichapong et al. 2015
ELISA[f]/ GICA[g]	-	Solid-liquid extraction	3.8 / 8 ng mL^{-1}	3.2-12.8	Li, Hua et al. 2014
Proposed method	PIF	QuEChERS	1.5 ng mL^{-1}	< 3	-

[a]Diode Array Detector; [b]Dispersive Solid Phase Extraction; [c]Dispersive Liquid–Liquid MicroExtraction; [d]Florescence Polarization ImmunoAssay; [e]Hydrophilic/Lipophilic Balanced; [f]Enzyme-Linked ImmunoSorbent Assay; [g]Gold ImmunoChromatographic Assay.

The ruggedness and robustness of the system were studied using a honey mixture sample because it was the sample with a more complex matrix. The ruggedness of the method was assessed by comparison of the intra- and inter-day assay results undertaken by two analysts. The RSD values (%) for intra- and inter-day assays did not exceed 3 and 5%, respectively, indicating the ruggedness of the sensor. In addition, the robustness was investigated under a variety of conditions such as small changes in sample and carrier solutions (0.014-0.016 mol L^{-1}

$C_2H_4O_2/NaC_2H_3O_2$), flow-rate (1.4-1.6 mL min^{-1}), and excitation/emission wavelengths (± 2 nm). The percent recoveries for clothianidin were in the range of 95–105% in all cases (considering the value obtained under optimum conditions as 100%), thus demonstrating the robustness of the proposed method.

3.6. Study of foreign species

Clothianidin can be determined in the presence of different amounts of other pesticides commonly used in agriculture, most of them strongly fluorescent (carbaryl, carbendazim or o-phenylphenol). The results are shown in **Table 3**.

Table 3
Study of interferences from pesticides.

Foreign species	**Tolerance level (foreign species/analyte, w/w)**
Na^+, K^+, NH_4^+, Ca^{2+}, Mg^{2+}, Al^{3+}, SO_4^{2-}, Cl^-, HCO_3^-, PO_4^{3-}, NO^{3-}	1000[a]
O-phenylphenol	25
Carbendazim	15
Carbaryl	15
Imidacloprid	5
Thiametoxam	3

[a]Maximum ratio tested.

The tolerance level was taken as the maximum concentration of the foreign species causing an error not exceeding ± 3% in the analytical signal, when compared with the signal obtained for the fluorescent photoproduct in the absence of the species. Due to the spectral overlapping, the determination of clothianidin in homogeneous solution

(without using solid support in the flow cell), in the presence of many of the pesticides tested, would be possible only with a previous separation of the latter. Specifically, in the case of imidacloprid and thiamethoxam, if the proposed method is compared to the same procedure in homogeneous solution, the obtained tolerance limits (w/w) were 0.1 in both cases. Therefore, the tolerance level to these compounds in the method here proposed is respectively about 50 and 30 times higher than that obtained in the solution method.

3.7. Analytical applications

Residues of clothianidin found in agricultural products and drinking water have been a great concern in recent years. The existence of this compound in dietary products is a very serious risk to human health, and its determination at trace levels is an acute analytical problem. The developed procedure was applied to the determination of clothianidin in spiked samples of tap and mineral water, rice and honey. Their pretreatment was described in the "*Sample treatment*" section. Taking into account that clothianidin levels were below the detection limit of the proposed method in all samples, a recovery study was carried out to evaluate the accuracy of the whole method (extraction and determination). The analytical signals obtained from the spiked samples were directly interpolated in the calibration graph because no matrix effect was detected.

Data obtained in the case of drinking water are shown in **Table 4**. With respect to the rice and honey, these were spiked with clothianidin concentrations in the range 0.3–10.0 mg kg^{-1}. These levels were close to the MRL established by CAC in rice grain, 0.5 mg kg^{-1} (EFSA,

2015). Results are detailed in **Table 5**. In all the studied samples, recovery values between 97% and 104% were obtained, with RSDs (*n=3*) lower than 3% in all cases.

Table 4

Determination of clothianidin in drinking water.

Water		**Added (ng mL^{-1})**	**Recovery (%)[a]**	**RSD (%)[a]**
Mineral	Sample 1	20	99.1	1.5
		90	98.4	1.2
		180	100.7	0.7
	Sample 2	80	101.2	1.6
		150	100.8	0.7
		300	99.6	0.4
	Sample 3	180	100.2	1.4
		300	100.9	0.4
		500	98.4	0.7
Tap	Sample 1	50	101.9	1.6
		150	103.6	0.6
		400	100.3	0.9
	Sample 2	120	102.2	2.1
		250	100.6	0.9
		500	103.1	1.8

[a] n=3

Table 5

Determination of clothianidin in honey and rice.

Sample	**Added (mg kg^{-1})**	**Recovery (%)[a]**	**RSD (%)[a]**
Rosemary honey 1	0.3	102.9	1.1
	3	103.1	0.7
	8	102.3	2.0

Rosemary honey 2	0.8	101.3	0.8
	2	100.4	0.4
	6	100.9	1.7
Orange blossom honey 1	0.5	102.3	1.2
	5	104.0	0.9
	7.5	101.6	1.0
Orange blossom honey 2	1	103.1	2.1
	4	101.9	0.6
	8	102.4	1.7
Thyme honey 1	1	101.9	1.6
	4	103.6	0.6
	10	100.3	0.9
Thyme honey 2	0.5	100.8	2.7
	3.5	102.2	0.8
	7	101.6	1.1
White rice 1 (white)	0.3	97.4	1.3
	1.5	99.8	1.5
	2.5	99.2	1.3
White rice 2 (white)	0.5	99.8	1.6
	3	98.8	1.1
	4	102.2	2.0
Brown rice 3	1	100.4	2.6
	3.5	98.3	1.7
	5	100.7	1.0
Brown rice 4	1.2	102.3	1.9
	3	102.6	0.9
	5	100.4	1.7

[a] n=3

The use of a 0.20 μm PTFE filter was necessary in the case of honey samples after obtaining the extract. This filter removed some interferences, thus making it possible to achieve better recoveries. It is worth mentioning that, due to the high dilution, no matrix effect was found and matrix-matched calibrations were not required. The obtained

results make the proposed method useful for environmental and food control against clothianidin.

The statistical study of the accuracy was carried out comparing the obtained results with an HPLC reference method (Zhang et al., 2013). Same samples were analyzed, but only one from each type of water, rice or honey was taken as representative for the analysis. Samples were prepared as described in section 2.3 and analyzed in triplicate. The results of the proposed method were compared with those obtained from this analysis by means of both *t*-test and *F*-criterion, showing that there is no significant statistical difference between the values obtained by both methods and indicating the utility of the proposed method for routine analytical control (**Table 6**).

Table 6

Comparison with HPLC reference method.

Sample	**Amount found[a] (ng mL^{-1})**		***t*[b]**	***F*[c]**
	Proposed method	**Reference method**		
Mineral water	99.99	101.32	1.11	1.29
Tap water	103.93	103.65	0.35	3.56
White rice	104.32	104.99	0.68	1.33
Brown rice	103.25	106.29	1.02	2.14
Rosemary honey	102.86	104.48	0.70	8.19
Orange blossom honey	103.59	103.96	0.36	2.03
Thyme honey	100.28	104.65	1.43	3.77

[a] Average of three determinations for 100 ng mL^{-1}.

[b] Theoretical value for t=4.30 (P=0.05).

[c] Theoretical value for F=39.00 (P=0.05).

4. Conclusions

A sensitive system based on PIF detection was successfully developed for analysis of clothianidin. The proposed method makes it easier and less expensive to determine clothianidin in water and foods, such as rice and honey, without the need for labor-intensive sample pretreatment, comparing with other methods usually used for detecting this analyte. The implementation of PIF as detection system in flow–SPS methodology widens its applicability to the determination of non-fluorescent species and provides advantages such as simplicity of the flow system, quicker derivatization reaction and use of fewer chemicals.

Thus we have shown that this multicommutation methodology contributes to low chemical consumption, simplicity in handling, enhancement in reproducibility, and higher sampling throughput. All this shows the feasibility of the system as a screening method and as an alternative to chromatographic methods for determination of clothianidin residues in agricultural products, therefore contributing to attaining the goal of better food safety for consumers.

Acknowledgements

J.J.L. acknowledges research scholarship from Spanish Government (Ministerio de Educación y Ciencia).

References

Anastassiades, M., Lehotay, S.J., Štajnbaher, D., Schenck, F.J., (2003). Fast and easy multiresidue method employing acetonitrile extraction/partitioning and "dispersive solid-phase extraction" for the determination of pesticide residues in produce. Journal of AOAC International 86(2), 412-431.

Ayora Cañada, M.J., Ruiz Medina, A., Frank, J., Lendl, B., (2002). Bead injection for surface enhanced Raman spectroscopy: Automated on-line monitoring of substrate generation and application in quantitative analysis. Analyst 127(10), 1365-1369.

Cerda, V., Pons, C., (2006). Multicommutated flow techniques for developing analytical methods. Trac-Trends in Analytical Chemistry 25(3), 236-242.

Costa-Fernandez, J.M., Pereiro, R., Sanz-Medel, A., (2006). The use of luminescent quantum dots for optical sensing. Trac-Trends in Analytical Chemistry 25(3), 207-218.

Chailapakul, O., Ngamukot, P., Yoosamran, A., Siangproh, W., Wangfuengkanagul, N., (2006). Recent electrochemical and optical sensors in flow-based analysis. Sensors 6(10), 1383-1410.

Chen, M., Collins, E.M., Tao, L., Lu, C., (2013). Simultaneous determination of residues in pollen and high-fructose corn syrup from eight neonicotinoid insecticides by liquid chromatography-tandem mass spectrometry. Analytical and Bioanalytical Chemistry 405(28), 9251-9264.

Chen, M.F., Huang, J.W., Wong, S.S., Li, G.C., (2005). Analysis of insecticide clothianidin and its metabolites in rice by liquid chromatography with a UV detector. Journal of Food and Drug Analysis 13(3), 279-283.

EFSA, (2015). Reasoned opinion on the review of the existing maximum residue levels (MRLs) for clothianidin and thiamethoxam according to Article 12 of Regulation (EC) No 396/2005.

Feres, M.A., Fortes, P.R., Zagatto, E.A.G., Santos, J.L.M., Lima, J.L.F.C., (2008). Multi-commutation in flow analysis: Recent developments and applications. Analytica Chimica Acta 618(1), 1-17.

Garcia, L.F., Eremin, S., Aaron, J.J., (1996). Flow-injection analysis of chlorophenoxyacid herbicides using photochemically induced fluorescence detection. Analytical Letters 29(8), 1447-1461.

Hou YY, B.H., Zhao XX, Hu YF, Su T, Wang XH, et al, (2011). Determination of nicotinoid residues in complicated matrix vegetables by solid phase extraction and HPLC method. Journal of Instrumental Analysis 30, 58-63.

Icardo, M.C., Calatayud, J.M., (2008). Photo-induced luminescence. Critical Reviews in Analytical Chemistry 38(2), 118-130.

Jiménez-López, J., Llorent-Martínez, E.J., Ortega-Barrales, P., Ruiz-Medina, A., (2014). Multi-commutated fluorometric optosensor for the determination of citrinin in rice and red yeast rice supplements. Food Additives and Contaminants - Part A

Chemistry, Analysis, Control, Exposure and Risk Assessment 31(10), 1744-1750.

Jiménez-López, J., Ortega-Barrales, P., Ruiz-Medina, A., (2016). Development of an semi-automatic and sensitive photochemically induced fluorescence sensor for the determination of thiamethoxam in vegetables. Talanta 149, 149-155.

Jovanov, P., Guzsvány, V., Franko, M., Lazić, S., Sakač, M., Šarić, B., Banjaca, V., (2013). Multi-residue method for determination of selected neonicotinoid insecticides in honey using optimized dispersive liquid-liquid microextraction combined with liquid chromatography-tandem mass spectrometry. Talanta 111, 125-133.

Kim, B.M., Park, J.S., Choi, J.H., Abd El-Aty, A.M., Na, T.W., Shim, J.H., (2012). Residual determination of clothianidin and its metabolites in three minor crops via tandem mass spectrometry. Food Chemistry 131(4), 1546-1551.

Li, L., Jiang, G., Liu, C., Liang, H., Sun, D., Li, W., (2012). Clothianidin dissipation in tomato and soil, and distribution in tomato peel and flesh. Food Control 25(1), 265-269.

Li, M., Hua, X., Ma, M., Liu, J., Zhou, L., Wang, M., (2014a). Detecting clothianidin residues in environmental and agricultural samples using rapid, sensitive enzyme-linked immunosorbent assay and gold immunochromatographic assay. Science of the Total Environment 499, 1-6.

Li, M., Liu, X., Hua, X., Yin, W., Fang, Q., Wang, M., (2014b). Fluorescence polarization immunoassay for highly efficient detection of clothianidin in agricultural samples. Analytical Methods 6(16), 6541-6547.

Llorent-Martínez, E.J., Jiménez-López, J., Fernández-de Córdova, M.L., Ortega-Barrales, P., Ruiz-Medina, A., (2013). Quantitation of hydroxytyrosol in food products using a sequential injection analysis fluorescence optosensor. Journal of Food Composition and Analysis 32(1), 99-104.

Llorent-Martínez, E.J., Ortega-Barrales, P., Fernández-de Córdova, M.L., Ruiz-Medina, A., (2011). Trends in flow-based analytical methods applied to pesticide detection: A review. Analytica Chimica Acta 684(1-2), 21-30.

Mbaye, M., Gaye Seye, M.D., Coly, A., Tine, A., Aaron, J.J., (2009). Usefulness of cyclodextrin media for the determination of α-cypermethrin by photochemically induced fluorescence: Analytical applications to natural waters. Analytical and Bioanalytical Chemistry 394(4), 1089-1098.

Molina-García, L., Ruiz-Medina, A., Fernández-de Córdova, M.L., (2011a). An automatic optosensing device for the simultaneous determination of resveratrol and piceid in wines. Analytica Chimica Acta 689(2), 226-233.

Molina-García, L., Ruiz-Medina, A., Fernández-de Córdova, M.L., (2011b). Automatic optosensing device based on photo-induced fluorescence for determination of piceid in cocoa-containing

products. Analytical and Bioanalytical Chemistry 399(2), 965-972.

Molina-García, L., Ruiz-Medina, A., Fernández-de Córdova, M.L., (2011c). A novel multicommuted fluorimetric optosensor for determination of resveratrol in beer. Talanta 83(3), 850-856.

Rastgar, S., Shahrokhian, S., (2014). Nickel hydroxide nanoparticles-reduced graphene oxide nanosheets film: Layer-by-layer electrochemical preparation, characterization and rifampicin sensory application. Talanta 119, 156-163.

Ruedas Rama, M.J., Ruiz Medina, A., Molina Díaz, A., (2004). A Prussian blue-based flow-through renewable surface optosensor for analysis of ascorbic acid. Microchemical Journal 78(2), 157-162.

Ruiz-Medina, A., Fernández-de Córdova, M.L., Molina-Díaz, A., (2001). A flow-through optosensing device with fluorimetric transduction for rapid and sensitive determination of dipyridamole in pharmaceuticals and human plasma. European Journal of Pharmaceutical Sciences 13(4), 385-391.

Sánchez-Bayo, F., Tennekes, H.A., Goka, K., (2013). Impact of systemic insecticides on organisms and ecosystems, in: Trdan, S. (Ed.), *Insecticides - Development of Safer and More Effective Technologies*. InTech, Rijeka, Croatia, pp. 365-414.

Tomizawa, M., Casida, J.E., (2005). Neonicotinoid insecticide toxicology: Mechanisms of selective action, *Annual Review of Pharmacology and Toxicology*, pp. 247-268.

Uchigashima, M., Watanabe, E., Ito, S., Iwasa, S., Miyake, S., (2012). Development of immunoassay based on monoclonal antibody reacted with the neonicotinoid insecticides clothianidin and dinotefuran. Sensors (Switzerland) 12(11), 15858-15872.

Uneme, H., (2011). Chemistry of clothianidin and related compounds. Journal of Agricultural and Food Chemistry 59(7), 2932-2937.

Vichapong, J., Burakham, R., Srijaranai, S., (2013). Vortex-assisted surfactant-enhanced-emulsification liquid-liquid microextraction with solidification of floating organic droplet combined with HPLC for the determination of neonicotinoid pesticides. Talanta 117, 221-228.

Vichapong, J., Burakham, R., Srijaranai, S., (2015). In-coupled syringe assisted octanol–water partition microextraction coupled with high-performance liquid chromatography for simultaneous determination of neonicotinoid insecticide residues in honey. Talanta 139, 21-26.

Wang, P., Yang, X., Wang, J., Cui, J., Dong, A.J., Zhao, H.T., Zhang, L.W., Wang, Z.Y., Xu, R.B., Li, W.J., Zhang, Y.C., Zhang, H., Jing, J., (2012). Multi-residue method for determination of seven neonicotinoid insecticides in grains using dispersive solid-phase extraction and dispersive liquid-liquid micro-extraction by high performance liquid chromatography. Food Chemistry 134(3), 1691-1698.

Xie, W., Han, C., Qian, Y., Ding, H., Chen, X., Xi, J., (2011). Determination of neonicotinoid pesticides residues in agricultural

samples by solid-phase extraction combined with liquid chromatography-tandem mass spectrometry. Journal of Chromatography A 1218(28), 4426-4433.

Zhang, Y., Xu, J., Dong, F., Liu, X., Li, X., Li, Y., Wu, X., Liang, X., Zheng, Y., (2013). Simultaneous determination of four neonicotinoid insecticides residues in cereals, vegetables and fruits using ultra-performance liquid chromatography/tandem mass spectrometry. Analytical Methods 5(6), 1449-1455.

Development of a semi-automatic and sensitive photochemically induced fluorescence sensor for the determination of thiamethoxam in vegetables

3. "Development of a semi-automatic and sensitive photochemically induced fluorescence sensor for the determination of thiamethoxam in vegetables"

J. Jiménez-López, P. Ortega-Barrales, A. Ruiz-Medina*

Publicado en Talanta, en Diciembre de 2016, volumen 149, páginas 149–155.

Resumen

En este trabajo se desarrolló un método para la determinación del tiametoxam (TMX), un plaguicida neonicotinoide ampliamente conocido. Para ello, se optimizó un optosensor en flujo continuo, empleando fluorescencia inducida fotoquímicamente (PIF) como técnica de detección y el Análisis por Inyección en Flujo Multiconmutado (MCFIA) como metodología de flujo.

El uso del PIF en un sistema de flujo continuo permitió llevar a cabo una rápida fotodegradación en línea del TMX para, posteriormente, preconcentrar y cuantificar ($\lambda_{exc}/\lambda_{em}$ = 353/407 nm/nm) el fotoproducto fluorescente generado una vez retenido en el soporte sólido (gel de sílice C_{18}) situado en la celda de flujo. Posteriormente, el fotoproducto era eluido por la misma disolución portadora. El método

analítico propuesto presenta un límite de detección de 3.6 ng mL^{-1} bajo las óptimas.

Se llevaron a cabo estudios de recuperación en diferentes tipos de vegetales a niveles iguales o inferiores al límite máximo de residuos legislado, y los resultados obtenidos demostraron la exactitud del método. De igual forma, se observaron ventajas adicionales tales como su simplicidad, alta sensibilidad y alta selectividad, cumplliendo con requisitos de interés para su aplicación en controles de calidad. Los resultados obtenidos en el análisis de muestras reales fortificadas a diferentes niveles estuvieron de acuerdo con las proporcionadas por un método de cromatografía líquida de referencia (HPLC).

Debido a que la calidad y la seguridad alimentaria son dos de los problemas globales más importantes en el campo de la alimentación, es importante el desarrollo de nuevos métodos de análisis para la determinación de residuos de contaminantes de forma rápida y fiable. Este estudio propone un método analítico que, además de ser una buena alternativa a los métodos cromatográficos (ya que presenta las ventajas anteriormente expuestas), puede considerarse un método de análisis *eco-friendly* (por su bajo consumo de reactivos y su baja generación de residuos), lo que lo hace adecuado para utilizar en un laboratorio de análisis y/o de control de calidad.

3. "Development of a semi-automatic and sensitive photochemically induced fluorescence sensor for the determination of thiamethoxam in vegetables"

Abstract

The determination of thiamethoxam (TMX), a widely known neonicotinoid pesticide, by a multicommutated optosensing device implemented with photochemically induced fluorescence (PIF) has been developed. The combination of both methodologies allows, on one hand a quick on-line photodegradation of TMX and, on the other hand, the preconcentration, quantification and desorption of the fluorescent photoproduct generated once retained on C_{18} silica gel filling the flow-cell which was monitored at 353 and 407 nm for excitation and emission wavelengths, respectively.

The proposed analytical method presents a detection limit of 3.6 ng mL^{-1} by using Multicommutated Flow Injection Analysis (MCFIA) as flow methodology. Recovery experiments have been carried out in different kinds of vegetables at levels same or below the legislated maximum residue limit, demonstrating that this method combines advantages such as simplicity, high sensibility and high selectivity, in addition to fulfill the requirements for its applications in quality control. The obtained results in the analysis of real samples were in good agreement with those provided by a reference liquid chromatography (HPLC) method.

Keywords: MCFIA; thiamethoxam; photo-induced fluorescence; vegetables

1. Introduction

The quality and food safety are, due to a convergence of factors, two of the most important global issues in the food field. Nevertheless, modern agricultural production is highly based on the use of agrochemicals, such as pesticides, applied to crops at various stages of cultivation and during the post-harvest storage. One of these pesticides is thiamethoxam (TMX) which has been widely used in last years. For this reason, the European Union has established its maximum residue limit (MRL) [1] in fruits and vegetables in the 0.05-7 mg kg^{-1} range, depending upon the type of food crop. Both foods are essentials and play basic roles in a healthful diet, so checking that they are below this range is vital. Specifically, the European Commission proposed to restrict the use of TMX (along with imidacloprid and clothianidin) for a period of 2 years from December 2013 [2]. This is the result of the disappearance of hundreds of millions of bees, a crisis that has been called the problem of colony collapse disorder, and could have been caused by the use of this insecticide, among others [3].

Currently, TMX is typically analyzed by liquid chromatography (LC) [4-7], gas chromatography (GC) [8, 9] and voltammetry [10], but information on residue determinations of TMX in leafy vegetables is very scarce. There is much interest in exploring inexpensive and reliable methods for the determination of TMX, being fluorescence methods a great proposal for these. TMX is not naturally fluorescent, and, therefore, it has to be converted into fluorescent species by a

derivatization method. An alternative is the use of photo-induced fluorescence (PIF) which is based on the photochemical transformation of a non-fluorescent or weakly fluorescent analyte into strongly fluorescent photoproduct(s) by using UV irradiation [11-16].

By coupling PIF and Solid Phase Spectrometry (SPS), the selectivity and sensitivity of the method can be increased. The combination of both methodologies allows both photodegradation of TMX and sorption of the fluorescent photoproduct generated on a suitable support placed in a commercial flow cell. Moreover, the implementation of SPS with Flow Injection Analysis (FIA), called Flow Injection-Solid Phase Spectroscopy (FI–SPS), has become a promising research area which is based on the selective on-line retention of the analyte or a derivate on an appropriate solid support and the direct measurement of its light absorption or emission (PIF in this case). Multicommutated Flow Injection Analysis (MCFIA) [17-19], which was designed making use of three-way solenoid valves automatically-controlled by a computer with home-made software, is a novel and interesting alternative to FIA. MCFIA, in addition to provide better results, has low-cost components, low consumption of reagents, high repeatability and sample throughput, robustness and simplicity of the system.

The objective of the study was the development of an original analytical approach based in the coupling of MCFIA-SPS-PIF methodologies. To our best knowledge, no photochemical reaction has been reported to date for the quantitative determination of TMX. The proposed system was successfully used to analyze this compound in different vegetables samples (spinach, lettuce and peppers). Taking into account that QuEChERS (quick, easy, cheap, effective, rugged and

safe) [20] approach represents the most commonly applied extraction method for the determination of pesticide residues in food samples, this one has been used as sample pre-treatment to extract and separate TMX from some interfering substances present in the matrix of the selected applications.

2. Experimental

2. 1. Instrumentation

Luminescence measurements were performed with a Cary-Eclipse Luminescence Spectrometer (Varian Inc., Mulgrave, Australia). The spectrometer was connected to a computer with a Cary-Eclipse (Varian) software package for data collection and treatment. Instrument excitation and emission slits were set at 10 and 10 nm, respectively. The detector voltage was 640V.

A Hellma flow cell 176.752-QS (25 μL of inner volume and a light path length of 1.5 mm) was used. The cell was filled with C_{18} silica gel microbeads, and was blocked at the outlet with glass wool to prevent displacement of the resin particles.

MCFIA system was built using a four-channel Gilson Minipuls-3 (Villiers Le Bel, France) peristaltic pump with rate selector and methanol-resistant pump tubes type Solvflex (Elkay Products, Shrewsbury, MA, USA). An electronic interface based on ULN 2803 integrate circuit was employed to generate the electric potential (12V) and current (100 mA) required to control the four 161T031 NResearch

three-way solenoid valves (Neptune Research, MA, USA). The software for controlling the system was written in Java.

A home-made continuous photochemical reactor was constructed by coiling PTFE tubing (180 cm, 0.8 mm i.d.) around a low-pressure mercury lamp (15 W, 254 nm). It was placed into an aluminium box to permit the maximum reflectance of UV light. Since the aluminium foil allowed the heat dissipation, no cooling device was needed and all the experiments were carried out at room temperature.

PTFE tubing and fittings were used for connecting the flow-through cell, the rotary valves and the solutions reservoirs.

A Mili-Q-Plus ultra-pure water system from Millipore (Milford, MA, USA) was used to obtain the HPLC-grade water used during all the experiments. A Sonorex Digital 10P (Bandelin Electronic, Berlin, Germany) ultrasonic bath, a pH-meter Crison GLP 21 (Crison Instruments, Barcelona, Spain) and a centrifuge Mixtasel-BL (Selecta, Barcelona, Spain) were also used.

For the validation of the proposed method, a high-performance liquid chromatography-ion trap-mass spectrometry (HPLC-ESI-IT-MS) method was used as reference. The HPLC system (consisting of vacuum degasser, autosampler, binary pump and diode array detector) (Agilent Series 1100, Agilent Technologies, Santa Clara, CA, USA) was equipped with a reversed phase Kinetex core–shell C_{18} analytical column of 50×2.1 mm and 2.6 μm particle size (Phenomenex, Torrance, CA, USA). A C_{18} Security Guard Ultra cartridge (Phenomenex) of 2.1 mm i.d. was also placed before the analytical column. The wavelength range was set at 210–520 nm in the diode

array detector. One microliter of extract was injected in each analytical run. The best separation was achieved by using a mobile phase consisting of methanol–formic acid (100:0.1, v/v) (A) and water–formic acid (100:0.1, v/v) (B). The following gradient program, with a total run time of 16 min, was used: 30 % A (0 min), 100 % A (8 min) and 30 % A (10-16 min). The mobile phase flow rate was 0.25 mL min^{-1}. The HPLC system was connected to an ion-trap mass spectrometer (Esquire 6000, Bruker Daltonics, Billerica, MA, USA) equipped with an electrospray interface operating in positive ion mode. The identification of TMX was done by using the protonated molecule of TMX ($[M+H]^+$, m/z 292). For the quantitation and construction of the analytical curve, the product ion at m/z 211 was used. The ESI conditions were as follows: capillary voltage 4000 V; nebulizer pressure 40 psi; dry gas 9 L min^{-1}; gas temperature 350 °C. A capillary exit voltage of 50.0 V was set. The instrument was operated in product ion scan MS/MS mode.

2.2. Reagents and solutions

TMX (99.6%) was purchased from Fluka (Sigma-Aldrich, Madrid, Spain). Stock solution of 150 μg mL^{-1} of this analyte was prepared in Mili-Q water (Sigma, Madrid, Spain). The solution was kept in dark at about 4 ºC. Working solutions were prepared daily by suitable dilution with Mili-Q water.

MeOH, acetonitrile, acetic acid, hydrochloric acid (HCl), anhydrous sodium acetate, sodium hydroxide (NaOH), sodium carbonate 10-hydrate ($Na_2CO_3 \cdot 10H_20$), sodium hydrogen carbonate

($NaHCO_3$), ammonium chloride (NH_4Cl), ammonia (NH_3), graphitized carbon (GCB), primary secondary amine (PSA) and anhydrous magnesium sulphate ($MgSO_4$) were obtained from Sigma. Sodium Dodecyl Sulfate (SDS) and Triton X-100 were purchased from Panreac (Barcelona, Spain). All of them were analytical reagent grade. Isolute QuEChERS extraction kit was acquired from Biotage (Sweden).

Sephadex-SP C-25 in sodium form, Sephadex-QAE A-25, Sephadex-CM C-25, all of them 40–120 μm average particle size (Sigma–Aldrich, Buchs, Switzerland) and C_{18} bonded phase silica gel beads (Waters, Milford, USA) with 55–105 μm of average particle size, were tested as solid supports.

2.3. Sample treatment

Vegetable samples were obtained from local markets. ‘‘Blank’’ extracts were used to prepare matrix-matched standards for optimization purposes. TMX was analyzed in 2 types of lettuce, spinach, red and green pepper. Before performing the extraction procedure, approximately 500 g of each sample were thoroughly ground, homogenized, and stored at 20º C until use.

Two types of the QuEChERS extraction procedures were applied. The first one was used for pigmented vegetable samples (peppers and spinach). This one was based on the original QuEChERS extraction method [20] but modified to eliminate the high influence of the extracted pigments [21]. In this method, 10 g of sample were weighed in a 50 mL PTFE centrifuge tube. Acetonitrile (10 mL) was added and the samples were shaken vigorously for 5 min to ensure the

solvent interacted adequately with the entire samples. The sample tubes were then stored in a freezer at -20º C for 20 min, taken out and then vortexed vigorously for 1 min. After that, 4 g $MgSO_4$ and 1 g NaCl were added, and the samples were vortexed immediately for 1 min. The extracts were then centrifuged for 5 min at relative centrifugal force (RCF) 4000 rpm. Then, a volume of 1.5 mL of prepared aliquot from the upper layer was transferred into a 2 mL centrifuge tube containing an amount of sorbent (10 mg GCB + 150 mg $MgSO_4$ for green pepper and 30 mg GCB + 150 mg $MgSO_4$ for red pepper and spinach). Finally, samples were again vortexed for 1 min and then centrifuged for 5 min at 3000 rpm.

The second extraction procedure, a QuEChERS extraction kit (Isolute QuEChERS), was used for slightly pigmented samples such as lettuce. For this method, 10 g of sample were weighed in a 50 mL PTFE centrifuge tube and acetonitrile (10 mL) was added. Then, the content of 15 mL tube extraction kit (4 g $MgSO_4$, 1 g $Na_3C_6H_5O_7$, 0.5 g $Na_2C_6H_6O_7 \cdot 1.5H_2O$ and 1 g NaCl) were added, and the samples were vortexed immediately for 1 min. The extracts were then centrifuged for 5 min at 4000 rpm. Then, a volume of 6 mL of prepared aliquot from the upper layer was transferred into a 15 mL dSPE (dispersive solid phase extraction) tube containing an amount of sorbent (150 mg PSA and 900 mg $MgSO_4$) and samples were again vortexed for 1 min and then centrifuged for 5 min at 4000 rpm.

In both extraction procedures an appropriate volume of the obtained extract was further diluted with deionized water previous to analysis by the proposed method.

2.4. General procedure

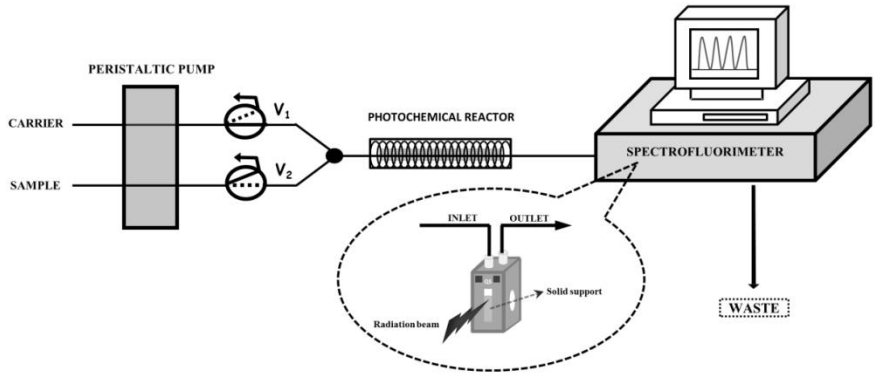

Fig. 1. Multicommutated flow-injection system, in which V_n=3-way solenoid valve n. Step 1: Sample's introduction, flowing through the photodegradation system to flow-cell. Step 2: The fluorescent photoproduct was transitorily retained and its relative fluorescence intensity was registered. Step 3: The system was returned to its initial position.

In **Fig. 1,** the manifold is shown. Each three-way solenoid valve can adopt two positions, "on" and "off", being the whole system assimilated to an electronic circuit with a variable number of active nodes. A flow-rate of 1.7 mL min^{-1} was used in all experiments. In the initial status, the carrier (MeOH:H_2O 25:75 (v:v)) was flowing through the flow-through cell while the sample wasbeing recycled to its respective vessel. The sample was introduced by simultaneously switching on valves V_1 and V_2 for 180 s (4.2 mL) (step 1). The sample solution was carried to the photoreactor where the photoconversion of TMX into a fluorescent compound took place (50 s, without stopping the flow). Afterwards, the fluorescent photoproduct reached the solid support placed in the flow-cell, was transitorily retained and its relative

fluorescence intensity was registered at 353/407 nm/nm (step 2). Finally, the system was returned to its initial position, flowing the carrier again and eluting itself the photoproduct from the solid support (step 3). In this way, the system remained ready for the next sample insertion.

Calibration standards and samples were analyzed by triplicate. The analytical signal was expressed as peak height mean values.

3. Results and discussion

3.1. Spectral characteristics and solid support

Preliminary experiments for evaluation of the effect of direct UV irradiation on TMX solutions revealed the formation of a fluorescent photodecomposition product in alkaline medium. Spectra of both TMX and fluorescent photoproduct in homogeneous solution are shown in Figure 2. As can be seen, TMX emission fluorescence is negligible. With the purpose of retaining the fluorescent photoproduct on a solid support several solid supports were tested. As the structure of this one was unknown, solid supports of different nature were checked, cationic (Sephadex SPC-25, Sephadex CMC-25), anionic (Sephadex QAE-A) and non-ionic ones (C_{18} silica gel). Finally, C_{18} silica gel was selected because the fluorescent photoproduct was strongly retained on it. No significant retention was observed on the rest of solid supports tested.

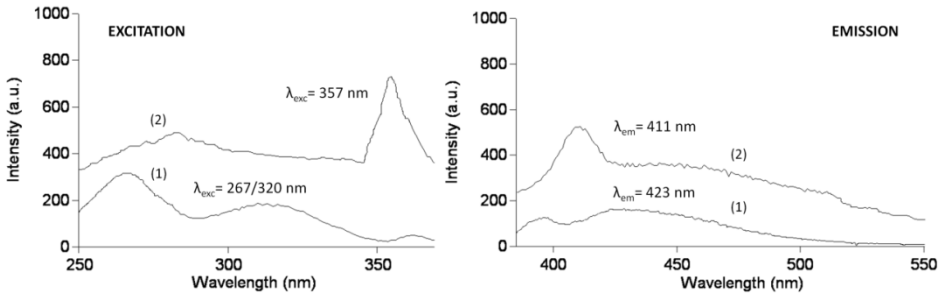

Fig. 2. Fluorescence spectra of TMX and its photoproduct. (1) TMX in homogeneous solution (20 μg mL^{-1}). (2) Photoproduct of TMX in homogeneous solution (2 μg mL^{-1} of TMX). Irradiation time: 50 s.

The photoproduct retained on the solid support chosen showed an emission peak at 407 nm and an excitation peak at 353 nm. The sorption of the fluorescent photoproduct of TMX on C_{18} silica gel and the consequent preconcentration process on this latter in the detector area itself provided a drastic enhancement in the analytical signal: 10-fold higher than that obtained in homogeneous solution under the same working conditions. The sensitivity obtained is the result of the retention of the analyte on a very little amount of solid support. It is necessary to point out that the cell was filled with the minimum amount of solid support, sufficient to allow the light beam to pass completely through it.

In order to ensure that the upper part of the solid support was just in the light path, the level of the resin packed in the flow cell had to be delicately selected to obtain the best sensitivity. Before starting the measuring process the carrier solution was passed through the sensing zone in order to condition it.

3.2. Instrumental variables

Luminescence measurements carried out in solid-phase media are usually affected by background signal, obviously due to the presence of the solid support in the irradiated zone. Therefore, instrumental parameters have to be carefully investigated in order to achieve the best possible signal-to-background ratio. For this reason, the instrument excitation and emission slit widths (5-20 nm) on the analytical signal and the influence of the voltage of the photomultiplier tube (400-800 V) had to be studied. The photomultiplier tube voltage was set at 640 V and the excitation and emission slit widths were fixed at 10 and 10 nm, respectively.

3.3. Chemical variables

The pH in sample solutions is a critical variable both in the generation of fluorescent photoproducts from an analyte and the sorption of a species on a solid support, so its value was studied over a range between 2.0 and 12.0, adjusting these pHs with HCl or NaOH solutions. It was observed that the rate of photodegradation of TMX was highly dependent on the pH.

As shown in **Fig. 3**, the peak height was maximum and constant around 9-10, and decreased outside this range. Although the structure of the fluorescent photoproduct generated is unknown, its retention on C_{18} silica gel at this pH value probably indicates a non-ionic character. Different buffer solutions at pH values between 9.0 and 10.0 ($Na_2CO_3/NaHCO_3$ and NH_3/NH_4Cl) were tested, but the maximum signal was obtained adjusting the pH of the sample with a $5x10^{-3}$ mol L^{-}

[1] NaOH solution. After the photoproduct was retained on the solid support and its analytical signal was recorded, it was totally eluted by the carrier solution in a time interval of 40 s, approximately, so it was not necessary an eluting solution in any type of real samples.

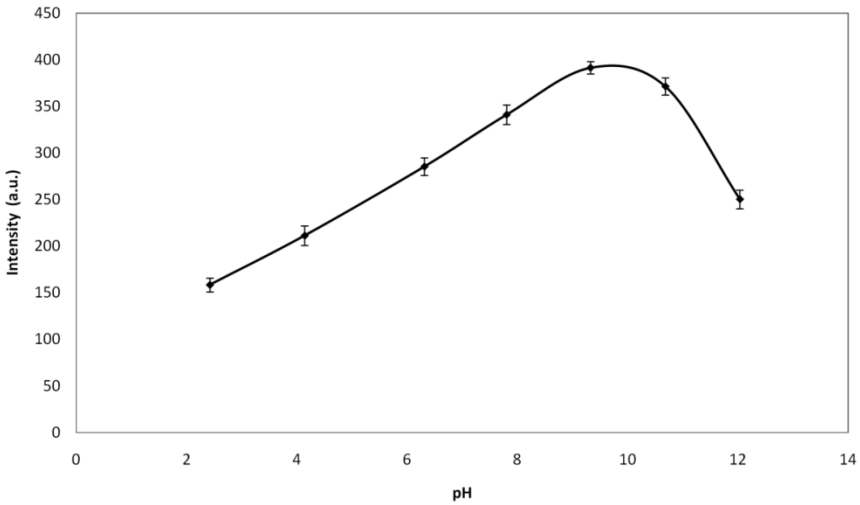

Fig. 3. Influence of pH of the sample. [TMX]= 400 ng mL^{-1}, irradiation time= 50 s.

The use of surfactant into the sample solution was studied to check the increase in the analytical signal. SDS and Triton X-100 were tested, observing higher sensitivity when SDS was used. For this reason its concentration was optimized by injecting in the system TMX solutions with increasing amounts of SDS (10^{-3}-10^{-2} mol L^{-1}). Finally, a $6x10^{-3}$ mol L^{-1} SDS solution was selected since it provided the highest analytical signal. Higher and lower surfactant concentrations caused a decreasing in the fluorescence signal. However, with the optimal concentration the signal increased only around 7 %. For this reason, being a harmful product, its use was not justified on routine analysis.

The nature of carrier and eluting solutions were other chemical variables under investigation. Taking into account the non-polar nature of C_{18} silica gel beads, several carrier solutions were tested containing methanol and water in different proportions, ranging from 0 to 50 % MeOH (v:v). According to **Fig. 4**, by increasing the concentration of methanol, the signal increased to a concentration of 25 % and then this signal decreased. At low concentrations the photoproduct did not reach the detection zone but an increase in % of methanol allowed the photoproduct reached this area, so obtaining the corresponding analytical signal. However, when methanol concentration was above 25% photoproduct elution was stronger than its own retention on the solid support. Regard to the peak time, higher concentrations of methanol produced higher sampling frequencies due to the quicker elution of the fluorescent photoproduct by the carrier itself. The best overall results were obtained with 25 % MeOH (v:v) solution, obtaining satisfactory sensitivity and complete desorption of the photoproduct from the support, so, finally, this percentage of methanol concentration was chosen as a compromise between sensitivity and throughput.

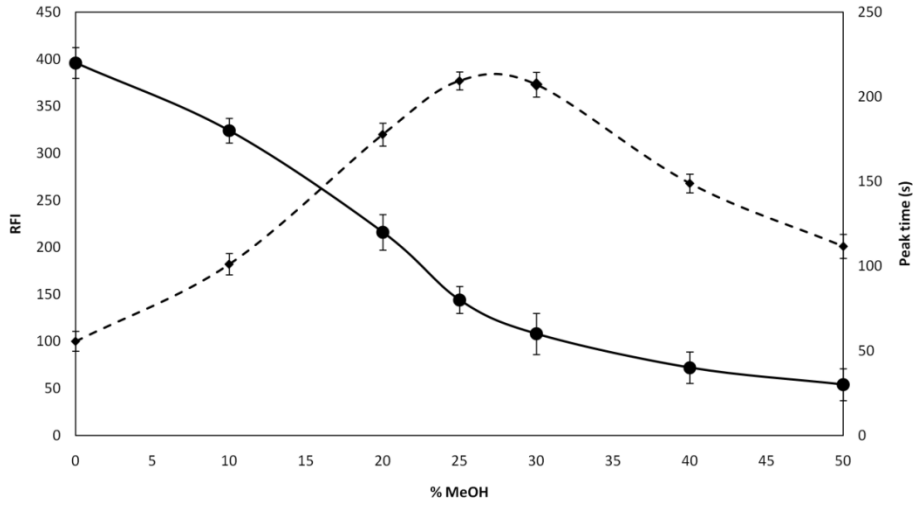

Fig. 4. Influence of methanol percentage in the carrier stream on (—) peak time and (- - -) relative fluorescence intensity (RFI).

3.4. Flow system variables

The sample introduction time and the flow-rate of the peristaltic pump were the flow variables studied.

In MCFIA-SPS systems sensitivity can be improved by increasing the sample volume injected. This is a consequence of the sorption of a higher amount of the species monitored on the same amount of solid support as the injection volume increases. This effect also allows working in a wider concentration range and makes possible to reduce the matrix effect by performing only an appropriate dilution of the sample. However, it is necessary to take also into account that the increase of the injection volume entails a simultaneous increase in

time of analysis and, consequently, both sensitivity and throughput have to be considered in the selection of this parameter. The study of the influence of this variable was carried out by injecting in the system different volumes of a 150 ng mL^{-1} TMX solution through different sample insertion times (range of 20–240 s). The fluorescence signal increased linearly with insertion time up to 180 s. Higher volumes did not provide a significant increase in the PIF signal. 180 s was selected as optimum insertion time of sample.

Also, the influence of the flow-rate was investigated from 1 up to 2 mL min^{-1}. A slight increase in the fluorescence signal was obtained for increasing flow-rate and the sampling frequency increased too. Nevertheless, flow-rates higher than 1.7 mL min^{-1} originated overpressure problems in the flow system due to the use of the solid support; for this reason this flow-rate value was finally chosen.

3.5. Optimization of the extraction and cleanup procedure

Two types of QuEChERS extraction methods were studied and a comparison was performed in order to obtain good final results.

The first one consisted in a modification of the conventional QuEChERS extraction method, described in Section 2.3, in order to improve the extraction of samples containing high amount of pigments which influenced in final recoveries. In our case, this procedure was used for spinach and peppers samples. Two different types of sorbent, PSA and GCB, were tested to investigate influence on recovery in the cleanup step. PSA has a weak anion exchange function and applies to remove various polar organic acids, polar pigments, some sugars and

fatty acid from the non-polar samples, which are mainly used for phase extraction. On the other hand, GCB is a weakly polar or non-polar sorbent, mainly used to remove hydrophobic interaction-based compounds, such as chlorophyll and carotenoids. Finally, GCB was selected because recoveries were better than using only PSA or PSA+GCB. Different levels of GCB (0-40 mg) were used to adsorb the pigments in sample extracts. Best recoveries were obtained in the presence of 10 mg GCB for green pepper and 30 mg CGB for red pepper and spinach (highly pigmented samples). The comparison for different samples can be seen in **Fig. 5**. Specifically, final recoveries ranged between 95 and 105 % were obtained. When this procedure was applied to lettuce samples, recoveries were less than 85 % and higher than 110 %.

The second extraction procedure was employed for lettuce samples because final recoveries for these samples were close to 100 % without the use of later clean-up with GCB. The absence of strong pigments in this kind of samples is the cause that this method reduces the cost of the reagents and time of pretreatment. With this procedure, recoveries ranged between 97 and 102 %. When this procedure was applied to spinach and pepper samples, recoveries were less than 80 % and higher than 115 %.

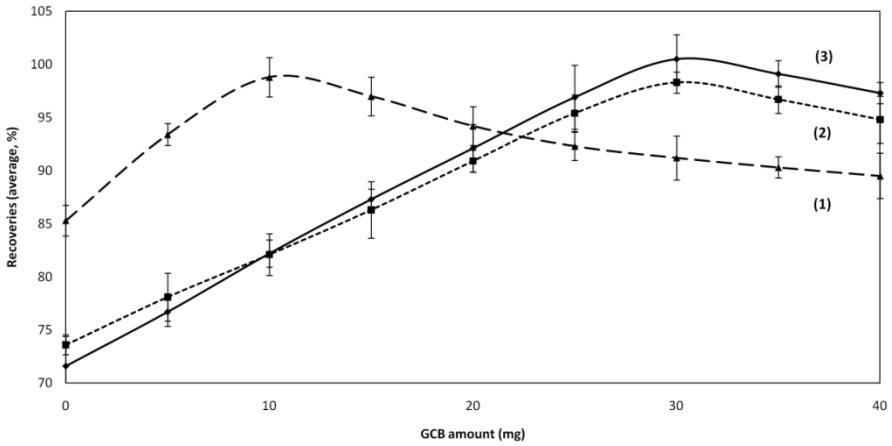

Fig. 5. Influence of GCB amount in final recoveries for vegetables samples. [TMX]= 600 ng mL^{-1}. Samples: (1) green pepper; (2) red pepper; and (3) spinach.

3.6. Photodegradation variables

One of the principal key variables is the irradiation time for the generation of fluorescent photoproducts. To establish the optimum irradiation time, a 500 ng mL^{-1} TMX solution was inserted into the system (sampling time, 180 s; flow rate, 1.7 mL min^{-1}), the flow was stopped just when the whole plug of sample was within the photoreactor (180 cm), and the sample was irradiated for increasing periods of time (10 to 100 s). The results showed that the kinetic of photodegradation of TMX in the working conditions is quite quick. The fluorescence signal increased with the irradiation time to reach a maximum value corresponding to the optimum value of this variable (50 s), and thereafter a decrease in fluorescence intensity was obtained. The shape of the curve obtained suggests a two-step photolysis

mechanism, consisting of the formation of a strongly fluorescent photoproduct and the posterior photodegradation of the latter compound into nonfluorescent product(s). Higher flow rates combined with longer photoreactors were assayed but overpressure problems in the system and a poor precision were observed. The use of lower flow rates combined with shorter photoreactors provided higher analytical signals but a decrease in throughput. The length of the transport system between the photochemical reactor and the flow cell was the minimum, allowing both units to be connected.

The effect of the temperature on the fluorescence intensity was also examined. Such an effect is of great theoretical significance and practical benefit. Increasing the temperature increases molecular thermal motion, thereby also increasing the probability of radiationless transitions and reducing the fluorescence quantum yield as a result. The influence of temperature was studied over the range 15−45 °C. As expected, the fluorescence intensity decreased as the temperature was raised. But it happened only when temperature was higher than 35 ºC. Because no significant heating is observed, the procedure was developed at room temperature.

3.7. Analytical parameters and study of foreign species

The analytical parameters of the system were studied (**Table 1**). The calibration curve was constructed by following the procedure above described after injecting sample solutions in triplicate, containing increasing concentrations of TMX. The data were fitted by standard

least-squares treatment and the quantification was carried out by using peak height as analytical signal.

Table 1. Analytical parameters.

Parameter	
Excitation/ emission slits (nm/nm)	10/10
Photomultiplier tube voltage (V)	640
Calibration graph	
Intercept	58.131
Slope (mL ng^{-1})	0.7662
Correlation coefficient	0.9972
Linear dynamic range (ng mL^{-1})	12-600
Detection limit (ng mL^{-1})	3.6
Quantitation limit (ng mL^{-1})	12
Intra-day RSD (%) (n=10)	
30 ng mL^{-1}	2.2
150 ng mL^{-1}	1.6
Inter-day RSD (%) (n=10)	
100 ng mL^{-1}	4.8
300 ng mL^{-1}	4.3
Sample throughput, h^{-1}	17

The proposed methodology replied linearly in the concentration range 12–600 ng mL^{-1}. The detection and quantification limits were 3.6 and 12 ng mL^{-1}. These limits were estimated as the concentration of analyte which produced an analytical signal equal to three and ten times, respectively, the standard deviation of the background fluorescence. The intra-day repeatability was established for ten independent analyses of sample solutions containing 30 and 150 ng mL^{-1} of TMX, RSDs being lower than 2.5 %. The inter-day repeatability was also performed for ten consecutive days by two different analysts, obtaining RSDs lower than 5 %. Method accuracy and recovery were evaluated by addition of standard solutions in "blank" vegetables.

The potential influence in the analytical signal from other species that might accompany the analyte in real samples was studied. The tolerance level was established as the maximum amount of foreign species that produced an error not exceeding ±3%. The study was focused on cations, anions, other fluorescent pesticides as *o*-phenylphenol, carbendazim and carbaryl, and the photodegradable pesticides thiacloprid, imidacloprid and clothianidin, commonly used in agriculture. Results are summarized in **Table 2**. Good tolerances were obtained due to the use of the solid support in the flow-cell. The use of this one increased the tolerance to tested compounds up to 10-fold, except in the case of clothianidin. Nevertheless, this neonicotinoid, from the same family and with similar structure to TMX, usually appears not together TMX in real samples.

Table 2. Study of interferences.

Foreign species	**Tolerance level (foreign species/analyte, w/w)**
Na^{+}, K^{+}, NH_4^{+}, Ca^{2+}, Mg^{2+}, Al^{3+}, SO_4^{2-}, Cl^{-}, HCO_3^{-}, PO_4^{3-}, NO^{3-}	1000[a]
O-phenylphenol	35
Carbendazim	25
Carbaryl, thiacloprid	20
Imidacloprid	10
Clothianidin	3

[a]Maximum ratio tested.

3.8. Analytical applications

To perform the recovery studies, fortified vegetable samples were prepared. Real samples were spiked with known amounts of TMX with concentrations (0.6-10 mg kg^{-1}) close to the established MRLs in these vegetables (lettuce: 5 mg kg^{-1}, spinach: 3 mg kg^{-1}, peppers: 0.7 mg kg^{-1}). In all the studied samples, recoveries values between 96% and 103% were obtained, as it can be observed in detail in **Table 3**, obtaining RSDs lower than 3% in all cases.

Table 3. Recovery studies of TMX in vegetables.

Sample	Spiked (mg kg^{-1})	Recovery (%)	RSD (%)
Spinach 1	2	98.7	1.8
	3	100.5	1.6
	7	98.5	0.3
Spinach 2	2.5	101.3	1.1
	4	103.0	0.7
	9	99.7	1.7
Lettuce 1	1	103.0	1.5
	4	100.9	0.9
	7	99.2	0.5
Lettuce 2	2	98.4	1.7
	5	101.8	2.2
	10	100.2	1.1
Red pepper 1	0.7	97.4	0.3
	3	99.5	1.6
	5	100.7	1.3
Red pepper 2	0.7	98.4	1.7
	4	96.9	2.3
	8	100.4	0.9
Green pepper 1	0.6	96.1	0.6

	1	98.8	1.1
	5	98.1	0.5
Green pepper 2	0.6	97.7	2.1
	2	98.3	1.0
	6	96.8	0.8

The statistical study of the accuracy was carried out comparing the obtained results with an HPLC-ESI-IT-MS reference method. Same samples were analyzed, but only one from each vegetable was taken as representative for the analysis. Samples were prepared as described in section 2.3 and analyzed in triplicate. The results of the proposed method were compared with those obtained with this one by means of a t-test and F-criterion, showing that there is no significant statistical difference between the values obtained by both methods and indicating the utility of the proposed method for routine analytical control (**Table 4**).

Table 4. Comparison with a HPLC-ESI-IT-MS reference method.

Sample	**Amount found [a] (ng mL^{-1})**		**t_{calc}[b]**	**F_{calc}[c]**
	Proposed method	Reference method		
Lettuce	248	253	1.93	1.00
Spinach	245	251	2.87	4.00
Green pepper	247	253	1.98	0.33
Red pepper	248	254	2.18	0.59

[a] Average of three determinations for 250 ng mL^{-1}.

[b] Theoretical value for t=4.30 (P=0.05).

[c] Theoretical value for F=39.00 (P=0.05).

4. Conclusions

A new, sensitive and selective flow-through method has been developed for the determination of TMX in vegetables by using the QuEChERS sample pre-treatment. A strongly fluorescent photoproduct generated in alkaline medium from TMX, after UV-irradiation through a PIF system, is reversibly retained on an appropriate solid support placed in the flow-cell of the detection area. This sensor allows the analysis of TMX concentrations below the MRL established by the European Commission for the analyzed samples and can be used as an alternative green method for the determination of TMX in vegetables with good recoveries close to 100%.

Usually, chromatographic techniques are employed for the quantitation of TMX, due to the high selectivity and sensitivity achieved. However, the results here presented show that other alternative methods such as the proposed one can also be useful for the determination of this analyte in vegetables. From our point of view, the implementation of MCFIA-SPS-PIF is a very attractive and fruitful research field, since these approaches are appropriate as pre-screening methods, in order to reduce the number of samples which need to be processed through conventional chromatographic methods.

Acknowledgements

J.J.L. acknowledges research scholarship from Spanish Government (Ministerio de Educación y Ciencia).

References

[1] http://www.efsa.europa.eu/en/efsajournal/doc/3918.pdf, Accesed March-2015.

[2] http://eurlex.europa.eu/LexUriServ/LexUriServ.do?uri=OJ:L:2013:139:0012:0026: EN:PDF, Accesed March-2015.

[3] http://europa.eu/rapid/press-release_IP-13-379_en.htm, Accesed March-2015.

[4] G.C.R.M. Andrade, S.H. Monteiro, J.G. Francisco, L.A. Figueiredo, R.G. Botelho, V.L. Tornisielo, Liquid

chromatography-electrospray ionization tandem mass spectrometry and dynamic multiple reaction monitoring method for determining multiple pesticide residues in tomato, Food Chem. 175 (2015) 57-65.

[5] P. Jovanov, V. Guzsvány, M. Franko, S. Lazić, M. Sakač, I. Milovanović, N. Nedeljković, Development of multiresidue DLLME and QuEChERS based LC-MS/MS method for determination of selected neonicotinoid insecticides in honey liqueur, Food Res. Int. 55 (2014) 11-19.

[6] M.M. Rahman, W. Farha, A.M. Abd El-Aty, M.H. Kabir, S.J. Im, D.I. Jung, J.H. Choi, S.W. Kim, Y.W. Son, C.H. Kwon, H.C. Shin, J.H. Shim, Dynamic behaviour and residual pattern of thiamethoxam and its metabolite clothianidin in Swiss chard using liquid chromatography-tandem mass spectrometry, Food Chem. 174 (2015) 248-255.

[7] D. Tomasini, M.R.F. Sampaio, S.S. Caldas, J.G. Buffon, F.A. Duarte, E.G. Primel, Simultaneous determination of pesticides and 5-hydroxymethylfurfural in honey by the modified QuEChERS method and liquid chromatography coupled to tandem mass spectrometry, Talanta 99 (2012) 380-386.

[8] F.P. Costa, S.S. Caldas, E.G. Primel, Comparison of QuEChERS sample preparation methods for the analysis of pesticide residues in canned and fresh peach, Food Chem. 165 (2014) 587-593.

[9] E.H.D.C. Morais, A.A.Z. Rodrigues, M.E.L.R.D. Queiroz, A.A. Neves, P.H.D. Morais, Determination of thiamethoxam,

triadimenol and deltamethrin in pineapple using SLE-LTP extraction and gas chromatography, Food Control 42 (2014) 9-17.

[10] P. Chorti, J. Fischer, V. Vyskocil, A. Economou, J. Barek, Voltammetric determination of insecticide thiamethoxam on silver solid amalgam electrode, Electrochim. Acta 140 (2014) 5-10.

[11] J. López Flores, M.L. Fernández De Córdova, A. Molina Díaz, Flow-through optosensing device implemented with photochemically-induced fluorescence for the rapid and simple screening of metsulfuron methyl in environmental waters, J. Environ. Monitor. 11 (2009) 1080-1085.

[12] O.M.A. Mbaye, M.D. Gaye Seye, A. Coly, A. Tine, M.A. Oturan, N. Oturan, J.J. Aaron, Photo-induced fluorescence properties of the propanil herbicide and analytical usefulness, Microchem. J. 110 (2013) 579-586.

[13] L. Molina-García, M.L. Fernández-de Córdova, A. Ruiz-Medina, Indirect determination of aflatoxin B1 in beer via a multi-commuted optical sensor, Food Addit. Contam. Part A Chem. Anal. Control Expo. Risk Assess. 29 (2012) 392-402.

[14] D.L. Rocha, M.Y. Kamogawa, F.R.P. Rocha, A critical review on photochemical conversions in flow analysis, Anal. Chim. Acta 896 (2015) 11-33.

[15] E.J. Llorent-Martínez, M.L. Fernández-de Córdova, P. Ortega-Barrales, A. Ruiz-Medina, Analysis of Agroalimentary and

Environmental Contaminants Using Flow-Through Chemical Optosensors, Appl. Spectrosc. Rev. 50 (2015) 527-556.

[16] P.A. Diaw, O.M.A. Mbaye, M.D. Gaye-Seye, J.J. Aaron, A. Coly, A. Tine, N. Oturan, M.A. Oturan, Photochemically-induced fluorescence properties of two benzoyl- and phenylurea pesticides and determination in natural waters, J. Fluoresc. 24 (2014) 1319-1330.

[17] J. Jiménez-López, E.J. Llorent-Martínez, P. Ortega-Barrales, A. Ruiz-Medina, Multi-commutated fluorometric optosensor for the determination of citrinin in rice and red yeast rice supplements, Food Addit. Contam. Part A Chem. Anal. Control Expo. Risk Assess. 31 (2014) 1744-1750.

[18] E.J. Llorent-Martínez, P.O. Barrales, M. Luisa Fernández-de Córdova, A. Ruiz-Medina, Multicommutation in flow systems: A useful tool for pharmaceutical and clinical analysis, Curr. Pharm. Anal. 6 (2010) 53-65.

[19] E.J. Llorent-Martínez, P. Ortega-Barrales, M.L. Fernández-de Córdova, A. Ruiz-Medina, Trends in flow-based analytical methods applied to pesticide detection: A review, Anal. Chim. Acta 684 (2011) 30-39.

[20] M. Anastassiades, S.J. Lehotay, D. Štajnbaher, F.J. Schenck, Fast and easy multiresidue method employing acetonitrile extraction/partitioning and "dispersive solid-phase extraction" for the determination of pesticide residues in produce, J. AOAC Int. 86 (2003) 412-431.

[21] Y. Zhang, J. Xu, F. Dong, X. Liu, X. Li, Y. Li, X. Wu, X. Liang, Y. Zheng, Simultaneous determination of four neonicotinoid insecticides residues in cereals, vegetables and fruits using ultra-performance liquid chromatography/tandem mass spectrometry, Anal. Method. 5 (2013) 1449-1455.

A photochemically induced fluorescence based flow-through optosensor for screening of nitenpyram residues in cruciferous vegetables

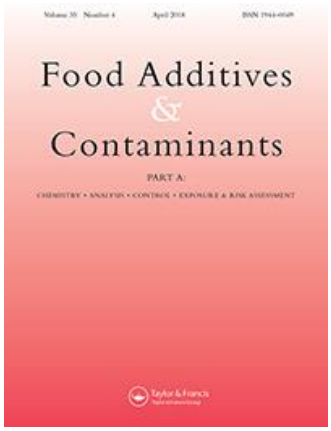

4. "A photochemically induced fluorescence based flow-through optosensor for screening of nitenpyram residues in cruciferous vegetables"

J. Jiménez-López, P. Ortega-Barrales, A. Ruiz-Medina*

Publicado en Food Additives & Contaminants: Part A, en Febrero de 2018, volumen 35, páginas 1-9.

Resumen

En este trabajo se ha determinado uno de los agroquímicos más utilizados en la producción agrícola, el nitenpiram (NTP), mediante el uso de un optosensor en flujo empleando la fluorescencia inducida fotoquímicamente (PIF) como técnica de detección. La combinación de los optosensores en flujo (en este caso, utilizando Análisis de Inyección por Flujo Multiconmutado) y el PIF permite, por un lado, una rápida fotodegradación en línea del NTP y, por otro lado, la preconcentración, la cuantificación y la desorción del fotoproducto fluorescente generado cuando se retiene en Sephadex QAE-A25 como soporte sólido. Las medidas analíticas se llevaron a cabo a longitudes de excitación y emisión de 295 y 362 nm, respectivamente.

El método analítico propuesto presentaba un límite de detección de 500 pg mL^{-1} y un rango dinámico lineal de 2 a 300 ng mL^{-1}. Se

llevaron a cabo estudios de recuperación (fortificando a niveles similares a los límites máximos de residuos) en diferentes tipos de vegetales de la familia de los crucíferos, obteniendo recuperaciones cercanas al 100% en todos los casos. Además, los resultados obtenidos se compararon con un método de referencia cromatográfico.

El método desarrollado podría ser una alternativa interesante a la determinación cromatográfica del analito, ya que presenta unos límites de detección similares a los que presentan estudios desarrollados con métodos cromatográficos. Además, el método presenta una alta frecuencia de muestreo (18 muestras por hora), no requiere de instrumentación costosa, y es sencillo de utilizar. Podría ser también considerado como un sistema analítico respetuoso del medio ambiente para la determinación de los residuos de nitenpiram debido a la mínima generación de residuos y al bajo consumo de reactivos durante el análisis, siendo adecuado para el análisis de rutina en controles de calidad.

4. "A photochemically induced fluorescence based flow-through optosensor for screening of nitenpyram residues in cruciferous vegetables"

Abstract

One of the most used agrochemicals in agricultural production, nitenpyram (NTP), has been determinated by using a flow-through optosensing device based on Photochemically Induced Fluorescence (PIF) detection. The combination of both methodologies allows, on one hand, a quick on-line photodegradation of NTP and, on the other hand, the preconcentration, quantification and desorption of the fluorescent photoproduct generated once retained on Sephadex QAE-A25 as solid support, which was monitored at 295 and 362 nm for excitation and emission wavelengths, respectively.

The proposed analytical method presents a detection limit of 500 pg mL^{-1} by using Multicommutated Flow Injection Analysis (MCFIA) as flow methodology. Recovery experiments have been carried out in different kinds of cruciferous vegetables at the same levels or below the maximum residue limit (MRL) established in Japan, demonstrating that this method combines advantages such as simplicity, high sensibility and high selectivity, in addition to fulfill the requirements for its applications in quality control. The obtained results in the analysis of real samples were in good agreement with those provided by a reference liquid chromatography (HPLC) method.

Keywords: MCFIA; nitenpyram; photo-induced fluorescence; vegetables; solid-phase spectroscopy

1. Introduction

In recent years, the presence of pesticides, parent compounds and their major metabolites or conversion products has become a serious environmental concern that is affecting food production and, as a consequence, its quality. No particular control or monitoring of the presence of all these compounds is currently performed. The use of neonicotinoids, whose purpose is to kill, repel, or control certain forms of plant or animal life that are considered to be pests, has been rapidly increasing in the agri-food sector. In fact, they are used on more than 140 crop varieties. Last decade, neonicotinoids had taken more than 24% share of the total insecticide market of €6.330 billion, assuming a wide reach within this market. They are applied in a wide variety of settings against pests in soil, seed, turf and timber, as well as treatments for cereals, cotton, legumes, fruits, rice and vegetables.

The determination of nitenpyram (NTP), one of these widely known neonicotinoids, is crucial for the quality control of the foods that are consumed daily. To date, the methods for its determination are liquid chromatography (Jiao, et al., 2016; Jovanov, et al., 2013; Sánchez-Hernández, Higes, Martín, Nozal, & Bernal, 2016), gas chromatography (Zhang, et al., 2010), coupled or not to mass spectrometric detection, and electrochemical methods (Lezi & Economou, 2015; Li, Ma, Cao, & Dong, 2013). Nevertheless, there are no alternative spectroscopic methods for the determination of this pesticide so the development of new strategies for its quantification is

an interesting field. One option is the use of photochemically induced fluorescence (PIF), which eliminates the limitation in the analysis of non-fluorescent pesticides. This detection technique provides excellent features like high reaction rates and low reagent consumption (Coly & Aaron, 1998; Jiménez-López, Ortega-Barrales, & Ruiz-Medina, 2016; L. Molina-García, A. Ruiz-Medina, & M. L. Fernández-de Córdova, 2011). The aim of the present work is to develop a new, sensitive and automatic screening method for the analysis of NTP as alternative to chromatographic methods. The procedure is based on the measurement of the fluorescence of the photoproduct generated by the on-line photodegradation of NTP in a flow system. The generated photoproduct is then retained on a solid support packed in a flow cell, where its analytical signal is monitored (Solid Phase Spectroscopy, SPS) (Capitán-Vallvey, Valencia, & Nicolás, 2003; Llorent-Martínez, Ortega-Barrales, Fernández-de Córdova, & Ruiz-Medina, 2013; Recalde-Ruiz, Andres-Garcia, & Diaz-Garcia, 2000). With the purpose of allowing independent handling of sample and carrier solutions, low sample and reagent consumption and the complete automation of the process, multicommutation principles were chosen for the flow-system (Rocha, et al., 2002). Specifically, Multicommutated Flow Injection Analysis (MCFIA) was used for the development of a flow through optosensor. This strategy presents well-known advantages, such as high sensitivity and selectivity, rapidity and simplicity (Jiménez-López, Llorent-Martínez, Ortega-Barrales, & Ruiz-Medina, 2014; Llorent-Martínez, Barrales, Luisa Fernández-de Córdova, & Ruiz-Medina, 2010; Lucía Molina-García, Antonio Ruiz-Medina, & Maria Luisa Fernández-de Córdova, 2011).

QueChERS method was employed in the sample pretreatment, thereby separating the analyte from other interfering substances present in vegetables. The method was successfully applied to the determination of NTP in cruciferous vegetables (cauliflower, Brussels sprouts, kale and broccoli). Although its maximum residue limit (MRL) is not still legislated for different agricultural products, recommendations have been proposed in official organisms such as Japan Food Chemical Research Foundation (JFCRF, 2017). To our knowledge, this work reports the first non-chromatographic luminiscence analytical method for the analysis of NTP in these products.

2. Experimental

2. 1. Instrumentation

By a Cary-Eclipse Luminescence Spectrometer (Varian Inc., Mulgrave, Australia), luminescence measurements were performed. The spectrometer was connected to a computer with a Cary-Eclipse (Varian) software package for data collection and treatment. The instrumental variable established were: 295 and 362 nm for excitation and emission wavelengths, respectively; 5 and 10 nm for excitation and emission slits, respectively; and 670 V for photomultiplier tube voltage. A Hellma flow cell 176.752-QS (25 μL of inner volume and a light path length of 1.5 mm) was used into the spectrofluorimeter being filled with Sephadex QAE-A25 solid phase microbeads. For preventing displacement of the resin particles, the cell was blocked at the outlet with glass wool.

Using a four-channel Gilson Minipuls-3 (Villiers Le Bel, France) peristaltic pump with rate selector and methanol-resistant pump tubes type Solvflex (Elkay Products, Shrewsbury, MA, USA), MCFIA system was built. An electronic interface based on ULN 2803 integrate circuit was employed to generate the electric potential (12V) and current (100 mA) required to control the four 161T031 NResearch three-way solenoid valves (Neptune Research, MA, USA). The software for controlling the system was written in Java. PTFE tubing and fittings were used for connecting the flow-through cell, the rotary valves and the solutions reservoirs.

A home-made continuous photochemical reactor was constructed by coiling PTFE tubing (180 cm, 0.8 mm i.d.) around a low-pressure mercury lamp (15 W, 254 nm). Placed into an aluminium box, it permits the maximum reflectance of UV light. Since the aluminium foil allowed the heat dissipation, no cooling device was needed and all the experiments were carried out at room temperature.

In order to obtain the HPLC-grade water used during all the experiments, a Milli-Q-Plus ultra-pure water system from Millipore (Milford, MA, USA) was used. A Sonorex Digital 10P (Bandelin Electronic, Berlin, Germany) ultrasonic bath, a centrifuge Mixtasel-BL (Selecta, Barcelona, Spain) and a pH-meter Crison GLP 21 (Crison Instruments, Barcelona, Spain) were also used.

A high-performance liquid chromatography-ion trap-mass spectrometry (HPLC-ESI-IT-MS) method was employed as reference for the validation of the proposed method. This method was adapted from the one proposed by Sánchez-Hernández et al. (Sánchez-Hernández, et al., 2016). The HPLC system (consisting of vacuum

degasser, autosampler, binary pump and diode array detector) (Agilent Series 1100, Agilent Technologies, Santa Clara, CA, USA) was equipped with a reversed-phase Kinetex core–shell C_{18} analytical column of 50×2.1 mm and 2.6 μm particle size (Phenomenex, Torrance, CA, USA). A C_{18} Security Guard Ultra cartridge (Phenomenex) of 2.1 mm i.d. was also placed before the analytical column. The wavelength range was set at 210-520 nm in the diode array detector. One microliter of extract was injected in each analytical run. The best separation was achieved by using a mobile phase consisting of water-formic acid (100:0.1, v/v) (A) and acetonitrile–formic acid (100:0.1, v/v) (B). The following gradient program was used: 90:10% A-B (0 min), 65:35% A-B (8 min), 60:40% A-B (13 min), 0:100% A-B (14 min), 0:100% A-B (15 min), 50:50% A-B (16 min), 90:10% A-B (17 min) and 90:10% A-B (24 min). The mobile phase flow rate was 0.5 mL min^{-1}. The HPLC system was connected to an ion-trap mass spectrometer (Esquire 6000, Bruker Daltonics, Billerica, MA, USA) equipped with an electrospray interface operating in positive ion mode. NTP was identified by using its protonated molecule ($[M+H]^+$, 271 m/z). The product ions at m/z 224 and 99 were used for quantitation of the analyte. The ESI conditions were as follows: capillary voltage 4000 V; nebulizer pressure 40 psi; dry gas 9 L min^{-1}; gas temperature 350 °C. A capillary exit voltage of 50.0 V was set. The instrument was operated in product ion scan MS/MS mode.

2.2. Reagents and solutions

NTP (99.6%) was obtained from Fluka (Sigma-Aldrich, Madrid, Spain). A stock solution of 50 μg mL^{-1} of this analyte was prepared in Milli-Q water (Millipore; Milford, MA). The solution was kept in dark at about 4 ºC and it was stable for at least 1 month in this conditions. Working solutions were prepared daily by appropriate dilution with Milli-Q water.

Acetonitrile, formic acid, ammonium chloride (NH_4Cl), ammonia (NH_3), graphitized carbon (GCB), Primary-secondary amine (PSA), hydrochloric acid (HCl), methanol (MeOH), sodium hydroxide (NaOH), sodium carbonate 10-hydrate ($Na_2CO_3 \cdot 10H_20$), sodium hydrogen carbonate ($NaHCO_3$), sodium phosphate dibasic (Na_2HPO_4) and potassium chloride (KCl) were purchased from Sigma (Sigma-Aldrich, Madrid, Spain). All of them were analytical reagent grade. Isolute QuEChERS extraction kit was acquired from Biotage (Sweden).

Sephadex QAE-A25, Sephadex CMC-25 and Sephadex SPC-25 in sodium form, all of them 40–120 μm average particle size (Sigma–Aldrich, Buchs, Switzerland) and C_{18} bonded phase silica gel beads (Waters, Milford, USA) with 55–105 μm of average particle size, were tested for their optimization as solid supports.

2.3. Sample treatment

Cruciferous vegetable samples were obtained from local markets. In order to prepare matrix-matched standards for optimization purposes, ‘‘blank’’ extracts were used. NTP was analyzed in 3 types of broccoli, Brussels sprouts, cauliflower and kale. Approximately 100 g

of each sample were thoroughly ground, homogenized, and stored at 4º C until use before performing the extraction procedure.

With the purpose of achieving lower detection limits and high sensitivity, a suitable sample clean-up is crucial prior to trace analysis. The QuEChERS extraction procedure was applied in this research (Anastassiades, Lehotay, Štajnbaher, & Schenck, 2003), but with slight modifications, similar to that proposed by our group in a previous research paper (Jiménez-López, Ortega-Barrales, & Ruiz-Medina, 2016). In this way, it was possible to eliminate the high influence of the extracted pigments in the samples.

A QuEChERS extraction kit (Isolute QuEChERS) with the use of Graphitized Carbon Black (GCB), for an improved clean-up, was used for all food samples. This non-polar sorbent (GBC) allowed removing hydrophobic interaction-based compounds such as chlorophyll and carotenoids. The amount of GCB (5-25 mg) was different depending on the sample pigmentation. Best recoveries were obtained in the presence of 5 mg for cauliflower, 15 mg for kale and 25 mg for Brussels sprouts and broccoli (highly pigmented samples). Specifically, final recoveries ranged between 98 and 103% were obtained. When the amount of GCB was fixed on 5 mg for all samples, recoveries were lower than 80% or higher than 115% in the case of kale, Brussels sprouts and broccoli. When the amount of GCB was fixed on 25 mg for all samples, recoveries were around 85% for cauliflower and 90% in the case of kale. This is because if all the pigments are not removed or if more of the appropriate amount is added, the pigments or the excess of GCB interfered in the signal. For

this reason, it was decided to use different amounts of GCB according to the type of sample since the sample treatment was not altered.

The method was used as follows: 10 g of sample were weighed in a 50 mL PTFE centrifuge tube and acetonitrile (10 mL) was added. Then, the content of 15 mL tube extraction kit (4 g $MgSO_4$, 1 g $Na_3C_6H_5O_7$, 0.5 g $Na_2C_6H_6O_7 \cdot 1.5H_2O$ and 1 g NaCl) were added, and the samples were vortexed immediately for 1 min. The extracts were then centrifuged for 5 min at 4000 rpm. Then, a volume of 6 mL of prepared aliquot from the upper layer was transferred into a 15 mL dSPE (dispersive solid phase extraction) tube containing an amount of sorbent (150 mg PSA and 900 mg $MgSO_4$), in addition to a certain amount of GCB (5 mg for cauliflower, 15 mg for kale and 25 mg for Brussels sprouts and broccoli). Samples were again vortexed for 1 min and then centrifuged for 5 min at 4000 rpm.

Previous to analysis by the proposed method, an appropriate volume of the obtained extract was further diluted with Milli-Q water adjusting the pH value at 12 with 0.5 M NaOH.

2.4. General procedure

The manifold is shown in **Fig. 1**. Each three-way solenoid valve can adopt two positions, "on" and "off", being the whole system assimilated to an electronic circuit with a variable number of active nodes. A flow-rate of 1.7 mL min^{-1} was used in all experiments. In the initial status, the carrier (0.01 mol L^{-1} NH_3/NH_4Cl pH=9.0 buffer solution) was flowing through the flow-through cell while all other solutions were being recycled to their respective vessels. The sample

was introduced by simultaneously switching on valves V_1 and V_2 for 90 s (2.25 mL) (step 1). The sample solution was carried to the photoreactor where the photoconversion of NTP into a fluorescent compound took place (85 s). Afterwards, the fluorescent photoproduct reached the solid support placed in the flow-cell, was transitorily retained and its relative fluorescence intensity was registered at 295/362 nm/nm (step 2). Then, NTP photoproduct was completely eluted from the solid support using an eluting solution of 0.005 mol L^{-1} HCl; this was achieved by switching on valves V_1 and V_3 for 10 s (step 3). In this way, the system remained ready for the next sample insertion.

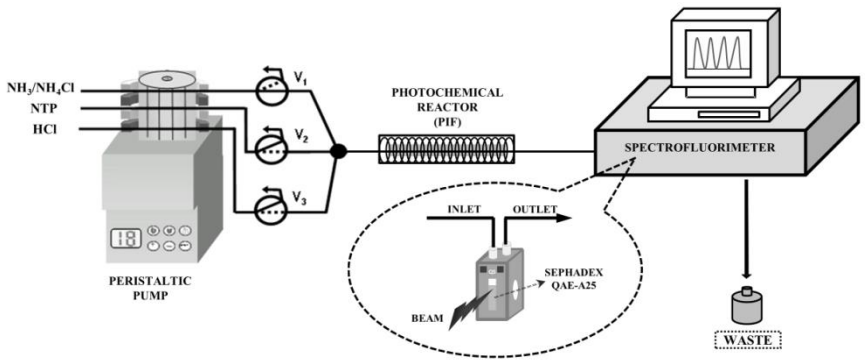

Fig. 1. Multicommutated flow-injection system.

Calibration standards and samples were analyzed by triplicate. The analytical signal was expressed as peak height mean values.

3. Results and discussion

3.1. Selection of the solid support

Preliminary experiments for evaluation of the effect of direct UV irradiation on NTP solutions revealed the formation of a fluorescent photodecomposition product in strong alkaline medium. Differents solid supports were tested with the aim of retaining this product on a solid support. As the structure of the fluorescent photoproduct generated was unknown, solid supports of different nature were checked: cationic (Sephadex SPC-25, Sephadex CMC-25), anionic (Sephadex QAE-A25) and non-ionic ones (C_{18} silica gel). Sephadex QAE-A25 was selected finally as the fluorescent photoproduct was strongly retained on it at a suitable pH. No significant retention was observed on the rest of solid supports tested due to the high pH required for the generation of the analyzed photoproduct.

The species of interest retained on the solid support chosen showed an emission peak at 362 nm and an excitation peak at 295 nm. The sorption of the fluorescent photoproduct of NTP on Sephadex QAE-A25 and the consequent preconcentration process on this latter in the detector area itself provided a drastic enhancement in the analytical signal: 15-fold higher than that obtained in homogeneous solution under the same working conditions. The sensitivity obtained is the result of the retention of the analyte on a very little amount of solid support. It is necessary to point out that the cell was filled with the minimum amount of solid support, sufficient to allow the light beam to pass completely through it. In addition, the photoproduct was not

distributed homogeneously on all the support filling the cell but it was strongly retained on a very little zone of this latter.

In order to ensure that the upper part of the solid support was just in the light path, the level of the resin packed in the flow cell had to be delicately selected to obtain the best sensitivity and selectivity. Before starting the measuring process the carrier solution was passed through the sensing zone in order to condition it.

3.2. Instrumental variables

Luminescence measurements carried out in solid-phase media are usually affected by background signal levels higher than those ones found in homogeneous solution, obviously due to the presence of the solid support in the irradiated zone. Therefore, instrumental parameters have to be carefully investigated in order to achieve the best possible signal-to-background ratio. For this reason, the instrument excitation and emission slit widths (5-20 nm) of the analytical signal and the influence of the voltage of the photomultiplier tube (400-800 V) had to be studied. The photomultiplier tube voltage was set at 670 V and the excitation and emission slit widths were fixed at 5 and 10 nm, respectively.

3.3. Chemical variables

The pH in sample solutions is a critical variable both in the generation of fluorescent photoproducts from the analyte and their sorption on the solid support, so its value was studied over a range

between 2.0 and 13.0, adjusting these pH values with HCl or NaOH solutions. It was observed that the rate of photodegradation of NTP was highly dependent on the pH, being maximum and constant the peak height around 11.5-12 (**Fig. 2**). Outside this range, the peak began to decrease. The retention of fluorescent photoproduct generated on QAE A-25 at this pH value probably indicates a strong ionic character although the structure is unknown. Different buffer solutions at pH values of 11.5-12 (Na_2HPO_4/NaOH and NaOH/KCl) were tested, but the maximum signal was obtained adjusting the pH of the sample with a 0.5 mol L^{-1} NaOH solution.

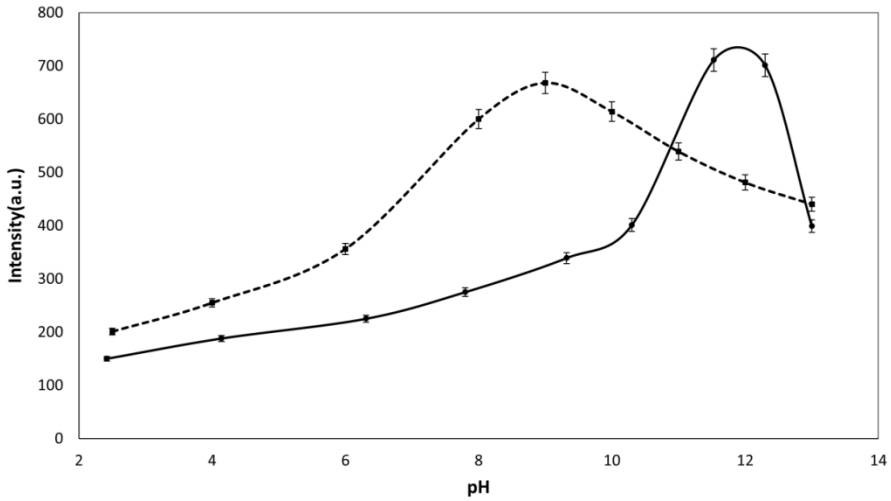

Fig. 2. Influence of pH of the sample (continuous line) and the carrier (discontinuous line). [NTP]= 250 ng mL^{-1}, irradiation time= 85 s.

The nature of carrier and eluting solutions were other chemical variables under investigation. Firstly, the pH of carrier solution was studied. The best results were obtained at pH 9 (**Fig. 2**), value in which the generated photoproduct probably could be deprotonated so allowing

its retention on the solid support. On the other hand, pH values higher than 10 produced a high deterioration of the solid support by the strong alkaline medium. The effect of ionic strength on the analytical signal was inquired by using a NH_3/NH_4Cl and $Na_2CO_3/NaHCO_3$ buffer solutions at 9 pH value, obtaining higher net signals with the first one. The study of the influence of its concentration was performed in the 0.005-0.05 mol L^{-1} range. The best overall results were obtained with 0.01 mol L^{-1} NH_3/NH_4Cl buffer solution (pH 9.0). The use of this carrier stream instead of water produced a remarkable improvement in the stability of the baseline.

Respect to the eluting solution, the baseline could be slightly regenerated by the carrier solution but it was observed that this regeneration was incomplete and the repeatability of the system worsened after several sample insertions. An eluting solution of 0.005 mol L^{-1} HCl was introduced into the system in order to avoid these handicaps.

3.4. Flow system variables

The sample introduction time and the flow-rate of the peristaltic pump were the flow variables studied.

In MCFIA-SPS systems sensitivity can be improved by increasing the sample volume injected. This is a consequence of the sorption of a higher amount of the species monitored on the same amount of solid support as the injection volume increases. This effect also allows working in a wider concentration range and makes possible to reduce the matrix effect by performing only an appropriate dilution

of the sample. However, it is necessary to take also into account that the increase of the injection volume entails a simultaneous increase in time of analysis and, consequently, both sensitivity and throughput have to be considered in the selection of this parameter. The study of the influence of this variable was carried out by injecting in the system different volumes of a 20 ng mL^{-1} NTP solution through different sample insertion times (range of 20–150 s). The fluorescence signal increased linearly with insertion time up to 90 s. Higher volumes did not provide a significant increase in the PIF signal, so 90 s was selected as optimum insertion time of sample.

Also, the influence of the flow-rate was investigated from 1 up to 2 mL min^{-1}. A slight increase in the fluorescence signal was obtained for increasing flow-rate and the sampling frequency increased too. On the other hand, flow-rates higher than 1.7 mL min^{-1} originated overpressure problems in the flow system due to the use of the solid support. Finally, this flow-rate value was chosen as a compromise between sensitivity and throughput.

3.5. Optimization of the cleanup procedure

QuEChERS extraction method was performed in order to obtain good final results. It consisted in a modification of the conventional QuEChERS extraction method, described in Section 2.3, in order to improve the extraction of samples containing high amount of pigments which influenced in final recoveries. In our case, this procedure was used for cauliflower, broccoli, Brussels sprouts and kale samples. Two different types of sorbent, PSA and GCB, were tested to investigate the

influence on recovery in the cleanup step. GCB is a weakly polar or non-polar sorbent, mainly used to remove hydrophobic interaction-based compounds, such as chlorophyll and carotenoids. On the other hand, PSA has a weak anion exchange function and applies to remove various polar organic acids, polar pigments, some sugars and fatty acid from the non-polar samples. Finally, GCB was selected because recoveries were better than using PSA (close to 100% for GCB and 90% for PSA). Different levels of GCB (0-30 mg) were used to adsorb the pigments in sample extracts. Best recoveries were obtained in the presence of 5 mg GCB for cauliflower (slightly pigmented sample), 15 mg GCB for kale and 25 mg GCB for Brussels sprouts and broccoli (highly pigmented samples).

3.6. Photodegradation variables

Irradiation time for the generation of fluorescent photoproducts is one of the principal key variables. Overpressure problems in the system and a poor precision were observed when higher flow rates combined with longer photoreactors were assayed. Higher analytical signals but a decrease in throughput were provided with the use of lower flow rates combined with shorter photoreactors, so a combination of a suitable flow rate with the size of photoreactor was used as optimum. The length of the transport system between the photochemical reactor and the flow cell was the minimum, allowing both units to be connected.

To establish the optimum irradiation time, a 200 ng mL^{-1} NTP solution was inserted into the system (sampling time, 90 s; flow rate,

1.7 mL min^{-1}), the flow was stopped just when the whole plug of sample was within the photoreactor (180 cm), and the sample was irradiated for increasing periods of time (10 to 150 s). The fluorescence signal increased with the irradiation time to reach a maximum value corresponding to the optimum value of this variable (85 s), and thereafter a decrease in fluorescence intensity was obtained. The shape of the curve obtained suggests a two-step photolysis mechanism, consisting of the formation of a strongly fluorescent photoproduct and the posterior photodegradation of the latter compound into nonfluorescent product(s).

Other variable like the effect of the temperature on the fluorescence intensity was also examined, whose effect is of great theoretical significance and practical benefit. Increasing the temperature increases molecular thermal motion, thereby also increasing the probability of radiationless transitions and reducing the fluorescence quantum yield as a result. The influence of temperature was studied over the range 10−40 °C. The fluorescence intensity decreased as the temperature was exceeded 35 ºC. The procedure was developed at room temperature because it was not observed significant heating.

3.7. Figures of merit and interference study

Under the optimized conditions, the analytical parameters of the system were carefully examined (**Table 1**). The calibration curve was constructed by following the procedure above described after injecting sample solutions in triplicate, containing increasing concentrations of NTP. As it is known, the data were fitted by standard least-squares treatment and the quantification was carried out by using peak height as

analytical signal. The existence of matrix effect was evaluated by comparing the slopes of aqueous standards and standard addition calibration graphs for different vegetable samples. Since there were no statistically significant differences between them, it was concluded that there was no matrix effect. Therefore, the determination of NTP was carried out by using external calibration.

Table 1. Analytical parameters

Parameter	
Excitation/ emission slits (nm/nm)	295/362
Photomultiplier tube voltage (V)	670
Calibration graph	
Intercept	14.406
Slope (mL ng^{-1})	3.6542
Correlation coefficient	0.9992
Linear dynamic range (ng mL^{-1})	2-300
Detection limit (ng mL^{-1})	0.5
Quantitation limit (ng mL^{-1})	2
Intra-day RSD (%) (n=10)	
20 ng mL^{-1}	2.6
120 ng mL^{-1}	3.1
Inter-day RSD (%) (n=10)	
50 ng mL^{-1}	4.5

175 ng mL^{-1}	3.8
Sample throughput, h^{-1}	18

The proposed methodology replied linearly in the concentration range 2–300 ng mL^{-1}. The detection and quantification limits were 0.5 and 2 ng mL^{-1}, being estimated as the concentration of analyte which produced an analytical signal equal to three and ten times, respectively, the standard deviation of the background fluorescence. These values are close to those found in electrochemical methods proposed by other authors (Lezi & Economou, 2015). The intra-day repeatability was established for ten independent analyses of sample solutions containing 20 and 120 ng mL^{-1} of NTP with RSDs lower than 3.1%. The inter-day repeatability was also carried out for ten consecutive days by two different analysts, getting RSDs lower than 4.5%. By addition of standard solutions in "blank" vegetables, method accuracy and recovery were evaluated.

Another important aspect of this work is the study of possible influence in the analytical signal from other species that might accompany the analyte in real samples. As the tolerance level was considered the maximum amount of foreign species that produced an error not exceeding ±3%. The study was focused on cations, anions, other fluorescent pesticides as *o*-phenylphenol, carbendazim and carbaryl, and the photodegradable pesticides thiacloprid, imidacloprid, acetamiprid, clothianidin and thiamethoxam, commonly used in agriculture. Results are summarized in **Table 2**. High tolerances were obtained, with levels up to 20-fold except in the case of thiamethoxam

and clothianidin. Nevertheless, these neonicotinoids, from the same family and with slightly similar structures to NTP, usually appear not together NTP in real samples. The determination of NTP would not be possible if it was developed in homogeneous solution. This is the result of the use of the solid support in the flow cell.

Table 2. Study of interferences

Foreign species	**Tolerance level (foreign species/analyte, w/w)**
Na^+, K^+, NH_4^+, Ca^{2+}, Mg^{2+}, Al^{3+}, SO_4^{2-}, Cl^-, HCO_3^-, PO_4^{3-}, NO^{3-}	1000[a]
o-phenylphenol	50
Carbendazim, carbaryl	35
Imidacloprid, thiacloprid, acetamiprid	20
Clothianidin	5
Thiamethoxam	3

[a]Maximum ratio tested

3.8. Analytical applications

Fortified vegetable samples were prepared to perform the recovery studies. Known amounts of NTP with concentrations (1-10 mg kg^{-1}) close to the MRLs (5 mg kg^{-1}) (JFCRF, 2017) were added in order to spike real samples. In all the studied samples, recoveries values between 98% and 103% were obtained, as it can be observed in detail in **Table 3**, obtaining RSDs lower than 4% in all cases.

Table 3. Recovery studies of NTP in cruciferous vegetables

Sample	Spiked (mg kg^{-1})	Recovery (%) ± RSD (%)
Cauliflower 1	1	102 ± 3
	3	103 ± 1
	6	101 ± 3
Cauliflower 2	1	102 ± 1
	4	102 ± 4
	8	101 ± 3
Cauliflower 3	1.5	100 ± 3
	4	102 ± 2
	7	99 ± 3
Brussels sprouts 1	1.5	99 ± 3
	4.5	99 ± 3
	8	98 ± 2
Brussels sprouts 2	2	101 ± 2
	4	99 ± 1
	6	100 ± 3
Brussels sprouts 3	2.5	100 ± 1
	6	100 ± 1
	10	102 ± 1
Kale 1	1	101 ± 4

	3	98 ± 3
	5	99 ± 1
Kale 2	1.5	101 ± 1
	4	101 ± 1
	6	101 ± 3
Kale 3	2	99 ± 3
	5	102 ± 3
	9	100 ± 1
Broccoli 1	3.5	102 ± 3
	5	100 ± 2
	10	101 ± 3
Broccoli 2	3	100 ± 3
	4.5	103 ± 2
	8	101 ± 2
Broccoli 3	2	102 ± 3
	6.5	99 ± 1
	9	100 ± 2

The statistical study of the accuracy was carried out comparing the obtained results with an HPLC-ESI-IT-MS reference method. Same samples were analyzed, but only one from each vegetable was taken as representative for the analysis. Samples were prepared as described in section 2.3 and analyzed in triplicate. The results of the proposed

method were compared with those obtained with this one by means of a t-test and F-criterion, showing that there is no significant statistical difference between the values obtained by both methods and indicating the utility of the proposed method for routine analytical control (**Table 4**).

Table 4. Comparison with a HPLC-ESI-IT-MS reference method

Sample	**Amount found[a] (ng mL^{-1})**		**t_{calc}[b]**	**F_{calc}[c]**
	Proposed method	Reference method		
Cauliflower	52	49	1.46	2.71
Brussels sprouts	51	50	0.54	5.57
Kale	50	51	0.71	6.33
Broccoli	51	52	0.78	1.59

[a] Average of three determinations: 50 ng mL^{-1}

[b] Theorical value for t=4.30 (P=0.05)

[c] Theorical value for F=39.00 (P=0.05)

4. Conclusions

A novel, simple and sensitive photochemically induced fluorescence based flow-through optosensor has been developed for the screening of NTP in cruciferous vegetables and veterinary medicinal products. To date, it is the first method based on PIF-MCFIA-SPS for determination of this analyte. The method makes use of the on-line photodegradation of NTP in a multicommuted flow-system and the

posterior monitoring of the generated highly fluorescent photoproduct in alkaline medium, once it is retained on an appropriate solid-support (Sephadex QAE-A25). This retention contributes to improve selectivity, allowing the exclusion of a large amount of organic species of the matrix. Moreover, sample treatments like QuEChERS method allow removing a large amount of pigments which cause serious interferences.

The method developed could be an interesting alternative to the chromatographic determination of the analyte, since it presents a large number of advantages like similar detection limits (Sun, et al., 2013; Vichapong, Burakham, & Srijaranai, 2015), higher throughputs (18 h^{-1}), low cost of instrumentation, rapidity and simplicity. The present work could be considered as an environmental friendly analytical system for the determination of NTP residues due to its minimal waste generation and low consumption of reagents, being suitable for routine analysis in industry quality control.

Acknowledgements

J.J.L. acknowledges research scholarship from Spanish Government (Ministerio de Educación y Ciencia). This study was funded by the "Ministerio de Economía y Competitividad" (grant number CTQ2016-7511-R).

References

Anastassiades, M., Lehotay, S. J., Štajnbaher, D., & Schenck, F. J. (2003). Fast and easy multiresidue method employing acetonitrile extraction/partitioning and "dispersive solid-phase extraction" for the determination of pesticide residues in produce. *Journal of AOAC International, 86*(2), 412-431.

Capitán-Vallvey, L. F., Valencia, M. C., & Nicolás, E. A. (2003). Simple Resolution of Butylated Hydroxyanisole and n-Propyl Gallate in Fatty Foods and Cosmetics Samples by Flow-Injection Solid-Phase Spectrophotometry. *Journal of Food Science, 68*(5), 1595-1599.

Coly, A., & Aaron, J.-J. (1998). Fluorimetric analysis of pesticides: Methods, recent developments and applications. *Talanta, 46*(5), 815-843.

JFCRF. (2017). Table of MRLs for Agricultural Chemicals- NITENPYRAM. http://www.m5.ws001.squarestart.ne.jp/foundation/agrdtl.php?a_inq=48600-last accessed May 2017.

Jiao, W., Xiao, Y., Qian, X., Tong, M., Hu, Y., Hou, R., & Hua, R. (2016). Optimized combination of dilution and refined QuEChERS to overcome matrix effects of six types of tea for determination eight neonicotinoid insecticides by ultra performance liquid chromatography-electrospray tandem mass spectrometry. *Food Chemistry, 210*, 26-34.

Jiménez-López, J., Llorent-Martínez, E. J., Ortega-Barrales, P., & Ruiz-Medina, A. (2014). Multi-commutated fluorometric optosensor for the determination of citrinin in rice and red yeast rice supplements. *Food Additives and Contaminants - Part A Chemistry, Analysis, Control, Exposure and Risk Assessment, 31*(10), 1744-1750.

Jiménez-López, J., Ortega-Barrales, P., & Ruiz-Medina, A. (2016). Development of an semi-automatic and sensitive photochemically induced fluorescence sensor for the determination of thiamethoxam in vegetables. *Talanta, 149*, 149-155.

Jovanov, P., Guzsvány, V., Franko, M., Lazić, S., Sakač, M., Šarić, B., & Banjaca, V. (2013). Multi-residue method for determination of selected neonicotinoid insecticides in honey using optimized dispersive liquid-liquid microextraction combined with liquid chromatography-tandem mass spectrometry. *Talanta, 111*, 125-133.

Lezi, N., & Economou, A. (2015). Voltammetric Determination of Neonicotinoid Pesticides at Disposable Screen-Printed Sensors Featuring a Sputtered Bismuth Electrode. *Electroanalysis, 27*(10), 2313-2321.

Li, S. P., Ma, X. R., Cao, X. H., & Dong, Y. W. (2013). Electro-catalytic degradation of nitenpyram wastewater using C/PTFE gas diffusion electrode. In *Advanced Materials Research, 699*, 747-752.

Llorent-Martínez, E. J., Barrales, P. O., Luisa Fernández-de Córdova, M., & Ruiz-Medina, A. (2010). Multicommutation in flow systems: A useful tool for pharmaceutical and clinical analysis. *Current Pharmaceutical Analysis, 6*(1), 53-65.

Llorent-Martínez, E. J., Ortega-Barrales, P., Fernández-de Córdova, M. L., & Ruiz-Medina, A. (2013). Quantitation of ochratoxin a in cereals and feedstuff using sequential injection analysis with luminescence detection. *Food Control, 30*(2), 379-385.

Molina-García, L., Ruiz-Medina, A., & Fernández-De Córdova, M. L. (2011). Automatic optosensing device based on photo-induced fluorescence for determination of piceid in cocoa-containing products. *Analytical and Bioanalytical Chemistry, 399*(2), 965-972.

Molina-García, L., Ruiz-Medina, A., & Fernández-de Córdova, M. L. (2011). A novel multicommuted fluorimetric optosensor for determination of resveratrol in beer. *Talanta, 83*(3), 850-856.

Recalde-Ruiz, D. L., Andres-Garcia, E., & Diaz-Garcia, M. E. (2000). Fluorimetric flow injection and flow-through sensing systems for cyanide control in waste water. *Analyst, 125*(11), 2100-2105.

Rocha, F. R. P., Reis, B. F., Zagatto, E. A. G., Lima, J. L. F. C., Lapa, R. A. S., & Santos, J. L. M. (2002). Multicommutation in flow analysis: concepts, applications and trends. *Analytica Chimica Acta, 468*(1), 119-131.

Sánchez-Hernández, L., Higes, M., Martín, M. T., Nozal, M. J., & Bernal, J. L. (2016). Simultaneous determination of neonicotinoid insecticides in sunflower-treated seeds (hull and kernel) by LC-MS/MS. *Food Additives and Contaminants - Part A Chemistry, Analysis, Control, Exposure and Risk Assessment, 33*(3), 442-451.

Sun, B. L., Shan, H., Li, Y. H., Zeng, Y. L., Shen, X. L., & Tong, C. F. (2013). Simultaneous determination of 6 neonicotinoid residues in soil using DLLME-HPLC and UV. *Guang Pu Xue Yu Guang Pu Fen Xi/Spectroscopy and Spectral Analysis, 33*(9), 2553-2557.

Vichapong, J., Burakham, R., & Srijaranai, S. (2015). In-coupled syringe assisted octanol–water partition microextraction coupled with high-performance liquid chromatography for simultaneous determination of neonicotinoid insecticide residues in honey. *Talanta, 139*, 21-26.

Zhang, G., Nie, S., Long, L., Zeng, D., Chen, J., Yang, H., & Chen, L. (2010). Determination of nitenpyram residue in cabbage and soil using gas chromatography. *Chinese Journal of Chromatography (Se Pu), 28*(11), 1103-1106.

Sensitive photochemically induced fluorescence sensor for the determination of nitenpyram and pyraclostrobin in grapes and wines

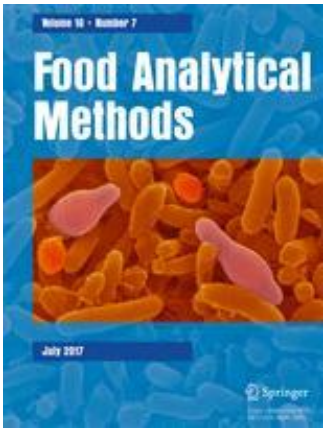

5. "Sensitive photochemically induced fluorescence sensor for the determination of nitenpyram and pyraclostrobin in grapes and wines"

J. Jiménez-López, E.J. Llorent-Martínez, P. Ortega-Barrales, A. Ruiz-Medina *

Enviado a Food Analytical Methods, en 2018.

Resumen

El objetivo principal de este estudio es proporcionar un nuevo enfoque para la determinación de plaguicidas, basado en el uso de sensores luminiscentes automáticos para el análisis de contaminantes. En este sentido, se han seleccionado dos plaguicidas ampliamente utilizados en agricultura, el nitenpiram y la piraclostrobina, como compuestos diana. El sistema propuesto hace uso del análisis por inyección en flujo multicommutado empleando la fluorescencia inducida fotoquímicamente como técnica de detección. Mediante irradiación UV *online* de los analitos, se obtuvieron productos de fotodegradación que resultaron ser fuertemente fluorescentes. Después, la separación *online* y la preconcentración de los fotoproductos se llevó a cabo en la superficie de un soporte sólido, gel de sílice C_{18}, situado dentro de la célula de flujo, en la cual se registró la señal analítica.

El método propuesto presenta un límite de detección de 7.5 ng mL^{-1} para ambos analitos. El método analítico desarrollado cumple con los límites máximos actuales de residuos en uvas (de mesa y de vino) y en el propio vino, a los cuales se realizó un tratamiento de muestra adecuado previa a la determinación de los plaguicidas. Los estudios de recuperación en uvas y vinos mostraron recuperaciones entre 96 y 107% en todos los casos. La simplicidad, bajo costo y alta sensibilidad del método propuesto lo convierten en un método con un enfoque atractivo para el análisis de estos dos plaguicidas en productos alimenticios.

Este estudio representa el primer optosensor biparámetro en flujo continuo con detección por fluorescencia inducida fotoquímicamente para el análisis de estos plaguicidas, y proporciona una novedosa alternativa para la cuantificación de plaguicidas no fluorescentes en muestras complejas, como las agroalimentarias.

5. "Sensitive photochemically induced fluorescence sensor for the determination of nitenpyram and pyraclostrobin in grapes and wines"

Abstract

The primary aim of this study is to report a new approach for pesticides determination, based on the use of automated luminescent sensors for the analysis of specific analytes. In this regard, we have selected two widely used pesticides - nitenpyram and pyraclostrobin - as target compounds. The proposed system makes use of Multicommutated Flow Injection Analysis by employing photochemically induced fluorescence as detection technique. Strongly fluorescent photodegradation products were obtained on-line by UV-irradiation of the analytes. Then, the on-line separation and pre-concentration of the analytes were carried out on the surface of C_{18} silica gel beads placed inside the flow-cell, where the analytical signal was recorded.

The proposed analytical method presents a detection limit of 7.5 ng mL^{-1} for both analytes. After an appropriate sample treatment, the method complies with the current maximum residue limits in table grapes and wine grapes. We carried out recovery experiments in grapes

and wines, obtaining recoveries between 96 and 107% in all cases. The simplicity, low-cost, and high sensitivity of the proposed method makes it an attractive approach for the analysis of these two pesticides in food commodities.

Keywords: Multicommutation; Sensor; Pesticide; Food; Photochemically-induced fluorescence

Introduction

Pesticides are the most abundant environmental pollutants and can be found in foods, soil, water, and agricultural products, among others. They present adverse effects on human health, even at low levels, hence the high number of analytical methodologies developed for their determination in the last decade. The most common analytical methods for pesticide determination are liquid or gas chromatography coupled to mass spectrometry detection (HPLC-MS, GC-MS) (Pano-Farias et al. 2017; Xiu-ping et al. 2017; Pérez-Fernández et al. 2017). However, different optical and electrochemical methods, many of them making use of flow methodologies, have also been developed as an alternative to chromatography (Trojanowicz 2009; Melchert et al. 2012).

An interesting approach for the analysis of pesticides in agri-food samples consists in the implementation of solid-phase spectroscopy (SPS) in flow analysis, obtaining the so-called flow-through optosensors or flow optosensors. In these systems, the species of interest is sorbed on a solid support, placed in the flow-through cell, in which the analytical signal is directly recorded, increasing selectivity and sensitivity (Llorent-Martínez et al. 2011). In particular, several flow monoparametric optosensors have been reported for the determination of pesticides in the agri-food sector, mainly with fluorescence detection (Jeanty et al. 2002; Sánchez-Barragán et al. 2007; Piccirilli et al. 2008; Trojanowicz 2009; Ruiz-Medina et al. 2012; Llorent-Martínez et al. 2012). However, not all the target analytes present native fluorescence, hence the necessity of other alternatives. One of the available strategies is photochemically induced fluorescence (PIF), which consists in the UV-irradiation of the sample solution with a UV lamp, producing fluorescent compound(s) by the photodegradation of the analyte (Piccirilli et al. 2008). Although the development of bi-parameter PIF optosensors is possible by achieving a proper separation of the analytes (Molina-García et al. 2011), this strategy has not been applied to the determination of pesticides, which is the main aim of this work. In this regards, two relatively new

pesticides have been selected as target analytes: nitenpyram (NTP) and pyraclostrobin (PYR).

PYR is a strobilurin fungicide that acts through inhibition of mitochondrial respiration by blocking electron transfer within the respiratory chain and results in cessation of fungal growth (de Oliveira et al. 2016). It is mainly analyzed by HPLC-MS (Fan et al. 2017; Wu et al. 2018) and electrophoresis (Souza et al. 2009). On the other hand, NTP is a neonicotinoid, a type of synthetic insecticides that act on the central nervous system of insects, causing paralysis and death. It is usually analyzed by HPLC with diode-array (Obana et al. 2002) or mass spectrometry (Yoshida et al. 2013) detection. Few non-chromatographic analytical methods have been reported for the determination of NTP (Brycht et al. 2012; Dong et al. 2014; Lezi & Economou 2015; Jiménez-López et al. 2018) or PYR (Dornellas et al. 2014). Hence, the development of novel methodologies can expand the possibilities for the determination of these pesticides in food samples.

To date, there are different flow methodologies at hand, each of them presenting advantages and handicaps. In this work, we have selected Multicommutated Flow Injection Analysis, which allows obtaining high sample throughput as well as low consumption of sample and reagents solutions. A detailed explanation of MCFIA

methodology and its implementation in flow-through optosensing can be found at Llorent-Martinez et al. (Llorent-Martinez et al. 2010).

This work is a continuation of a previous PIF method that was applied to the quantitation of NTP in vegetables (Jiménez-López et al. 2018). Here, the novel flow manifold has been successfully applied to the analysis of PYR and NTP in wine and grapes. Both target analytes suffered on-line UV irradiation, producing fluorescent compounds that were separated and independently detected on a solid support placed in the flow-cell. This work reports the first bi-parameter flow-through optosensor with PIF detection for the analysis of pesticides, providing a novel alternative for the quantification of non-fluorescent pesticides in complex samples. To our best knowledge, this is the first analytical method for the simultaneous determination of PYR and NTP.

Experimental

Reagents and solutions

NTP (99.6%) and PYR (99.9 %) were obtained from Fluka (Sigma-Aldrich, Madrid, Spain). Stock solutions of 40 μg mL^{-1} of these analytes were prepared in Mili-Q water. The solutions were kept in the dark at 4 ºC and were stable for at least one month. Working solutions were prepared daily by appropriate dilution with Mili-Q water.

Acetonitrile, graphitized carbon black (GCB), hydrochloric acid (HCl), methanol (MeOH), sodium phosphate dibasic (Na_2HPO_4), and sodium hydroxide (NaOH) were purchased from Sigma (Sigma-Aldrich, Madrid, Spain). All reagents and standards were of analytical reagent grade. Discovery DSC-18 (500 mg) solid-phase extraction cartridges were purchased from Supelco (Sigma-Aldrich). Isolute QuEChERS extraction kits were acquired from Biotage (Sweden): the extraction tube contained 4 g $MgSO_4$, 1 g $Na_3C_6H_5O_7$, 0.5 g $Na_2C_6H_6O_7 \cdot 1.5H_2O$ and 1 g NaCl, whereas the sorbent tube contained 150 mg primary and secondary amine (PSA) and 900 mg $MgSO_4$.

Ultrapure water (Milli-Q Waters purification system, Millipore, Milford, MA, USA) was used for all analyses.

Sephadex QAE-A25, 40–120 μm average particle size (Sigma–Aldrich, Buchs, Switzerland) and C_{18} bonded phase silica gel beads (Waters, Milford, MA, USA) with 55–105 μm of average particle size, were tested as solid supports.

Instrumentation and apparatus

Luminescence measurements were performed with a Cary-Eclipse Luminescence Spectrometer (Varian Inc., Mulgrave, Australia). The

spectrometer was connected to a computer with a Cary-Eclipse (Varian) software package for data collection and treatment.

A Hellma flow cell 176.752-QS (Hellma, Mülheim, Germany) (25 μL of inner volume and a light path length of 1.5 mm) was used. The cell was filled with C_{18} solid phase microbeads and was blocked at the outlet with glass wool to prevent displacement of the particles.

A four-channel Gilson Minipuls-3 (Villiers Le Bel, France) peristaltic pump with rate selector and methanol-resistant pump tubes type Solvflex (Elkay Products, Shrewsbury, MA, USA) were used. An electronic interface based on ULN 2803 integrate circuit (Motorola, Phoenix, AZ, USA) was employed to generate the electric potential (12V) and current (100 mA) required to control the four 161T031 NResearch three-way solenoid valves (Neptune Research, West Caldwell, NJ, USA). The software for controlling the system was written in Java. Flow lines of 0.8 mm internal diameter PTFE tubing and methacrylate connections were used.

A home-made continuous photochemical reactor was constructed by coiling PTFE tubing (180 cm, 0.8 mm i.d.) around a low-pressure mercury lamp (15 W, 254 nm). It was contained in an aluminium box, permitting maximum reflectance of UV light. Since the aluminium foil

allowed heat dissipation, no cooling device was needed and all the experiments were carried out at room temperature.

A pH-meter Crison GLP21 (Crison Instruments, Barcelona, Spain) and a centrifuge Mixtasel-BL (Selecta, Barcelona, Spain) were also used.

Sample Preparation

Different wines (red and white) and grapes (red and white table grapes; red and white wine grapes) produced in different areas of Spain were purchased in local markets. Grape samples were kept at 4ºC in the fridge until extraction, which was carried out within 24 hours. Wine bottles were kept at room temperature; after opening the bottles, the extraction was performed within 24 h. Before extraction, whole grape samples were thoroughly ground, homogenized, and stored at 20º C, whereas wine samples were hand-shaking homogenized.

We performed two different sample treatments: a) solid phase-extraction (SPE) for wines; b) Quick, Easy, Cheap, Effective, Rugged, and Safe (QuEChERS) method for grapes and wines.

a) The SPE treatment was adapted from Economou et al. (Economou et al. 2009). An accurately measured volume of 10 mL of wine sample was diluted to a final volume of 100 mL with Milli-Q

water. Cartridges were conditioned with 6 mL of methanol and 6 mL of Milli-Q water. Then, wine samples were percolated through the cartridges at a flow-rate of 5 mL min^{-1}. The cartridges were rinsed with 5 mL of Milli-Q water and vacuum-dried for 10 min. Finally, the retained pesticides were eluted with 2×5 mL of methanol. The eluent was reduced to about 0.5 mL by vacuum rotary evaporation on a water bath at 40 ºC. The residue was redissolved in 10 mL H_2O. For red wine samples, a clean-up with GCB (20 mg) was needed. In this case, GCB was added to the flask, mixed for 15 seconds and filtered, removing pigments that can interfere with the analysis.

b) The QuEChERS method was as follows: 10 g of sample was weighed in a 50 mL PTFE centrifuge tube and 10 mL acetonitrile was added. The content of a 15 mL tube extraction kit was added, and the samples were vortexed for 1 min. The extracts were centrifuged for 5 min at 4000 rpm. Then, 6 mL of the supernatant was transferred into a 15 mL dSPE (dispersive solid phase extraction) tube containing the sorbent. An additional 20 mg of GCB was required for the treatment of red wine grapes, red table grapes, and red wine. Samples were again vortexed for 1 min and centrifuged for 5 min at 4000 rpm.

In both extraction procedures, an appropriate volume of the obtained extract was further diluted with deionized water previous to analysis.

General Procedure

The flow manifold is shown in **Figure 1**. In the initial status, all valves are switched off and the carrier, 10% MeOH, flows through the flow-through cell while all other solutions are recycled to their vessels. The sample (NTP + PYR, pH 12.0) is introduced by simultaneously switching valves V_1 and V_2 on for 100 s. Both NTP and PYR are carried towards the photochemical reactor, where they are UV-irradiated, and their fluorescent photoproducts are obtained. Then, these photoproducts are carried towards the flow-through cell, which is filled with C_{18} silica gel. NTP photoproduct is slightly retained on the solid microbeads, being eluted by the same carrier solution, while PYR photoproduct is strongly retained on the upper part of the C_{18} solid support (above the irradiation area). Hence, the signal corresponding to NTP is obtained whereas PYR photoproduct is still retained on the solid support. Then, a 65% MeOH eluting solution is inserted into the system by activating valves V_1 and V_3 for 50 s. The eluting solutions desorbs PYR photoproduct from the solid support (while the carrier

solution is recycled) and its analytical signal is recorded when reaching the detection area. After the signal from both photoproducts is obtained, the carrier solution flows through the whole system for 30 s, so it is prepared for the next sample insertion.

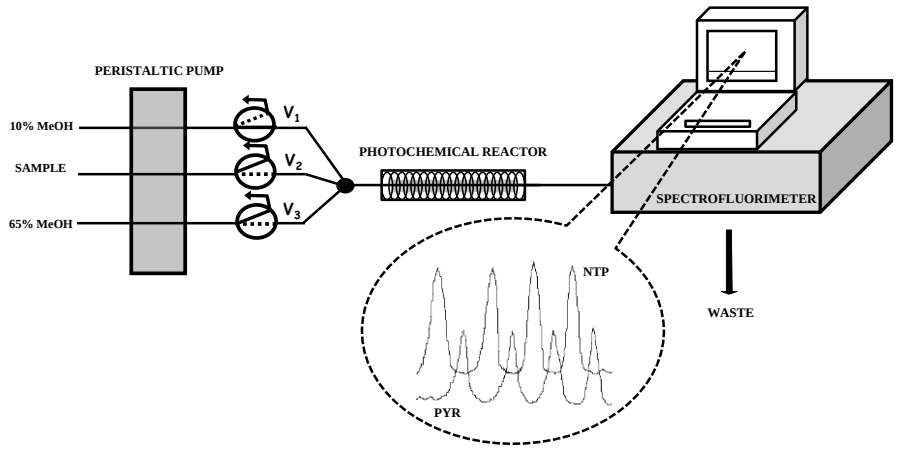

Figure 1. Manifold. V_i = three-way solenoid valves. Insert: typical flow profile of the signal recorded for both analytes.

Calibration standards and samples were analyzed in triplicate. Luminescence measurements were recorded at excitation/emission wavelengths of 295/361 and 309/419 nm respectively for NTP and PYR photoproducts, respectively. For red wines and red grapes, the solid support had to be cleaned with 100% MeOH each 15-20 sample insertions.

Results and discussion

Preliminary studies

The native fluorescence signal of the target analytes was very low, particularly for NTP ($\lambda_{exc}/\lambda_{em}$ at 280/442 and 270/329 for NTP and PYR, respectively). Hence, we studied the influence of UV irradiation to obtain photoproducts with enhanced fluorescence signal. The UV irradiation in alkaline medium produced fluorescent photoproducts for both analytes. Hence, the chemical parameters were optimized to obtain the highest fluorescent products. Also, we optimized the separation of the photoproducts produced by each pesticide, so their sequential determination could be performed selectively.

Selection of the solid support

Different solid supports were tested for the retention of each analyte. As explained later, fluorescent photoproducts were obtained at basic pH values. Therefore, an anionic-exchange (QAE A-25) and a non-ionic exchange (C_{18}) solid supports were tested for their retention, as no signal was expected for cationic-exchange supports. The photoproducts of NTP and PYR were retained in both QAE A-25 and C_{18} solid supports, although the analytical signal was higher in C_{18} silica beads (approximately 30% increase). Also, both analytes could be separated

previously to their analysis on this selected solid support, by using an extra amount of solid support in the same flow-through cell (placed just above the detection area). Hence, we selected C_{18} silica beads for further experiments.

Instrumental variables

The fluorescence spectra of NTP and PYR photoproducts were firstly recorded in aqueous solutions. However, the wavelengths can vary when the photoproducts are retained on the solid support, due to bathochromic or hypsochromic effects. Hence, both photoproducts were individually retained on the C_{18} solid support, observing maximum fluorescence wavelengths at 295/361 and 309/419 nm for NTP and PYR photoproducts, respectively. Also, the background fluorescence signal – almost absence in aqueous solutions- is higher when the signal is recorded on a solid support. Hence, instrumental parameters have to be carefully optimized to take into account this fact. Hence, we optimized the excitation and emission slit widths (5-20 nm) and the voltage of the photomultiplier tube (400-800 V). The best signals (analyte minus background signal) were observed for a photomultiplier tube voltage of 700 V and excitation and emission slit widths of 5 and 10 nm, respectively. With these parameters, the

background signal was low enough to obtain a proper linear dynamic range, obtaining detection limits that complied with the maximum residue limits in grapes and wine, which were the target samples.

Chemical Variables

Chemical variables can affect in two different ways: a) generation of fluorescent photoproducts of NTP and PYR; b) separation/retention on the solid support. Hence, the first variable to consider was the pH of sample solutions to obtain photoproducts. We observed that PYR yielded fluorescence photoproducts no matter the pH value. However, fluorescent photoproducts from NTP were only obtained at basic pH values, observing the highest fluorescence signals at pH values higher than 11.5 (70% reduction in fluorescence signal for lower pH values). The pH value was adjusted to 12.0 using both phosphate buffer (0.05-0.5 mol L^{-1}) and 0.01 mol L^{-1} NaOH solutions. The adjustment of the pH with NaOH provided the best analytical signal, so we prepared the sample in this solution.

The next step consisted in the optimization of the carrier and eluting solutions, testing different percentages of methanol:water solutions, which is the conventional approach when C_{18} microbeads are used as solid support. PYR photoproduct was firmly retained on the

upper part of the solid support, whereas NTP photoproduct was only slightly retained on the solid support and could be eluted using a 10% MeOH carrier solution, recording its analytical signal without any interference from the other analyte. After the analytical signal from NTP photoproduct was recorded, an additional eluting solution (higher percentage of MeOH) was required to elute PYR photoproduct from the upper part of the solid support, so its signal could be recorded in the detection area. The use of carrier and eluting solutions of 10% and 65% MeOH, respectively, provided the complete separation and individual recording of both analytes, achieving their sequential quantification.

Irradiation time

In addition to the pH of the sample solution, the irradiation time is a crucial variable for the generation of fluorescent photoproducts. To establish the optimum irradiation time, 250 ng mL^{-1} of each pesticide were inserted in the system individually, the flow was stopped when the whole plug of the sample was within the photoreactor, and the sample was irradiated for increasing periods of time (10–120 s). The results are shown in **Figure 2**.

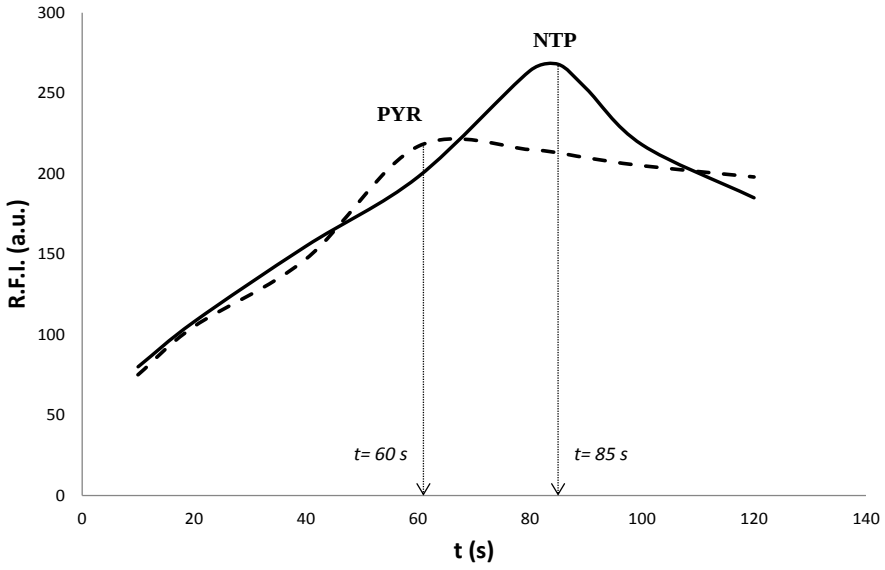

Figure 2. Influence of the UV irradiation time on the fluorescence signal of NTP (300 ng mL^{-1}) and PYR (250 ng mL^{-1}). R.F.I. (a.u.), relative fluorescence intensity (arbitrary units).

It can be observed that the fluorescence signals increased with the irradiation time, reaching maximum values at 85 s for NTP and 60 s for PYR. For higher irradiation times, the analytical signal of NTP photoproduct diminished continually. However, only a slight decrease was observed for PYR photoproduct. Hence, an irradiation time of 80 s was selected for both analytes. The shape of the curves obtained could suggest a two-step photolysis mechanism, consisting of the formation of a strongly fluorescent photoproduct and the posterior photodegradation of the latter compound into nonfluorescent product(s) or different photoproduct(s) with lower fluorescence emission.

The residence time of NTP and PYR in the photoreactor and, consequently, the irradiation time, can be controlled by both the flow rate of the carrier solution and the length of the tubing around the UV lamp. The optimum irradiation time (80 s) was established by using the maximum flow rate allowed by the flow system, 1.6 mL min^{-1}, combined with a 200-cm photoreactor. Longer photoreactor lengths involved higher flow rates and, consequently, overpressure problems. Shorter tubing lengths allowed working at lower flow rates, although they caused a significant reduction in sample throughput, without any improvement in the analytical signals. Hence, a high flow-rate and short tubing length were selected with the shorter length of the transport system between the photochemical reactor and the flow cell.

Flow parameters

In MCFIA-SPS systems, the sensitivity can be improved by increasing the sample volume inserted, which produces the sorption of higher amounts of the analytes on the same amount of solid support, leading to a pre-concentration in the same flow-cell. However, it is necessary to consider that the increase of the insertion volume entails a simultaneous increase in the time of analysis and, consequently, both sensitivity and sample throughput have to be considered for the

optimization of this parameter. For this optimization, different volumes of 150 ng mL^{-1} NTP and PYR were inserted for increasing sample insertion times (20–150 s). The fluorescence signal increased linearly up to 100 s, but higher volumes did not provide a significant increase in the PIF signal, so we selected 100 s as sample insertion time. **Figure 3** shows the influence of this parameter on the signal of both analytes.

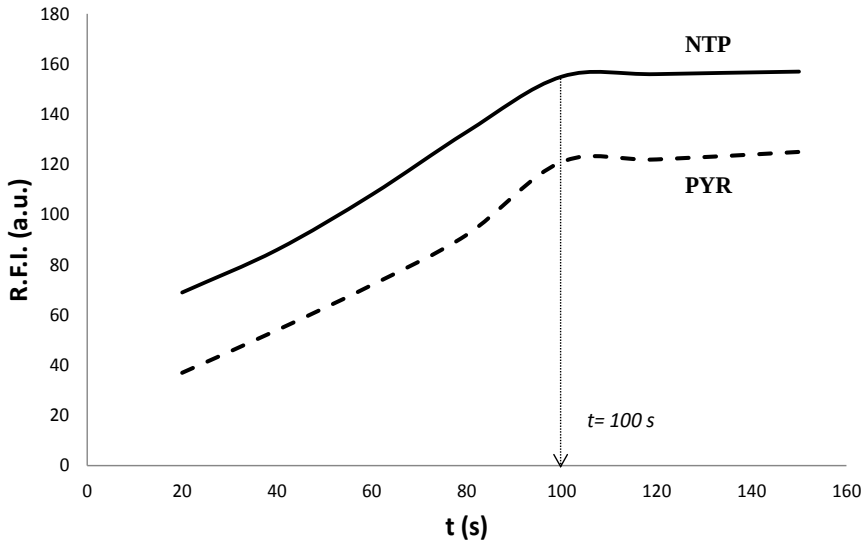

Figure 3. Influence of the sample insertion time on the analytical signal of NTP (200 ng mL^{-1}) and PYR (150 ng mL^{-1}). R.F.I. (a.u.), relative fluorescence intensity (arbitrary units).

Figures of merit

The analytical parameters of the system were studied using the optimized conditions previously discussed. **Table 1** contains the figures of merit of the proposed method, using a sample insertion time of 100

s. The calibration graph was constructed fitting the data by standard least-squares treatment. Detection and quantitation limits were calculated using the 3σ and 10σ criterion. The detection limit was 7.5 ng mL^{-1} for both analytes, and linear dynamic ranges between 25 and 650 ng mL^{-1} were obtained. Repeatability was lower than 3%, whereas intermediate precision (3 consecutive days) was lower than 5% for both NTP and PYR. A sample throughput of 16 samples per hour was obtained.

Table 1. Analytical parameters.

Parameter	**NTP**	**PYR**
Calibration graph		
Intercept	9.085	14.436
Slope (mL ng^{-1})	0.8231	0.7799
Correlation coefficient	0.9991	0.9981
Linear dynamic range (ng mL^{-1})	25-650	25-650
Detection limit (ng mL^{-1})	7.5	7.5
Quantitation limit (ng mL^{-1})	25	25
Repeatability (%) (n=10)		
50 ng mL^{-1}	1.8	1.5
180 ng mL^{-1}	2.3	2.8

Intermediate precision (%) (n=10)[a]		
75 ng mL^{-1}	3.5	3.0
200 ng mL^{-1}	4.1	3.7
Sample throughput, h^{-1}	16	16

[a] 3 consecutive days

The detection limits of NTP and PYR compare satisfactorily with those reported by author authors using non-chromatographic analytical methods. The detection limit of NTP is similar to that reported by Zhang et al. (Zhang et al. 2017), and lower than those reported by other authors (Papp et al. 2011; Brycht et al. 2012; Dong et al. 2014; Lezi & Economou 2015; Jiménez-López et al. 2018), whereas the limit of detection of PYR is lower than the obtained in (Dornellas et al. 2014).

Interference study

We studied the potential interference of different species that can be present in the analyzed samples. This study was carried out for 200 µg L^{-1} of each analyte. Tolerance level was defined as the level of foreign species that produced an error lower than 3% in the determination of the analytes. We selected different pesticides as potential interferents, including several neonicotinoids, and also the most common ions that can be present in the extracts of food samples.

Table 2 shows the results, observing that both NTP and PYR can be selectively quantified in the presence of the studied species.

Table 2. Interference study.

Foreign species	Tolerated interferent/analyte (w/w) ratio [a]	
	NTP	**PYR**
Na^+, K^+, NH_4^+, Ca^{2+}, Mg^{2+}, Al^{3+}, SO_4^{2-}, Cl^-, HCO_3^-, PO_4^{3-}, NO^{3-}	1000[b]	1000[b]
Clothianidin	10	40
Carbaryl	30	40
Imidacloprid, thiacloprid	20	25
Thiamethoxam	5	15
Glyphosate, o-phenylphenol	5	5

[a] 200 ng mL^{-1} of NTP or PYR
[b] Maximum ratio tested

Analytical applications

This flow optosensor was applied to the determination of NTP and PYR in different grapes and wine samples commercially available. Both red and white wines were selected. Different types of red and white grapes were also analyzed: a) wine grapes, which are used for wine making; and b) table grapes, which are used for direct consumption. The maximum residue limits for PYR (European Union

and Codex Alimentarius) are 1 mg kg^{-1} in table grapes and 2 mg kg^{-1} in wine grapes. No maximum residue limit has been set for NTP in the European Union, although a temporary limit of 5 mg kg^{-1} has been set by the Japan Food Chemical Research Foundation for NTP in grapes. There are not maximum residue limits for these pesticides in wines. Hence, we carried out recovery experiments in different samples at NTP and PYR concentrations close to the maximum residue limits established in grapes. First of all, blank extracts were analyzed to assess the absence of these pesticides. Using these extracts, the absence of matrix effect was confirmed so that external calibration could be used. Then, samples were spiked with appropriate volumes of NTP and PYR standard solutions. After thorough homogenization, samples were kept at room temperature overnight, and then the extraction procedure was carried out as previously explained. The obtained results are shown in **Tables 3 and 4**. It can be observed that remarkable recoveries were obtained in all samples, with both the QuEChERS and SPE procedures.

Table 3

Recovery experiments in different grapes using QuEChERS procedure.

Sample	Spiked (mg kg^{-1})	Recovery (%) ± RSD (n=3)	
		NTP	PYR
White wine grapes 1	0.7	98 ± 2	98 ± 4
	1.5	100 ± 2	97 ± 3
	3.0	102 ± 2	99 ± 4
White wine grapes 2	0.9	103 ± 2	101 ± 3
	1.8	99 ± 1	102 ± 5
	3.5	101 ± 1	102 ± 2
Red wine grapes 1	0.8	98 ± 4	96 ± 4
	1.5	104 ± 5	97 ± 3
	3.5	97 ± 1	96 ± 5
Red wine grapes 2	1.0	97 ± 3	104 ± 3
	2.0	102 ± 2	104 ± 5
	4.0	98 ± 4	103 ± 5
White table grapes 1	0.7	99 ± 1	99 ± 3
	0.9	99 ± 1	98 ± 3
	2.0	98 ± 2	98 ± 4
White table grapes 2	0.8	103 ± 2	98 ± 3
	1.5	101 ± 3	99 ± 4
	2.5	98 ± 2	97 ± 4
Red table grapes 1	0.7	97 ± 2	95 ± 2
	1.0	102 ± 3	96 ± 2
	2.0	97 ± 1	96 ± 3
Red table grapes 2	0.8	97 ± 2	96 ± 1
	1.2	99 ± 2	96 ± 4
	2.5	96 ± 3	97 ± 2

Table 4

Recovery experiments in wine samples using QuEChERS and SPE procedures.

Sample	Spiked (mg L^{-1})	Recovery (%) ± RSD (n=3)			
		QuEChERS		SPE	
		NTP	PYR	NTP	PYR
White wine 1	0.8	101 ± 2	97 ± 3	104 ± 2	105 ± 3
	2.0	103 ± 1	99 ± 5	98 ± 3	97 ± 2
	3.0	98 ± 1	97 ± 3	102 ± 2	106 ± 3
White wine 2	1.0	99 ± 3	99 ± 2	95 ± 1	94 ± 4
	2.5	102 ± 2	103 ± 3	107 ± 4	107 ± 1
	4.0	97 ± 2	103 ± 4	105 ± 5	99 ± 3
Red wine 1	1.0	104 ± 2	96 ± 3	98 ± 3	107 ± 5
	2.5	103 ± 2	104 ± 2	105 ± 5	102 ± 4
	3.5	104 ± 4	105 ± 4	102 ± 1	98 ± 2
Red wine 2	1.5	98 ± 4	104 ± 5	101 ± 2	107 ± 4
	3.0	102 ± 3	105 ± 4	104 ± 1	96 ± 5
	4.0	102 ± 1	98 ± 5	96 ± 4	106 ± 4

To assess the accuracy of the method, we used the method of the average recovery (González et al. 1999) for grapes and wine samples. In all cases, the experimental t values were lower than the tabulated t values at a 95% confidence level (1.714 and 1.796 for n=24 and 12, respectively).

Conclusions

Here we have reported a novel strategy for the quantification of selected pesticides in food commodities. The use of PIF detection can expand the applicability of automated flow systems. Also, the use of multicommutated manifolds allows simple integration of on-line UV irradiation, separation, pre-concentration, and detection of the analytes, obtaining high sample throughputs. The bi-parameter system for the determination of NTP and PYR was satisfactorily applied to the analysis of these pesticides in grapes and wine samples, fulfilling the current maximum residue limits. Although chromatography is the preferred and most suitable option for the analysis of a high number of analytes, the development of quick and straightforward methods of analysis, such as the approach here reported, can be useful for the analysis of a small number of pesticides in food samples, providing an alternative for quality control purposes.

Acknowledgments

J.J.L. acknowledges a research scholarship from the Spanish Government (Ministerio de Educación y Ciencia). This study was funded by the "Ministerio de Economía y Competitividad" (grant number CTQ2016-7511-R).

Compliance with Ethical Standards

Funding This study was funded by "Ministerio de Economía y Competitividad" (grant number CTQ2016-7511-R).

Conflict of Interest Julia Jiménez-López declares that she has no conflict of interest. Eulogio J. Llorent-Martínez declares that he has no conflict of interest. Pilar Ortega-Barrales declares that she has no conflict of interest. Antonio Ruiz-Medina declares that he has no conflict of interest.

Ethical Approval This article does not contain any studies with human participants or animals performed by any of the authors.

Informed Consent Not applicable.

References

Brycht M, Vajdle O, Zbiljić J, et al (2012) Renewable silver-amalgam film electrode for direct cathodic SWV determination of clothianidin, nitenpyram and thiacloprid neonicotinoid insecticides reducible in a fairly negative potential range. Int J Electrochem Sci 7:10652–10665

de Oliveira LAB, Pacheco HP, Scherer R (2016) Flutriafol and pyraclostrobin residues in Brazilian green coffees. Food Chem 190:60–63

Dong X, Jiang D, Liu Q, et al (2014) Enhanced amperometric sensing for direct detection of nitenpyram via synergistic effect of copper nanoparticles and nitrogen-doped graphene. J Electroanal Chem

734:25–30

Dornellas RM, Nogueira DB, Aucélio RQ (2014) The boron-doped diamond electrode voltammetric method for ultra-trace determination of the fungicide pyraclostrobin and evaluation of its photodegradation and thermal degradation. Anal Methods 6:944–950

Economou A, Botitsi H, Antoniou S, Tsipi D (2009) Determination of multi-class pesticides in wines by solid-phase extraction and liquid chromatography-tandem mass spectrometry. J Chromatogr A 1216:5856–5867

Fan X, Zhao S, Chen X, Hu J (2017) Simultaneous determination of pyraclostrobin, prochloraz, and its metabolite in apple and soil via RRLC-MS/MS. Food Anal Methods 1–9

González AG, Herrador MA, Asuero AG (1999) Intra-laboratory testing of method accuracy from recovery assays. Talanta 48:729–736

Jeanty G, Wojciechowska A, Marty J-L, Trojanowicz M (2002) Flow-injection amperometric determination of pesticides on the basis of their inhibition of immobilized acetylcholinesterases of different origin. Anal Bioanal Chem 373:691–695

Jiménez-López J, Ortega-Barrales P, Ruiz-Medina A (2018) A photochemically induced fluorescence based flow-through optosensor for screening of nitenpyram residues in cruciferous vegetables. Food Addit Contam Part A 35:941–949

Lezi N, Economou A (2015) Voltammetric Determination of neonicotinoid pesticides at disposable screen-printed sensors featuring a sputtered bismuth electrode. Electroanalysis 27:2313–2321

Llorent-Martinez E, Barrales P, Fernandez-de Cordova M, Ruiz-Medina A (2010) Multicommutation in Flow Systems: A useful tool for pharmaceutical and clinical analysis. Curr Pharm Anal 6:53–65

Llorent-Martínez EJ, Alcántara-Durán J, Ruiz-Medina A, Ortega-Barrales P (2012) Determination of carbendazim in food products using a sequential injection analysis optosensor. Food Anal Methods 6:1278–1283

Llorent-Martínez EJ, Ortega-Barrales P, Fernández-de Córdova ML, Ruiz-Medina A (2011) Trends in flow-based analytical methods applied to pesticide detection: A review. Anal Chim Acta 684:30–39

Melchert WR, Reis BF, Rocha FRP (2012) Green chemistry and the evolution of flow analysis. A review. Anal Chim Acta 714:8–19

Molina-García L, Ruiz-Medina A, Fernández-de Córdova ML (2011) An automatic optosensing device for the simultaneous determination of resveratrol and piceid in wines. Anal Chim Acta 689:226–233

Obana H, Msahiro Okihashi, Kazuhiko Akutsu, et al (2002) Determination of acetamiprid, imidacloprid, and nitenpyram residues in vegetables and fruits by high-performance liquid chromatography with diode-array detection. J Agric Food Chem 50:4464–4467

Pano-Farias NS, Ceballos-Magaña SG, Muñiz-Valencia R, Gonzalez J (2017) Validation and assessment of matrix effect and uncertainty of a gas chromatography coupled to mass spectrometry method for pesticides in papaya and avocado samples. J Food Drug Anal 25:501–509

Papp Z, Guzsvány V, Švancara I, Vytřas K (2011) Voltammetric monitoring of photodegradation of clothianidin, nitenpyram and imidacloprid insecticides using a tricresyl phosphate-based carbon paste electrode. Int J Electrochem Sci 6:5161–5171

Pérez-Fernández V, Mainero Rocca L, Tomai P, et al (2017) Recent advancements and future trends in environmental analysis: Sample preparation, liquid chromatography and mass spectrometry. Anal Chim Acta 983:9–41

Piccirilli G, Escandar G, Cañada F, et al (2008) Flow-through photochemically induced fluorescence optosensor for the determination of linuron. Talanta 77:852–857

Ruiz-Medina A, Llorent-Martínez EJ, Fernández-de Córdova ML, Ortega-Barrales P (2012) Automated optosensor for the determination of carbaryl residues in vegetable edible oils and table olive extracts. J Food Compos Anal 26:66–71

Sánchez-Barragán I, Karim K, Costa-Fernández JM, et al (2007) A molecularly imprinted polymer for carbaryl determination in water. Sensors Actuators B Chem 123:798–804

Souza CF, da Cunha ALMC, Aucélio RQ (2009) Determination of picoxystrobin and pyraclostrobin by MEKC with on-line analyte concentration. Chromatographia 70:1461–1466

Trojanowicz M (2009) Recent developments in electrochemical flow detections—A review: Part I. Flow analysis and capillary electrophoresis. Anal Chim Acta 653:36–58

Wu S, Zhang H, Zheng K, et al (2018) Simultaneous determination and method validation of difenoconazole, propiconazole and pyraclostrobin in pepper and soil by LC–MS/MS in field trial samples from three provinces, China. Biomed Chromatogr 32:1-9

Xiu-ping Z, Lin M, Lan-qi H, et al (2017) The optimization and establishment of QuEChERS-UPLC–MS/MS method for simultaneously detecting various kinds of pesticides residues in fruits and vegetables. J Chromatogr B 1060:281–290

Yoshida T, Murakawa H, Toda K (2013) Determination of nitenpyram and its metabolites in agricultural products by using hydrophilic interaction liquid chromatography-tandem mass spectrometry. J Pestic Sci 38:27–32

Zhang M, Zhang H, Zhai X, et al (2017) Application of b-cyclodextrin–reduced graphene oxide nanosheets for enhanced electrochemical sensing of the nitenpyram residue in real samples. New J Chem 41:2169–2177

Parte II

Automated determination of Rifamycins making use of MPA–CdTe quantum dots

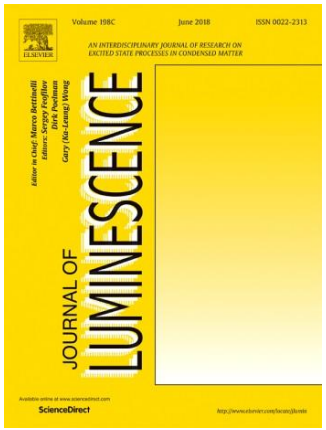

6. "Automated determination of Rifamycins making use of MPA–CdTe quantum dots"

J. Jimenez-López[1], L. Molina-García[1], S.S.M. Rodrigues[2], J.L.M. Santos[2], P. Ortega-Barrales[1], A. Ruiz-Medina[1]*

Publicado en Journal of Luminescence, en Julio de 2016, volumen 175, páginas 158–164.

Resumen

Las rifamicinas son un grupo de antibióticos particularmente efectivos contra las micobacterias y son usados para el tratamiento de enfermedades y trastornos importantes como la tuberculosis, el cáncer, la encefalopatía hepática o infecciones intestinales. Teniendo en cuenta el gran potencial clínico de estos medicamentos, es importante el desarrollo de procedimientos rápidos, simples y fiables para su control de calidad. Este artículo presenta un método analítico automático basado en el uso de *quantum dots* (puntos cuánticos) en un sistema de flujo multiconmutado. La detección se basa en el efecto *quenching* que la rifampicina y la rifaximina (dos importantes derivados de la rifamicina) producen sobre la fluorescencia de los *quantum dots* de CdTe con un capping de ácido mercaptopropiónico, siendo la principal ventaja de estos *quantum dots* su solubilidad en agua, lo que facilita su uso en el desarrollo de métodos analíticos.

Bajo las condiciones óptimas, la relación entre la intensidad de fluorescencia de los puntos cuánticos y las concentraciones de rifampicina o rifaximina fue lineal en el rango de 5-80 y 3-40 mg mL^{-1}, con límites de detección de 1.5 y 1.0 mg mL^{-1}, respectivamente. Se observaron desviaciones estándar relativas inferiores al 3% en todos los casos. Se obtuvo una frecuencia de muestreo de 70 muestras por hora, y los estudios de recuperación sirvieron para demostrar la exactitud del método propuesto, que se aplicó a la determinación de rifamicinas en formulaciones farmacéuticas y orina humana.

Este trabajo ha supuesto una nueva demostración de las ventajas que supone para la química analítica el empleo de los nanomateriales (*quantum dots* en este trabajo en particular) para el desarrollo y la mejora de métodos analíticos para la cuantificación de compuestos de interés. La simplicidad, rapidez, alta precisión y alta frecuencia de muestreo hacen de este método una nueva opción para el control de productos farmacéuticos en la industria.

6. "Automated determination of Rifamycins making use of MPA–CdTe quantum dots"

Abstract

Rifamycins are a group of antibiotics particularly effective against mycobacteria and they are used for the treatment of important diseases and disorders such as tuberculosis, cancer, hepatic encephalopathy or intestinal infections. Taking into account the great clinical potential of these drugs it is important to develop a rapid, simple and reliable strategy for its quantification. This paper presents an automated quantum dots-based analytical method making use of a multicommutated flow system and the quenching effect that rifampicin and rifaximin, two important rifamycin derivatives, have on the fluorescence of water-soluble mercaptopropionic acid-capped CdTe quantum dots.

Under the optimized conditions, the relationship between the fluorescence intensity of the quantum dots and rifampicin or rifaximin concentrations were linear in the range of 5-80 and 3-40 μg mL^{-1}, with a detection limit of 1.5 and 1.0 μg mL^{-1}, respectively. Relative standard deviations (RSD) lower than 3% were observed in all cases. A sample throughput of 70 determinations per hour and good recoveries were also achieved. The proposed method was satisfactory applied to the determination of rifamycins in pharmaceutical formulations and human urine.

Keywords: Rifamycins, Clinical analysis, Luminescence, CdTe quantum dots

1. Introduction

Rifamycins (RF) are complex macrocyclic antibiotics gained from an Actinomycete bacterium and they play a preponderant role as antibiotics in therapeutics against tuberculosis and various other mycobacterial infections. Two of their most useful and well established semisynthetic derivatives are Rifampicin (RFP) and Rifaximin (RFX) [1]. RFP is used in the treatment of tuberculosis worldwide [2, 3] and its inhibiting effect on the growth of a variety of human cancer cells has also been demonstrated, being considered to have potent antiangiogenic properties, especially in targeting hepatobiliary tumor [4-7]**.** On the other hand, RFX is useful in the treatment of other important disorders with enterobacteria involvement including hepatic encephalopathy [8] and intestinal infections such as travellers' diarrhoea and diverticular and crohn's diseases [9, 10].

Taking into account the great clinical potential of these drugs, the high use of them and the new formulations and synthetic methods [1], it is important to develop rapid, simple, accurate and reliable strategies for its quality control analysis. Various methods have been described in scientific literature for the determination of RF in plasma and cellular [3, 11-14], rat serum [15, 16], pharmaceuticals [17, 18] or urine [19-21]. Among the determinations above mentioned High-Performance Liquid Chromatography (HPLC) is the most analytical technique utilized, being coupled to Mass Spectrometry (MS), Tandem Mass Spectrometry (MS/MS) or Ultraviolet (UV) detectors. Moreover,

fluorescence methods based on quenching effect [22, 23] or voltammetric quantification by using nickel hydroxide nanoparticles [24] were also applied to the analysis of pharmaceutical preparations.

Quantum dots (QDs) are colloidal semiconductor nanocrystals formed from group II–IV, III–V or IV–VI materials, such as those made of CdSe and CdTe. They can be prepared readily in aqueous media or made water soluble by appropriate capping with hydrophilic ligands [25]. In the aqueous synthesis, QDs are stabilized by some functional ligands, such as mercaptopropionic acid (MPA) and glutathione (GSH), among others, and exhibit some unique properties such as lower cost, less toxicity, water solubility, and biocompatibility. Thanks to recent advances in nanotechnology and nanomaterials they have been proposed as an alternative to conventional organic fluorophores because of their unique and superior optical properties such as high photo-bleaching threshold, good chemical stability, size-tunable photoluminescence spectra, broad absorption, narrow emission wavelengths and excellent photostability [26, 27]. The field of light-emitting nanoparticles has experienced an enormous development over the past two decades, being numerous the QDs articles focused on theoretical studies. In addition, these nanoparticles have been using for the design of fluorescence chemical and biological probes with different applications, such as the determination of biomolecules [26, 28, 29]. Simple and sensitive fluorescence sensors using QDs have also been developed for the determination of different kinds of analytes that could quench the fluorescence of QDs [30-33].

New innovations and application regarding QDs and related technologies are continuously demanded. An interesting possibility is implementing the use of QDs in flow systems, thus automating the

whole analytical procedure. Automatic schemes and non-manual sample handling and measuring methodologies making use of QDs are still scarce. The use of automated flow methodologies have proved to be an excellent tool for handling solutions and they permit the development of environmentally friendly methods preventing operators from coming into contact with toxic material as QDs. Flow methodologies also allow lower reagents' consumption and waste generation, and an increase in the degree of automation and miniaturization. Multicommutated Flow Injection Analysis (MCFIA) is one of the most versatile flow methodologies and it is based on the use of discrete commutation devices (3-way solenoid valves) to control the flow of solutions, being all the system automatically controlled by an appropriate software [34, 35].

In this paper RFP and RFX have been determined by their quenching effect produced on the fluorescence of MPA- capped CdTe QDs. It is noteworthy that, in comparison with chromatography methods which are characterized to be technically complex, cost-effective and time consuming, the alternated proposed approach has the advantages of allowing a simple and fast analysis and obtaining high repeatability and sample throughput as a consequence of the use of MCFIA. For the first time, a QDs-based flow method has been developed for RF quantitation in pharmaceutical formulations and human urine.

2. Materials and methods

2.1. Reagents and solutions

For the synthesis of the CdTe QDs, cadmium chloride hemi (pentahydrate) ($CdCl_2 \cdot 2.5\ H_20$, 99%), sodium telluride (100 mesh, 99%), tellurium powder (200 mesh, 99.8%), sodium borohydride ($NaBH_4$, 99%), L-glutathione reduced (GSH ≥ 98%) were pursached from Sigma-Aldrich (St. Louis, MO, USA). Trisodium citrate dehydrate and 3-mercaptopropionic acid (MPA 99%) were obtained from Fluka (St. Louis MO, USA). Absolute ethanol (99.5%) was pursached by Panreac (Barcelona, Spain).

RFP (≥97%; Sigma, Madrid, Spain) and RFX (Sigma, Madrid, Spain) stock solutions of 300 mg L^{-1} was prepared by dissolving the required weight in a methanol:water solution (25% (v:v)). All of them were kept in the dark under refrigeration at 4º C and remained stable for at least 2 months.

Hydrochloric acid (HCl, 37%), sodium hydroxide (NaOH, 98%), sodium carbonate 10- hydrate ($Na_2CO_3 \cdot 10\ H_20$, 99%), sodium hydrogen carbonate ($NaHCO_3$, 99.9%), ammonium chloride (NH_4Cl, 99.9%), potassium dihydrogen phosphate (KH_2PO_4, 99%) and ammonia (NH_3, 30%), all of them of reagent grade, were obtained from Panreac (Barcelona, Spain). NaOH and HCl (1 and 5 $\cdot 10^{-2}$ mol L^{-1}) solutions were used to adjust the pH when required. All the excipients, ions or compounds, used in the interference study were obtained from Sigma-Aldrich.

2.2. Instrumentation

For the characterization of the synthesized QDs, absorbance and fluorescence spectra were recorded using a Jasco V-660 spectrophotometer and a PerkinElmer LS 50B luminescence spectrometer (Lisboa, Portugal), respectively. QDs centrifugation was performed with a ThermoElectron Jouan BR4I refrigerated centrifuge.

Luminescence measurements in the MCFIA system were performed with a Cary-Eclipse Luminescence Spectrometer (Varian Inc., Mulgrave, Australia) controlled by a computer equipped with a Cary-Eclipse (Varian) software package for data collection and treatment. Instrument excitation and emission slit widths were set at 5 and 10 nm, respectively. The detector voltage was 580 and 610 V and the excitation and emission wavelengths were 340 and 637 nm, for RFP and RFX, respectively. A Hellma flow-cell 176.752-QS (25 µL of inner volume and a light path length of 1.5 mm) was used too. All experiments were carried out at room temperature.

The flow system (**Fig. 1**) was built with: one four-channel Gilson Minipuls-3 peristaltic pump (Villiers le Bel, France), fitted with a rate selector and pump tubing type Solvflex (Elkay Products, Shrewsbury, MA, USA); three 161T031 NResearch three-way solenoid valves (Neptune Research, MA, USA); and an electronic interface, based on ULN 2803 integrate circuits, to generate the electric potential (12 V) and current (100 mA) required to control the valves. PTFE tubing (0.8 mm i.d.) and methacrylate connections were also used. The software for controlling the system was developed by our research group using Visual Basic 6.0.

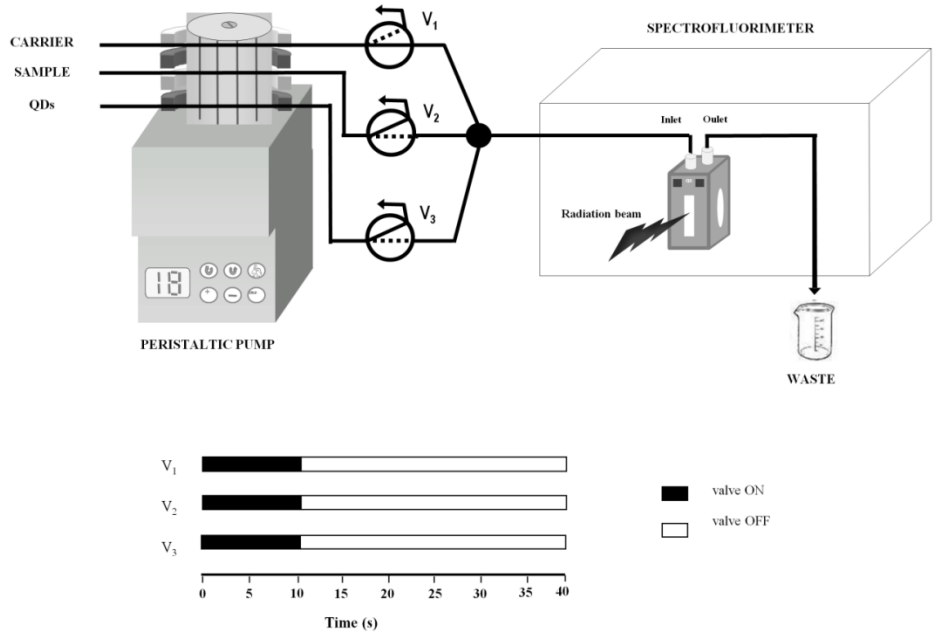

Fig.1. Upper part: MCFIA manifold; V_1, V_2, V_3 refer to three-way solenoid valves.

Bottom part: valves scheme.

The morphology and microstructure of QDs were examined by Transmission Electron Microscopy (TEM) with a JEOL JEM 1010 with an accelerating voltage of 80 kV. The samples for TEM were made by dropping an aqueous solution onto a 200-mesh copper grid coated with a Formvar-carbon film. It allows 5000x magnification range from up to 600k. The microscope has a digital images capture camera Gatan model 782. DigitalMicrograph is employed as control software and image processing.

2.3. Synthesis and characterization of QDs

Three different diameters of MPA-capped CdTe QDs were synthesized as described by Zou et al. [36] with some modifications. The size of the synthesized nanoparticles decreased from 1.36 to 3.72

nm. Briefly, 1.6×10^{-3} mol of $NaHB_4$ reacted with 0.4×10^{-3} mol of tellurium powder in N_2 saturated water inside a 50 mL flask at 80 ºC for 30 min under constant stirring. The resulting NaHTe aqueous solution was transferred to another flask containing 4.0×10^{-3} mol $CdCl_2$ and 6.8×10^{-3} mol MPA in a 100 mL of N_2 saturated water solution. The pH of the solution was adjusted to 11.5 by addition of 1 mol L^{-1} NaOH. The Cd^{2+}:Te^{2-}: MPA molar ratio was fixed as 1:0.1:1.7.

GSH-capped CdTe QDs (with three diameters varying from 2.57 to 3.47 nm) were synthesized using L-glutathione reduced and were prepared in a one-step route by modified Qian's procedure [37]. Briefly, $CdCl_2$, Na_2TeO_3 and GSH (Cd:Te:GSH molar ratio 1:0.2:1.2) were added into a single reaction pot with $NaBH_4$, trisodium citrate and water. The solution pH was adjusted to 10.5 by the addition of 1.0 mol L^{-1} NaOH and the resulting solution was heated with vigorous stirring at 100 ˚C under reflux for QDs growth.

The CdTe QD size was tuned by varying the heating time. In order to remove the contaminants, purification of QDs was performed by precipitation in absolute ethanol. The precipitate fractions were subsequently centrifuged; vacuum dried, kept in amber flasks and kept in the refrigerator. All the fractions obtained were re-suspended in deionized water maintaining the initial synthesis concentration and the diameter of CdTe QDs was calculated by the following expression [38]:

$$D = (9.8127\times10^{-7})\,\lambda^3 - (1.7147\times10^{-3})\,\lambda^2 + (1.0064)\,\lambda - 194.84$$

Where D is the diameter of the nanocrystals (nm); λ is the wavelength of maximum absorbance corresponding to the first excitonic absorption peak of the crystal.

To facilitate the preparation of the QDs solutions was also necessary to calculate the molar weight of the different sized nanocrystals. This was carried out by establishing firstly the extinction coefficient (ε) by using the expression [38]:

$$\varepsilon = 3450\ \Delta E(D)^{2.4}$$

where ΔE is the transition energy corresponding to the first absorption peak and the unit is in eV. Knowing ε it was simple to reach the molar mass by measuring the absorbance of a known concentration solution and by applying the Lambert–Beer law.

The morphology of MPA-capped CdTe QDs was confirmed by TEM, as depicted in **Fig. 2**. Well-dispersed spherical QDs with uniform particle size and crystallinity can be observed. Consequently the used MPA-capped CdTe QDs exhibited narrow fluorescence bandwidth.

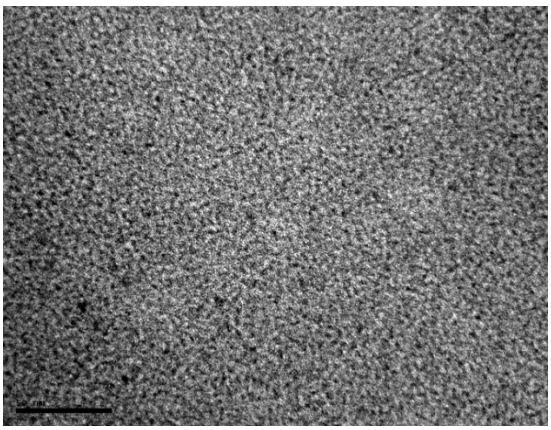

Fig.2. TEM image of aqueous MPA-capped CdTe QDs. Magnification: 500kx.

2.4. Sample preparation

Several pharmaceutical formulations containing RFP or RFX available in the Spanish and US Pharmacopoeia were analyzed.

In order to obtain a homogeneous sample, three tablets of each pharmaceutical formulation were accurately weighed and finely ground. A portion of the powder obtained, equivalent to the average weight of a tablet (depending on the drug), was transferred to a 500 mL volumetric flask and dissolved in a methanol:water solution (25% (v:v)). Appropriate dilutions with 0.02 mol L^{-1} Na_2CO_3/$NaHCO_3$ buffer were realized.

Human urine samples were obtained from healthy volunteers and required no further pre-treatment. Only when turbidity was observed, a filtration step was required. The samples were spiked with a suitable RFP or RFX concentration, diluted (1:25 (v/v)) with 0.02 mol L^{-1} Na_2CO_3/$NaHCO_3$ buffer and directly inserted in the flow system.

2.5. General MCFIA procedure

The schematic valve system diagram is shown in **Fig. 1**. In the initial status, all valves were switched off and the carrier (0.02 mol L^{-1} Na_2CO_3/$NaHCO_3$ buffer solution, pH 9 or 9.5) was flowing through the flow-cell while all other solutions were recycled to their vessels. Then, all valves (V_1, V_2 and V_3) were switched on for 10 s and the direct confluence between QDs and sample solutions (both prepared in 0.02 mol L^{-1} Na_2CO_3/$NaHCO_3$ buffer solution, pH 9 or 9.5) took place, whereas the carrier solution was recycled to its vessel. The QDs-sample mixture was directed to the spectrofluorimeter, recording the

corresponding analytical signal. A blank has to be recorded before any sample analysis, because the analytical signal used is the fluorescence decrease (quenching effect induced by RFP or RFX). A flow-rate of 2.3 mL min^{-1} was employed.

3. Results and discussion

3.1. Chemical variables

Preliminary tests showed that RFP and RFX interacted with both GSH-capped CdTe and MPA-capped CdTe QDs, reducing their photoluminescence emission by means of a quenching mechanism. It was in accordance with others previous studies where the quenching effect that RF have on serum albumin and CdTe/ZnS QDs fluorescence were also used for its own determination in pharmaceuticals and urine samples [22, 23].

QDs have a large fraction of their atoms arrayed on their surfaces and are capped with organic ligands, which make their photoluminescence highly sensitive to charge-transfer processes. A possible mechanism of the quenching effect that RF provokes on CdTe QDs relies on an electron transfer-process [39, 40]. The establishment of interactions between electron-donor groups on each analyte molecule and incompletely coordinated Cd^{2+} on the QDs surface, resulting on the establishment of mid-gap energy levels that act as electron-trapping states preventing electron-hole recombination and yielding a quenching of the nanocrystal photoluminescence.

In addition, the Stern-Volver plot was constructed. The dynamic process in which quenching mechanism is mainly due to collision is governed by the linear Stern-Volmer equation [41]:

$$\frac{I_0}{I} = 1 + K_{SV}[Q]$$

where I_0 is luminescence intensity of solute in the absence of quencher and I the luminescence intensity in the presence of quencher, K_{SV} ($=k_q\tau$ where k_q is quenching rate parameter and τ is the lifetime of the solute in the absence of quencher) is the Stern-Volmer constant and [Q] is the quencher concentration. The previous equation is applicable as long as the experimental results show linear variation. In our case, the plot obtained was (for RFP and RFX, respectively):

$$\frac{I_0}{I} = 1.1823 + 0.0068[RFP] \qquad r=0.9963$$

$$\frac{I_0}{I} = 1.1095 + 0.0274[RFX] \qquad r=0.9969$$

The Stern-Volmer constant (K_{SV}) for both analytes is indicated in Table 1.

QDs size, concentration and pH value, the most influencing variables on the net analytical signal, had to be studied. All experiments were carried out with the MCFIA system already described, performing the on-line confluence between QDs and sample solutions.

Respect to QDs size, several diameters of the different QDs (MPA-capped CdTe: 1.36, 3.14 and 3.72 nm; GSH-capped CdTe: 2.57, 3.19 and 3.47 nm) were evaluated, using the optimum range of QDs' concentrations depending on the diameter (higher concentrations are required for lower sizes). Firstly, the effect of the pH was studied. At

pH values lower than 6.0 a precipitate was generally formed, no matter the size of the QDs. Hence, a precise study of this variable was carried out in the pH range between 6.0 and 11.0 by using 5 x 10^{-2} mol L^{-1} HCl or NaOH solutions. The highest net signal (highest quenching) was obtained at pH values around 9.0 for the MPA-capped CdTe QDs with 3.72 nm of diameter and GSH-capped CdTe QDs with 3.47 nm of diameter. However, lower reproducibility were observed when GSH-capped CdTe QDs were used being the QDs capped with MPA selected as optimum. The pH values finally selected were 9.0 and 9.5 for RFP and RFX, respectively since they provided the higher quenching effect on the MPA-capped CdTe QDs (**Fig. 3**).

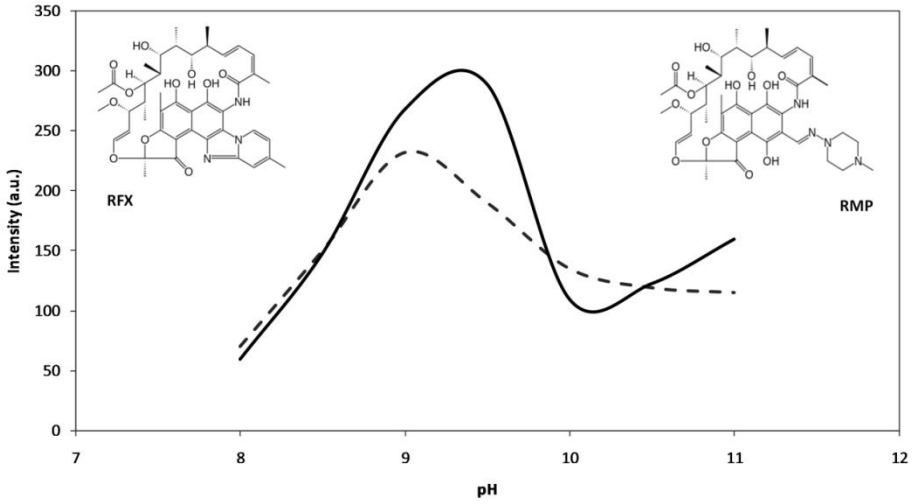

Fig.3. Influence of the pH over analytical signal. MPA- capped CdTe QDs (1.5 μmol L^{-1}, 3.72 nm diameter). 20 μg mL^{-1} of RFP and RFX. (Dotted line: RFP; Solid line: RFX).

The effect of ionic strength on the analytical signal was studied by using a $Na_2CO_3/NaHCO_3$ and NH_3/NH_4Cl buffer solutions at pH values of 9.0 and 9.5 (depending on the analyte). Similar behavior was

observed for both analytes, RFP and RFX. Higher net signals were obtained with the use of Na_2CO_3/$NaHCO_3$ buffer solution (see RFP in Fig. 4). Therefore it was selected for further experiments. In addition, the study of the influence of buffer concentration was performed in the 0.0075–0.05 mol L^{-1} range. As it can be also seen in **Fig. 4**, the best results were achieved when using 0.02 mol L^{-1}. Hence, all solutions were prepared in 0.02 mol L^{-1} Na_2CO_3/$NaHCO_3$ buffer solution (pH=9) and 0.02 mol L^{-1} Na_2CO_3/$NaHCO_3$ buffer solution (pH=9.5) for RFP and RFX samples, respectively.

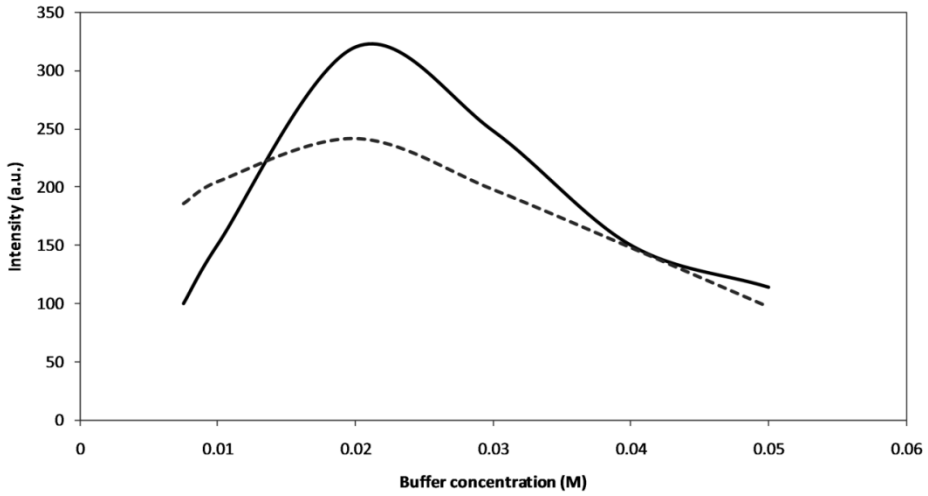

Fig.4. Effect of both ionic strength and buffer concentration over analytical signal. MPA- capped CdTe QDs (1.5 μmol L^{-1}, 3.72 nm diameter). 25 μg mL^{-1} of RFP. (Dotted line: NH_3/NH_4Cl buffer solution; Solid line: Na_2CO_3/$NaHCO_3$ buffer solution).

The QDs' concentration was also studied for both RF. In this case three different ranges of concentration were established according to the sizes of the QDs (MPA and GSH, respectively): 1–4 μmol L^{-1} (diameter of 3.72 and 3.47 nm), 2–8 μmol L^{-1} (diameters of 3.14 and

3.19 nm) and 7–15 μmol L^{-1} (diameters of 1.36 and 2.57 nm). Similar behavior was observed in all cases: the net signal increased up to the middle value of the tested range and then decreased for higher concentrations (**Fig. 5**). This effect could be explained by a decrease of QDs' fluorescence when the QDs' concentration reached too high values, mainly due to the inner filter effect as a result of re-absorption of emitted radiation. Finally, 1.5 μmol L^{-1} QDs solution of 3.72 nm diameter (0.02 mol L^{-1} Na_2CO_3/$NaHCO_3$ buffer, pH 9.0 and 9.5) was selected as optimum value, since it provided the best sensitivity.

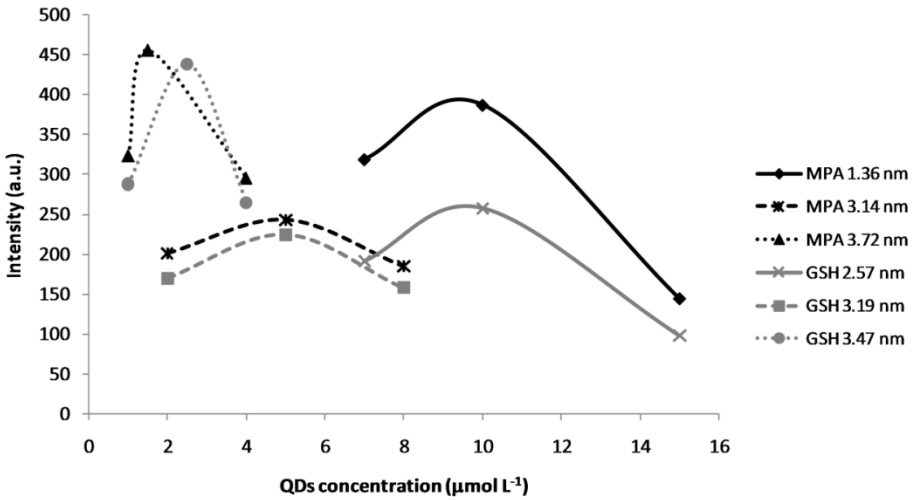

Fig.5. Influence of QDs' concentration over analytical signal. 20 μg mL^{-1} of RFP.

3.2. Instrumental variables

The most outstanding characteristics of QDs are their broad absorption spectra, enabling excitation at a wider range of wavelengths, and symmetric and narrow emission spectra. In addition, the same particles of different sizes present specific emission wavelengths, and

this emission increases proportionally with QDs diameters through a red-shift phenomenon [42]. The QD fluorescence spectra for the different sized QDs assayed in this work (1.36, 3.14 and 3.72 nm of MPA-capped CdTe QDs and 2.57, 3.19 and 3.47 nm of GSH-capped CdTe QDs) showed maximum excitation and emission wavelengths at 344/521, 482/583, 340/637, 446/537, 480/585 and 353/617 nm, respectively.

Taking into account the QDs (MPA-capped CdTe) and the size (3.72 nm) optimum for the determination of RFP and RFX, the selected wavelengths were 340/637 nm/nm ($\lambda_{exc}/\lambda_{em}$).

Then, the emission and excitation slits (5-20 nm), and voltage of the photomultiplier tube (450-750 V) were optimized to obtain the best sensitivity. Results showed that, under the optimum conditions described previously, the best signal was obtained when instrumental conditions were fixed to provide the highest possible signal from the blank solution (QDs in 0.02 mol L^{-1} Na_2CO_3/$NaHCO_3$ buffer solution). Finally, voltage of the photomultiplier tube for RFP and RFX was set at 580 and 610 V, respectively, whereas excitation and emission slits were selected at 5 and 10 nm for both analytes.

3.3. Figures of merit

Figures of merit are shown in **Table 1**.

Table 1

Analytical parameters.

Parameter	**RFP**	**RFX**
Excitation/ emission slits (nm/nm)	5/10	5/10
Photomultiplier tube voltage (V)	580	610
Calibration graph		
Intercept	159.76	124.59
Slope (mL μg^{-1})	2.952	7.757
Correlation coefficient	0.9993	0.9952
Linear dynamic range ($\mu g\ mL^{-1}$)	5-80	3-40
Detection limit ($\mu g\ mL^{-1}$)	1.5	1.0
Quantitation limit ($\mu g\ mL^{-1}$)	5.0	3.0
Intra-day RSD (%) (n=7)		
10 $\mu g\ mL^{-1}$	1.9	2.1
30 $\mu g\ mL^{-1}$	2.8	2.5
Inter-day RSD (%) (n=7)		
10 $\mu g\ mL^{-1}$	3.8	4.7
30 $\mu g\ mL^{-1}$	4.2	4.2
Sampling frequency / h^{-1}	70	70
K_{SV} (mL μg^{-1})	0.0068	0.0274

The proposed method offered good linearity for both RFP and RFX. The linearity was in the range of 5-80 $\mu g\ mL^{-1}$ and 3-40 $\mu g\ mL^{-1}$, respectively. The obtained data was fitted by standard least-squares calibration. Detection and quantitation limits were estimated as the concentrations of analyte that produced analytical signals equal to three and ten times, respectively, the standard deviation of the luminescence of the blank solution. The detection limits obtained were 1.5 $\mu g\ mL^{-1}$ for RFP and 1.0 $\mu g\ mL^{-1}$ for RFX.

The ruggedness and robustness of the method were also studied with RFP and RFX solutions. The ruggedness of the method was assessed by comparison of the intra- and inter-day assay results under

taken by two analysts; the RSD values did not exceed 3% and 5%, respectively. The robustness of the method was also studied under a variety of conditions such as small changes in the pH of sample solution (8.8–9.2 for RFP and 9.3-9.7 for RFX), flow-rate (2.1–2.5 mL min^{-1}), buffer concentration (0.01-0.03 mol L^{-1}), and excitation/emission wavelengths (±2 nm). The percent recoveries for RFP and RFX were in the 95–105% range in all cases (considering 100% the value obtained under the optimum conditions). With both studies the ruggedness and robustness of the MCFIA system were demonstrated.

3.4. Interference study

The potential interfering effect of excipients commonly found in pharmaceutical formulations containing RFP and RFX were also studied. Experiments were carried out using a solution containing 30 μg mL^{-1} of both analytes. Tolerance level was defined as the amount of foreign species that produced an error not exceeding ±3% in the determination of the analyte. The tolerated interferent/analyte (w/w) ratio was higher than 120 for starch, glucose, saccharose, lactose and polyethylene glycol. As a result, RFP and RFX could be analyzed, without significant errors, in the presence of high concentrations of potentially interfering compounds in pharmaceuticals.

In the same way, the tolerated interferent/analyte (w/w) ratio was studied for human urine, being this ratio higher than 1000 for some ions (Na^+, K^+, NH_4^+, Cl^-, SO_4^{2-}, NO_3^- and PO_4^{3-}) and higher than 10 for uric acid and urea. In all cases, the tolerated ratios observed were higher than the ones normally found in real samples.

3.5. Analytical applications

Pharmaceutical samples, prepared as described under "*Sample preparation*" section, were analyzed by triplicate. Four pharmaceuticals available in the Spanish and US Pharmacopoeia (tablets) and 2 human urines were analyzed. For RFP, human urinary elimination accounts for about 30% of the drug administration, whereas for RFX, the elimination is only about 0.32%. Therefore, the determination in human urine is possible mainly for RFP where this compound appears accompanied by various metabolites such as 3-formylrifamycin SV, rifampicin N-oxidation and 25-desacetyl rifampicin [21].In the case of pharmaceuticals, RFP and RFX amounts determined by the proposed method were in good agreement with those ones provided by the manufacturer. A recovery study was also performed in both pharmaceuticals and urine (only for RFP) in order to evaluate the accuracy of the method. It was carried out by spiking three different levels of RFP and RFX concentrations to the analyzed samples. The obtained results are shown in **Table 2** and **Table 3**, with recoveries ranging from 97% up to 103% and RSDs lower than 3% in all cases.

Table 2

Recovery study of RF in pharmaceuticals.

SAMPLE	ADDED (mg)	RECOVERY (%)	RSD (%)[a]
RIFALDIN, *Ltd. Sanofi Aventis* (600 mg RFP/tablet)	-	99	2
	150	97	1
	400	98	1
	700	97	< 1
RIFATER, *Ltd. Sanofi Aventis* (120 mg RFP/tablet)	-	99	1
	75	97	< 1
	150	98	2
	300	97	1
SPIRAXIN, *Ltd. Bama-Geve* (200 mg RFX/tablet)	-	101	2
	100	100	1
	200	103	3
	400	100	< 1
XIFAXAN, *Ltd. Salix Pharmaceuticals* (200 mg RFX/tablet)	-	99	1
	50	99	1
	175	99	2
	400	101	1

[a]Means of three determinations

Table 3

Recovery study of RFP in human urine.

SAMPLE	ADDED (μg mL^{-1})	RECOVERY (%)	RSD (%)[a]
URINE 1	10	101	1
	20	102	2
	50	103	< 1
URINE 2	7	101	2
	25	102	1
	60	100	1

[a]Means of three determinations

4. Conclusions

An automated, simple, rapid, low-cost and reliable multicommutated QDs-based analytical method is described for the satisfactory determination of RF in pharmaceutical preparations and human urine needing no pretreatment, only filtration or dilution of the samples. The system is based on the quenching effect that these drugs have on the fluorescence of MPA-capped CdTe QDs. The employment of the multicommutation principles permits to automate the system and to obtain a high sample throughput. It makes the proposed method suitable for the routine analysis of RF being useful for for pharmacokinetic studies, recommendations and assessment of environmental contamination as well as quality control in clinical industry. Moreover, the low consumption of reagents and low waste generation offer an environmental friendly analytical system. It is worth mentioning that it is the first analytical method described for the determination of RF where the attachment of automatic scheme and QDs fluorescence quenching is used together. The quenching effect that RF have on the fluorescence of water-soluble MPA-CdTe QDs could be considered for future analytical purposes and applied for different formats of RF assays. Taking into account the effectiveness of these compounds in the treatment of tumors, it could be of great interest their monitoring and analysis directly in blood or human cells.

Acknowledgements

J.J.L. acknowledges research scholarship from Spanish Government (Ministerio de Educación y Ciencia).

References

[1] K. Bujnowski, L. Synoradzki, T.A. Zevaco, E. Dinjus, E. Augustynowicz-Kopec, A. Napiorkowska, Tetrahedron 71 (2015) 158-169.

[2] R. van Crevel, B. Alisjahbana, W.C.M. de Lange, F. Borst, H. Danusantoso, J.W.M. van der Meer, D. Burger, R.H.H. Nelwan. Int. J. Tuberc. Lung Dis. 6 (2002) 497-502.

[3] K.H. Hee, J.J. Seo, L.S. Lee, J. Pharm. Biomed. Anal. 102 (2015) 253-260.

[4] M. Shichiri, N. Fukai, Y. Kono, Y. Tanaka, Cancer Res. 69 (2009) 4760-4768.

[5] A. Courtois, L. Payen, L. Vernhet, E.G.E. de Vries, A. Guillouzo, O. Fardel, Cancer Lett. 139 (1999) 97-104.

[6] J. Chuan, Y. Li, L. Yang, X. Sun, Q. Zhang, T. Gong, Z. Zhang, J. Nanopart. Res. 15 (2013) 1-9.

[7] N.A. Zainal, S.R.A. Shukor, H.A.A. Wab, K.A. Razak, Chem. Eng. Trans. (2013) 2245-2250.

[8] E. Mattila, P. Arkkila, P.S. Mattila, E. Tarkka, P. Tissari, V.J. Anttila, Aliment. Pharmacol. Ther. (2013) 122-128.

[9] G.W. Robins, K. Wellington, Drugs 65 (2005) 1697-1713.

[10] S. Maccaferri, B. Vitali, A. Klinder, S. Kolida, M. Ndagijimana, L. Laghi, F. Calanni, P. Brigidi, G.R. Gibson, A. Costabile, J. Antimicrob. Chemother. 65 (2010) 2556-2565.

[11] R.C. Hartkoorn, S. Khoo, D.J. Back, J.F. Tjia, C.J. Waitt, M. Chaponda, G. Davies, A. Ardrey, S. Ashleigh, S.A. Ward, J. Chromatogr. B-Anal. Technol. Biomed. Life Sci. 857 (2007) 76-82.

[12] X. Zhang, J. Duan, K. Li, L. Zhou, S. Zhai, J. Chromatogr. B-Anal. Technol. Biomed. Life Sci. 850 (2007) 348-355.

[13] R.N. Rao, R.M. Vali, B. Ramachandra, P.K. Maurya, Biomed. Chromatogr. 25 (2011) 1201-1207.

[14] A.L. Allanson, M.M. Cotton, J.N.A. Tettey, A.C. Boyter, J. Pharm. Biomed. Anal. 44 (2007) 963-969.

[15] R.N. Rao, R.M. Vali, A.V.P. Rao, J. Sep. Sci. 35 (2012) 1945-1952.

[16] X. Zhang, R. Wang, H. Xie, Z. Jia, W. Li, J. Zhang, Y. Wang, Biomed. Chromatogr. 29 (2015) 475-480.

[17] J. Liu, J. Sun, W. Zhang, K. Gao, Z. He, J. Pharm. Biomed. Anal. 46 (2008) 405-409.

[18] M.Y. Khuhawar, F.M.A. Rind, J. Chromatogr. B-Anal. Technol. Biomed. Life Sci. 766 (2002) 357-363.

[19] S. Stets, T.M. Tavares, P.G. Peralta-Zamora, C.A. Pessoa, N. Nagata, J. Braz. Chem. Soc. 24 (2013) 1198-1205.

[20] R.N. Rao, D.D. Shinde, S.B. Agawane, Biomed. Chromatogr. 23 (2009) 563-567.

[21] Y.D. Liang, J.F. Song, M. Xu, Spectrochim. Acta A-Mol. Biomol. Spectrosc. 67 (2007) 430-436.

[22] J.D. Yang, S.X. Deng, Z.F. Liu, L. Kong, S.P. Liu, Luminescence 22 (2007) 559-566.

[23] Z. Liu, P. Yin, H. Gong, P. Li, X. Wang, Y. He, J. Lumin. 132 (2012) 2484-2488.

[24] S. Rastgar, S. Shahrokhian, Talanta 119 (2014) 156-163.

[25] C.I.C. Silvestre, C. Frigerio, J.L.M. Santos, J.L.F.C. Lima, Anal. Chim. Acta 699 (2011) 193-197.

[26] X. Wang, M.J. Ruedas-Rama, E.A.H. Hall, Anal. Lett. 40 (2007) 1497-1520.

[27] M.J. Ruedas-Rama, J.D. Walters, A. Orte, E.A.H. Hall, Anal. Chim. Acta 751 (2012) 1-23.

[28] D.B. Cordes, S. Gamsey, B. Singaram, Angew. Chem.-Int. Ed. 45 (2006) 3829-3832.

[29] J. Lei, H. Ju, Trac-Trend. Anal. Chem. 30 (2011) 1351-1359.

[30] E.M. Ali, Y. Zheng, H.-h. Yu, J.Y. Ying, Anal. Chem. 79 (2007) 9452-9458.

[31] R. Gill, L. Bahshi, R. Freeman, I. Willner, Angew. Chem.-Int. Ed. 47 (2008) 1676-1679.

[32] M. Liu, L. Xu, W. Cheng, Y. Zeng, Z. Yan, Spectrochim. Acta A-Mol. Biomol. Spectrosc. 70 (2008) 1198-1202.

[33] R. Tu, B. Liu, Z. Wang, D. Gao, F. Wang, Q. Fang, Z. Zhang, Anal. Chem. 80 (2008) 3458-3465.

[34] E.J. Llorent-Martinez, P.O. Barrales, M. Luisa Fernandez-de Cordova, A. Ruiz-Medina, Curr. Pharm. Anal. 6 (2010) 53-65.

[35] V. Cerda, C. Pons, Trac-Trend. Anal. Chem. 25 (2006) 236-242.

[36] L. Zou, Z. Gu, N. Zhang, Y. Zhang, Z. Fang, W. Zhu, X. Zhong, J. Mater. Chem. 18 (2008) 2807-2815.

[37] H.F. Qian, C.Q. Dong, J.F. Weng, J.C. Ren, Small 2 (2006) 747-751.

[38] W.W. Yu, L.H. Qu, W.Z. Guo, X.G. Peng, Chem. Mater. 15 (2003) 2854-2860.

[39] X. Ji, G. Palui, T. Avellini, H.B. Na, C. Yi, K.L. Knappenberger, H. Mattoussi, J. Am. Chem. Soc. 134 (2012) 6006-6017.

[40] A. Xiangzhao, M. Qiang, S. Xingguang, Microchim. Acta 180 (2013) 269-277.

[41] R.M. Melavanki, R.A. Kusanur, J.S. Kadadevaramath, M.V. Kulakarni, J. Lumin. 129 (2009) 1298-1303.

[42] J.M. Costa-Fernandez, R. Pereiro, A. Sanz-Medel, Trac-Trend. Anal. Chem. 25 (2006) 207-218.

New perspectives of quantum dots in the food field: determination of β-carotene in tropical fruit juices and food supplements

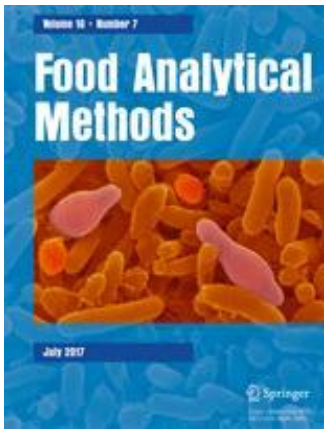

7. "New perspectives of quantum dots in the food field: determination of β-carotene in tropical fruit juices and food supplements"

J. Jiménez-López[1], J.L.M. Santos[2], P. Ortega-Barrales[1], A. Ruiz-Medina[1]*

Publicado en Food Analytical Methods, en Enero de 2017, volumen 10: 7, páginas 2412–2421.

Resumen

En este trabajo se ha propuesto un método novedoso y sencillo para la determinación de β-caroteno, un carotenoide abundante en plantas y frutas. Se ha aplicado el Análisis por inyección en flujo multiconmutado (MCFIA) como metodología de flujo automatizado para el análisis de β-caroteno en zumos de frutas tropicales y complementos alimenticios, haciendo uso del efecto atenuante (quenching) causado por este analito sobre la fluorescencia de quantum dots (puntos cuánticos, QDs) de CdTe con un recubrimiento de glutationa. En condiciones óptimas, el método se comportó de forma lineal en el rango de 0.3-15 μg mL^{-1}, con un límite de detección de 0.09 μg mL^{-1} y desviaciones estándar relativas inferiores al 3%. La frecuencia de muestreo fue de, aproximadamente, 80 muestras por hora, y los resultados obtenidos se compararon tanto con los

proporcionados por el fabricante, como con los obtenidos por un método de referencia cromatográfica, sin observar diferencias significativas entre nuestros resultados y los del fabricante o el método cromatográfico. De esta forma, se pudo comprobar la exactitud del método propuesto.

Se seleccionó el β-caroteno como analito debido a su gran importancia, que se deriva de su capacidad antioxidante, con los consiguientes beneficios para la salud. En este estudio, se ha hecho uso de las amplias ventajas que presentan las nuevas tecnologías como son los QDs para llevar a cabo la determinación del analito. Gracias a la combinación de los sistemas automatizados con la utilización de los QDs, ha sido posible desarrollar dicho método analítico, cuyas principales ventajas son su sencillez y bajo consumo de reactivos.

7. "New Perspectives of Quantum Dots in the Food Field: Determination of β-Carotene in Tropical Fruit Juices and Food Supplements"

Abstract

A novel and simple method for thedetermination of β-carotene, a carotenoid abundant in plants and fruits, is proposed. Multicommutated Flow Injection Analysis (MCFIA) has been applied as automated flow methodology to the analysis of β-carotene in tropical fruit juices and food supplements, making use of the quenching effect caused by this analyte over glutathione-capped CdTe quantum dots (QDs) fluorescence signal. Under optimized conditions, the method was linear in the range of 0.3-15 μg mL^{-1}, with a detection limit of 0.09 μg mL^{-1} and relative standard deviations lower than 3%. The determination rate was of about 80 h^{-1} and results were in good agreement with those provided by both the manufacturer and a chromatographic reference method.

Keywords: β-Carotene, Luminescence, Glutathione-capped CdTe quantum dots, Fruit juices, Food supplements

Introduction

Plant foods, such as fruits and vegetables, contain many components that are beneficial to human health, and customers increasingly demand healthier foods with functional compounds that might improve their life quality. Research has demonstrated that some of them, as part of an overall healthful diet, have the potential to delay the onset of many age-related diseases. These observations have led to continuing research aimed at identifying specific bioactive components in foods, such as antioxidants, which may be responsible for improving and maintaining health. Antioxidants (including carotenoids) have been studied for their ability to prevent these diseases. Carotenoids, especially β-carotene, occur abundantly in the nature, being the most prevalent carotenoid in the plant sources of food chain and also known as pro-vitamin A. β-carotene is a strongly colored organic compound which has been used to treat various disorders and to reduce the risk of some types of cancer and age-related macular degeneration. The estimated average amount of total β-carotene presently consumed in Europe and the U.S. is below the recommended intake. Research studies suggest that dietary intake of foods high in β-carotene has positive association with decreased risk of cardio-vascular disease as well as of occurrence of oral cavity and lung cancers (Mayne 1996; Group 1994; Garewal and Schantz 1995). Moreover, being an important flavonoid compound, β-carotene has powerful antioxidant functions that help the body scavenge free radicals, thereby limiting damage to cell membranes, DNA and protein structures in the tissues, which could be regarded as some of its main benefits. Different methods of analysis like high-performance liquid chromatography

(HPLC) (Andrés et al. 2014; Brabcová et al. 2013; Chiosa et al. 2005; Giuffrida et al. 2013) and near-infrared spectroscopy (NIRS) (De Nardo et al. 2009; Rungpichayapichet et al. 2015) have been used for ß-carotene determination. Seeking the attainment of increased simplicity and more cost-effective analytical processes there is an enormous interest in the development of new methodologies for the analysis of this compound.

Quantum Dots (QDs) nanoparticles are, usually, semiconductor crystals formed by atoms from groups (12-16), (13-15), or (14-16) of the periodic table, like CdSe and CdTe. In the aqueous hydrothermal synthesis, QDs are stabilized by some functional ligands, such as mercaptopropionic acid (MPA) and glutathione (GSH), among others, and exhibit some unique properties such as lower preparation cost, high water solubility and stability, and high and adjustable reactivity towards selected functional groups or chemical species. QDs need only a small amount of energy to be excited and this can be achieved by a single blue or ultraviolet wavelength beam. Characterized by advantageous intrinsic properties (size-tunability, wide absorbance and narrow emission ranges, excellent photostability, etc) (Ruedas-Rama et al. 2012; Costa-Fernandez et al. 2006; Frigerio et al. 2012), straightforward aqueous preparation and great simplicity of surface-modification and functionalization, QDs have obtained a great recognition as versatile and valuable chemical sensors for application in the fluorescence-based quantification of different molecules (Raymo and Yildiz 2007; Yuan et al. 2009; Li et al. 2015; Yang et al. 2015), offering a worthwhile alternative to other molecular probes. Other great benefits of QDs are that they can be used in various forms, e.g. as small crystals in liquid solutions, as quantum dust, and in bead form. All

these existing forms make their range of applications even wider. Moreover, there are multiple methods to develop them easily and cost effectively. These methods include lithographic techniques, epitaxial techniques, and colloidal synthesis.

Their use in continuous flow systems could be a prospect of enormous potentiality seeking the automating of the entire analytical process. However, a literature survey shows that the employment of QDs in automatic procedures and non-manual sample handling and measuring methodologies is still limited. The adoption of automated flow methodologies for the development of environmentally friendly analytical procedures taking advantage of QDs features is a promising perspective not only because flow methods prevent operators from coming into contact with potential toxic material (Rodrigues et al. 2014) but also because they allow the carrying out of measurements in non-equilibrium conditions. This is a relevant issue since the QDs-analyte interactions associated with the signaling process usually affect markedly QDs solubility that tended to precipitate impairing detection. Among the available flow techniques, Multicommutated Flow Injection Analysis (MCFIA) is one of the most versatile providing a high automation level both in solutions manipulation and in the establishing of the reaction zone. It is based on the utilization of discrete commutation devices (3-way solenoid valves) to direct the flow of solutions assuring an automated computer control of the whole system (Llorent-Martínez et al. 2013a; Llorent-Martínez et al. 2013b; Jiménez-López et al. 2016; Molina-García et al. 2012). MCFIA, in addition, provides good results, has low-cost components, low consumption of reagents, high repeatability and sample throughput, robustness and high simplicity of the flow system.

In the present work a novel method of analysis based on the quenching effect induced by β-carotene on glutathione (GSH)-capped CdTe QDs fluorescence signal is performed. To the best of our knowledge, this is the first strategy based on the use of QDs for the determination of this analyte. The procedure described here is rapid and simple, and was applied successfully to the analysis of fruit juices and food supplements.

Materials and methods

Reagents and solutions

Sodium tellurite (100 mesh, 99%), tellurium powder (200 mesh, 99.8%), cadmium chloride hemi (pentahydrate) ($CdCl_2 \cdot 2.5\ H_20$, 99%), sodium borohydride ($NaBH_4$, 99%) and L-glutathione reduced (GSH ≥ 98%) were obtained from Sigma-Aldrich (St. Louis, MO, USA) and used for the synthesis of the CdTe QDs. Trisodium citrate dehydrate and 3-mercaptopropionic acid (MPA 99%) were purchased from Fluka (St. Louis MO, USA).

Sodium hydroxide (NaOH, 98%), sodium carbonate 10- hydrate ($Na_2CO_3 \cdot 10\ H_20$, 99%), sodium hydrogen carbonate ($NaHCO_3$, 99.9%), acetone (C_3H_6O, 99.9%), sodium chloride (NaCl, 99%), hydrochloric acid (HCl, 37%) and absolute ethanol (C_2H_5OH, 99.5%), all of them of reagent grade, were purchased from Panreac (Barcelona, Spain). HCl and NaOH (10^{-2} mol L^{-1}) solutions were used to adjust the pH when required. Hexane (C_6H_{14}, > 97%), anhydrous sodium sulphate (Na_2SO_4, > 99%), all the excipients or compounds used in the

interference study and solutions used in chromatographic reference method were purchased from Sigma-Aldrich.

Instrumentation

For the characterization of the synthesized QDs, absorbance and fluorescence spectra were recorded using a Jasco V-660 spectrophotometer and a PerkinElmer LS 50B luminescence spectrometer (Lisboa, Portugal). A ThermoElectron Jouan BR4I refrigerated centrifuge was used for QDs centrifugation.

For the luminescence measurements in the MCFIA system, a Cary-Eclipse Luminescence Spectrometer (Varian Inc., Mulgrave, Australia) was employed. Treatment and control of data collection was performed by a computer equipped with a Cary-Eclipse (Varian) software package. Instrument conditions were set as follows: excitation and emission slit widths were 5 and 10 nm, respectively, the detector voltage was established at 600 V and the excitation and emission wavelengths were 353 and 617 nm for β-carotene, respectively. For the measurements in the flow system, a Hellma flow-cell 176.752-QS (25 µL of inner volume and a light path length of 1.5 mm) was used.

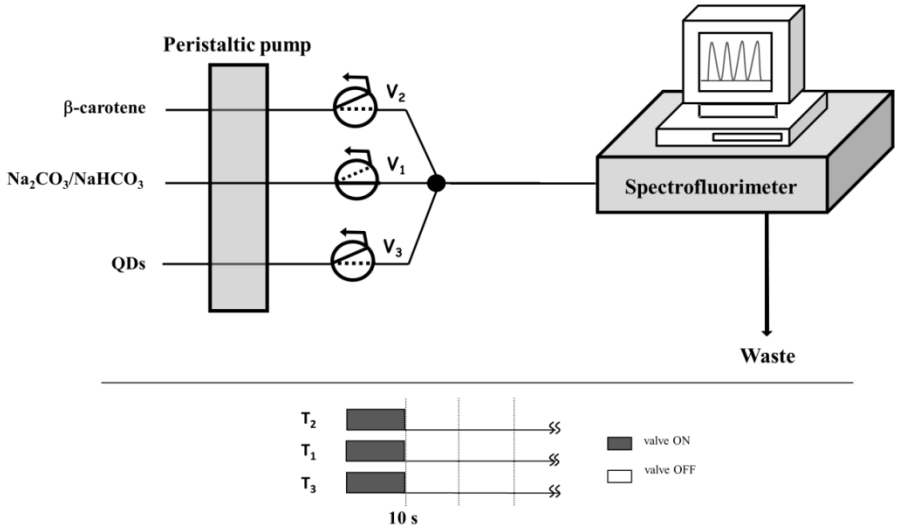

Fig.1 Upper part: MCFIA manifold; V_1, V_2, V_3 refer to three-way solenoid valves. Bottom part: valves scheme. T_n corresponds to the timing course of V_n. The filled rectangles above the time lines for each valve indicate the times at which the corresponding valve was switched on.

The analytical flow system (**Fig. 1**) was arranged by making use of: (1) one four-channel Gilson Minipuls-3 peristaltic pump (Villiers le Bel, France), which was fitted with a rate selector; (2) three 3-way 161T031 NResearch solenoid valves (Neptune Research, MA, USA); (3) pump tubing of Solvflex type (Elkay Products, Shrewsbury, MA, USA); and (4) an electronic interface, based on ULN 2803 integrate circuits, to generate the electric potential (12 V) and current (100 mA) required to control the valves. The software for operating and controlling the analytical system was developed by our research group using Visual Basic 6.0. PTFE tubing (0.8 mm i.d.) and methacrylate connections were also utilized.

By means of Transmission Electron Microscopy (TEM) with a JEOL JEM 1010 with an accelerating voltage of 80 kV, the morphology and microstructure of QDs were examined. The samples for TEM were made by depositing an aqueous solution onto a 200-mesh copper grid coated with a Formvar-carbon film. It allows 500x magnification range from up to 600k. Digital images were captured by using a camera Gatan model 782 with image processing and control software developed by DigitalMicrograph.

For the validation of the proposed method, a high-performance liquid chromatography-diode array detection (HPLC-DAD) method was used as reference. This method was adapted from the one proposed by Andrés et al. (Andrés et al. 2014). The HPLC system consisted of a Shimadzu LC-20AC (Shimadzu, Kyoto, Japan) equipped with a Shimadzu SPD-M20A photodiode array detector (DAD) and a SIL-20ACHT autosampler. The system was equipped with a reversed phase Spherisorb ODS2 analytical column of 250×4.6 mm and 5 μm particle size (Waters, Milford, MA, USA) coupled with a C_{18} Security Guard Ultra cartridge of 5 mm i.d. precolumn. The data processing was carried out with Shimadzu LabSolutions software for LC systems. The chromatographic method was carried out in isocratic mode, at a flow rate 0.8 mL/min, by using a methanol: tetrahydrofuran: water 67:27:6 (v/v/v) solution as mobile phase. Compounds were monitored by a DAD at 440 nm (β-carotene). For identification purposes the retention times were compared with those obtained with pure standards, co-elution with a spike of standard and the specific spectrum of each analysed compound. In order to prevent degradation of the pro-vitamin, all operations were performed in amber flasks and ensuring that the samples were not heated to over 40 ºC.

Synthesis of QDs

Both MPA and GSH-capped CdTe QDs have been synthesized and studied to determinate which of them was more appropriate for the analysis in the present research [22].

Some modifications were performed to the described method by Zou et al. (Zou et al. 2008) for the synthesis of MPA-capped CdTe QDs. The size of the synthesized nanoparticles ranged from 1.36 to 3.72 nm. The Cd^{2+}:Te^{2-}: MPA molar ratio was fixed as 1:0.1:1.7. Briefly, 1.6×10^{-3} mol of $NaHB_4$ reacted with 0.4×10^{-3} mol of tellurium powder in N_2 saturated water inside a 50 mL flask at 80 ºC for 30 min under constant stirring. The resulting NaHTe aqueous solution was transferred to another flask containing 4.0×10^{-3} mol $CdCl_2$ and 6.8×10^{-3} mol MPA in a 100 mL of N_2 saturated water solution. The pH of the solution was adjusted to 11.5 by addition of NaOH (10^{-2} mol L^{-1}).

Using a one-step route by modified Qian's procedure (Qian et al. 2006), GSH-capped CdTe QDs were synthesized using L-glutathione reduced. Three sizes were obtained, varying from 2.57 to 3.47 nm. Shortly, $CdCl_2$, Na_2TeO_3 and GSH (Cd:Te:GSH molar ratio 1:0.2:1.2) were added into a single reaction pot with $NaBH_4$, trisodium citrate and water. The solution pH was adjusted to 10.5 by the addition of NaOH (10^{-2} mol L^{-1}) and the resulting solution was heated with vigorous stirring at 100 ˚C under reflux for QDs growth.

Purification of QDs was performed by precipitation in absolute ethanol in order to remove the contaminants. The precipitate fractions were afterwards centrifuged, vacuum dried, stored in amber flasks and kept in the refrigerator.

Sample preparation

The applied procedure is the one followed by Andrés et al. (Andrés et al. 2014) with some modifications. In the case of fruit juices, 25 mL of a mixture of hexane:acetone 1:1 (v/v) were added to 20 mL of each of the drinks under analysis. The mixture was then centrifuged (3700 rpm, 15 min), followed by vigorous shaking and sonication from 15 min. The content was subsequently transferred into a separating funnel and the organic phase was washed with sodium chloride solution for three times. Likewise, the aqueous phase was washed for four times with hexane and it was scrapped. The organic phases were pooled and dewatered with anhydrous sodium sulphate. The extract was evaporated to dryness under N_2 stream and dissolved in different amounts of ethanol, depending on the necessary dilution. The redissolution was accomnplished by sonication (15 min) and, finally, samples were passed through a 0.45 mm nylon filter.

For food supplements, it was only necessary to break the capsule and to properly dissolve its content in ethanol.

General MCFIA procedure

The MCFIA manifold is shown in **Fig. 1**. Initially, the carrier (0.01 mol L^{-1} Na_2CO_3/$NaHCO_3$ buffer solution, pH 10) was flowing through the flow-cell while the other two solutions (sample and QDs) were recycled to their vessels. Then all valves (V_1, V_2 and V_3) were switched on for 10 s and the direct confluence between QDs and sample solution (both prepared in 0.01 mol L^{-1} Na_2CO_3/$NaHCO_3$ buffer solution, pH 10) took place, whereas the carrier solution was recycled to its vessel. The QDs-sample mixture was subsequently

directed towards the detector and the corresponding analytical signal (quenching effect of the QDs) was recorded. A blank has to be also recorded before any sample is analysed. A flow rate of 2.8 mL min^{-1} was employed.

Results and discussion

Characterization of QDs and spectral characteristics

By modifying the heating time, the CdTe QD size was tuned. A well-defined absorption maximum for the first excitonic transition was observed for all samples, which substantiate a narrow size distribution, further confirmed by FWHM (Full Width at Half Maximum) values of about 47 nm. All the fractions obtained were re-suspended in deionized water maintaining the initial synthesis concentration and the diameter of CdTe QDs was calculated by the following expression (Yu et al. 2003), where D is the diameter of the nanocrystals and λ is the wavelength of maximum absorbance corresponding to the first excitonic absorption peak of the crystal:

$$D = (9.8127\times10^{-7})\,\lambda^3 - (1.7147\times10^{-3})\,\lambda^2 + (1.0064)\,\lambda - 194.84$$

To calculate the molar weight of the different sized nanocrystals, which was essential to prepare QDs solutions with the required concentration, the extinction coefficient (ε) was initially established by using the expression (Yu et al. 2003):

$$\varepsilon = 3450\ \Delta E(D)^{2.4}$$

(ΔE: transition energy corresponding to the first absorption peak)

The morphology of MPA and GSH-capped CdTe QDs can be seen in **Fig.2** through the TEM images, confirming that the

nanoparticles, with an average size around the diameter calculated, are well-dispersed spherical QDs with uniform particle size and crystallinity. Narrow fluorescence bandwidth is consequently exhibited by the used MPA and GSH-capped CdTe QDs.

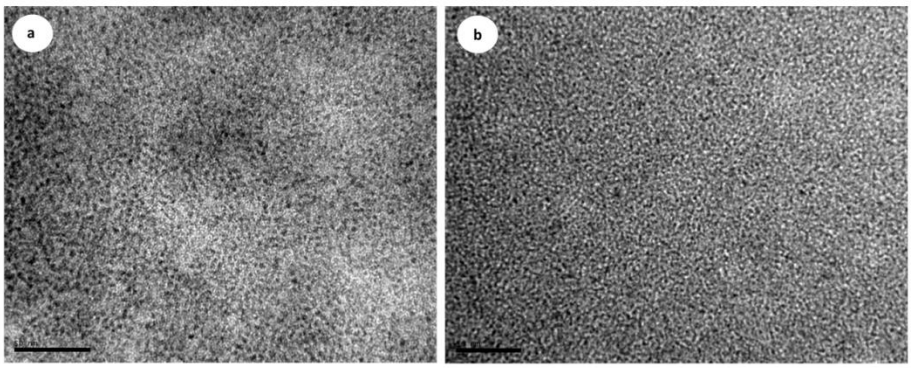

Fig.2 TEM image of: (a) GSH-capped (3.47 nm) and MPA-capped (1.36 nm) CdTe QDs. Magnification: 500 kx.

The remarkable quality of QDs particles is clearly seen from several features in the absorption spectra such as the steepness of the absorption onset, the narrow absorption band and the occurrence of higher energy transitions. Their high quality also results in strong ‘‘band- edge’’ emission, which is tunable by varying particle size. Three different sizes of MPA capped CdTe (1.36, 3.14 and 3.72 nm) and GSH-capped CdTe (2.57, 3.19 and 3.47 nm) QDs were used, showing maximum excitation/emission wavelengths at 344/521, 482/583, 340/637, 446/537, 480/585 and 353/617 nm, respectively for MPA and GSH. The same particles of different sizes present specific emission wavelengths, and this emission increases proportionally with

QDs diameters through a red-shift phenomenon (Costa-Fernandez et al. 2006) (**Fig. 3**).

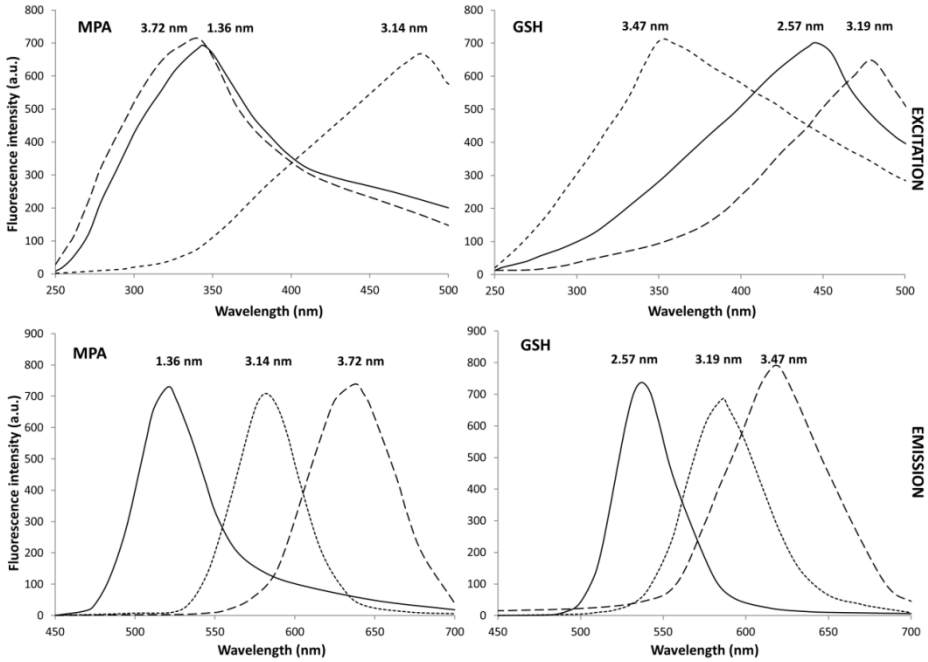

Fig.3 Excitation and emission spectra of QDs for different diameters of MPA and GSH-capped CdTe.

Quenching mechanism of QDs

An electron transfer process reliance could be a possible mechanism for explaining the quenching effect that β-carotene induces on MPA or GSH-capped CdTe QDs (Ji et al. 2012; Xiangzhao et al. 2013). Upon photoexcitation of the QDs with visible light, the oxidation of β-carotene occurs when the QDs accept the electron from electron donor groups on the β-carotene molecules. Interactions between electron donor groups on the β-carotene molecules and partially coordinated Cd^{2+} on the QDs' surface could result in the

establishment of mid-gap energy levels that could behave as electron-trapping states impeding electron-hole recombination and yielding a quenching of the nanocrystal photoluminescence. The Stern–Volmer plot was constructed considering that the dynamic process, in which the quenching mechanism is mainly due to collision, is ruled by the linear Stern–Volmer equation (Melavanki et al. 2009). The plots obtained in our case were (I_0: luminescence intensity of solute in the absence of quencher; I: luminescence intensity in the presence of quencher):

$$\frac{I_0}{I} = 1.1268 + 0.0831[\beta - carotene] \qquad r = 0.9924 \quad (GSH)$$

$$\frac{I_0}{I} = 1.2381 + 0.0772[\beta - carotene] \qquad r = 0.9907 \quad (MPA)$$

The obtained Stern-Volmer constants are 0.0831 and 0.0772 for GSH (3.47 nm) and MPA (1.36 nm) capped CdTe QDs, respectively. The equation is relevant as long as the experimental results show linear variation.

Chemical variables

Preliminary studies showed that QDs size, QDs concentration and pH value were the most influencing variables on the net analytical signal (Jimenez-López et al. 2016; Molina-García et al. 2013). All experiments were carried out with the MCFIA system already described and its conditions were optimized in order to obtain the highest fluorescence signal ($\Delta F=F_0-F$), where F_0 and F are the

fluorescence emission of the blank and the sample solution, respectively.

Taking into account QDs size, the obtained results revealed that the smaller MPA QDs were clearly more sensitive to β-carotene, whereas for the case of GSH QDs bigger sizes were more sensitive promoting higher quenching. Moreover, the effect of the pH was studied. When pH values were lower than 6.0 a precipitate was generally formed (no matter the size of the QDs). Hence, a precise study of this variable was carried out in the 6.0-11.0 pH range by using NaOH or HCl solutions (10^{-2} mol L^{-1}) to adjust this value. The highest quenching effect was produced at pH values around 6.0 for the MPA-capped CdTe QDs with 1.36 nm of diameter and around 10.0 for the GSH-capped CdTe QDs with 3.47 nm of diameter (**Fig. 4**). Comparing both QDs a lower reproducibility and analytical signal were obtained with MPA respect to GSH-capped CdTe QDs. For this reason QDs capped with GSH with 3.47 nm of diameter at a pH value of 10.0 were chosen as optimum.

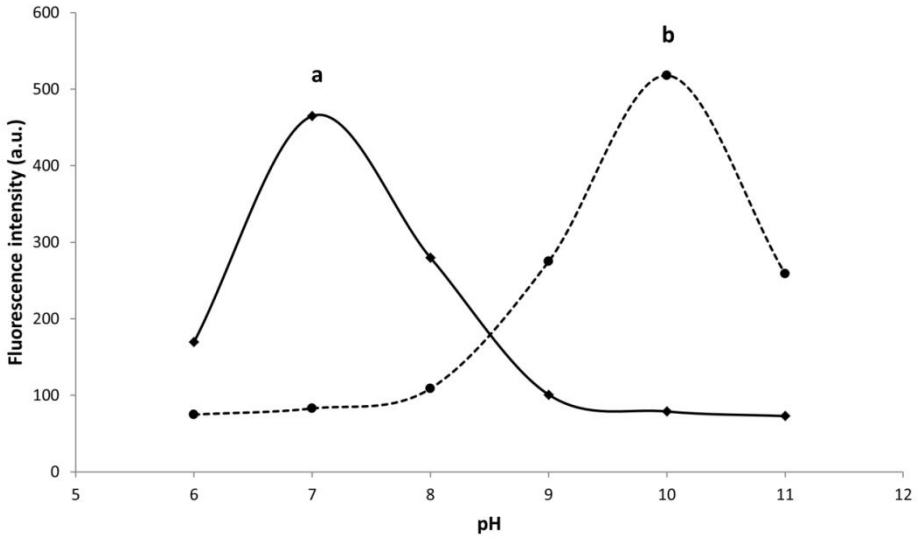

Fig.4 Effect of the pH in QDs: (a) MPA 1.36 nm and (b) GSH 3.47 nm.

Different ranges of concentration were established for the selected GSH-capped CdTe QDs. Net signal increased up to the middle value of the tested range (1–4 μmol L^{-1}) and then decreased for higher concentrations. This effect could be explained by a decrease of QDs' fluorescence when the QDs' concentration reached too high values, mainly due to the inner filter effect as a result of re-absorption of emitted radiation. Finally, 2.5 μmol L^{-1} GSH-capped CdTe QDs solution (3.47 nm diameter, pH 10) was selected as optimum value since it provided the best sensitivity.

The effect of ionic strength on the analytical signal was studied by using a $Na_2CO_3/NaHCO_3$ and $NaHCO_3/NaOH$ buffer solutions at 10 pH value, obtaining higher net signals with the first one. The study of the influence of its concentration was performed in the 0.005-0.05 mol L^{-1} range. The best results were achieved when using 0.01 mol L^{-1}. Hence, carrier, sample and QDs solutions were prepared in 0.01 mol L^{-1} $Na_2CO_3/NaHCO_3$ buffer solution, pH 10.

Instrumental variables

According to showed spectral characteristics of GSH-capped CdTe QDs with 3.47 nm of diameter, selected working wavelengths for further experiments were 353/617 nm/nm ($\lambda_{exc}/\lambda_{em}$). In order to obtain the best sensitivity it was necessary to optimize the emission and excitation slits (5-20 nm) as well as voltage of the photomultiplier tube (450-750 V). Results showed that, under the optimum conditions described previously, the best signal was obtained when instrumental conditions were fixed to provide the highest possible signal from the blank solution (QDs in 0.01 mol L^{-1} $Na_2CO_3/NaHCO_3$ buffer solution): voltage of the photomultiplier tube was set at 600 V whereas excitation and emission slits were selected at 5 and 10 nm, respectively.

MCFIA variables

Concerning the MCFIA variables, one of the main differences between this technique and other flow methodologies is that insertion volumes are replaced with insertion times, which constitutes one of the most important parameters demanding optimization for sample and QDs solutions [29]. When required, the volume can be easily calculated taking into consideration the flow-rate and the insertion time. First variable to contemplate is the flow rate provided by the peristaltic pump, which was studied in the range 1.5-3.5 mL min^{-1}. Sample throughput and repeatability of the system were the analytical parameters considered in order to select the working flow-rate. A 2.8 mL min^{-1} flow rate was selected as the most adequate since it allowed obtaining a high sample throughput providing a good repeatability. Higher flow-rates diminished the repeatability of the signals.

To study the influence of QDs and sample insertion times, the same times (5-40 s range) were employed for both solutions (2.5 μmol L^{-1} QDs and 2 μg mL^{-1} β-carotene), promoting a direct confluence between them just before the flow cell. The highest analytical signal was attained at 10 s and persisted constant for higher values. This value could be justified taking into account the following explanation. There is a relationship between sample-carrier mixture and reaction development and analytical signal magnitude since the sample is continuously diluted by the carrier solution. When the insertion time is very low, a high dilution of the reaction zone is observed, yielding a low analytical signal. However, there is a critical point (10 s) that maximizes the reaction, and therefore detection, minimizing the sample dilution. Above this value sample dilution is no longer perceived. Since higher sample times do not increase the analytical signal (they just make the peak wider and diminish sample throughput), this time (10 s) was selected as optimum.

Analytical performance

Under the above established optimum conditions, the analytical parameters of the system were studied. The proposed method was able to produce analytical fits with good linearity in the range 0.3-15 μg mL^{-1}. Three replicates of eight concentration levels were prepared from the β-carotene stock solution to construct the calibration graph. The obtained data were fitted by standard least-squares calibration. The LOD (detection limit) and LOQ (quantitation limit), 0.09 and 0.3 μg mL^{-1}, respectively, were estimated as the concentrations of analyte that produced analytical signals equal to three and 10 times, respectively, the standard deviation (SD) of the background luminescence. The

sample throughput was calculated as 80 samples per hour, a high sample throughput if it is compared with those obtained with chromatographic methods, hence the high interest of the proposed method for routine analysis.

The robustness and ruggedness of the method were also evaluated obtaining in both cases good results. The robustness was studied under a variety of conditions such as small changes in the pH of sample solution (9.6-10.4), buffer concentration (0.005-0.015 mol L^{-1}), flow-rate (2.5–3.1 mL min^{-1}) and excitation/emission wavelengths (±2 nm). The percent recoveries were in the 96–105% range in all cases (considering 100% the value obtained under the optimum conditions), so there was no alteration to small variations such as those indicated. The ruggedness of the method was assessed by comparison of the intra- and inter-day assay results under taken by two analysts; the RSD values did not exceed 3% and 5%, respectively, so demonstrating its high repeatability. All these values are shown in **Table 1**.

Table 1 Analytical parameters.

Parameter	
Calibration graph	
Intercept	128.8
Slope (mL μg^{-1})	24.3
Correlation coefficient	0.9982
Linear dynamic range ($\mu g\ mL^{-1}$)	0.3-15
Detection limit ($\mu g\ mL^{-1}$)	0.09
Quantitation limit ($\mu g\ mL^{-1}$)	0.3
Intra-day RSD (%) (n=7)	
3 $\mu g\ mL^{-1}$	2.5
13 $\mu g\ mL^{-1}$	2.7
Inter-day RSD (%) (n=7)	
1 $\mu g\ mL^{-1}$	4.9
6 $\mu g\ mL^{-1}$	4.3

K_{SV} GSH 3.47 nm (mL μg^{-1})	0.0831
K_{SV} MPA 1.36 nm (mL μg^{-1})	0.0772
Sampling frequency / h^{-1}	80

Interference study

QDs reactivity is very high and for that reason sometimes they could lack selectivity. In the case of the glutathione-capped CdTe QDs, due to the reducing nature of the passivating layer, the major problem in terms of reactivity would result from the presence of oxidant interfering species, which upon reaction might be able to destabilize de QDs, reducing their quantum yield, with the consequent fluorescence decrease. However, β-carotene is a reducing molecule, likewise glutathione, and this type of interaction is not expected in the analyzed samples.

In order to determine the effect of possible interferences, a tolerance study was carried out with some compounds that usually could be found along with β-carotene in fruit juices and food supplements. The study was carried out with 5 μg mL^{-1} of β-carotene. Potentially interfering compounds were added to the samples at concentrations higher than those usually found in these food supplements. Tolerance level was defined as the amount of foreign species that produced an error not exceeding ±3% in the determination of the analyte. Depending on the behavior of these foreign species with GSH-capped CdTe QDs, the tolerated interferent/analyte (w/w) ratio was different. The obtained values indicated the selectivity of the proposed method. The tolerated interferent/analyte ratio was higher than 100 for glucose, saccharose, L-carnitine, citric acid, acesulfame K and sucralose. In the case of ascorbic acid (used as antirust), this ratio

was higher than 10. As a result, β-carotene could be analyzed, without significant errors, inasmuch as the tolerance of potentially interfering compounds and their ratios were higher than the ones usually found in real samples.

Analytical applications

β-carotene is considered as a fundamental active component of foods that are intended to be consumed as part of the normal diet, offering the potential to promote health or reduce the risk of disease. Thus, if it is not consumed in the normal diet, should be dispensed through dietary supplements provide the necessary amount of β-carotene that the human body requires. For these reasons the method was applied to different types of fruit juices (as representative of daily food) and food supplements, being all of them analyzed by triplicate. The juices selected were tropical fruit juices as they contain moderate doses of β-carotene. Three different types were selected: passion fruit, mango and guava.

An important matrix effect was observed in some juices samples when the method was applied to the analysis of them, as it was not completely eliminated by the pre-treatment procedure developed. Therefore, the standard addition method was used for calibration in these cases. The slope of the calibration curve obtained by spiking the final juice extracts with β-carotene was different to that obtained by spiking the original samples (mainly, passion fruit and guava juices), and both differed to that obtained by external calibration. This matrix effect is due to the presence in the final extracts of interfering species or the incomplete recovery of β-carotene after sample pre-treatment.

Consequently, calibration curves were constructed with matrix-matched standard, i.e. the analysis was carried out by spiking different aliquots of a juice sample with increasing amounts of β-carotene before subjecting them to the whole analytical procedure. The obtained results are shown in **Table 2**, with RSDs lower than 4% in all cases.

In the case of food supplement samples no matrix effect was found. Recovery experiments, spiking each sample at two different β-carotene concentration levels, were performed in four commercial products. The obtained results are shown in **Table 3**, with RSDs lower than 3% in all cases.

The statistical study of the accuracy was carried out comparing the obtained results with an HPLC-DAD reference method. Samples were prepared as described in section *Instrumentation* and analyzed in triplicate. The results of the proposed method were compared with those obtained with this one by means of a t-test and F-criterion. **Tables 2** and **3** show that there is no significant statistical difference between the values obtained by both methods. Thus it is evident the utility of the proposed method for routine analytical control in food analysis laboratories.

Table 2 Recovery study and its comparison with a HPLC-DAD reference method for juice samples.

Sample	Proposed method		Reference method	RSD (%)[a]	t_{calc}[b]	F_{calc}[c]
	Added (μg mL^{-1})	Found (μg mL^{-1})	Found (μg mL^{-1})			
Passion	-	2.45	2.36	1.5	2.80	0.58
fruit	2	4.39	4.48	0.9	2.92	1.29
juice 1	5	7.61	7.44	0.5	2.39	0.64
Passion	-	2.88	2.68	1.4	3.44	0.48
fruit	2	5.09	4.89	2.1	2.86	1.16
juice 2	5	7.94	7.79	1.3	1.87	1.64
Mango	-	10.79	10.86	0.7	2.50	3.25
juice 1	0.5	11.31	11.25	2.9	1.63	6.08
	2	12.82	12.95	3.1	3.79	1.75
Mango	-	9.48	9.57	2.2	2.51	0.03
juice 2	0.5	9.96	10.06	1.7	2.01	1.84
	2	11.40	11.44	0.3	1.84	4.33
Guava	-	7.18	6.99	0.8	3.14	4.00
juice 1	1	8.25	8.18	1.2	1.93	1.29
	3	10.09	10.16	3.3	1.38	1.00
Guava	-	7.31	7.37	1.9	2.43	0.08
juice 2	1	8.34	8.28	0.6	1.63	7.44
	3	10.28	10.49	1.3	3.61	4.00

[a] Average of three determinations.
[b] Theorical value for t=4.30 (P=0.05).
[c] Theorical value for F=39.00 (P=0.05).

Table 3 Recovery study and its comparison with a HPLC-DAD reference method for food supplements samples.

Sample	Proposed method		Reference method	RSD (%)[a]	t_{calc}[b]	F_{calc}[c]
	Added (mg)	Found (mg)	Found (mg)			
Natural Source Oceanic Beta-Carotene, *Ltd. Solgar* (7 mg β-carotene/tablet)	-	7.10	7.14	0.9	1.1	2.08
	5	12.02	12.19	1.2	3.6	6.33
	10	17.28	17.06	1.9	4.0	4.75
Betacaroteno, *Ltd. Sotya* (9.6 mg β-carotene/tablet)	-	9.69	9.72	0.7	1.2	1.76
	6	15.77	15.68	1.7	2.6	1.86
	12	21.66	21.73	0.4	1.9	1.11
Natural Beta Carotene, *Ltd. Lamberts* (14.2 mg β-carotene/tablet)	-	14.27	14.22	0.5	2.5	1.75
	10	24.29	24.37	2.2	2.3	2.58
	20	34.31	34.39	1.1	2.6	0.06
Beta Caroteno, *Ltd. Megadiet* (15 mg β-carotene/tablet)	-	15.06	15.08	1.8	1.0	5.78
	8	23.11	23.02	0.4	2.2	5.57
	18	33.15	33.08	1.3	1.9	0.90

[a] Average of three determinations.
[b] Theorical value for t=4.30 (P=0.05).
[c] Theorical value for F=39.00 (P=0.05).

Conclusions

Research about antioxidants continues to grow and being subject to a great attention as new beneficial components of food are discovered. They are potentially actives in reducing the risk of disease and may be beneficial to human health. For this reason there is a huge interest in analyzing antioxidants such as β-carotene in real samples. This work proposes a valuable and useful analytical methodology for the determination of β-carotene in fruit juices and food supplements samples based on the use of GSH-capped CdTe QDs. This novel fluorometric method has been efficaciously implemented in an automatic multicommutated flow system, whose approach have demonstrated to be a potential tool for automation of QDs-based sensing schemes since accurate, precise and reliable results were obtained assuring, at same time, high sample throughput and low reagents consumption.

Acknowledgements

J.J.L. acknowledges research scholarship from Spanish Government ("Ministerio de Educación y Ciencia").

Compliance with Ethical Standards

Funding: This study was funded by the "Ministerio de Economía y Competitividad" (grant number CTQ2016-7511-R).

Conflict of Interest: All authors declare that they have no conflict of interest.

Ethical approval: This article does not contain any studies with human participants or animals performed by any of the authors.

References

Andrés V, Villanueva MJ & Tenorio MD (2014) Simultaneous determination of tocopherols, retinol, ester derivatives and β-carotene in milk- and soy-juice based beverages by HPLC with diode-array detection. LWT - Food Sci Technol 58:557-562.

Brabcová I, Hlaváčková M, Šatínský D & Solich P (2013) A rapid HPLC column switching method for sample preparation and determination of β-carotene in food supplements. Food Chem 141:1433-1437.

Costa-Fernandez JM, Pereiro R & Sanz-Medel A (2006) The use of luminescent quantum dots for optical sensing. Trac-Trend Anal Chem 25:207-218.

Chiosa V, Mandravel C, Kleinjans JCS & Moonen E (2005) Determination of b-carotene concentration in orange and apple juice and in vitamin supplemented drinks. An Univ Bucuresti : Chimie 1-2:253-258.

De Nardo T, Shiroma-Kian C, Halim Y, Francis D & Rodriguez-Saona LE (2009) Rapid and Simultaneous Determination of Lycopene and β-Carotene Contents in Tomato Juice by Infrared Spectroscopy. J Agr Food Chem 57:1105-1112.

Frigerio C, Ribeiro DSM, Rodrigues SSM, Abreu VLRG, Barbosa JAC, Prior JAV, Marques KL & Santos JLM (2012) Application of quantum dots as analytical tools in automated chemical analysis: A review. Anal Chim Acta 735: 9-22.

Garewal HS & Schantz S (1995) EMerging role of β-carotene and antioxidant nutrients in prevention of oral cancer. Arch Otolaryngol Head Neck Surg 121:141-144.

Giuffrida D, Torre G, Dugo P & Dugo G (2013) Determination of the carotenoid profile in peach fruits, juice and jam. Fruits 68:39-44.

Group TA-TBCCPS (1994) The Effect of Vitamin E and Beta Carotene on the Incidence of Lung Cancer and Other Cancers in Male Smokers. N Engl J Med 330:1029-1035.

Ji X, Palui G, Avellini T, Na HB, Yi C, Knappenberger KL & Mattoussi H (2012) On the pH-Dependent Quenching of Quantum Dot Photoluminescence by Redox Active Dopamine. J Am Chem Soc 134:6006-6017.

Jimenez-López J, Molina-García L, Rodrigues SSM, Santos JLM, Ortega-Barrales P & Ruiz-Medina A (2016) Automated determination of Rifamycins making use of MPA–CdTe quantum dots. J Lumin 175:158-164.

Jiménez-López J, Ortega-Barrales P & Ruiz-Medina A (2016) Development of an semi-automatic and sensitive photochemically induced fluorescence sensor for the determination of thiamethoxam in vegetables. Talanta 149:149-155.

Li Q, Tan X, Li J, Pan L & Liu X (2015) Glutathione-capped CdTe nanocrystals as probe for the determination of fenbendazole. Spectrochim Acta Part A Mol Biomol Spectrosc 141:10-15.

Llorent-Martínez EJ, Molina-García L, Fernández-de Córdova ML, Santos JLM, Rodrigues SSM & Ruiz-Medina A (2013a) A novel multi-commutated method for the determination of hydroxytyrosol in enriched foods using mercaptopropionic acid-capped CdTe quantum dots. Food Addit Contam Part A Chem Anal Control Expo Risk Assess 30:1485-1492.

Llorent-Martínez EJ, Molina-García L, Kwiatkowski R & Ruiz-Medina A (2013b) Application of quantum dots in clinical and alimentary

fields using multicommutated flow injection analysis. Talanta 109:203-208.

Mayne ST (1996) Beta-carotene, carotenoids, and disease prevention in humans. FASEB J 10:690-701.

Melavanki RM, Kusanur RA, Kadadevaramath JS & Kulakarni MV (2009) Quenching mechanisms of 5BAMC by aniline in different solvents using Stern–Volmer plots. J Lumin 129:1298-1303.

Molina-García L, Fernández-de Córdova ML & Ruiz-Medina A (2012) Analysis of Bisphenol A in milk by using a multicommuted fluorimetric sensor. Talanta 96:195-201.

Molina-García L, Llorent-Martínez EJ, Fernández-de Córdova ML, Santos JLM, Rodrigues SSM & Ruiz-Medina A (2013) Study of the quenching effect of quinolones over CdTe-quantum dots using sequential injection analysis and multicommutation. J Pharm Biomed Anal 80:147-154.

Qian HF, Dong CQ, Weng JF & Ren JC (2006) Facile one-pot synthesis of luminescent, water-soluble, and biocompatible glutathione-coated CdTe nanocrystals. Small 2:747-751.

Raymo FM & Yildiz I (2007) Luminescent chemosensors based on semiconductor quantum dots. Phys Chem Chem Phys 9:2036-2043.

Rodrigues SSM, Ribeiro DSM, Molina-Garcia L, Ruiz Medina A, Prior JAV & Santos JLM (2014) Fluorescence enhancement of CdTe MPA-capped quantum dots by glutathione for hydrogen peroxide determination. Talanta 122:157-165.

Ruedas-Rama MJ, Walters JD, Orte A & Hall EAH (2012) Fluorescent nanoparticles for intracellular sensing: A review. Anal Chim Acta 751:1-23.

Rungpichayapichet P, Mahayothee B, Khuwijitjaru P, Nagle M & Müller J (2015) Non-destructive determination of β-carotene content in mango by near-infrared spectroscopy compared with colorimetric measurements. J Food Compos Anal 38:32-41.

Xiangzhao A, Qiang M & Xingguang S (2013) Nanosensor for dopamine and glutathione based on the quenching and recovery of the fluorescence of silica-coated quantum dots. Microchim Acta 180:269-277.

Yang Q, Tan X & Yang J (2015) Sensitive determination of enoxacin in pharmaceutical formulations by its quench effect on the fluorescence of glutathione-capped CdTe quantum dots. Luminescence 31:241-246.

Yu WW, Qu LH, Guo WZ & Peng XG (2003) Experimental determination of the extinction coefficient of CdTe, CdSe, and CdS nanocrystals. Chem Mater 15:2854-2860.

Yuan J, Guo W, Yin J & Wang E (2009) Glutathione-capped CdTe quantum dots for the sensitive detection of glucose. Talanta 77:1858-1863.

Zou L, Gu Z, Zhang N, Zhang Y, Fang Z, Zhu W & Zhong X (2008) Ultrafast synthesis of highly luminescent green- to near infrared-emitting CdTe nanocrystals in aqueous phase. J Mater Chem 18:2807-2815.

Multicommutated flow system for the determination of glyphosate based on its quenching effect on CdTe-quantum dots fluorescence

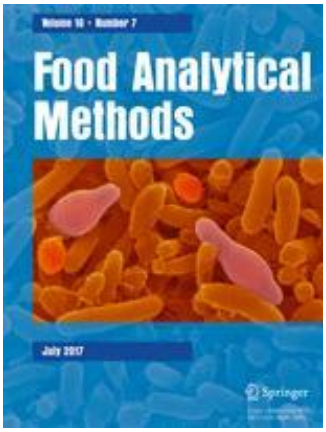

8. "Multicommutated flow system for the determination of glyphosate based on its quenching effect on CdTe-quantum dots fluorescence"

Julia Jiménez-López, Eulogio J. Llorent-Martínez, Pilar Ortega-Barrales, Antonio Ruiz-Medina*

Publicado en Food Analytical Methods, en Febrero de 2018, volumen 11, páginas 1840–1848.

Resumen

El glifosato es el herbicida más utilizado a día de hoy en el mundo. Presenta un amplio espectro de acción, de ahí su uso en una gran diversidad de cultivos. Las agencias reguladoras han mencionado a menudo el bajo riesgo de este herbicida para los mamíferos. Sin embargo, la Agencia Internacional para la Investigación del Cáncer concluyó en 2015 que el glifosato es probablemente carcinogénico para el ser humano. Por esta razón, es importante el desarrollo de métodos analíticos fiables para estudiar el destino y los niveles de glifosato en muestras ambientales. En este trabajo, proponemos un método de análisis de flujo multiconmutado para la determinación de glifosato, basado en el efecto atenuante de la señal producido por este herbicida en la fluorescencia de *quantum dots* de CdTe (λ_{exc} / λ_{em} 400/548 nm / nm).

El método analítico propuesto presenta unos límites de detección y cuantificación de 0.5 y 1.7 μg mL^{-1}, respectivamente. Se logró una frecuencia de muestreo de 30 muestras por hora usando un flujo de muestra de 2.5 ml min^{-1}. Se llevaron a cabo estudios de interferencias para evaluar la selectividad del método, sin observar la interferencia de otros plaguicidas comúnmente utilizados. Finalmente, se llevaron a cabo estudios de recuperación en agua y muestras de cereal (amaranto, cebada, avena y quinoa). Se obtuvieron recuperaciones entre 92 y 108% en todos los análisis de las muestras. Se usó un método de cromatografía de líquidos- espectrometría de masas (HPLC-MS / MS) como método de referencia para evaluar la exactitud de la metodología propuesta, y no se observaron diferencias significativas entre ambos métodos analíticos.

En base a los resultados obtenidos, puede concluirse que se cumplió con el principal objetivo de este trabajo: el desarrollo de un método analítico simple, selectivo y rápido para la cuantificación del glifosato con potencial aplicación en el control de calidad en el sector agroalimentario.

8. "Multicommutated Flow System for the Determination of Glyphosate Based on Its Quenching Effect on CdTe-Quantum Dots Fluorescence".

Abstract

Glyphosate is the most widely used herbicide at the moment. It presents a broad spectrum of action, hence its use for many different crops. Regulatory agencies have constantly mentioned the low hazard potential to mammals. However, the International Agency for Research on Cancer concluded in 2015 that glyphosate is "probably carcinogenic to humans". For this reason, it is important to develop reliable analytical methods to study the fate and levels of glyphosate in environmental samples. In this work, we propose a multicommutated flow analysis method for the determination of glyphosate, based on the quenching effect produced by this herbicide on the fluorescence of CdTe quantum dots ($\lambda_{exc}/\lambda_{em}$: 400/548 nm/nm). The proposed analytical method presents detection and quantitation limits of 0.5 and 1.7 µg mL^{-1}, respectively. A sample throughput of 30 samples per hour was achieved using a 2.5 mL min^{-1} flow-rate. Interference studies were carried out to assessing the selectivity of the method, observing no interference from other common pesticides. Finally, we carried out recovery experiments in water and cereal samples (amaranth, barley, oat, and quinoa). We obtained recovery yields between 92 and 108% in all the analyzed samples. HPLC-MS/MS was used as reference method to assess the accuracy of the proposed methodology.

Keywords: Multicommutation; Pesticide; Glyphosate; Cereal; Quantum dots

Introduction

Glyphosate, the most widely used herbicide worldwide, was first introduced in the market in 1974 but its practice was somehow limited because it could only be sprayed if the intention was to kill all vegetation (Benbrook 2016). However, the introduction of genetically engineered herbicide-tolerant crops in 1996 considerably increased the applications of this pesticide (Benbrook 2016; Tarazona et al. 2017). Nowadays, glyphosate is used for weed control in agriculture, vegetation control in non-agricultural areas, and harvesting aid as crop desiccant (Tarazona et al. 2017). In some cases, farmers increase glyphosate application rates and spray more often to combat weeds less sensitive to this pesticide. Glyphosate has thus become a concern due to its ubiquitous use in the last few years. Although glyphosate potential toxicity to mammals has commonly been described as low, the International Agency for Research on Cancer (IARC) assessed glyphosate as "probably carcinogenic to humans (Group 2A)" in 2015 (IARC 2015). This assessment has generated controversy, as neither the European Union (Tarazona et al. 2017) nor several independent expert panels (Williams et al. 2016) confirmed the conclusions of the IARC. However, due to the high amounts of glyphosate normally used, as well as its high solubility in water (12 g L^{-1}), the presence of this herbicide can easily spread and become a risk to the environment and human health. As a result, it is important to develop reliable analytical methods to control glyphosate levels in different samples.

Glyphosate determination is usually performed by liquid chromatography with mass spectrometry (Chamkasem and Harmon 2016; Ding et al. 2016; Guo et al. 2016) or fluorescence detection after a previous derivatization step (Sun et al. 2017; Wang et al. 2016). However, other analytical methods have been also proposed, including the use of spectrophotometry (Cetin et al. 2017; Jan et al. 2009) or voltammetry (Martínez-Gil et al. 2013; Xu et al. 2017). Concerning the use of fluorescence detection, the non-fluorescent nature of glyphosate makes it necessary to use fluorescent probes, such as quantum dots (QDs) (Guo et al. 2014) or carbon dots (Yuan et al. 2017). These nanoparticles have been used as an alternative to conventional organic fluorophores in the last few years. The main advantages of QDs include their high quantum yield, broad absorption and narrow emission spectra, large Stokes shifts, size-tunable fluorescent emission, etc. (Ruedas-Rama et al. 2012).

One strategy to improve the characteristics of QDs-based analytical methods consists in the use of flow methodologies to automate the analytical system (Sklenářová et al. 2017). They present interesting advantages such as the easy-handling of solutions, low reagents consumption, high repeatability, and the possibility to miniaturize the analytical systems. Among the different flow methodologies, multicommutation provides a high degree of automation and increases the versatility of the systems. In this work, we have selected Multicommutated Flow Injection Analysis (MCFIA) due to its simplicity and easy automation, being all steps computer-controlled (Jiménez-López et al. 2016). In MCFIA, the systems are usually constructed using 3-way solenoid valves, which can adopt two positions – ON and OFF – acting as independent switches, although

other kinds of solenoid valves can be used too. MCFIA has been used in a wide variety of analytical methods due to the ease to carry out online reactions (Pokrzywnicka et al. 2016) or to determine several analytes in the same sample insertion (Gilbert-López et al. 2007; Molina-García et al. 2011).

The aim of this work was to propose an MCFIA system for the determination of glyphosate based on its quenching effect on CdTe QDs fluorescence. Glyphosate is used for weed control in many cultivars, which can lead to the presence of this pesticide not only in crops but also in environmental waters, especially due to its high solubility in water. Hence, we analyzed different cereals and waters using the developed method. The results obtained in the interference studies and recovery experiments indicated the selectivity and accuracy of the proposed method.

Experimental

Reagents and solutions

All reagents and standards were of analytical reagent grade. Ultrapure water (Milli-Q Waters purification system; Millipore; Milford, MA) was used for analysis.

Sodium hydroxide, sodium chloride, potassium dihydrogen phosphate, potassium hydrogen phosphate, ethanol, acetic acid, acetonitrile, activated charcoal, anhydrous sodium acetate, anhydrous magnesium sulfate, and all the tested interferents were bought from Sigma-Aldrich (Madrid, Spain). Siliceous earth purified and calcined was purchased from Panreac (Barcelona, Spain).

For the synthesis of MPA-capped and GSH-capped CdTe quantum dots, sodium tellurite (Na_2TeO_3, ≥99 %), sodium borohydride ($NaBH_4$, >99%), cadmium chloride ($CdCl_2$, >99%), sodium citrate tribasic dihydrate ($C_6H_5Na_3O_7 \cdot 2H_2O$, ≥99%), 3-mercaptopropionic acid (MPA, >99%), and L-glutathione reduced (GSH, ≥98%) were purchased from Sigma-Aldrich. QDs solutions were prepared in ultrapure water.

Glyphosate ($C_3H_8NO_5P$, ≥99.7%; Sigma-Aldrich) weekly stock solution of 500 mg L^{-1} was prepared in ultrapure water and kept protected from light at room temperature. Suitable dilutions were also made in ultrapure water.

Instrumentation

Luminescence measurements were recorded in a Cary-Eclipse Luminescence Spectrometer (Varian Inc., Mulgrave, Australia) using a Cary-Eclipse (Varian) software package for data collection and treatment.

The manifold is illustrated in Fig. 1. A four-channel Gilson Minipuls-3 (Villiers Le Bel, France) peristaltic pump with rate selector was used. An electronic interface based on an ULN 2803 integrate circuit (Motorola, Phoenix, AZ, USA) generated the electric potential (12V) and current (100 mA) required by the 161T031 NResearch three-way solenoid valves (Neptune Research, West Caldwell, NJ, USA). The valves were controlled using a home-made software written in Java. A Hellma flow cell 176.752-QS (Hellma, Mülheim, Germany) (25 μL inner volume; light path length of 1.5 mm) was also used.

The synthesis and characterization of QDs were performed using a CEM Discover SP® microwave synthesis platform with SynergyTM software (Matthews, NC, US). Reactions were carried out in borosilicate glass vessels. The photoluminescence of QDs was recorded in a Quantaurus QY-C11347-11 Absolute QY Spectrometer equipped with an integration sphere (Hamamatsu, Japan). Absorption and emission spectra were recorded on a Jasco V-660 spectrophotometer (Easton, MD, USA) and an LS-50B Perkin Elmer luminescence spectrometer (Waltham, MA, USA), respectively. FT-IR spectra were obtained with a PerkinElmer Frontier spectrophotometer (Waltham) equipped with a universal ATR Diamond/ZnSe support. QDs morphology was observed by transmission electron microscopy (TEM) using an electron microscope JEOL model JEM-2200FS (Tokyo, Japan), at an acceleration voltage of 200 kV. A Thermo Electron Jouan BR4I refrigerated centrifuge (Waltham) was also used.

The HPLC system was an Agilent Series 1100 (Agilent Technologies, Santa Clara, CA, USA), with an Aminex HPX-87H column (300 x 7.8 mm; 9 µm particle size) from Bio-Rad (Madrid, Spain). The mobile phase was water-formic acid (100:0.1, v/v) at a flow-rate of 0.6 mL min^{-1}. 20 µL of sample was injected, and the detection was carried out with an ion trap mass spectrometer (Esquire 6000, Bruker Daltonics, Billerica, MA, USA) equipped with an electrospray interface. The instrument was operated in negative ionization mode, in both full-scan mode (m/z range 50-1000) and MS/MS mode (168→150 for glyphosate quantification).

Synthesis and characterization of CdTe-QDs

The synthesis of the QDs has been adapted from a previous study by Ribeiro et al. (2017). CdTe nanocrystals were synthesized using MPA and GSH as stabilizing ligands in aqueous solutions. The preparation of QDs was performed in a one-step synthetic route assisted by microwave irradiation.

For the synthesis of MPA-CdTe QDs, equimolar amounts of $CdCl_2$ and MPA were mixed in 125 mL of deionized water. Appropriate amounts of Na_2TeO_3, $NaBH_4$, and citrate were separately placed in a beaker. The $CdCl_2$ and MPA solution was added to the beaker and the pH was adjusted to 11 with a NaOH solution. The preparation of GSH-capped CdTe QDs was similar to the previous one, with slight modifications in the molar ratios of the reagents. The pH of the precursor was also adjusted to 9.8 instead of 11.

Subsequently, 25 mL of the CdTe precursor solution was transferred into a 35 mL reaction vessel and placed in the microwave. A series of CdTe QDs were prepared at different temperatures and times in order to obtain various diameters. At the end of the synthesis, the reaction vessel was rapidly cooled to 70ºC, and the obtained CdTe QDs solutions were collected. QDs purification was carried out by precipitation with absolute ethanol followed by centrifugation at 4000 rpm for 10 min. Then, they were dried under vacuum and kept protected from light.

Nanocrystals sizes were estimated using the wavelengths of maximum absorption corresponding to the first electronic transition (λ) (Yu et al. 2003):

$$D = (9.8127\times10^{-7})\,\lambda^3 - (1.7147\times10^{-3})\,\lambda^2 + (1.0064)\,\lambda - 194.84$$

where D is the diameter of the nanocrystals (nm); λ is the wavelength of maximum absorbance corresponding to the first excitonic absorption peak of the crystal. The emission wavelength increases with QDs size through a red-shift phenomenon.

The average sizes of the synthesized QDs analyzed by TEM were in accordance with the diameter values calculated by the previous empirical formula. The complete characterization of these QDs is detailed in (Riberio et al. 2017).

Sample treatment

Several water samples (river, well, spring, and irrigation) and cereal samples (amaranth, barley, oat, and quinoa) were analyzed. Water samples were filtered before the analysis. Food samples were ground and homogenized. Then, we used a QuEChERS method for the extraction of glyphosate.

The original QuEChERS extraction method (Anastassiades et al. 2003) was designed for samples with a high water percentage. For the analysis of the selected samples, which were dry, we used a modified QuEChERS method. We weighed 5 g of sample in a 50 mL PTFE centrifuge tube and added 10 mL of water and 10 mL of 1% (v:v) acetic acid in acetonitrile. After shaking the tube by hand for 1 min, we added 0.43 g of anhydrous sodium acetate and 0.75 g of anhydrous $MgSO_4$. After shaking the tube for 1 min, we centrifuged it at 3700 rpm for 8 min. Then, we transferred 5 mL of supernatant (acetonitrile phase) to a 15 mL centrifuge tube. After the addition of 300 mg anhydrous $MgSO_4$ and 200 mg siliceous earth purified and calcined, we shook the tube by hand for 1 min and centrifuged again for 8 min at 3000 rpm.

We collected the supernatant, added a small amount of activated charcoal to decolorize, and filtered. Further dilutions were performed with ultrapure water before analysis.

General Procedure

The flow network procedure is shown in Fig. 1. A flow-rate of 2.5 mL min^{-1} was used. In the initial status, all valves were switched off (position OFF) and the carrier, deionized water, flowed through the flow-through cell, while sample (1.7-15 mg L^{-1} glyphosate) and MPA-capped CdTe QDs (2 µmol L^{-1}) solutions were recycled to their corresponding vessels. For each measurement, all valves were activated (position ON) for 15 s, so the carrier was recycled, whereas sample and QDs solutions were directed towards the detector (they were mixed by a direct confluence placed before the detector).

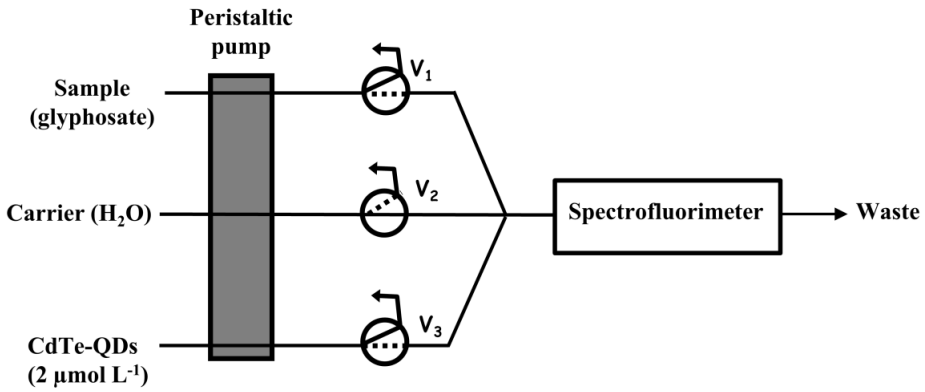

Fig. 1 MCFIA manifold

Calibration standards and samples were analyzed in triplicate. Fluorescence signals were recorded at excitation/emission wavelengths

of 400/548 nm/nm. Excitation/emission slit widths of 10/20 nm/nm and a photomultiplier tube voltage of 650 V were used. A typical signal recording can be observed in Fig. 2**.**

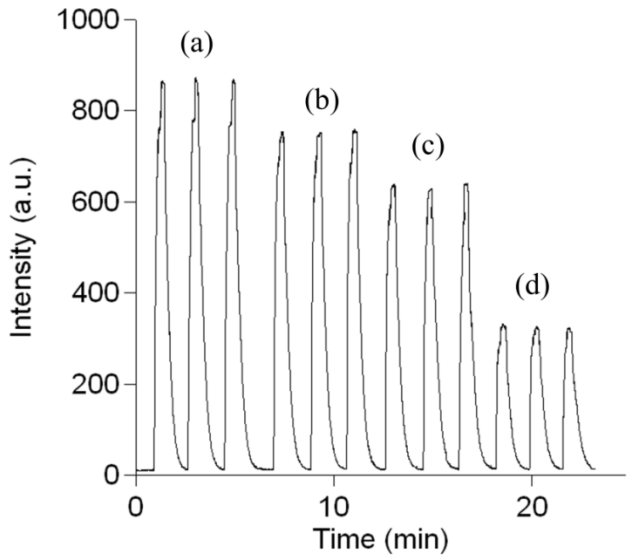

Fig. 2 MCFIA flow profile for different glyphosate concentrations: (a) 0 µg mL^{-1}; (b) 2 µg mL^{-1}; (c) 5 µg mL^{-1}; (d) 10 µg mL^{-1}; a.u. = arbitrary units

Results and discussion

Selection of type and concentration of CdTe-QDs

In preliminary experiments, we observed that the addition of glyphosate to a solution containing CdTe-QDs produced a quenching in the QDs fluorescence (the signal decrease was proportional to glyphosate concentration). Hence, we studied this quenching effect in order to propose an analytical method for glyphosate determination. From now on, analytical signal (fluorescence intensity, arbitrary units) refers to the quenched analytical signal (or net signal), that is, blank

signal (CdTe-QDs solution) minus signal for a given glyphosate concentration.

Two different kinds of CdTe-QDs, along with different diameters for each type of QDs, were synthesized: GSH-capped CdTe-QDs (1.22, 2.99, and 3.15 nm) and MPA-capped CdTe-QDs (1.36, 2.04, 2.50, and 3.29 nm). The highest signal was obtained with MPA-capped CdTe QDs, so we selected them for further experiments. The analytical signals obtained with each diameter are shown in Fig. 3a, observing that the maximum sensitivity was achieved for a 2.04 nm diameter, at excitation and emission wavelengths of 400 and 548 nm, respectively. Different concentrations of these nanoparticles were studied, between 1 and 10 μmol L^{-1}. We observed that the best result was obtained using a 2 μmol L^{-1} QDs concentration; the signal diminished at higher concentrations (Fig. 3b). Hence, 2.04 nm MPA-capped CdTe QDs, at a concentration of 2 μmol L^{-1}, were selected for further experiments.

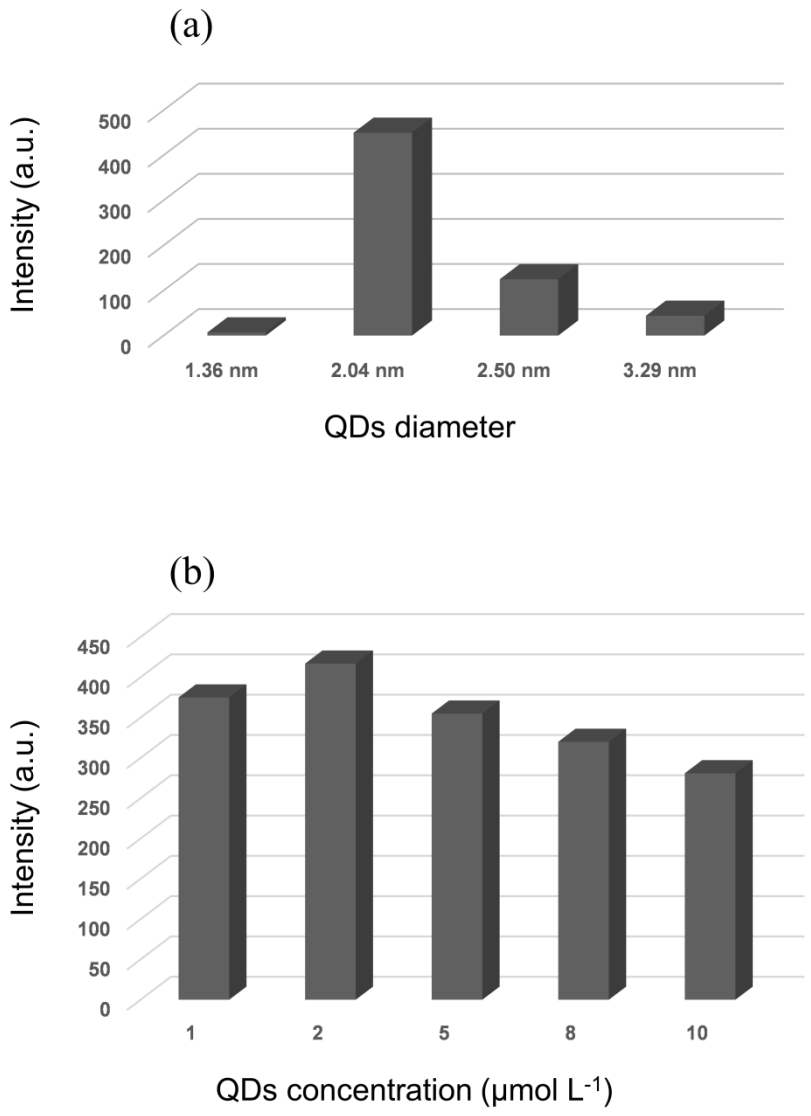

Fig. 3 (3a) Selection of the optimum diameter of QDs; 8 µg mL^{-1} glyphosate; (3b) Influence of QDs (2.04 nm) concentration; 8 µg mL^{-1} glyphosate; a.u. = arbitrary units

Optimization of pH

The pH value of sample and QDs solutions can be a critical parameter, affecting the fluorescence of QDs. Hence, we studied this parameter for values between 3 and 12, adjusting glyphosate and QDs solutions at the same pH value, using NaOH or HCl solutions. At acidic pH values, QDs tend to aggregate and precipitate, as confirmed by the absence of fluorescence at pH values lower than 6. Glyphosate produced the highest quenching at pH values between 7 and 9, observing a decrease at higher pH values. We thus selected the optimum pH between 7 and 9. Then, we studied the effect of the ionic strength by using NaCl and phosphate buffers in the sample and carrier solutions at different concentrations, but the analytical signal did not improve. Taking into account that the pH of glyphosate-QDs solution is approximately 7-7.5, without adjusting the pH, we prepared all solutions directly in ultrapure water.

Instrumental variables

First of all, the optimum excitation and emission wavelengths were 400 and 548 nm, respectively. Using these wavelengths in all experiments, we optimized the excitation/emission slit widths (5-20 nm) and the photomultiplier tube (PMT) detector voltage (600-800 V), using a solution of 5 mg L^{-1} glyphosate. After careful optimization, the highest analytical signal was observed for the following parameters: excitation/emission slit widths of 10/20 nm/nm; PMT voltage of 650 V. Hence, we used these parameters for following experiments.

Flow parameters

The flow rate and insertion times/volumes of sample and QDs solutions are important parameters that have to be studied. In flow methodologies, the most common approach is to measure the volumes of solutions. However, volumes are replaced by insertion times in MCFIA systems, as the solenoid valves are activated for a fixed period of time. However, volumes can be calculated by measuring the flow rate.

As it can be observed in Fig. 1, QDs and sample solutions are mixed online by a direct confluence just before the flow-cell. Hence, we used the same times (10-30 s) for all solenoid valves in order to obtain a homogeneous mixture. The analytical signal increased up to 15 s and then remained constant. Therefore, we selected this insertion time as optimum. We also studied the influence of the flow rate between 1.6 and 3.6 mL min^{-1}. The analytical signal was maximum between 2.4 and 2.7 mL min^{-1} (Fig. 4). Signal intensity decreased for flow rates higher than 2.7 mL min^{-1}, probably due to an incomplete interaction between glyphosate and QDs. Finally, we selected a flow rate of 2.5 mL min^{-1}. Taking into account this flow-rate, 15 s of insertion time corresponds to 625 µL.

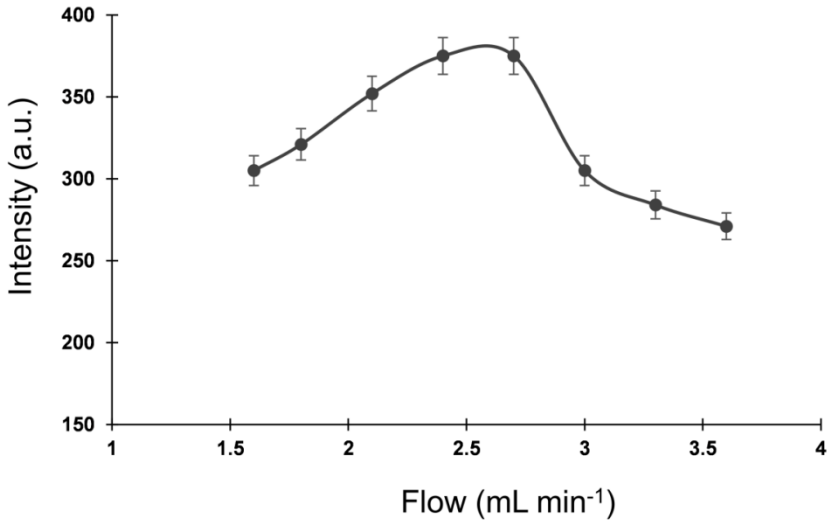

Fig. 4 Effect of the flow rate on the analytical signal; 8 µg mL^{-1} glyphosate; a.u. = arbitrary units

Figures of merit and interference study

Using the previously optimized chemical and instrumental conditions, we constructed a calibration curve for glyphosate using peak height as the analytical signal. We prepared a blank (2 µmol L^{-1} QDs) and eight standard solutions at different glyphosate concentrations (1.7-15 µg mL^{-1} glyphosate). All of them were analyzed in triplicate. The analytical signal was net fluorescence signal (blank minus calibration standard signal), and data were fitted by standard least-squares treatment. The proposed analytical methodology presents a detection limit of 0.52 µg mL^{-1} glyphosate. We also obtained a sample throughput of at least 30 samples per hour. All analytical parameters are shown in **Table 1.**

Table 1 Analytical parameters

Parameter	
Calibration Graph	
Intercept	-11.429
Slope (mL μg^{-1})	50.429
Correlation coefficient	0.9994
Linear dynamic range / $\mu g\ mL^{-1}$	1.7-20.0
Detection limit / $\mu g\ mL^{-1}$	0.52
Quantitation limit / $\mu g\ mL^{-1}$	1.7
RSD (%) (n= 10) [a]	3.7

[a] 6 $\mu g\ mL^{-1}$ glyphosate.

The limit of detection of the proposed method (0.52 $\mu g\ mL^{-1}$) is similar to other spectrophotometric or fluorescent methods (0.1-1.1 $\mu g\ mL^{-1}$) (Silva et al. 2011; Çetin et al. 2017; Yuan et al. 2017), although lower than chromatographic methods (Chamkasem and Harmon 2016; Ding et al. 2016; Wang et al. 2016).

The aim of this work was to propose a novel analytical method to analyze glyphosate in food and water samples. Hence, we calculated the tolerated interferent/analyte ratio for several inorganic ions and different pesticides that may be found in the target samples. We assumed that no interference took place if the variation of the signal was lower than 4% - the RSD in the absence of any interfering compound – after the addition of a potential interferent. Results are summarized in **Table 2**. It can be observed that similar concentrations of other pesticides, as well as high levels of common ions, produced no interference, so allowing the selective determination of the target pesticide. As mentioned before, glyphosate concentration in the environment may be very high. Hence, we tested the interference from

other pesticides at a 1:1 ratio, as their concentrations in the environment would be much lower than glyphosate.

Table 2 Interference study

Foreign species	Tolerance interferent/analyte (w/w) ratio
K^+, Na^+, Cl^-, NO_3^-	20[a]
Mg^{2+}, PO_4^{3-}, CO_3^{2-}	10[a]
SO_4^{2-}	8
Ni^{2+}	6
Carbaryl, carbendazim, fipronil, imidacloprid, malathion, nitenpyram, o-phenylphenol, pyraclostrobin, thiabendazole, thiacloprid, thiamethoxam	1[a]

[a] Maximum ratio tested

The selective quenching of glyphosate on MPA-QDs fluorescence is probably due to the interaction between the carboxylic acid group in glyphosate and the MPA in the outer shell of QDs. The interaction between glyphosate and MPA (Avigliano and Schenone 2015; Yadav et al. 2017), as well as glyphosate and thioglycolic acid (similar structure than MPA) (Liu et al. 2012) has been previously reported.

Analytical applications

Cereal samples, all of them ecological products manufactured in Spain, were purchased from local markets. Water samples were collected from different locations of Andalucía (a region in southern Spain). As glyphosate was not present in the analyzed samples, we performed

recovery experiments to study the suitability of the proposed methodology.

The Environmental Protection Agency has set a maximum residue limit (MRL) of 0.7 mg L^{-1} of glyphosate in drinking waters (USEPA 2009), although higher levels are expected in environmental waters. In addition, MRLs in Codex alimentarius for barley and oat are 400 and 100 mg kg^{-1}, respectively (FAO and WHO 2006). Hence, we spiked each sample at three different glyphosate levels (close to MRLs) and analyzed each sample in triplicate. We obtained satisfactory recoveries in all cases (Tables 3 & 4), with RSD values similar to those found in the analysis of standard solutions. To assess the accuracy of the analytical method, we used the method of the average recovery (González et al. 1999) as a significant test. We carried out the calculations separately for water and cereal samples, as the matrices are completely different. The average recovery was calculated from the individual recoveries (**Tables 3 & 4**), and experimental *t* values of 0.149 and 0.579 were obtained for water and cereal samples, respectively (n=24 in each case). The tabulated *t* value for n-1 degrees of freedom and a 95% confidence level is 1.714. As the experimental Student *t* values were lower than the theoretical one, the method was considered accurate for both types of samples.

Table 3 Recovery study in water samples

Sample	Added (mg L^{-1})	Recovery ± RSD (%)[a]	Recovery ± RSD (%)[a,b]
Well water-1	30	95 ± 4	97 ± 2
	40	101 ± 3	100 ± 3
	50	98 ± 3	97 ± 3

Well-water-2	20	104 ± 3	102 ± 4
	60	102 ± 4	103 ± 3
	100	98 ± 3	100 ± 2
Spring water-1	10	98 ± 3	100 ± 3
	15	98 ± 3	97 ± 4
	20	95 ± 2	96 ± 2
Spring water-2	25	97 ± 3	95 ± 3
	50	104 ± 4	103 ± 2
	75	102 ± 4	104 ± 3
River water-1	15	98 ± 3	102 ± 5
	20	108 ± 4	107 ± 3
	25	106 ± 3	101 ± 4
River water-2	20	105 ± 3	106 ± 5
	40	95 ± 3	97 ± 3
	60	98 ± 2	95 ± 3
Irrigation water-1	10	103 ± 3	103 ± 4
	20	92 ± 3	94 ± 4
	30	98 ± 2	97 ± 3
Irrigation water-2	20	96 ± 4	98 ± 4
	40	104 ± 3	105 ± 5
	60	102 ± 4	103 ± 3

[a] n=3; [b] HPLC-MS/MS reference method

Table 4 Recovery study in cereal samples

Sample	Added (mg kg^{-1})	Recovery ± RSD (%)[a]	Recovery ± RSD (%)[a,b]
Amaranth-1	100	94 ± 4	95 ± 3
	200	106 ± 3	108 ± 3
	400	97 ± 3	96 ± 4
Amaranth-2	150	96 ± 4	98 ± 4
	250	99 ± 4	99 ± 4
	350	103 ± 3	100 ± 5
Barley-1	120	101 ± 4	104 ± 4
	240	96 ± 4	95 ± 2
	480	98 ± 3	99 ± 2
Barley-2	150	99 ± 4	97 ± 3
	250	105 ± 3	102 ± 3
	350	102 ± 4	104 ± 5
Oat-1	150	95 ± 3	93 ± 5
	300	104 ± 3	107 ± 3
	450	105 ± 4	102 ± 3
Oat-2	120	105 ± 4	103 ± 3
	240	99 ± 4	98 ± 2
	480	104 ± 4	101 ± 3
Quinoa-1	100	99 ± 3	100 ± 3
	200	103 ± 4	104 ± 3
	300	97 ± 3	95 ± 4
Quinoa-2	125	104 ± 3	106 ± 5
	250	105 ± 4	101 ± 4
	350	95 ± 4	97 ± 3

[a] n=3; [b] HPLC-MS/MS reference method

We used an HPLC-MS/MS method as reference method to assess the accuracy of the results (**Tables 3 & 4**). The precision and recovery of both methods were compared by using the F criterion and t values, observing no significant differences between the proposed method and the chromatographic reference method.

Conclusions

In this work, we have developed and optimized a novel method for the analysis of glyphosate in cereals and waters. The proposed method is based on the quenching effect that this analyte produces on the CdTe QDs fluorescence. The study of potential interferences, as well as the recovery studies presented, demonstrate the suitability of this methodology for the intended applications. Taking into account the potential risks caused by high levels of glyphosate, although these risks are still being evaluated by different authors, it is important to have different analytical methodologies at hand for the determination of this ubiquitous herbicide. The high sample throughput of the proposed method makes it suitable for screening purposes in order to dismiss non-contaminated samples, although positive results would have to be confirmed by mass spectrometry. Hence, we consider that the simplicity, selectivity, and rapidity of this method make it an interesting alternative to other existing methodologies for the analysis of glyphosate in agri-food samples.

Acknowledgments

J.J.L. acknowledges research scholarship from Spanish Government (Ministerio de Educación y Ciencia) (FPU13/03869).

Compliance with Ethics Requirements

Funding This study was funded by "Ministerio de Economía y Competitividad" (grant number CTQ2016-7511-R).

Conflict of Interest Julia Jiménez-López declares that she has no conflict of interest. Eulogio J. Llorent-Martínez declares that he has no conflict of interest. Pilar Ortega-Barrales declares that she has no conflict of interest. Antonio Ruiz-Medina declares that he has no conflict of interest.

Ethical Approval This article does not contain any studies with human or animal subjects.

Informed Consent Not applicable.

References

Anastassiades M, Lehotay SJ, Štajnbaher D, Schenck FJ (2003) Fast and easy multiresidue method employing acetonitrile extraction/partitioning and 'dispersive solid-phase extraction' for the determination of pesticide residues in produce. J AOAC Int 86:412–431

Avigliano E, Schenone NF (2015) Human health risk assessment and environmental distribution of trace elements, glyphosate, fecal coliform and total coliform in Atlantic Rainforest mountain rivers (South America). Microchem J 122:149-158

Benbrook CM (2016) Trends in glyphosate herbicide use in the United States and globally. Environ Sci Eur 28:3

Çetin E, Şahan S, Ülgen A, Şahin U (2017) DLLME-spectrophotometric determination of glyphosate residue in legumes. Food Chem 230:567-571

Chamkasem N, Harmon T (2016) Direct determination of glyphosate, glufosinate, and AMPA in soybean and corn by liquid

chromatography/tandem mass spectrometry. Anal Bioanal Chem 408:4995-5004

Ding J, Jin G, Jin G, Shen A, Guo Z, Yu B, Jiao Y, Yan J, Liang X (2016) Determination of underivatized glyphosate residues in plant-derived food with low matrix effect by solid phase extraction-liquid chromatography-tandem mass spectrometry. Food Anal Methods 9:2856-2863

FAO, WHO (2006) Codex alimentarius. International food standards. Available at http://www.fao.org/fao-who-codexalimentarius/codex-texts/dbs/pestres/en/

Gilbert-López B, Llorent-Martínez EJ, Ortega-Barrales P, Molina-Díaz A (2007) Development of a multicommuted flow-through optosensor for the determination of a ternary pharmaceutical mixture. J Pharm Biomed Anal 43:515-521

González AG, Herrador MA, Asuero AG (1999) Intra-laboratory testing of method accuracy from recovery assays. Talanta 48:729-736

Guo J, Zhang Y, Luo Y, Shen F, Sun C (2014) Efficient fluorescence resonance energy transfer between oppositely charged CdTe quantum dots and gold nanoparticles for turn-on fluorescence detection of glyphosate. Talanta 125:385-392

Guo H, Riter LS, Wujcik CE, Armstrong DW (2016) Direct and sensitive determination of glyphosate and aminomethylphosphonic acid in environmental water samples by high performance liquid chromatography coupled to electrospray tandem mass spectrometry. J Chromatogr A 1443:93-100

IARC (2015) Monographs, volume 112: some organophosphate insecticides and herbicides: tetrachlorvinphos, parathion,

malathion, diazinon and glyphosate. IARC Monographs on the evaluation of carcinogenic risks to humans. IARC working group, Lyon

Jan MR, Shah J, Muhammad M, Ara B (2009) Glyphosate herbicide residue determination in samples of environmental importance using spectrophotometric method. J Hazard Mater 169:742-745

Jimenez-López J, Molina-García L, Rodrigues SSM, Santos JLM, Ortega-Barrales P, Ruiz-Medina A (2016) Automated determination of Rifamycins making use of MPA-CdTe quantum dots. J Lumin 175:158-164

Liu Z, Liu S, Yin P, He Y (2012) Fluorescence enhancement of CdTe/CdS quantum dots by coupling of glyphosate and its application for sensitive detection of copper ion. Anal Chim Acta 745:78-84

Martínez-Gil P, Laguarda-Miro N, Camino JS, Peri RM (2013) Glyphosate detection with ammonium nitrate and humic acids as potential interfering substances by pulsed voltammetry technique. Talanta 115:702-705

Molina-García L, Ruiz-Medina A, Fernández-de Córdova ML (2011) An automatic optosensing device for the simultaneous determination of resveratrol and piceid in wines. Anal Chim Acta 689:226-233

Pokrzywnicka M, Kamiński J, Michalec M, Koncki R, Tymecki L (2016) A multicommutated tester of bioreactors for flow analysis. Talanta 160:233-240

Ribeiro DSM, de Souza GCS, Melo A, Soares JX, Rodrigues SSM, Araújo AN, Montenegro MCBSM, Santos JLM (2017) Synthesis of distinctly thiol-capped CdTe quantum dots under microwave

heating: multivariate optimization and characterization. J Mater Sci 52:3208-3224

Ruedas-Rama MJ, Walters JD, Orte A, Hall EAH (2012) Fluorescent nanoparticles for intracellular sensing. A review. Anal Chim Acta 751:1-23

Silva AS, Tóth IV, Pezza L, Pezza HR, Lima JL (2011) Determination of glyphosate in water samples by multi-pumping flow system coupled to a liquid waveguide capillary cell. Anal Sci 27:1031-1036

Sklenářová H, Voráčová I, Chocholouš P, Polášek M (2017) Quantum dots as chemiluminescence enhancers tested by sequential injection technique: Comparison of flow and flow-batch conditions. J Lumin 184:235-241

Sun L, Kong D, Gu W, Guo X, Tao W, Shan Z, Wang Y, Wang N (2017) Determination of glyphosate in soil/sludge by high performance liquid chromatography. J Chromatogr A 1502:8-13

Tarazona JV, Court-Marques D, Tiramani M, Reich H, Pfeil R, Istace F, Crivellente F (2017) Glyphosate toxicity and carcinogenicity: a review of the scientific basis of the European Union assessment and its differences with IARC. Arch Toxicol 91:2723-2743

United States Environmental Protection Agency (2009) National primary drinking water regulations. EPA 816-F-09-004

Wang S, Liu B, Yuan D, Ma J (2016) A simple method for the determination of glyphosate and aminomethylphosphonic acid in seawater matrix with high performance liquid chromatography and fluorescence detection. Talanta 161:700-706

Williams GM, Aardema M, Acquavella J, Berry SC, Brusick D, Burns MM, de Camargo JLV, Garabrant D, Greim HA, Kier LD,

Kirkland DJ, Marsh G, Solomon KR, Sorahan T, Roberts A, Weed DL (2016) A review of the carcinogenic potential of glyphosate by four independent expert panels and comparison to the IARC assessment. Crit Rev Toxicol 46:3-20

Xu J, Zhang Y, Wu K, Zhang L, Ge S, Yu J (2017) A molecularly imprinted polypyrrole for ultrasensitive voltammetric determination of glyphosate. Microchim Acta 184:1959-1967

Yadav V, Kaur P, Kaur P (2017) Effect of light conditions and chemical characteristics of water on dissipation of glyphosate in aqueous medium. Environ Monit Assess 189:613-622

Yu WW, Qu L, Guo W, Peng X (2003) Experimental determination of the extinction coefficient of CdTe, CdSe, and CdS nanocrystals. Chem Mater 15:2854–2860

Yuan Y, Jiang J, Liu S, Yang J, Zhang H, Yan J, Hu X (2017) Fluorescent carbon dots for glyphosate determination based on fluorescence resonance energy transfer and logic gate operation. Sens Act B 242:545-553

Exploiting the fluorescence resonance energy transfer (FRET) between CdTe quantum dots and Au nanoparticles for the determination of bioactive thiols

9. "Exploiting the fluorescence resonance energy transfer (FRET) between CdTe quantum dots and Au nanoparticles for the determination of bioactive thiols"

J. Jiménez-López[1], S.S.M. Rodrigues[2], D.S.M. Ribeiro[2], P. Ortega-Barrales[1], A. Ruiz-Medina[1], J.L.M. Santos[2*]

Enviado a Spectrochimica Acta Part A, en 2018.

Resumen

En este trabajo se propone la implementación de los procesos de transferencia de energía de resonancia de fluorescencia (FRET) entre *quantum dots* (QDs) de CdTe, que actúan como donadores, y nanopartículas de oro (AuNPs), que se comportan como aceptores, para la determinación de varios tioles bioactivos o de interés biológico. Los QDs y las AuNPs se recubrieron con "cappings" adecuados, ácido mercaptopropiónico y cisteamina, respectivamente, para que de esta manera se garantizase una fuerte interacción electrostática entre ellos y se promoviese la formación de procesos FRET estables. Una vez establecido este proceso entre las nanopartículas, la emisión de fluorescencia de los QDs disminuyó se extinguió por presencia de las AuNPs. Los analitos de interés analizados fueron capaces de romper la unión donador-aceptor produciendo una reversión del proceso FRET

relacionada con la concentración de cada analito y recuperando la emisión de fluorescencia de los QDs. Para la explicación de la recuperación que ocurre en proceso FRET, existen diferentes mecanismos, como pueden ser: potenciación del rendimiento cuántico del QD, aglomeración de las AuNPs, desprendimiento de las nanopartículas, etc.

El estudio que se ha desarrollado muestra buenos rangos analíticos de trabajo y presenta una buena sensibilidad para el análisis de los compuestos ensayados, mostrándose como una buena alternativa de gran potencialidad para su implementación en metodologías de detección rápidas y simples para el monitoreo de especies farmacéuticas, alimentarias y ambientales. Además, muestra una gran versatilidad analítica, ya que es posible adaptar fácilmente la superficie, tanto de QDs como de AuNPs, a la naturaleza química del analito objetivo.

En conclusión, en este estudio se ha desarrollado un nanosensor multiconmutado que hace uso de nanopartículas para la detección de compuestos de interés biológico. El estudio plantea una novedosa alternativa para la cuantificación de este tipo de compuestos no fluorescentes o débilmente fluorescentes, no solo en muestras de tipo farmacológico, sino también en muestras complejas, como las agroalimentarias y las biológicas.

9. Exploiting the fluorescence resonance energy transfer (FRET) between CdTe quantum dots and Au nanoparticles for the determination of bioactive thiols

Abstract

This work focused the implementation of FRET processes between CdTe quantum dots (QDs), acting as donors, and gold nanoparticles (AuNPs), behaving as acceptors, for the determination of several bioactive thiols such as captopril, glutathione, L-cysteine, thiomalic acid and coenzyme M. The surface chemistry of the QDs and AuNPs was adjusted with adequate capping ligands, i.e. mercaptopropionic acid and cysteamine, respectively, to guarantee the establishment of strong electrostatic interaction between them and promoting the formation of stable FRET assemblies. Under these circumstances the fluorescence emission of the QDs was completely suppressed by the AuNPs. The assayed target analytes were capable of disrupting the donor-acceptor assemblies yielding a concentration-related reversion of the FRET process and restoring QDs fluorescence emission. Distinct mechanisms, involving enhancing of the QDs quantum yield (QY), AuNPs agglomeration, nanoparticles detachment, etc, could be proposed to explain the referred FRET reversion. The developed approach assured good analytical working ranges and demonstrate adequate sensitivity for the assayed compounds, anticipating great prospective for implementing rapid, simple and

reliable sensing methodologies for the monitoring of pharmaceutical, food and environmental species. Moreover, it shows a great analytical versatility since it is possible to easily adapt the surface chemistry, of both QDs and AuNPs, to the chemical nature of the target analyte.

Keywords: FRET; CdTe; quantum dots; Gold nanoparticles; Fluorescence; Chemical analysis.

1. Introduction

One of the key challenges in the design of new and improved analytical methodologies is the development of robust, rapid, cost-effective, flexible, and miniaturized sensing platforms that can offer sensitive and selective determinations and the possibility to detect simultaneously multiple analytes in real samples. To fulfil these great demands, it is fundamental to combine the knowledge from different fields, such as, physics, chemistry, biology, material sciences and nanotechnology [1]. The fluorescence resonance energy transfer (FRET) is a technique that illustrates the cooperative combination of all these sciences [2]. Generally, FRET is a nonradiative process that involves an energy transfer between an electronically excited state donor luminophore (D) and an acceptor (A), which can be either a luminophore or a non-luminescent FRET quencher in its ground state, through long-range dipole-dipole interactions [3]. The efficiency of the FRET process is dependent on the orientation of the dipole moments of the donor and acceptor, the extent of spectral overlap between the donor emission and the acceptor absorption spectra, and the distance

among FRET pair (1-10 nm) [4]. In this sense, many works have exploited the use of quantum dots (QDs) in FRET systems, not only due to their size-dependent photoluminescent characteristics, that make them excellent donors [4, 5] but also because it is easy to prepare QDs emitting at any fitting wavelength. QDs may be considered excellent probes for optical sensing, due to their distinct photophysical properties, such as, high resistance to photobleaching, high fluorescence quantum yields, high molar extinction coefficients, size-controlled luminescence properties, broad excitation spectra, narrow and symmetric emission spectra, biocompatibility and long fluorescence lifetimes when compared with conventional organic dyes [6-8]. In fact, when QDs are used as donors in a FRET process, the size-tunable obtained during their synthesis allows to vary the distance between the donor/acceptor pair and to match the QDs emission with the absorption band of the acceptor, generating sensing systems with enhanced sensitivity [5, 9]. Nevertheless, the selection of QDs as acceptors has rarely been explored, since their broad absorption bands favor excitation crosstalk [9].

The surface coating of the QDs is a parameter that must be also taken into account, as it can affect the distance between the donor-acceptor pair and the ability of the semiconductor to bind to another molecule, compromising the FRET effectiveness [9, 10]. Consequently, the optimization of the thickness of the ligands of the nanoparticles is a crucial step [11]. In a different perspective, the coating could be used to adjust reactivity towards selected analytes, which, when interacting, could modulate (either enhance or impair) the FRET process. The short-chained thiol molecules, generally used as surface ligands in QDs, besides controlling the stability of the nanoparticles and

determining their surface charge and reactivity, could also provide platforms for posterior functionalization [12-14]. In fact, the functionalization of the QDs with appropriate molecules or ligands is very important to increase the interaction possibilities, selectivity and efficiency of the FRET process [13].

In recent years, gold nanoparticles (AuNPs) emerged as excellent fluorescence acceptors, replacing traditional organic quenchers in FRET systems, and opening new perspectives for the sensitive determination of different (bio)molecules and compounds. AuNPs possess high molar extinction coefficients and broad energy bandwidth within the visible light region that overlaps the emission wavelengths of common FRET donors [1, 15, 16].

The sensing platforms based on QDs-AuNPs donor-acceptor pairs are very appealing for chemical and biological applications and have resulted in several scientific publications. The QDs-AuNPs FRET approaches have been employed in inhibition assays methods for the detection of glycoproteins [17], enzymes [18], DNA [19], glucose [16], fungicides and pesticides [15, 20], ions [21], melamine [22] among others. In all applications, the substances under determination attenuated the FRET mechanism promoting a fluorescence recovery.

Inspired in these assays, we aimed at designing a FRET strategy based on the modulation of the FRET efficiency between mercaptopropionic acid (MPA)-capped CdTe QDs and cysteamine (CS)-capped AuNPs. Firstly, by electrostatic interaction, the negatively charged CdTe QDs form FRET donor-acceptor assemblies with positively charged AuNPs, inducing a strong quenching of the quantum dots fluorescence emission. The presence of selected analytes inhibits the FRET process and restores the emission efficiency of CdTe QDs.

Different mechanisms are presented to explain the fluorescence recovery of the quenched semiconductor quantum dots.

2. Materials and methods

2.1. Chemicals

All solutions were prepared with Milli-Q water and analytical grade reagents without any treatment process or further purification.

For the synthesis of MPA-capped and GSH-capped CdTe quantum dots, sodium tellurite (100 mesh, Na_2TeO_3, ≥ 99 %), sodium borohydride ($NaBH_4$, > 99 %), cadmium chloride ($CdCl_2$, > 99 %), sodium citrate tribasic dihydrate ($C_6H_5Na_3O_7 \cdot 2H_2O$, ≥ 99 %), 3-mercaptopropionic acid (MPA, > 99%) and L-glutathione reduced (GSH, ≥ 98%) were purchased from Sigma-Aldrich (St. Louis, MO, USA); sodium hydroxide (NaOH, ≥ 99 %) and absolute ethanol (> 99 %) were obtained from Panreac (Barcelona, Spain).

For the synthesis of CS-AuNPs, hydrogen tetrachloroaurate(III) tetrahydrate ($HAuCl_4 \cdot 4H_2O$, 99.9%), cysteamine hydrochloride (CS, ≥ 97 %) and sodium borohydride ($NaBH_4$, > 99 %) were obtained from Sigma-Aldrich (St. Louis, MO, USA).

For the analysis of thiols, L-glutathione (GSH, 98%), captopril (CTP, ≥98%), L-cysteine (L-Cys, 97%), thioglycolic acid (TGA, 98%), 3-mercaptopropionic acid (MPA, > 99%) and 2-mercaptoethanesulfonate (MES, ≥98%) were obtained from Sigma Aldrich. Mercaptosuccinic acid (MA, 98%) was obtained from Fluka.

For the preparation of buffers, Tris(hydroxymethyl)aminomethane and diethylbarbituric acid were obtained from Sigma Aldrich (St. Louis, MO, USA), and potassium dihydrogenphosphate hydrochloric acid, boric acid, sodium hydroxide, sodium carbonate and sodium bicarbonate were obtained from Panreac (Barcelona, Spain).

2.2. Apparatus

CdTe QDs synthesis was carried out by using a single mode CEM Discover SP® microwave synthesis platform operated using SynergyTM software (Matthews, NC, US), which assured control of irradiation time, reaction temperature (30–300ºC), pressure (0–200 psi), power (0–300 W) and stirring. The reactions were conducted in borosilicate glass vessels with 35 mL volume. Through an integrated infrared (IR) sensor, temperature was continuously monitored. The microwave was equipped with an automated pressure control/sensing system (ActiVentTM), making possible to perform the synthesis under controlled pressure, and an active cooling system (PowerMAXTM) that assured a fast decrease of the reaction vessel temperature at the end of the synthesis. The measurement of the photoluminescence (PL) QY of all synthesized CdTe QDs was performed in a Quantaurus QY—C11347-11 Absolute QY Spectrometer equipped with an integration sphere (Hamamatsu, Japan). By using a Jasco V-660 spectrophotometer (Easton, MD, USA) and a model LS-50B Perkin Elmer luminescence spectrometer (Waltham, MA, USA), QDs absorption and emission spectra were obtained. Samples were precipitated with ethanol and a

Thermo Electron Jouan BR4I refrigerated centrifuge (Waltham MA, USA) was used for the separation of the precipitated QDs.

2.3. Synthesis of MPA and GSH-capped CdTe QDs

CdTe nanocrystals were synthesized using 3-mercaptopropionic acid (MPA) and glutathione reduced (GSH) as stabilizing ligands in aqueous solution. The preparation of all CdTe QDs in aqueous phase was performed in a one-step synthetic route assisted by microwave irradiation [23]. For the synthesis of CdTe-MPA QDs, a fixed amount of $1.25x10^{-3}$ mol of $CdCl_2$ and an equimolar quantity of MPA was initially mixed in 125 mL of deionized water. Then, $2.5x10^{-3}$ mol of Na_2TeO_3, $4 \cdot 10^{-3}$ mol of $NaBH_4$, and $1.25x10^{-3}$ mol of citrate were separately placed in a beaker. The solution of the mixture of $CdCl_2$ and MPA was added to the beaker and the pH of the final solution was adjusted to 11 under magnetic stirring, by the addition of 1.0 mol L^{-1} NaOH. The molar ratio of Cd^{2+}/Te^{2-}/MPA was set as 1:0.2:1. Subsequently, 25 mL of CdTe precursor solution was transferred into a 35-mL reaction vessel. A series of CdTe QDs were prepared at different temperatures and time under microwave irradiation. At the end of the synthesis, the reaction vessel was rapidly cooled to 70ºC using a high-pressure air stream (≥25 psi) coupled to the synthesizer and the obtained CdTe QDs solutions were reserved.

The preparation of QDs capped with GSH was very similar to the one used for MPA, with only slight modifications: the pH of the precursor was adjusted to 9.8 and the molar ratio of Cd^{2+}/Te^{2-}/GSH was set to 1:0.2:0.77. A molar ratio of BH^{4-} to TeO_3^{2-} of 16:1 and a molar ratio citrate/Cd^{2+} of 1:1 was used in all syntheses. Molar ratios were

adjusted relatively to the amount of Cd^{2+} which was fixed at $1.25x10^{-3}$ mol.

The CdTe QD size was tuned by varying the heating temperature and the microwave irradiation time, synthesizing four different sizes for each ligand of CdTe QD. The purification of CdTe QDs was achieved by precipitation with absolute ethanol to remove the contaminants, the excess stabilizer and cadmium ions. The precipitate was subsequently separated by centrifugation at 4000 rpm for 10 min, dried under vacuum, kept in amber flasks and protected from light, for posterior use.

The nanocrystals sizes (D) were estimated according to the empirical formula (**Eq. 1**) proposed by Yu et al. [24], by using the wavelengths of maximum absorption corresponding to the first electronic transition (λ).

$$D = (9.8127\times10^{-7})\,\lambda^3 - (1.7147\times10^{-3})\,\lambda^2 + (1.0064)\,\lambda - 194.84$$

Eq. 1

where D is the diameter of the nanocrystals (nm) and λ is the wavelength of maximum absorbance corresponding to the first excitonic absorption peak of the crystal.

2.4. Synthesis of CS-AuNPs

The solution of 40 nm CS-AuNPs was prepared according to the reported literature [25] as followed:

All glassware was soaked overnight in freshly prepared concentrated HCl/HNO_3 (3:1, v/v) and thoroughly rinsed with Milli-Q water prior to use. Briefly, 500 μL of 0.213 mol L^{-1} cysteamine

hydrochloride and 50 mL of $1.40x10^{-3}$ mol L^{-1} $HAuCl_4 \cdot 4H_2O$ were mixed in a 100 mL round-bottom flask. The mixture was stirred for 20 min at room temperature in the dark. 12.5 μL of freshly prepared $NaBH_4$ solution ($10x10^{-3}$ mol L^{-1}) was then quickly added into the above aqueous solution under vigorous stirring, and the mixture was further stirred for 30 min. The resulting wine-red solution was filtered by 0.45 μm filter and stored in the fridge (4ºC) before use.

2.5. General procedures for fluorescence detection of target analytes

A typical FRET-based analysis of target analytes was performed as follow: 188 μL CdTe QDs (10 μmol L^{-1}) and different concentrations of CS-AuNPs (optimized for each pH) and different volumes of buffer (filling up to 2 mL) were added into 2 mL centrifuge tubes with several concentrations of target analytes. The mixture was incubated at room temperature in darkness for 15 min. Afterwards, the fluorescence emission spectra were recorded with the excitation of 400 nm. The calibration curves for the different analytes was established according to the fluorescence enhancement efficiency, which was monitored by $(PL–PL_0)/PL_0$ where PL_0 and PL are the maximum emission intensity of the system in the absence and presence of analytes, respectively.

3. Results and discussion

3.1. Selection of type and size of AuNPs and CdTe QDs

Four different AuNPs were synthesized, by using distinct capping ligands, in order to evaluate the performance and stability of

the FRET system. The assayed cappings were polyethylene glycol 6000, polyethylene glycol 8000, citrate and cysteamine. The stability study involved the monitoring of the nanoparticles maximum absorption for a 7-days period, during which the AuNPs were kept in the dark and refrigerated. The obtained results confirmed that the nanoparticles with the greatest stability were those prepared with cysteamine, while citrate yielded the more unstable ones (considering the referred 7-days period, although citrate provided higher stability for longer periods). Concerning the profile of the absorption spectrum, the nanoparticles prepared with PEG 8000 and PEG 6000 exhibited broad absorption bands with no defined absorption maximum (Figure 1). In contrast, the absorption bands of the AuNPs prepared with cysteamine and citrate were more resolved with absorption maximum of 523 and 531 nm, respectively (Figure 1). Although the citrate-stabilized AuNPs showed and entirely coincident donor-acceptor wavelength, the higher stability of the Cs-AuNPs and the complementary positive surface charge they exhibit, with respect to the negatively charged QDs, provided a more stable FRET pair and improved results.

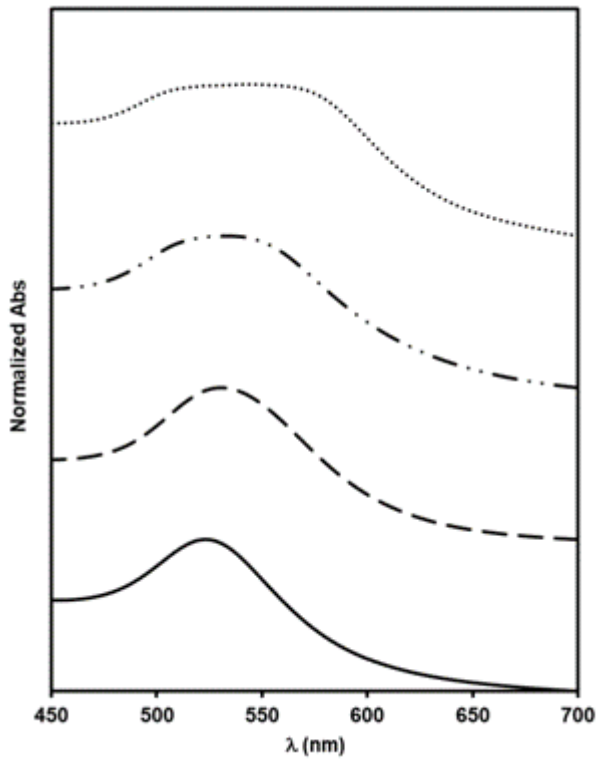

Figure 1. Normalized absorption spectra of AuNPs capped with cysteamine (——); citrate (— —), PEG 6000 (— ·) and PEG 8000(·····).

Two different types of CdTe QDs, capped with MPA and GSH, and exhibiting dissimilar sizes (2.04, 2.50, 3.38 and 3.73 nm for MPA, and 1.22, 2.99 and 3.15 nm for GSH) were also synthesized for this study. The main goal was to select the nanocrystals combining a high emission intensity with an emission wavelength overlapping the maximum of absorption of the AuNPs, which would favor the FRET process, and adequate reactivity for signaling the target analytes. The emission spectra of the prepared nanocrystals showed that the MPA-capped with sizes around 2.04 and 2.50 nm and GSH-capped with 1.22 and 2.99 nm, where those with highest emission at wavelengths close to 523 nm, which matches the optimal absorption of the AuNPs. When

evaluated in the implementation of FRET processes of these four QDs, the MPA-capped ones were those providing the best results, with both quenching and recovery signals greater than those attained with the GSH-capped QDs. Presumably, steric hindrance was minimized when MPA is the capping ligand, which favored the interaction with the analytes). Concerning QDs size it was verified the smaller QDs (2.04 nm) assured better results than the 2.50 nm ones, mostly because of a superior donor-acceptor coupling between the emission spectrum of the MPA-CdTe QD 2.04 nm and the absorption spectrum of the gold nanoparticles.

3.2. Optical characteristics of MPA-CdTe-QDs and CS-AuNPs

Before performance optimization both nanoparticles selected to implement the FRET system were characterized in terms of optical properties. The emission spectrum of MPA-CdTe-QDs is displayed in **Figure 2** (solid line) and showed a maximum fluorescence centered at c. 532 nm. It can also be seen that the emission band is relatively narrow and symmetric, which indicates that the obtained nanocrystals are nearly monodisperse and homogenous.

CS-AuNPs display an intense plasmon absorption centered at 523 nm (dotted line in **Figure 2**), which is just near the maximum fluorescence emission of MPA-CdTe-QDs. It is clear that the absorption spectrum of the gold nanoparticles overlaps well with the emission spectrum of GSH and MPA-CdTe-QDs, demonstrating that, if guaranteeing an adequate distance, it is possible to implement a non-radiative transfer of energy between them, acting the latter as donors and the Au-NPs as acceptors.

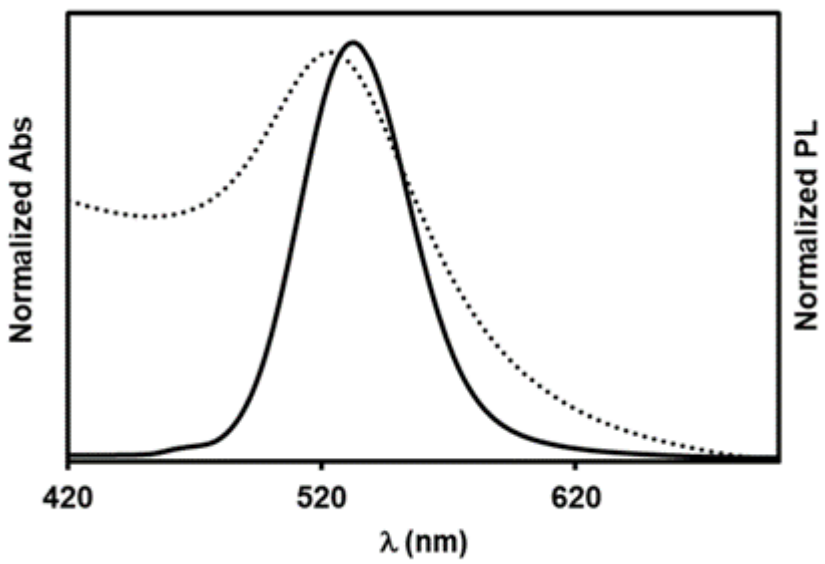

Figure 2. Normalized absorption spectrum of CS-capped AuNPs (▪▪▪▪▪) and normalized photoluminescence spectrum of MPA-capped CdTe QDs (——).

MPA-CdTe QDs and CS-AuNPs spectroscopic signals must also be well resolved to extract experimental information for the studied system although, mainly, good spectral overlap is paramount for high transfer efficiency.

3.3. FRET-based nanoscale assemblies of MPA-CdTe-QDs and CS-AuNPs

The study of the FRET mechanism involving MPA-CdTe-QDs and CS-AuNPs assemblies anticipates that this is strongly affected by the establishment of electrostatic interactions between them. These interactions occurred between negatively charged carboxylic moieties resulting from dissociation of the –COOH group of MPA, on the QDs

surface, and positive charges resulting from the protonation of the $-NH_2$ group in the CS ligand of AuNPs. On the other hand, it is well known that the FRET efficiency is extremely sensitive to the distance separating donor and acceptor. In this regard, the electrostatic interactions bring the two nanoparticles into close proximity to each other enabling the energy transfer between them, and, as a consequence, the QDs fluorescence was strongly quenched (**Figure 3**). In order to confirm the quenching mechanism, a test experiment was carried out involving the utilization of negatively charged citrate-stabilized AuNPs, absorbing at the same wavelength, as acceptors. In this case, no obvious fluorescence change was observed, confirming that the electrostatic repulsion between the two negatively charged nanoparticles did not allow their proximity preventing the occurrence of the FRET process.

Since the occurrence of surface charges depended on pH, the efficiency of the FRET process at variable AuNPs concentration was also studied at distinct pH values. As can be seen in **Figure 3**, with a higher pH value, a bigger quantity of AuNPs is necessary for a total quenching of the signal from the QDs.

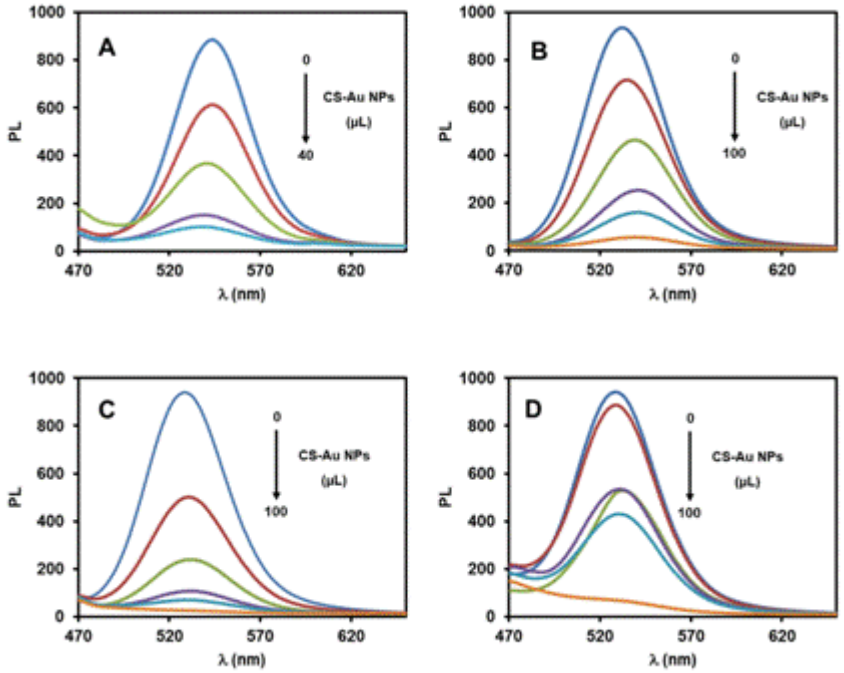

Figure 3. Evaluation of the FRET process upon the interaction of MPA-capped CdTe QDs with CS-capped AuNPs in Tris HCl buffer at pH 7 (A), pH 8 (B) and in phosphate buffer at pH 7 (C) and pH 8 (D).

3.4. Evaluation of FRET incubation times

Different incubation times were assayed to check if the increment of the reaction time between donor and acceptor affected the magnitude of the FRET signal. These assays were carried out in the dark. By using reaction times of 0, 15 and 30 min it was verified that the highest quenching response was attained for t = 15 min, while at 0 and 30 min the QDs fluorescence emission was still noticeable corresponding to a lower quenching effect.

3.5. Evaluation of FRET process in the presence of target analytes

As it was previously mentioned, oppositely charged MPA-CdTe-QDs and CS-AuNPs can form FRET donor–acceptor assemblies due to electrostatic interactions, resulting in effective quenching of QDs emission. Any analyte capable of interacting with this system, either by inducing aggregation of CS-AuNPs or de-passivation of QDs surface, both accompanied by absorption and/or emission spectral changes, or by preventing the occurrence of nanoparticles interaction, could affect the magnitude of the FRET process. This way, the FRET process could be used as an expeditious approach to quantify the occurrence of the interfering analyte. With this purpose, several analytes with analytical relevance and exhibiting specific functional groups were selected for assay. It was payed a noteworthy attention to the occurrence in the analyte molecule of easily protonated thiol groups, particularly suitable for interacting with the positively charged AuNPs, averting FRET establishment and allowing the recovery of the original QDs fluorescence. Beside analyte type and concentration, in the referred assays was also studied the influence of pH and buffer nature. The assayed buffers were the Britton–Robinson, phosphate, KH_2PO_4/NaOH and Na_2CO_3/$NaHCO_3$ buffers. The studies with different buffers covered a pH range (7 to 9) that yielded the highest FRET. The results of these studies are shown below:

Captopril:

Captopril (CTP) is an angiotensin-converting enzyme (ACE) inhibitor, so it is used to treat high blood pressure (hypertension), congestive heart failure, kidney problems caused by diabetes, and to improve survival after a heart attack.

After studying the influence of captopril in the FRET process, it was concluded that at pH=7, in addition to verify the need for a smaller amount of AuNPs to achieve total fluorescence quenching, it was also observed, depending on CTP concentration, an inhibition of the FRET and enhancing of the original QDs fluorescence. Indeed, complete reversion of the FRET and total recovery of the QDs original fluorescence occurred at a concentration of $0.15x10^{-3}$ mol L^{-1} (**Figure 4**). For higher concentrations, it was observed a fluorescence emission that was even higher than the original one, revealing that CTP could presumably improve the QDs QY. A similar phenomenon was observed at pH=8. In this case the concentration of AuNPs required for complete quenching was greater that at pH=7. At pH=9, a similar situation occurs but, in this case, not even the original fluorescence was possible to restore.

Mercaptosuccinic acid:

Mercaptosuccinic acid (MSA) is a dicarboxylic acid used in complexation concealment, biochemical research, heavy metal antidotes and rubber industries.

After studying the behavior of MSA in the FRET process, we observed that, similarly to what happened with captopril, at pH=7 there was a FRET reversion for increasing concentrations. In this case, the complete reversion occurred at a concentration of $0.150x10^{-3}$ mol L^{-1} (**Figure 5**). For higher MSA concentrations the fluorescence never exceeded the original QDs signal.

At pH=8 and pH=9, one could observe that despite a fluorescence increase due to FRET reversion it was not possible to even reach the QDs original signal, so it could be assumed that complete FRET reversion was never achieved.

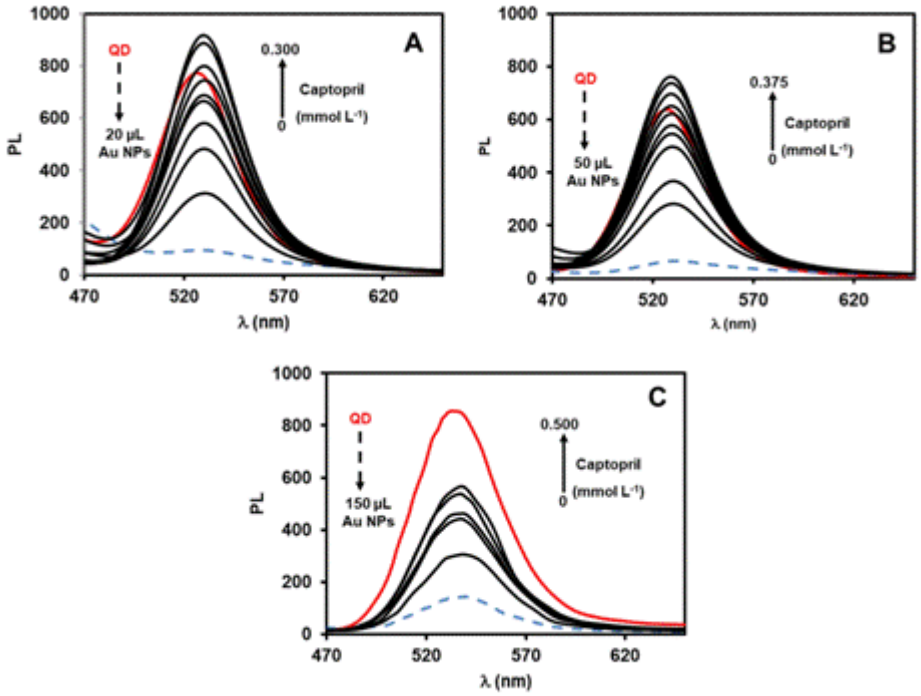

Figure 4. PL emission spectra of CdTe QDs (——), CdTe QDs-AuNPs in the absence (– – –) and in the presence of increasing concentrations of Captopril (——) at different pH, namely, 7 (A), 8 (B) and 9 (C).

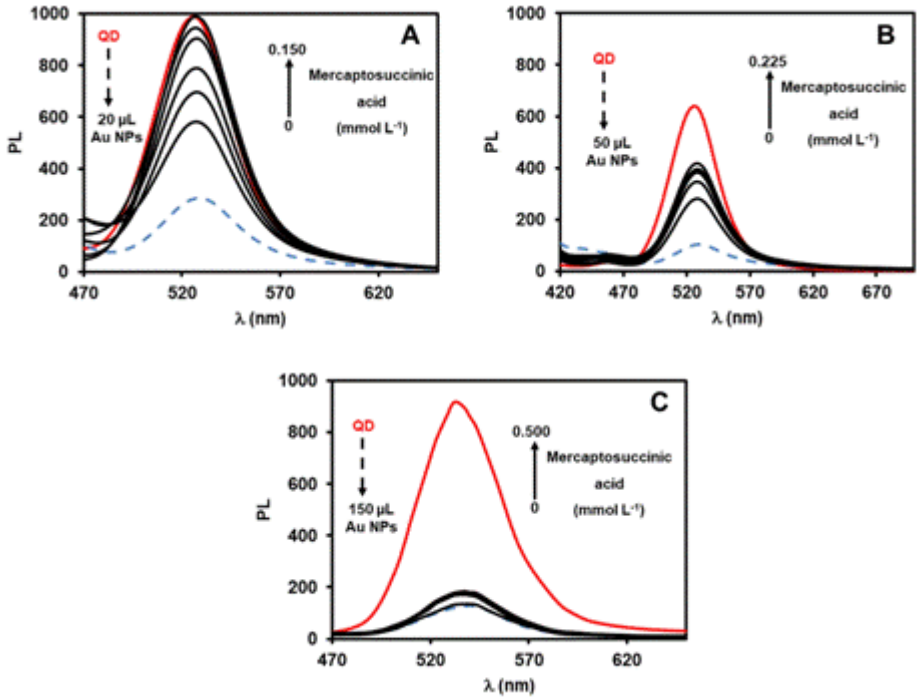

Figure 5. PL emission spectra of CdTe QDs (—), CdTe QDs-AuNPs in the absence (– –) and in the presence of increasing concentrations of Mercaptosuccinic acid (—) at different pH, namely, 7 (A), 8 (B) and 9 (C).

Gluthathione:

Gluthathione (GSH) is an important antioxidant in plants, animals, fungi, and some bacteria and archaea. Glutathione is capable of preventing damage to important cellular components caused by reactive oxygen species such as free radicals, peroxides, lipid peroxides, and heavy metals.

The study of the behavior of gluthathione in the FRET process showed that, like MSA and CTP, at pH=7 GSH is capable of inducing a FRET reversion with a concomitant increase of fluorescence. The complete reversion occurred at a concentration of $0.125x10^{-3}$ mol L^{-1} (**Figure 6**). Equal to CTP, for higher concentration values the

fluorescence emission was above the original one. This phenomenon did not occur at pH=8, since fluorescence recovery never exceeded the QD signal.

At pH=9, total reversion did not occur and the enhancing of fluorescence was marginal, remaining relatively unchanged for concentrations values of up to $0.125x10^{-3}$ mol L^{-1}.

L-Cysteine:

L-Cysteine (CYS) is an essential amino acid, which is an important component of skin, hair and nails, so its use is mainly intended for anti-ageing, healthy immune system and hair.

The results obtained in the study of CYS showed, at pH=7, a behavior similar to that of GSH or MSA with total FRET reversion at a concentration of $0.1x10^{-3}$ mol L^{-1} (**Figure 7**).

For pH=8 and pH=9, and although reversion was not completely attained, like with MSA, the intensity of the signals was significantly lower than that of the original QDs.

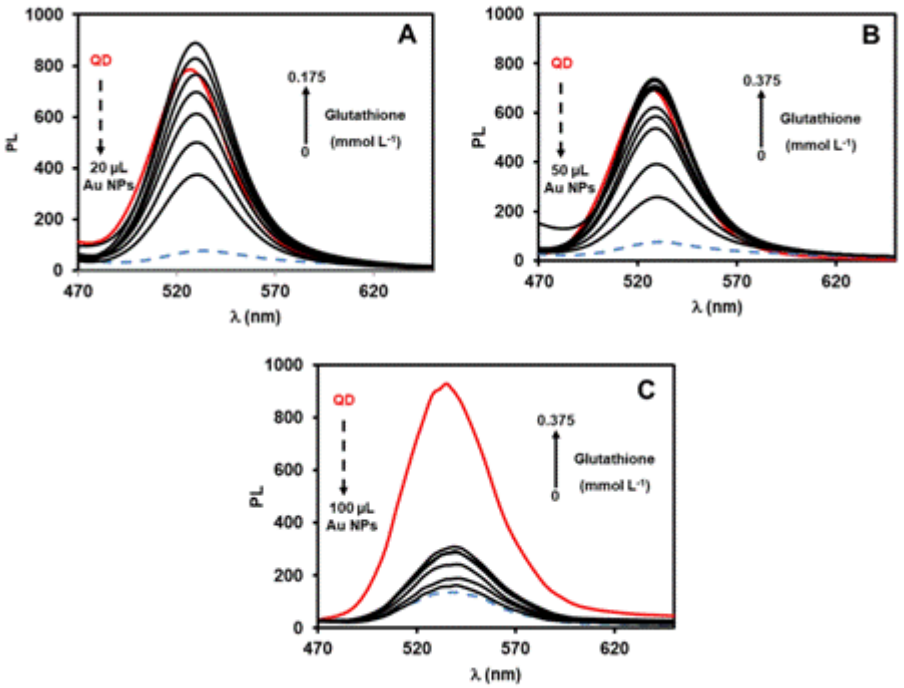

Figure 6. PL emission spectra of CdTe QDs ( ), CdTe QDs-AuNPs in the absence ( ) and in the presence of increasing concentrations of Glutathione ( ) at different pH, namely, 7 (A), 8 (B) and 9 (C).

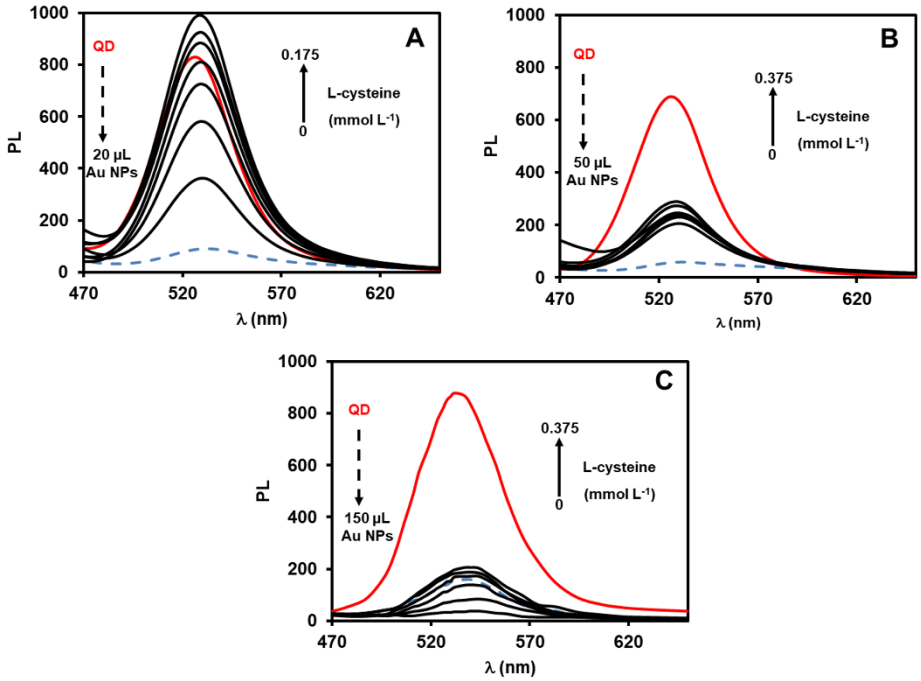

Figure 7. PL emission spectra of CdTe QDs (—), CdTe QDs-AuNPs in the absence (- - -) and in the presence of increasing concentrations of L-Cysteine (—) at different pH, namely, 7 (A), 8 (B) and 9 (C).

Coenzim M:

Coenzim M (sodium 2-mercaptoethanesulfonate) is a water soluble uroprotective agent. It reduces the incidence of hemorrhagic cystitis and hematuria in cancer chemotherapy. It is considered one of the most important medications needed in a basic health system.

The study of the behavior of glutathione in the FRET process showed that, contrary to what happened with the other analytes, neither the reversion nor the enhancing of fluorescence occurred. The behavior for this analyte was similar for pH=7, 8 and 9, although the fluorescence intensity was higher in the case of pH=7. For this pH, there was a very slight fluorescence enhancement which could be hardly attributed to FRET reversion.

For all analytes, the use of distinct buffers such as KH_2PO4 / NaOH (pH=7 and 8) or Na_2CO_3/$NaHCO_3$ (pH=9), produced similar results. A pH=7 was considered the most adequate for carrying out the FRET process, and therefore selected for the assays by using the Britton–Robinson buffer.

3.6. Linear regression analysis

From the obtained results, a linear relationship between PL enhancement efficiency ($(PL–PL_0)/PL_0$) and the logarithm of the analyte concentration was observed being the regression equations resumed in Table S1 – supplementary materials. In Table 1 are summarized the linear range, the correlation coefficient and the regression linear sensitivity values of each analyte at the different pH tested. The obtained results showed that the determination of Captopril was optimized at pH = 8 since a higher sensitivity was achieved. In the case of Glutathione, the sensitivity decreased by increasing the pH thus demonstrating that its determination was more efficient at pH = 7. For L-cysteine and mercaptosuccinic acid, it was impossible the obtaining of a linear relationship between PL enhancement efficiency and the logarithm of the concentration. However, pH = 7 revealed to be ideal for a more accurate determination of L-cysteine while for the mercaptosuccinic acid both pH =7 and 8 allow a similar sensitivity for its determination despite the lower values obtained.

Table 1. Calibration curves values obtained for the different analytes.

	pH = 7		
	Sensitivity	**Correlation coefficient (R)**	**Linear range (mmol L^{-1})**
Captopril	2.8	0.9963 (n = 8)	0.025 – 0.250
Glutathione	7.8	0.9917 (n = 7)	0.025 – 0.175
L-Cysteine	8.1	0.9995 (n = 7)	0.025 – 0.175
Mercaptosuccinic acid	1.9	0.9904 (n = 6)	0.025 – 0.150

	pH = 8		
	Sensitivity	**Correlation coefficient (R)**	**Linear range (mmol L^{-1})**
Captopril	6.5	0.9944 (n = 10)	0.025 – 0.375
Glutathione	6.9	0.9942 (n =6)	0.025 – 0.175
L-Cysteine	1.2	0.9894 (n = 5)	0.025 – 0.375
Mercaptosuccinic acid	1.8	0.9967 (n = 3)	0.025 – 0.100

	pH = 9		
	Sensitivity	**Correlation coefficient (R)**	**Linear range (mmol L^{-1})**
Captopril	1.9	0.9908 (n= 4)	0.025 – 0.250
Glutathione	1.2	0.9822 (n= 5)	0.025 – 0.250
L-Cysteine	n/a	n/a	n/a
Mercaptosuccinic acid	n/a	n/a	n/a

4. Conclusions

This work has enabled the implementation of a sensitive, fast, simple and reliable fluorometric procedure to carry out the assessment of bioactive thiols with pharmaceutical relevance based on their effect on FRET process occurring between oppositely charged MPA-CdTe-QDs and CS-AuNPs. These MPA-CdTe-QDs and CS-AuNPs can form FRET donor–acceptor assemblies resulting from electrostatic interactions, which can effectively quench the fluorescence emission of the MPA-CdTe-QDs.

In the presence of the analytes, the FRET process is reverted, mostly because of impairment of MPA-CdTe-QDs-AuNPs assemblies, with a concomitant enhancement of the fluorescence emission. This method is easy to implement and operate and presents valuable analytical working ranges and sensitivity. Furthermore, nanoparticles like QDs exhibit remarkable advantages, including high fluorescence quantum yields, excellent photostability, and good water solubility, which, in combination with the straightforwardly prepared AuNPs, could be exploited to develop efficient FRET-based methodologies for the detection of a wide range of bioactive compounds.

The pharmaceutically active thiols were selected for analysis due to their industrial and therapeutic relevance and broad perspectives of use in the near future. The present research, has demonstrated its high susceptibility to analysis through a FRET process, which confirmed the previously mentioned advantages. Implementation of similar FRET mechanisms by using solid supports, such as paper or polymeric materials, could enable the development of simple and expeditious sensing devices for application in the monitoring of a

panoply of similar organic molecules in pharmaceutical analysis, food safety and environmental monitoring.

Acknowledgements

J.J.L. acknowledges research scholarship from Spanish Government (Ministerio de Educación y Ciencia) and scholarship of University of Jaén in order to obtain International Ph.D. This study was funded by the "Ministerio de Economía y Competitividad" (grant number CTQ2016-7511-R).

J.J.L. also acknowledges the possibility of work in new areas of knowledge to improve her research future provided by LAQV/REQUIMTE and Department of Applied Chemistry of Faculty of Pharmacy (UP).

David S.M. Ribeiro thanks FCT (Fundação para a Ciência e Tecnologia) and POPH (Programa Operacional Potencial Humano) for his Post-Doc grant ref. SFRH/BPD/104638/2014. S. Sofia M. Rodrigues is grateful to the financial support from Operação NORTE-01-0145-FEDER-000011 – Qualidade e Segurança Alimentar—uma abordagem (nano) tecnológica.

This work received financial support from the European Union (FEDER funds POCI/01/0145/ FEDER/007265) and National Funds (FCT/MEC, Fundação para a Ciência e Tecnologia and Ministério da Educação e Ciência) under the Partnership Agreement PT2020UID/QUI/50006/2013.

References

[1] K. Saha, S.S. Agasti, C. Kim, X. Li, V.M. Rotello, Gold nanoparticles in chemical and biological sensing, Chem. Rev. 112 (2012) 2739-2779.

[2] O.A. Goryacheva, N.V. Beloglazova, A.M. Vostrikova, M.V. Pozharov, A.M. Sobolev, I.Y. Goryacheva, Lanthanide-to-quantum dot Förster resonance energy transfer (FRET): Application for immunoassay, Talanta 164 (2017) 377-385.

[3] N. Hildebrandt, K.D. Wegner, W.R. Algar, Luminescent terbium complexes: superior Förster resonance energy transfer donors for flexible and sensitive multiplexed biosensing, Coord. Chem. Rev. 273-274 (2014) 125-138.

[4] G. Chen, F. Song, X. Xiong, X. Peng, Fluorescent Nanosensors Based on Fluorescence Resonance Energy Transfer (FRET), Ind. Eng. Chem. Res. 52 (2013) 11228-11245.

[5] C. Frigerio, D.S.M. Ribeiro, S.S.M. Rodrigues, V.L.R.G. Abreu, J.A.C. Barbosa, J.A.V. Prior, K.L. Marques, J.L.M. Santos, Application of quantum dots as analytical tools in automated chemical analysis: A review, Anal. Chim. Acta 735 (2012) 9-22.

[6] V. Bagalkot, L. Zhang, E. Levy-Nissenbaum, S. Jon, P.W. Kantoff, R. Langer, O.C. Farokhzad, Quantum dot-aptamer conjugates for synchronous cancer imaging, therapy, and sensing of drug delivery based on bi-fluorescence resonance energy transfer, Nano Lett. 7 (2007) 3065-3070.

[7] A.M. Dennis, W.J. Rhee, D. Sotto, S.N. Dublin, G. Bao, Quantum Dot–Fluorescent Protein FRET Probes for Sensing Intracellular pH, ACS Nano 6 (2012) 2917-2924.

[8] J. Saha, A. Datta Roy, D. Dey, D. Bhattacharjee, S. Arshad Hussain, Role of quantum dot in designing FRET based sensors, Mater. Today 5 (2018) 2306-2313.

[9] U. Resch-Genger, M. Grabolle, S. Cavaliere-Jaricot, R. Nitschke, T. Nann, Quantum dots versus organic dyes as fluorescent labels, Nat. Methods 5 (2008) 763.

[10] K.E. Sapsford, L. Berti, I.L. Medintz, Materials for fluorescence resonance energy transfer analysis beyond traditional donor-acceptor combinations, Angew. Chem. Int. Ed. 45 (2006) 4562-4589.

[11] H.R. Chandan, J.D. Schiffman, R.G. Balakrishna, Quantum dots as fluorescent probes: Synthesis, surface chemistry, energy transfer mechanisms, and applications, Sens. Actuators B Chem. 258 (2018) 1191-1214.

[12] S.S.M. Rodrigues, D.S.M. Ribeiro, J.X. Soares, M.L.C. Passos, M.L.M.F.S. Saraiva, J.L.M. Santos, Application of nanocrystalline CdTe quantum dots in chemical analysis: Implementation of chemo-sensing schemes based on analyte-triggered photoluminescence modulation, Coord. Chem. Rev. 330 (2017) 127-143.

[13] J. Zhou, Y. Liu, J. Tang, W. Tang, Surface ligands engineering of semiconductor quantum dots for chemosensory and biological applications, Mater. Today 20 (2017) 360-376.

[14] J. Donegan, Y. Rakovich, Cadmium Telluride Quantum Dots: Advances and Applications, CRC Press, Boca Raton, Florida, 2013.

[15] J. Guo, Y. Zhang, Y. Luo, F. Shen, C. Sun, Efficient fluorescence resonance energy transfer between oppositely charged CdTe quantum dots and gold nanoparticles for turn-on fluorescence detection of glyphosate, Talanta 125 (2014) 385-392.

[16] T. Bo, C. Lihua, X. Kehua, Z. Linhai, G. Jiechao, L. Qingling, Y. Lijuan, A new nanobiosensor for glucose with high sensitivity and selectivity in serum based on fluorescence resonance energy transfer (FRET) between CdTe quantum dots and Au nanoparticles, Chem. Eur. J. 14 (2008) 3637-3644.

[17] L. Chang, X. He, L. Chen, Y. Zhang, A fluorescent sensing for glycoproteins based on the *FRET* between *quantum dots* and Au nanoparticles, Sens. Actuators B Chem. 250 (2017) 17-23.

[18] X. Fu, X. Fu, Q. Wang, L. Sheng, X. Huang, M. Ma, Z. Cai, Fluorescence switch biosensor based on *quantum dots* and gold nanoparticles for discriminative detection of lysozyme, Int. J. Biol. Macromol. 103 (2017) 1155-1161.

[19] Z. Dai, J. Zhang, Q. Dong, N. Guo, S. Xu, B. Sun, Y. Bu, Adaption of Au nanoparticles and CdTe quantum dots in DNA detection, Chin. J. Chem. Eng. 15 (2007) 791-794.

[20] G. Liu, X. Huang, S. Zheng, L. Li, D. Xu, X. Xu, Y. Zhang, H. Lin, Novel triadimenol detection assay based on fluorescence resonance energy transfer between gold nanoparticles and cadmium telluride quantum dots, Dyes Pigments 149 (2018) 229-235.

[21] M. Xue, X. Wang, L. Duan, W. Gao, L. Ji, B. Tang, A new nanoprobe based on *FRET* between functional *quantum dots* and gold nanoparticles for fluoride anion and its applications for biological imaging, Biosens. Bioelectron. 36 (2012) 168-173.

[22] J. Zhao, H. Wu, J. Jiang, S. Zhao, Label-free fluorescence turn-on sensing for melamine based on fluorescence resonance energy transfer between CdTe/CdS quantum dots and gold nanoparticles, RSC Adv. 4 (2014) 61667-61672.

[23] D.S.M. Ribeiro, G.C.S. de Souza, A. Melo, J.X. Soares, S.S.M. Rodrigues, A.N. Araújo, M.C.B.S.M. Montenegro, J.L.M. Santos, Synthesis of distinctly thiol-capped CdTe quantum dots under microwave heating: multivariate optimization and characterization, J. Mater. Sci. 52 (2017) 3208-3224.

[24] W.W. Yu, L. Qu, W. Guo, X. Peng, Experimental Determination of the Extinction Coefficient of CdTe, CdSe, and CdS Nanocrystals, Chem. Mater. 15 (2003) 2854-2860.

[25] J. Zheng, H. Zhang, J. Qu, Q. Zhu, X. Chen, Visual detection of glyphosate in environmental water samples using cysteamine-stabilized gold nanoparticles as colorimetric probe, Anal. Methods 5 (2013) 917-924.

Conclusiones/Conclusions

5. Conclusiones

En esta Memoria de Investigación se presentan nueve sistemas luminiscentes multiconmutados en flujo, que, a través del uso de una serie de optosensores y de nanopartículas que actúan como nanosensores, han sido aplicados para el análisis de diversos compuestos de interés dentro de los campos agroalimentario y farmacológico.

Los resultados obtenidos de los diferentes estudios han permitido establecer las siguientes conclusiones:

- Se han desarrollado un total de cinco optosensores luminiscentes, de los cuales cuatro son monoparámetro y uno multiparámetro. La resolución de la mezcla se consigue mediante la llegada secuencial de los analitos al detector, debido a la retención selectiva en el soporte sólido empleado. La estrategia para efectuar la separación de los analitos ha sido el uso una cantidad adicional de soporte sólido en la misma célula de flujo.
- Cuatro de estos optosensores usan los fotones como "reactivos" gracias a la Fluorescencia Inducida Fotoquímicamente, que permite convertir analitos no fluorescentes (o que presentan débil fluorescencia) en fotoproductos altamente fluorescentes para su detección con dicha técnica. Además de proporcionar ciertas características interesantes a estos analitos, la derivatización fotoquímica presenta numerosas ventajas frente a la derivatización química, como son: decrecimiento en el tiempo de análisis empleado, simplicidad en el montaje del

sistema en flujo, menor coste del análisis en sí, menor cantidad de desechos e incremento en la sensibilidad del sistema desarrollado, entre otras.

- La sensibilidad y selectividad obtenida en estos sistemas luminiscentes reside principalmente en el hecho de que se produce la retención y detección del analito (o su producto de fotodegradación) en un soporte sólido adecuado, colocado en la célula de flujo que se ubica en el área de detección.
- La inclusión de nanopartículas (QDs), que se ha visto reflejada en cuatro de los nueve estudios de esta Memoria, en los sistemas multiconmutados en flujo proporciona nuevos enfoques en dichos sistemas, generando sistemas analíticos de última generación sensibles y selectivos, con grandes perspectivas de futuro.
- La ampliación de la utilización de este tipo de sistemas que utilizan nanosensores a campos como el agroalimentario, donde existen pocos estudios sobre el tema en cuestión, además del uso de la transferencia de energía de resonancia de fluorescencia en ellos, hacen que estos sistemas analíticos resulten muy atractivos para aplicaciones químicas y biológicas.
- Como conclusión final, gracias al desarrollo de estos sistemas luminiscentes multiconmutados en flujo, se ha confirmado la gran versatilidad y aplicabilidad analítica que surge de la combinación de los optosensores/nanosensores y los sistemas automatizados en flujo. Se han propuesto nuevos métodos con alta sensibilidad y selectividad que permiten la determinación de compuestos de alto interés en diferentes campos, debido a su simplicidad, bajo coste de análisis y capacidad para aplicarse en

matrices complejas. Se trata de una alternativa a los métodos cromatográficos de análisis.

Esta Memoria permite plantear como perspectivas de futuro nuevas e innovadoras metodologías analíticas que hagan uso de los sistemas de última generación que en ella se presentan. Tal es el caso de los sistemas de flujo basados en QDs u otros tipos de nanopartículas que puedan dar lugar a la detección de otras nanopartículas o, por otro lado, la creación de sensores que puedan servir como nanopruebas aplicables a los diferentes campos de investigación gracias a la inmovilización, adsorción o unión en la superficie de un soporte sólido.

Conclusions

In this Research Report, nine luminescent multicommutated flow systems are presented. They can be divided into flow-through optosensors and nanosensors, in which nanoparticles have been used to improve the performance of the methods developed. The reported analytical methods have been applied to the analysis of several compounds of interest within the agri-food and pharmacological fields.

The results obtained from the different studies have allowed establishing the following conclusions:

- Five luminiscent flow-through optosensors have been developed, four monoparametric and one biparametric. The resolution of the mixtures is achieved by the sequential arrival of the analytes to the detection area, due to the selective retention in the solid support used. The strategy employed for obtaining the analytes separation has been the use of an additional amount of solid support in the same detection cell.
- Four of these optosensors make use of photons as "reactives" thanks to Photochemically Induced Fluorescence. This technique allows the conversion of non-fluorescent or weakly fluorescent analytes (that require a previous derivatization for luminescence detection) into highly fluorescent photoproducts. The photoderivatization presents several advantages when compared to chemical derivatization: lower time of analysis (higher sample throughput), simplicity of the flow system, lower cost of analysis, reduction of waste and enhanced sensitivity.

- The obtained sensitivity and selectivity in these luminescent systems are consequences of the retention and detection of the analyte (or its photodegradation product), due to its retention in a suitable solid support, located in the detection flow cell.
- The inclusion of nanoparticles (QDs), which has been reflected in four of the nine studies in this Report, in the multicommutated flow systems provides new approaches in these systems, generating last-generation analytical systems with high sensitivity and selectivity, with great future perspectives.
- The extension of the use of the systems that use nanosensors in fields such as agri-food (where there are few studies), besides the use of the fluorescence resonance energy transfer in them, make these analytical systems very attractive for chemical and biological applications.
- As a final conclusion, thanks to the development of these luminescent multicommutated flow systems, the great versatility and analytical applicability arising from the combination of optosensors / nanosensors and automated flow systems has been confirmed. New methods with high sensitivity and selectivity that allow the determination of compounds of high interest in different fields have been proposed. These analytical methods may represent a good alternative to the chromatographic methods of analysis due to the simplicity, low cost of analysis and ability to be applied in complex matrices.

This Report allows the proposal of new and innovative analytical methodologies as future trends in analytical chemistry. Such

is the case of flow systems based on QDs or other types of nanoparticles that can lead to the detection of other nanoparticles or, on the other hand, the creation of sensors that can serve as nanoproves applied to different fields thanks to the immobilization, adsorption or bonding on the surface of a solid support.

Bibliografía

6. Bibliografía

[1] L.T. Skeggs, *An automatic method for colorimetric analysis*, American Journal of Clinical Pathology, 28 (1957) 311-322.

[2] J. Růžička, E.H. Hansen, *Flow injection analyses: Part I. A new concept of fast continuous flow analysis*, Analytica Chimica Acta, 78 (1975) 145-157.

[3] M.D. Luque de Castro, M. Valcárcel, *Automatic Methods of Analysis*, Elsevier Science, 1988.

[4] K.K. Stewart, G.R. Beecher, P.E. Hare, *Rapid analysis of discrete samples: The use of nonsegmented, continuous flow*, Analytical Biochemistry, 70 (1976) 167-173.

[5] R.C. Prados-Rosales, J.L. Luque-García, M.D. Luque de Castro, *Valves and flow injection manifolds: an excellent marriage with unlimited versatility*, Analytica Chimica Acta, 480 (2003) 181-192.

[6] J. Ruzicka, G.D. Marshall, *Sequential injection: a new concept for chemical sensors, process analysis and laboratory assays*, Analytica Chimica Acta, 237 (1990) 329-343.

[7] B.F. Reis, M.F. Giné, E.A.G. Zagatto, J.L.F.C. Lima, R.A. Lapa, *Multicommutation in flow analysis. Part 1. Binary sampling: concepts, instrumentation and spectrophotometric determination of iron in plant digests*, Analytica Chimica Acta, 293 (1994) 129-138.

[8] F.R.P. Rocha, B.F. Reis, E.A.G. Zagatto, J.L.F.C. Lima, R.A.S. Lapa, J.L.M. Santos, *Multicommutation in flow analysis: concepts, applications and trends*, Analytica Chimica Acta, 468 (2002) 119-131.

[9] M. Catalá Icardo, J.V. García Mateo, J. Martínez Calatayud, *Multicommutation as a powerful new analytical tool*, TrAC Trends in Analytical Chemistry, 21 (2002) 366-378.

[10] B.G.-T. Corominas, *Nuevos métodos de análisis en flujo (F.I.A. y multiconmutación) aplicados a la determinación por quimiluminiscencia directa de fenoles y polifenoles*, Universidad de Valencia, 2003.

[11] A. Ghosh, C.T. Bates, S.K. Seeley, J.V. Seeley, *High speed deans switch for low duty cycle comprehensive two-dimensional gas chromatography*, Journal of Chromatography A, 1291 (2013) 146-154.

[12] V. Cerdà, J.M. Estela, R. Forteza, A. Cladera, E. Becerra, P. Altimira, P. Sitjar, *Flow techniques in water analysis*, Talanta, 50 (1999) 695-705.

[13] R.A.S. Lapa, J.L.F.C. Lima, B.F. Reis, J.L.M. Santos, E.A.G. Zagatto, *Multi-pumping in flow analysis: concepts, instrumentation, potentialities*, Analytica Chimica Acta, 466 (2002) 125-132.

[14] J. Ruzicka, *Lab-on-valve: universal microflow analyzer based on sequential and bead injection*, Analyst, 125 (2000) 1053-1060.

[15] D. Nacapricha, P. Sastranurak, T. Mantim, N. Amornthammarong, K. Uraisin, C. Boonpanaid, C. Chuyprasartwattana, P. Wilairat, *Cross injection analysis: Concept and operation for simultaneous injection of sample and reagents in flow analysis*, Talanta, 110 (2013) 89-95.

[16] M.I. Pascual-Reguera, G. Pérez Parras, A. Molina Díaz, *A single spectroscopic flow-through sensing device for*

determination of ciprofloxacin, Journal of Pharmaceutical and Biomedical Analysis, 35 (2004) 689-695.

[17] P. Ortega-Barrales, A. Ruiz-Medina, M.L. Fernández-de Córdova, A. Molina-Díaz, *A flow-through solid-phase spectroscopic sensing device implemented with FIA solution measurements in the same flow cell: Determination of binary mixtures of thiamine with ascorbic acid or acetylsalicylic acid*, Analytical and Bioanalytical Chemistry, 373 (2002) 227-232.

[18] A. Molina-Díaz, I. Ortega-Carmona, M.I. Pascual-Reguera, *Indirect spectrophotometric determination of ascorbic acid with ferrozine by flow-injection analysis*, Talanta, 47 (1998) 531-536.

[19] A. Dhaouadi, L. Monser, S. Sadok, N. Adhoum, *Flow-injection methylene blue-based spectrophotometric method for the determination of peroxide values in edible oils*, Analytica Chimica Acta, 576 (2006) 270-274.

[20] C.E. López Pasquali, P. Fernández Hernando, J.S. Durand Alegría, *Spectrophotometric simultaneous determination of nitrite, nitrate and ammonium in soils by flow injection analysis*, Analytica Chimica Acta, 600 (2007) 177-182.

[21] S. Kulmala, J. Suomi, *Current status of modern analytical luminescence methods*, Analytica Chimica Acta, 500 (2003) 21-69.

[22] J. Kuijt, F. Ariese, U.A.T. Brinkman, C. Gooijer, *Room temperature phosphorescence in the liquid state as a tool in analytical chemistry*, Analytica Chimica Acta, 488 (2003) 135-171.

[23] S.G. Schulman, A. Fernández-Gutiérrez, *Fosforescencia molecular analítica: una aproximación práctica*, Universidad de Granada, 2001.

[24] W. R. G. Baeyens. A.M. García-Campaña, *Chemiluminiscence in Analytical Chemistry*, Ed. Marcel Dekker, 2001.

[25] T. Pérez-Ruiz, C. Martínez-Lozano, A. Sanz, A. Guillén, *Successive determination of thiamine and ascorbic acid in pharmaceuticals by flow injection analysis*, Journal of Pharmaceutical and Biomedical Analysis, 34 (2004) 551-557.

[26] J. López-Flores, A. Molina-Díaz, M.L. Fernández-de Córdova, *Development of a photochemically induced fluorescence-based optosensor for the determination of imidacloprid in peppers and environmental waters*, Talanta, 72 (2007) 991-997.

[27] J.M. Traviesa-Alvarez, J.M. Costa-Fernández, R. Pereiro, A. Sanz-Medel, *Direct screening of tetracyclines in water and bovine milk using room temperature phosphorescence detection*, Analytica Chimica Acta, 589 (2007) 51-58.

[28] I. Sánchez-Barragán, J.M. Costa-Fernández, A. Sanz-Medel, M. Valledor, J.C. Campo, *Room-temperature phosphorescence (RTP) for optical sensing*, TrAC Trends in Analytical Chemistry, 25 (2006) 958-967.

[29] K. Robards, P.J. Worsfold, *Analytical applications of liquid-phase chemiluminescence*, Analytica Chimica Acta, 266 (1992) 147-173.

[30] Z. Zhang, S. Zhang, X. Zhang, *Recent developments and applications of chemiluminescence sensors*, Analytica Chimica Acta, 541 (2005) 37-46.

[31] K. Mervartová, M. Polášek, J. Martínez Calatayud, *Recent applications of flow-injection and sequential-injection analysis techniques to chemiluminescence determination of pharmaceuticals*, Journal of Pharmaceutical and Biomedical Analysis, 45 (2007) 367-381.

[32] L. Gámiz-Gracia, A.M. García-Campaña, F. Alés Barrero, L. Cuadros Rodríguez, *Determination of albumin in biological fluids by flow injection analysis using the peroxyoxalate chemiluminescent system in micellar medium*, Analytical and Bioanalytical Chemistry, 377 (2003) 281-286.

[33] J.F. Huertas-Pérez, L. Gámiz-Gracia, A.M. García-Campaña, A. González-Casado, J.L. Martínez Vidal, *Chemiluminescence determination of carbofuran at trace levels in lettuce and waters by flow-injection analysis*, Talanta, 65 (2005) 980-985.

[34] X. Liu, A. Li, C. Wu, J. Lu, *Flow Injection Chemiluminescence Determination of Fenitrothion Pesticide Using Luminol-Hydrogen Peroxide System*, Analytical Letters, 40 (2007) 2737-2746.

[35] J.L. López-Paz, M. Catalá-Icardo, *Analysis of Pesticides by Flow Injection Coupled with Chemiluminescent Detection: A Review*, Analytical Letters, 44 (2011) 146-175.

[36] W. Ruengsitagoon, S. Liawruangrath, A. Townshend, *Flow injection chemiluminescence determination of paracetamol*, Talanta, 69 (2006) 976-983.

[37] B. Haghighi, S. Bozorgzadeh, *Flow injection chemiluminescence determination of isoniazid using luminol and silver nanoparticles*, Microchemical Journal, 95 (2010) 192-197.

[38] N. Arnaud, J. Georges, *Improved detection of salicylic acids using terbium-sensitized luminescence in aqueous micellar solutions of cetyltrimethylammonium chloride*, Analyst, 124 (1999) 1075-1078.

[39] M. P. Aguilar-Caballos, A. Gómez-Hens, D. Pérez-Bendito, *Simultaneous determination of benzoic acid and saccharin in soft drinks by using lanthanide-sensitized luminescence*, Analyst, 124 (1999) 1079-1084.

[40] A. Dominguez-Vidal, E. J. Llorent-Martínez, P. Ortega-Barrales, A. Molina-Díaz *Fast determination of salicylic acid in pharmaceuticals by using a terbium-sensitized luminescent SIA optosensor*, Journal of Pharmaceutical Sciences, 97 (2008) 791-797.

[41] P. Ortega-Barrales, M. J. Ayora-Cañada, A. Molina-Díaz, S. Garrrigues, M. de la Guardia, *Solid phase Fourier transform near infrared spectroscopy*, Analyst, 124 (1999) 579-582.

[42] M.J. Ayora-Cañada, A. Ruiz-Medina, B. Lendl, *Determination of Free Fatty Acids in Edible Oils by Continuous-Flow Analysis with FT-IR Spectroscopic Detection*, Applied Spectroscopy, 55 (2001) 356-360.

[43] S. Armenta, G. Quintás, J. Moros, S. Garrigues, M. de la Guardia, *Fourier transform infrared spectrometric strategies for the determination of Buprofezin in pesticide formulations*, Analytica Chimica Acta, 468 (2002) 81-90.

[44] M. Gallignani, M.d.R. Brunetto, *Infrared detection in flow analysis — developments and trends (review)*, Talanta, 64 (2004) 1127-1146.

[45] M.J. Ruedas-Rama, M. López-Sánchez, A. Ruiz-Medina, A. Molina-Díaz, M.J. Ayora-Cañada, *Flow-through sensor with Fourier transform Raman detection for determination of sulfonamides*, Analyst, 130 (2005) 1617-1623.

[46] M.J. Ayora-Cañada, A. Ruiz-Medina, J. Frank, B. Lendl, *Bead injection for surface enhanced Raman spectroscopy: automated on-line monitoring of substrate generation and application in quantitative analysis*, Analyst, 127 (2002) 1365-1369.

[47] S. Lee, J. Choi, L. Chen, B. Park, J.B. Kyong, G.H. Seong, J. Choo, Y. Lee, K.H. Shin, E.K. Lee, S.W. Joo, K.H. Lee, *Fast and sensitive trace analysis of malachite green using a surface-enhanced Raman microfluidic sensor*, Analytica Chimica Acta, 590 (2007) 139-144.

[48] L.G. Thygesen, K. Jørgensen, B.L. Møller, S.B. Engelsen, *Raman spectroscopic analysis of cyanogenic glucosides in plants: development of a flow injection surface-enhanced Raman scatter (FI-SERS) method for determination of cyanide*, Applied Spectroscopy, 58 (2004) 212-217.

[49] A. Sanz-Medel, R. Pereiro, *Flow Injection Analysis Techniques in Atomic Spectroscopy*, Encyclopedia of Analytical Chemistry, 2011.

[50] M. Burguera, J.L. Burguera, M.R. Brunetto, M. de la Guardia, A. Salvador, *Flow-injection atomic spectrometric determination of inorganic arsenic (III) and arsenic (V) species by use of an aluminium-column arsine generator and cold-trapping arsine collection*, Analytica Chimica Acta, 261 (1992) 105-113.

[51] M.C. Yebra, *Continuous automatic determinations of organic compounds by flow injection–atomic absorption spectrometry*, TrAC Trends in Analytical Chemistry, 19 (2000) 629-641.

[52] G.E. Roscoe, R. Miles, C.G. Taylor, *Determination of potassium in gasoline and lubricating oils by a flow-injection technique with flame atomic emission spectrometric detection*, Analytica Chimica Acta, 234 (1990) 439-444.

[53] N.V. Semenova, L.O. Leal, R. Forteza, V. Cerdà, *Multisyringe flow-injection system for total inorganic arsenic determination by hydride generation-atomic fluorescence spectrometry*, Analytica Chimica Acta, 455 (2002) 277-285.

[54] N. Yunes, S. Moyano, S. Cerutti, J.A. Gásquez, L.D. Martinez, *On-line preconcentration and determination of nickel in natural water samples by flow injection-inductively coupled plasma optical emission spectrometry (FI-ICP-OES)*, Talanta, 59 (2003) 943-949.

[55] R. De Marco, B. Pejcic, M. Loan, M. Wilcox, *Continuous flow analysis of iron in zinc electrowinning electrolyte using an iron chalcogenide glass ion-selective electrode: Part I. Synthetic media*, Talanta, 57 (2002) 115-121.

[56] A.P.S. Paim, C.M.N.V. Almeida, B.F. Reis, R.A.S. Lapa, E.A.G. Zagatto, J.L.F. Costa Lima, *Automatic potentiometric flow titration procedure for ascorbic acid determination in pharmaceutical formulations*, Journal of Pharmaceutical and Biomedical Analysis, 28 (2002) 1221-1225.

[57] M.N. Abbas, A.A. Radwan, *Novel lipoate-selective membrane sensor for the flow injection determination of α-lipoic acid in*

pharmaceutical preparations and urine, Talanta, 74 (2008) 1113-1121.

[58] Y.M. Issa, M.M. Khalil, S.I.M. Zayed, A. Hussein, *Flow injection potentiometric sensor for determination of phenylpropanolamine hydrochloride*, Arabian Journal of Chemistry, 2 (2009) 41-46.

[59] J.J. Pedrotti, I.G.R. Gutz, *Ultra-simple adaptor to convert batch cells with mercury drop electrodes in voltammetric detectors for flow analysis*, Talanta, 60 (2003) 695-705.

[60] M. Amatatongchai, W. Sroysee, S. Chairam, D. Nacapricha, *Amperometric flow injection analysis of glucose using immobilized glucose oxidase on nano-composite carbon nanotubes-platinum nanoparticles carbon paste electrode*, Talanta, 166 (2017) 420-427.

[61] S. Pati, M. Quinto, F. Palmisano, *Flow injection determination of choline in milk hydrolysates by an immobilized enzyme reactor coupled to a selective hydrogen peroxide amperometric sensor*, Analytica Chimica Acta, 594 (2007) 234-239.

[62] R.E. Gyurcsányi, Z. Fehér, G. Nagy, *Study of the determination of acetylcholine after enzymatic hydrolysis by triangle programmed coulometric flow titration*, Talanta, 47 (1998) 1021-1031.

[63] Z.K. He, B. Fuhrmann, U. Spohn, *Calibrationless determination of creatinine and ammonia by coulometric flow titration*, Analytical Biochemistry, 283 (2000) 166-174.

[64] P. Norouzi, S. Shirvani-Arani, P. Daneshgar, M.R. Ganjali, *Sub-second adsorptive fast Fourier transform coulometric technique as a novel method for the determination of nanomolar*

concentrations of sodium valproate in its pharmaceutical preparation in flowing solution systems, Biosensors and Bioelectronics, 22 (2007) 1068-1074.

[65] K. Grudpan, P. Sritharathikhun, J. Jakmunee, *Flow injection conductimetric or spectrophotometric analysis for acidity in fruit juice*, Analytica Chimica Acta, 363 (1998) 199-202.

[66] G. Altiokka, N.Ö. Can, H.Y. Aboul-Enein, *Determination of Amoxicillin by Flow Injection Analysis using UV-Detection, Potentiometry, and Conductometry in Pharmaceutical Preparations*, Journal of Liquid Chromatography & Related Technologies, 30 (2007) 1333-1341.

[67] M.S. Pena, F. Salinas, M.C. Mahedero, J.J. Aaron, *Spectrofluorimetric determination of sulphonamides in pharmaceutical compounds and foods*, Journal of Pharmaceutical and Biomedical Analysis, 10 (1992) 805-808.

[68] B. Laassis, J.J. Aaron, M.C. Mahedero, *Photochemically induced fluorescence determination of biomedically important phenothiazines in aqueous media at different pH values*, Analytica Chimica Acta, 290 (1994) 27-33.

[69] A. Coly, J.J. Aaron, *Photochemical–spectrofluorimetric method for the determination of several aromatic insecticides*, Analyst, 119 (1994) 1205-1209.

[70] D.M. Hercules, *Analytical photochemistry and photochemical analysis: Solids, solutions, and polymers (Fitzgerald, J. M.)*, Journal of Chemical Education, 49 (1972) A434.

[71] R.J. Lukasiewicz, J.M. Fitzgerald, *Digital integration method for fluorimetric studies of photochemically unstable compounds*, Analytical Chemistry, 45 (1973) 511-517.

[72] T. Pérez-Ruiz, C. Martínez-Lozano, J. Martín, M.D. García, *Automatic determination of phylloquinone in vegetables and fruits using on-line photochemical reduction and fluorescence detection via solid phase extraction and flow injection*, Analytical and Bioanalytical Chemistry, 384 (2006) 280-285.

[73] A.H.M.T. Scholten, P.L.M. Welling, U.A.T. Brinkman, R.W. Frei, *Use of PTFE coils in post-column photochemical reactors for liquid chromatograph — application to pharmaceuticals*, Journal of Chromatography A, 199 (1980) 239-248.

[74] C. González-Barreiro, M. Lores, M.C. Casais, R. Cela, *Simultaneous determination of neutral and acidic pharmaceuticals in wastewater by high-performance liquid chromatography–post-column photochemically induced fluorimetry*, Journal of Chromatography A, 993 (2003) 29-37.

[75] P.P. Vázquez, A.R. Mughari, M.M. Galera, *Application of solid-phase microextraction for determination of pyrethroids in groundwater using liquid chromatography with post-column photochemically induced fluorimetry derivatization and fluorescence detection*, Journal of Chromatography A, 1188 (2008) 61-68.

[76] X.Q. Guo, J.G. Xu, Y.Z. Wu, Y.B. Zhao, X.Z. Huang, G.Z. Chen, *Determination of thiamine (vitamin B1) by in situ sensitized photochemical spectrofluorimetry*, Analytica Chimica Acta, 276 (1993) 151-160.

[77] D. Chen, A. Ríos, M.D.L.d. Castro, M. Valcárcel, *Simultaneous flow-injection determination of chlorpromazine and promethazine by photochemical reaction*, Talanta, 38 (1991) 1227-1233.

[78] D. Chen, A. Rios, M.D. Luque de Castro, M. Valcarcel, *Photochemical–spectrofluorimetric determination of phenothiazine compounds by unsegmented-flow methods*, Analyst, 116 (1991) 171-176.

[79] R.S. Guerrero, C.G. Benito, J.M. Calatayud, *On-line photoreaction and fluorimetric determination of diazepam*, Journal of Pharmaceutical and Biomedical Analysis, 11 (1993) 1357-1360.

[80] C. Gómez Benito, T. García Sancho, J. Martínez Calatayud, *Spectrofluorimetric determination of emetine by flow injection using barium peroxide and UV derivatization*, Analytica Chimica Acta, 279 (1993) 293-298.

[81] C. Huang, Q. He, H. Chen, *Flow injection photochemical spectrofluorimetry for the determination of carbamazepine in pharmaceutical preparations*, Journal of Pharmaceutical and Biomedical Analysis, 30 (2002) 59-65.

[82] J. López-Flores, M.L. Fernández-de Córdova, A. Molina-Díaz, *Implementation of flow-through solid phase spectroscopic transduction with photochemically induced fluorescence: determination of thiamine*, Analytica Chimica Acta, 535 (2005) 161-168.

[83] J. López-Flores, M.L. Fernández-de Córdova, A. Molina-Díaz, *Flow-through optosensor combined with photochemically induced fluorescence for simultaneous determination of binary mixtures of sulfonamides in pharmaceuticals, milk and urine*, Analytica Chimica Acta, 600 (2007) 164-171.

[84] S. Irace-Guigand, E. Leverend, M.D. Seye, J. J. Aaron, *A new on-line micellar-enhanced photochemically-induced*

fluorescence method for determination of phenylurea herbicide residues in water, Luminescence, 20 (2005) 138-142.

[85] J. López-Flores, M.L. Fernámdez-de Córdova, A. Molina-Díaz, *Simultaneous Flow-Injection Solid-Phase Fluorometric Determination of Thiabendazole and Metsulfuron Methyl Using Photochemical Derivatization*, Analytical Sciences, 25 (2009) 681-686.

[86] L. Molina-García, A. Ruiz-Medina, M.L. Fernández-de Córdova, *Automatic optosensing device based on photo-induced fluorescence for determination of piceid in cocoa-containing products*, Analytical and Bioanalytical Chemistry, 399 (2011) 965-972.

[87] L. Molina-García, M.L. Fernández-de Córdova, A. Ruiz-Medina, *Indirect determination of aflatoxin B1 in beer via a multi-commuted optical sensor*, Food Additives & Contaminants: Part A, 29 (2012) 392-402.

[88] M. Fujimoto, *Mikroanalyse Mit Hilfe von Ionenaustauschenden Harzen I. Über Den Nachweis Geringer Menge Des Kobalts Mit Ammoniumrhodanid*, Bulletin of the Chemical Society of Japan, 27 (1954) 48-50.

[89] M. Fujimoto, *Mikroanalyse mit Hilfe von ionenaustauschenden Harzen. II. Über den Nachweis geringer Menge des Chroms mit Wasserstoffperoxyde*, Bulletin of the Chemical Society of Japan, 27 (1954) 347-350.

[90] K. Yoshimura, H. Waki, S. Ohashi, *Ion-exchanger colorimetry—I: Micro determination of chromium, iron, copper and cobalt in water*, Talanta, 23 (1976) 449-454.

[91] C.A. Heller, R.R. McBride, M.A. Ronning, *Detection of trinitrotoluene in water by fluorescent ion-exchange resins*, Analytical Chemistry, 49 (1977) 2251-2253.

[92] A. Molina-Diaz, J.M. Herrador-Mariscal, M.I. Pascual-Reguera, L.F. Capitan-Vallvey, *Determination of traces of aluminium with chrome azurol S by solid-phase spectrophotometry*, Talanta, 40 (1993) 1059-1066.

[93] P. Ortega-Barrales, M.L. Fernández-de Córdova, A. Molina-Díaz, *Microdetermination of Vitamin B1 in the Presence of Vitamins B2, B6, and B12 by Solid-Phase UV Spectrophotometry*, Analytical Chemistry, 70 (1998) 271-275.

[94] A. Ruiz-Medina, M.L. Fernández-de Córdova, A. Molina-Díaz, *A rapid and selective solid-phase UV spectrophotometric method for determination of ascorbic acid in pharmaceutical preparations and urine*, Journal of Pharmaceutical and Biomedical Analysis, 20 (1999) 247-254.

[95] J.L. Vilchez, M. del Olmo, R. Avidad, L.F. Capitán-Vallvey, *Determination of polycyclic aromatic hydrocarbon residues in water by synchronous solid-phase spectrofluorimetry*, Analyst, 119 (1994) 1211-1214.

[96] O. Ballesteros, J.L. Vílchez, A. Navalón, *Determination of the antibacterial ofloxacin in human urine and serum samples by solid-phase spectrofluorimetry*, Journal of Pharmaceutical and Biomedical Analysis, 30 (2002) 1103-1110.

[97] J. Růžička, E.H. Hansen, *Optosensing at active surfaces — a new detection principle in flow injection analysis*, Analytica Chimica Acta, 173 (1985) 3-21.

[98] M. Valcárcel, M.D.L. de Castro, *Flow-through (bio)chemical sensors—Plenary lecture*, Analyst, 118 (1993) 593-600.

[99] Á.I. López-Lorente, M. Valcárcel, *The third way in analytical nanoscience and nanotechnology: Involvement of nanotools and nanoanalytes in the same analytical process*, TrAC Trends in Analytical Chemistry, 75 (2016) 1-9.

[100] A.O. A. Ekimov, *Quantum size effect in three-dimensional microscopic semiconductor crystals*, ZhETF Pis ma Redaktsiiu, 34 (1981) 363-366.

[101] W.C.W. Chan, S. Nie, *Quantum Dot Bioconjugates for Ultrasensitive Nonisotopic Detection*, Science, 281 (1998) 2016-2018.

[102] M. Bruchez, M. Moronne, P. Gin, S. Weiss, A.P. Alivisatos, *Semiconductor Nanocrystals as Fluorescent Biological Labels*, Science, 281 (1998) 2013-2016.

[103] A.P. Alivisatos, *Semiconductor Clusters, Nanocrystals, and Quantum Dots*, Science, 271 (1996) 933-937.

[104] R. Peter, P. Myriam, L. Liang, *Core/Shell Semiconductor Nanocrystals*, Small, 5 (2009) 154-168.

[105] W. Horst, *Colloidal Semiconductor Q-Particles: Chemistry in the Transition Region Between Solid State and Molecules*, Angewandte Chemie International Edition in English, 32 (1993) 41-53.

[106] M.A. El-Sayed, *Small Is Different: Shape-, Size-, and Composition-Dependent Properties of Some Colloidal Semiconductor Nanocrystals*, Accounts of Chemical Research, 37 (2004) 326-333.

[107] L.E. Brus, *A simple model for the ionization potential, electron affinity, and aqueous redox potentials of small semiconductor crystallites*, The Journal of Chemical Physics, 79 (1983) 5566-5571.

[108] A.S. Lima, S.S.M. Rodrigues, M.G.A. Korn, D.S.M. Ribeiro, J.L.M. Santos, L.S.G. Teixeira, *Determination of copper in biodiesel samples using CdTe-GSH quantum dots as photoluminescence probes*, Microchemical Journal, 117 (2014) 144-148.

[109] S.S.M. Rodrigues, A.S. Lima, L.S.G. Teixeira, M.d.G.A. Korn, J.L.M. Santos, *Determination of iron in biodiesel based on fluorescence quenching of CdTe quantum dots*, Fuel, 117 (2014) 520-527.

[110] M. Tayebi, M. Tavakkoli Yaraki, M. Ahmadieh, M. Tahriri, D. Vashaee, L. Tayebi, *Determination of total aflatoxin using cysteamine-capped CdS quantum dots as a fluorescence probe*, Colloid and Polymer Science, 294 (2016) 1453-1462.

[111] E.J. Llorent-Martínez, L. Molina-García, R. Kwiatkowski, A. Ruiz-Medina, *Application of quantum dots in clinical and alimentary fields using multicommutated flow injection analysis*, Talanta, 109 (2013) 203-208.

[112] N. Gaponik, A.L. Rogach, *Thiol-capped CdTe nanocrystals: progress and perspectives of the related research fields*, Physical Chemistry Chemical Physics, 12 (2010) 8685-8693.

[113] C. Frigerio, D.S.M. Ribeiro, S.S.M. Rodrigues, V.L.R.G. Abreu, J.A.C. Barbosa, J.A.V. Prior, K.L. Marques, J.L.M. Santos, *Application of quantum dots as analytical tools in*

automated chemical analysis: A review, Analytica Chimica Acta, 735 (2012) 9-22.

[114] F.M. Raymo, J. Callan, *Quantum Dot Sensors: Technology and Commercial Applications*, Pan Stanford, 2013.

[115] R. Freeman, I. Willner, *Optical molecular sensing with semiconductor quantum dots (QDs)*, Chemical Society Reviews, 41 (2012) 4067-4085.

[116] S. Ghosh, A. Priyam, S.C. Bhattacharya, A. Saha, *Mechanistic Aspects of Quantum Dot Based Probing of Cu (II) Ions: Role of Dendrimer in Sensor Efficiency*, Journal of Fluorescence, 19 (2009) 723-731.

[117] S.S.M. Rodrigues, Z. Oleksiak, D.S.M. Ribeiro, E. Poboży, M. Trojanowicz, J.A.V. Prior, J.L.M. Santos, *Selective determination of sulphide based on photoluminescence quenching of MPA-capped CdTe nanocrystals by exploiting a gas-diffusion multi-pumping flow method*, Analytical Methods, 6 (2014) 7956-7966.

[118] S.S.M. Rodrigues, D.S.M. Ribeiro, L. Molina-Garcia, A. Ruiz Medina, J.A.V. Prior, J.L.M. Santos, *Fluorescence enhancement of CdTe MPA-capped quantum dots by glutathione for hydrogen peroxide determination*, Talanta, 122 (2014) 157-165.

[119] J.A.C. Barbosa, V.L.R.G. Abreu, S.S.M. Rodrigues, C. Frigerio, J.L.M. Santos, *A CdTe–MPA quantum dot fluorescence enhancement flow method for chlorhexidine determination*, Analytical Methods, 6 (2014) 4240-4246.

[120] A.P.S. Paim, S.S.M. Rodrigues, D.S.M. Ribeiro, G.C.S. de Souza, J.L.M. Santos, A.N. Araújo, C.G. Amorim, É. Teixeira-Neto, V.L. da Silva, M.C.B.S.M. Montenegro, *Fluorescence*

probe for mercury(ii) based on the aqueous synthesis of CdTe quantum dots stabilized with 2-mercaptoethanesulfonate, New Journal of Chemistry, 41 (2017) 3265-3272.

[121] E.J. Llorent-Martínez, L. Molina-García, M.L. Fernández-de Córdova, J.L.M. Santos, S.S.M. Rodrigues, A. Ruiz-Medina, *A novel multi-commutated method for the determination of hydroxytyrosol in enriched foods using mercaptopropionic acid-capped CdTe quantum dots*, Food Additives & Contaminants: Part A, 30 (2013) 1485-1492.

[122] L. Molina-García, E.J. Llorent-Martínez, M.L. Fernández-de Córdova, J.L.M. Santos, S.S.M. Rodrigues, A. Ruiz-Medina, *Study of the quenching effect of quinolones over CdTe-quantum dots using sequential injection analysis and multicommutation*, Journal of Pharmaceutical and Biomedical Analysis, 80 (2013) 147-154.

[123] N. Hildebrandt, K.D. Wegner, W.R. Algar, *Luminescent terbium complexes: Superior Förster resonance energy transfer donors for flexible and sensitive multiplexed biosensing*, Coordination Chemistry Reviews, 273-274 (2014) 125-138.

[124] G. Chen, F. Song, X. Xiong, X. Peng, *Fluorescent Nanosensors Based on Fluorescence Resonance Energy Transfer (FRET)*, Industrial & Engineering Chemistry Research, 52 (2013) 11228-11245.

[125] U. Resch-Genger, M. Grabolle, S. Cavaliere-Jaricot, R. Nitschke, T. Nann, *Quantum dots versus organic dyes as fluorescent labels*, Nature Methods, 5 (2008) 763.

[126] K. E. Sapsford, L. Berti, I. L. Medintz, *Materials for Fluorescence Resonance Energy Transfer Analysis: Beyond*

Traditional Donor–Acceptor Combinations, Angewandte Chemie International Edition, 45 (2006) 4562-4589.

[127] H.R. Chandan, J.D. Schiffman, R.G. Balakrishna, *Quantum dots as fluorescent probes: Synthesis, surface chemistry, energy transfer mechanisms, and applications*, Sensors and Actuators B: Chemical, 258 (2018) 1191-1214.

[128] S.S.M. Rodrigues, D.S.M. Ribeiro, J.X. Soares, M.L.C. Passos, M.L.M.F.S. Saraiva, J.L.M. Santos, *Application of nanocrystalline CdTe quantum dots in chemical analysis: Implementation of chemo-sensing schemes based on analyte-triggered photoluminescence modulation*, Coordination Chemistry Reviews, 330 (2017) 127-143.

[129] J. Zhou, Y. Liu, J. Tang, W. Tang, *Surface ligands engineering of semiconductor quantum dots for chemosensory and biological applications*, Materials Today, 20 (2017) 360-376.

[130] J. Donegan, Y. Rakovich, *Cadmium Telluride Quantum Dots: Advances and Applications*, Pan Stanford, 2013.

[131] J. Guo, Y. Zhang, Y. Luo, F. Shen, C. Sun, *Efficient fluorescence resonance energy transfer between oppositely charged CdTe quantum dots and gold nanoparticles for turn-on fluorescence detection of glyphosate*, Talanta, 125 (2014) 385-392.

[132] T. Bo, C. Lihua, X. Kehua, Z. Linhai, G. Jiechao, L. Qingling, Y. Lijuan, *A new nanobiosensor for glucose with high sensitivity and selectivity in serum based on fluorescence resonance energy transfer (FRET) between CdTe quantum dots and Au nanoparticles*, Chemistry – A European Journal, 14 (2008) 3637-3644.

[133] L. Chang, X. He, L. Chen, Y. Zhang, *A fluorescent sensing for glycoproteins based on the FRET between quantum dots and Au nanoparticles*, Sensors and Actuators B: Chemical, 250 (2017) 17-23.

[134] Z. Dai, J. Zhang, Q. Dong, N. Guo, S. Xu, B. Sun, Y. Bu, *Adaption of Au Nanoparticles and CdTe Quantum Dots in DNA Detection*, Chinese Journal of Chemical Engineering, 15 (2007) 791-794.

[135] M. Xue, X. Wang, L. Duan, W. Gao, L. Ji, B. Tang, *A new nanoprobe based on FRET between functional quantum dots and gold nanoparticles for fluoride anion and its applications for biological imaging*, Biosensors and Bioelectronics, 36 (2012) 168-173.

[136] J. Zhao, H. Wu, J. Jiang, S. Zhao, *Label-free fluorescence turn-on sensing for melamine based on fluorescence resonance energy transfer between CdTe/CdS quantum dots and gold nanoparticles*, RSC Advances, 4 (2014) 61667-61672.

[137] http://www.fao.org/fao-who-codexalimentarius/es/.

[138] F. Wu, J.D. Groopman, J.J. Pestka, *Public Health Impacts of Foodborne Mycotoxins*, Annual Review of Food Science and Technology, 5 (2014) 351-372.

[139] B.J. Xu, X.Q. Jia, L.J. Gu, C.K. Sung, *Review on the qualitative and quantitative analysis of the mycotoxin citrinin*, Food Control, 17 (2006) 271-285.

[140] B. Nigović, M. Sertić, A. Mornar, *Simultaneous determination of lovastatin and citrinin in red yeast rice supplements by micellar electrokinetic capillary chromatography*, Food Chemistry, 138 (2013) 531-538.

[141] V. Dohnal, L. Pavlíková, K. Kuča, *Rapid and sensitive method for citrinin determination using high-performance liquid chromatography with fluorescence detection*, Analytical Letters, 43 (2010) 786-792.

[142] K. Markov, J. Pleadin, M. Bevardi, N. Vahčić, D. Sokolić-Mihalak, J. Frece, *Natural occurrence of aflatoxin B1, ochratoxin A and citrinin in Croatian fermented meat products*, Food Control, 34 (2013) 312-317.

[143] J.F. Huertas-Pérez, N. Arroyo-Manzanares, A.M. García-Campaña, L. Gámiz-Gracia, *High-throughput determination of citrinin in rice by ultra-high-performance liquid chromatography and fluorescence detection (UHPLC-FL)*, Food Additives and Contaminants - Part A Chemistry, Analysis, Control, Exposure and Risk Assessment, 32 (2015) 1352-1357.

[144] G.P. Kononenko, A.A. Burkin, *A survey on the occurrence of citrinin in feeds and their ingredients in Russia*, Mycotoxin Research, 24 (2008) 3-6.

[145] F.J. Arévalo, A.M. Granero, H. Fernández, J. Raba, M.A. Zón, *Citrinin (CIT) determination in rice samples using a micro fluidic electrochemical immunosensor*, Talanta, 83 (2011) 966-973.

[146] Y. Li, H. Wu, L. Guo, Y. Zheng, Y. Guo, *Microsphere-based flow cytometric immunoassay for the determination of citrinin in red yeast rice*, Food Chemistry, 134 (2012) 2540-2545.

[147] N. Atar, M.L. Yola, T. Eren, *Sensitive determination of citrinin based on molecular imprinted electrochemical sensor*, Applied Surface Science, 362 (2016) 315-322.

[148] A. Mornar, M. Sertić, B. Nigović, *Development of a rapid LC/DAD/FLD/MSn method for the simultaneous determination of monacolins and citrinin in red fermented rice products*, Journal of Agricultural and Food Chemistry, 61 (2013) 1072-1080.

[149] M. Wang, N. Jiang, H. Xian, D. Wei, L. Shi, X. Feng, *A single-step solid phase extraction for the simultaneous determination of 8 mycotoxins in fruits by ultra-high performance liquid chromatography tandem mass spectrometry*, Journal of Chromatography A, 1429 (2016) 22-29.

[150] X. Cao, X. Li, J. Li, Y. Niu, L. Shi, Z. Fang, T. Zhang, H. Ding, *Quantitative determination of carcinogenic mycotoxins in human and animal biological matrices and animal-derived foods using multi-mycotoxin and analyte-specific high performance liquid chromatography-tandem mass spectrometric methods*, Journal of Chromatography B: Analytical Technologies in the Biomedical and Life Sciences, 1073 (2018) 191-200.

[151] A.L. Manizan, M. Oplatowska-Stachowiak, I. Piro-Metayer, K. Campbell, R. Koffi-Nevry, C. Elliott, D. Akaki, D. Montet, C. Brabet, *Multi-mycotoxin determination in rice, maize and peanut products most consumed in Côte d'Ivoire by UHPLC-MS/MS*, Food Control, 87 (2018) 22-30.

[152] https://ec.europa.eu/food/plant/pesticides_en.

[153] M. Tomizawa, J.E. Casida, *Neonicotinoid Insecticides: Highlights of a Symposium on Strategic Molecular Designs*, Journal of Agricultural and Food Chemistry, 59 (2011) 2883-2886.

[154] BOE, *REGLAMENTO DE EJECUCIÓN (UE) No 485/2013 DE LA COMISIÓN de 24 de mayo de 2013 por el que se modifica el Reglamento de Ejecución (UE) no 540/2011 en lo relativo a las condiciones de aprobación de las sustancias activas clotianidina, tiametoxam e imidacloprid, y se prohíben el uso y la venta de semillas tratadas con productos fitosanitarios que las contengan*, 2013.

[155] P. Jovanov, V. Guzsvány, M. Franko, S. Lazić, M. Sakač, B. Šarić, V. Banjaca, *Multi-residue method for determination of selected neonicotinoid insecticides in honey using optimized dispersive liquid-liquid microextraction combined with liquid chromatography-tandem mass spectrometry*, Talanta, 111 (2013) 125-133.

[156] M. Laurent PH, M. Ribiere-Chabert and M.P. Chauzat, *A pan-European epidemiological study on honeybee colony losses 2012-2014*, 2016.

[157] Z. Lu, N. Fang, Z. Zhang, B. Wang, Z. Hou, Y. Li, *Simultaneous Determination of Five Neonicotinoid Insecticides in Edible Fungi Using Ultrahigh-Performance Liquid Chromatography-Tandem Mass Spectrometry (UHPLC-MS/MS)*, Food Analytical Methods, 11 (2018) 1086-1094.

[158] W. Jiao, Y. Xiao, X. Qian, M. Tong, Y. Hu, R. Hou, R. Hua, *Optimized combination of dilution and refined QuEChERS to overcome matrix effects of six types of tea for determination eight neonicotinoid insecticides by ultra performance liquid chromatography-electrospray tandem mass spectrometry*, Food Chemistry, 210 (2016) 26-34.

[159] M. Chen, E.M. Collins, L. Tao, C. Lu, *Simultaneous determination of residues in pollen and high-fructose corn syrup from eight neonicotinoid insecticides by liquid chromatography–tandem mass spectrometry*, Analytical and Bioanalytical Chemistry, 405 (2013) 9251-9264.

[160] J. Vichapong, R. Burakham, S. Srijaranai, *In-coupled syringe assisted octanol–water partition microextraction coupled with high-performance liquid chromatography for simultaneous determination of neonicotinoid insecticide residues in honey*, Talanta, 139 (2015) 21-26.

[161] M. Li, E. Sheng, L. Cong, M. Wang, *Development of Immunoassays for Detecting Clothianidin Residue in Agricultural Products*, Journal of Agricultural and Food Chemistry, 61 (2013) 3619-3623.

[162] L. Li, G. Jiang, C. Liu, H. Liang, D. Sun, W. Li, *Clothianidin dissipation in tomato and soil, and distribution in tomato peel and flesh*, Food Control, 25 (2012) 265-269.

[163] K. Węgiel, B. Baś, *Voltammetric characteristics and determination of clothianidin using a bismuth bulk annular band electrode regenerated in situ*, Ionics, 23 (2017) 3187-3195.

[164] S. Valverde, A.M. Ares, J.L. Bernal, M.J. Nozal, J. Bernal, *Simultaneous determination of thiamethoxam, clothianidin, and metazachlor residues in soil by ultrahigh performance liquid chromatography coupled to quadrupole time-of-flight mass spectrometry*, Journal of Separation Science, 40 (2017) 1083-1090.

[165] P. Jovanov, V. Guzsvány, M. Franko, S. Lazić, M. Sakač, I. Milovanović, N. Nedeljković, *Development of multiresidue DLLME and QuEChERS based LC–MS/MS method for determination of selected neonicotinoid insecticides in honey liqueur,* Food Research International, 55 (2014) 11-19.

[166] M.M. Rahman, W. Farha, A.M. Abd El-Aty, M.H. Kabir, S.J. Im, D.I. Jung, J.H. Choi, S.W. Kim, Y.W. Son, C.H. Kwon, H.C. Shin, J.H. Shim, *Dynamic behaviour and residual pattern of thiamethoxam and its metabolite clothianidin in Swiss chard using liquid chromatography–tandem mass spectrometry*, Food Chemistry, 174 (2015) 248-255.

[167] E.H. da Costa Morais, C.H. Collins, I.C.S.F. Jardim, *Pesticide determination in sweet peppers using QuEChERS and LC–MS/MS*, Food Chemistry, 249 (2018) 77-83.

[168] F.P. Costa, S.S. Caldas, E.G. Primel, *Comparison of QuEChERS sample preparation methods for the analysis of pesticide residues in canned and fresh peach*, Food Chemistry, 165 (2014) 587-593.

[169] M.F. Zayats, S.M. Leschev, M.A. Zayats, *A novel method for the determination of some pesticides in vegetable oils based on dissociation extraction followed by gas chromatography-mass spectrometry*, Food Additives and Contaminants - Part A Chemistry, Analysis, Control, Exposure and Risk Assessment, 33 (2016) 1337-1345.

[170] P. Chorti, J. Fischer, V. Vyskocil, A. Economou, J. Barek, *Voltammetric determination of insecticide thiamethoxam on silver solid amalgam electrode*, Electrochimica Acta, 140 (2014) 5-10.

[171] L. Sánchez-Hernández, M. Higes, M.T. Martín, M.J. Nozal, J.L. Bernal, *Simultaneous determination of neonicotinoid insecticides in sunflower-treated seeds (hull and kernel) by LC-MS/MS*, Food Additives and Contaminants - Part A Chemistry, Analysis, Control, Exposure and Risk Assessment, 33 (2016) 442-451.

[172] G. Zhang, S. Nie, L. Long, D. Zeng, J. Chen, H. Yang, L. Chen, *Determination of nitenpyram residue in cabbage and soil using gas chromatography*, Chinese Journal of Chromatography (Se Pu), 28 (2010) 1103-1106.

[173] M. Zhang, H. Zhang, X. Zhai, X. Yang, H. Zhao, J. Wang, A. Dong, Z. Wang, *Application of β-cyclodextrin-reduced graphene oxide nanosheets for enhanced electrochemical sensing of the nitenpyram residue in real samples*, New Journal of Chemistry, 41 (2017) 2169-2177.

[174] N. Lezi, A. Economou, *Voltammetric Determination of Neonicotinoid Pesticides at Disposable Screen-Printed Sensors Featuring a Sputtered Bismuth Electrode*, Electroanalysis, 27 (2015) 2313-2321.

[175] L.A.B. de Oliveira, H.P. Pacheco, R. Scherer, *Flutriafol and pyraclostrobin residues in Brazilian green coffees*, Food Chemistry, 190 (2016) 60-63.

[176] Z. Mu, X. Feng, Y. Zhang, H. Zhang, *Trace analysis of three fungicides in animal origin foods with a modified QuEChERS method and liquid chromatography-tandem mass spectrometry*, Analytical and Bioanalytical Chemistry, 408 (2016) 1515-1522.

[177] X. Fan, S. Zhao, X. Chen, J. Hu, *Simultaneous determination of pyraclostrobin, prochloraz, and its metabolite in apple and soil*

via RRLC-MS/MS, Food Analytical Methods, 11 (2018) 1312–1320.

[178] S. Wu, H. Zhang, K. Zheng, B. Meng, F. Wang, Y. Cui, S. Zeng, K. Zhang, D. Hu, *Simultaneous determination and method validation of difenoconazole, propiconazole and pyraclostrobin in pepper and soil by LC–MS/MS in field trial samples from three provinces*, China, Biomedical Chromatography, 32 (2018) e4052.

[179] L. Rong, X. Wu, J. Xu, F. Dong, X. Liu, X. Pan, P. Du, D. Wei, Y. Zheng, *Simultaneous determination of three pesticides and their metabolites in unprocessed foods using ultraperformance liquid chromatography-tandem mass spectrometry*, Food Additives and Contaminants - Part A Chemistry, Analysis, Control, Exposure and Risk Assessment, 35 (2018) 273-281.

[180] R.M. Dornellas, D.B. Nogueira, R.Q. Aucelio, *The boron-doped diamond electrode voltammetric method for ultra-trace determination of the fungicide pyraclostrobin and evaluation of its photodegradation and thermal degradation*, Analytical Methods, 6 (2014) 944-950.

[181] C.M. Benbrook, *Trends in glyphosate herbicide use in the United States and globally*, Environmental Sciences Europe, 28 (2016) 3.

[182] J.V. Tarazona, D. Court-Marques, M. Tiramani, H. Reich, R. Pfeil, F. Istace, F. Crivellente, *Glyphosate toxicity and carcinogenicity: a review of the scientific basis of the European Union assessment and its differences with IARC*, Archives of Toxicology, 91 (2017) 2723-2743.

[183] IARC, *Monographs, volume 112: some organophosphate insecticides and herbicides: tetrachlorvinphos, parathion, malathion, diazinon and glyphosate., IARC Monographs on the evaluation of carcinogenic risks to humans*, 2015.

[184] G.M. Williams, M. Aardema, J. Acquavella, S.C. Berry, D. Brusick, M.M. Burns, J.L.V. de Camargo, D. Garabrant, H.A. Greim, L.D. Kier, D.J. Kirkland, G. Marsh, K.R. Solomon, T. Sorahan, A. Roberts, D.L. Weed, *A review of the carcinogenic potential of glyphosate by four independent expert panels and comparison to the IARC assessment*, Critical Reviews in Toxicology, 46 (2016) 3-20.

[185] H. Guo, H. Wang, J. Zheng, W. Liu, J. Zhong, Q. Zhao, *Sensitive and rapid determination of glyphosate, glufosinate, bialaphos and metabolites by UPLC–MS/MS using a modified Quick Polar Pesticides Extraction method*, Forensic Science International, 283 (2018) 111-117.

[186] N. Chamkasem, T. Harmon, *Direct determination of glyphosate, glufosinate, and AMPA in soybean and corn by liquid chromatography/tandem mass spectrometry*, Analytical and Bioanalytical Chemistry, 408 (2016) 4995-5004.

[187] J. Ding, G. Jin, G. Jin, A. Shen, Z. Guo, B. Yu, Y. Jiao, J. Yan, X. Liang, *Determination of underivatized glyphosate residues in plant-derived food with low matrix effect by solid phase extraction-liquid chromatography-tandem mass spectrometry*, Food Analytical Methods, 9 (2016) 2856-2863.

[188] L. Sun, D. Kong, W. Gu, X. Guo, W. Tao, Z. Shan, Y. Wang, N. Wang, *Determination of glyphosate in soil/sludge by high*

performance liquid chromatography, Journal of Chromatography A, 1502 (2017) 8-13.

[189] S. Wang, B. Liu, D. Yuan, J. Ma, *A simple method for the determination of glyphosate and aminomethylphosphonic acid in seawater matrix with high performance liquid chromatography and fluorescence detection*, Talanta, 161 (2016) 700-706.

[190] E. Çetin, S. Şahan, A. Ülgen, U. Şahin, *DLLME-spectrophotometric determination of glyphosate residue in legumes*, Food Chemistry, 230 (2017) 567-571.

[191] C.V. Waiman, M.J. Avena, M. Garrido, B. Fernández Band, G.P. Zanini, *A simple and rapid spectrophotometric method to quantify the herbicide glyphosate in aqueous media. Application to adsorption isotherms on soils and goethite*, Geoderma, 170 (2012) 154-158.

[192] M.L. Xu, Y. Gao, Y. Li, X. Li, H. Zhang, X.X. Han, B. Zhao, L. Su, *Indirect glyphosate detection based on ninhydrin reaction and surface-enhanced Raman scattering spectroscopy*, Spectrochimica Acta - Part A: Molecular and Biomolecular Spectroscopy, (2018).

[193] P. Martínez Gil, N. Laguarda-Miro, J.S. Camino, R.M. Peris, *Glyphosate detection with ammonium nitrate and humic acids as potential interfering substances by pulsed voltammetry technique*, Talanta, 115 (2013) 702-705.

[194] J. Xu, Y. Zhang, K. Wu, L. Zhang, S. Ge, J. Yu, *A molecularly imprinted polypyrrole for ultrasensitive voltammetric determination of glyphosate*, Microchimica Acta, 184 (2017) 1959-1967.

[195] E.H. Duarte, J. Casarin, E.R. Sartori, C.R.T. Tarley, *Highly improved simultaneous herbicides determination in water samples by differential pulse voltammetry using boron-doped diamond electrode and solid phase extraction on cross-linked poly(vinylimidazole)*, Sensors and Actuators, B: Chemical, 255 (2018) 166-175.

[196] S.T. Mayne, *Beta-carotene, carotenoids, and disease prevention in humans*, The FASEB Journal, 10 (1996) 690-701.

[197] Alpha-Tocopherol, Beta Carotene Cancer Prevention Study Group, *The effect of vitamin E and beta carotene on the incidence of lung cancer and other cancers in male smokers*, New England Journal of Medicine, 330 (1994) 1029-1035.

[198] H.S. Garewal, S. Schantz, *Emerging role of β-carotene and antioxidant nutrients in prevention of oral cancer*, Archives of Otolaryngology–Head & Neck Surgery, 121 (1995) 141-144.

[199] A. Zeb, *A simple, sensitive HPLC-DAD method for simultaneous determination of carotenoids, chlorophylls and α-tocopherol in leafy vegetables*, Journal of Food Measurement and Characterization, 11 (2017) 979-986.

[200] I. Brabcová, M. Hlaváčková, D. Šatínský, P. Solich, *A rapid HPLC column switching method for sample preparation and determination of β-carotene in food supplements*, Food Chemistry, 141 (2013) 1433-1437.

[201] V. Andrés, M.J. Villanueva, M.D. Tenorio, *Simultaneous determination of tocopherols, retinol, ester derivatives and β-carotene in milk- and soy-juice based beverages by HPLC with diode-array detection*, LWT - Food Science and Technology, 58 (2014) 557-562.

[202] D. Giuffrida, G. Torre, P. Dugo, G. Dugo, *Determination of the carotenoid profile in peach fruits, juice and jam*, Fruits, 68 (2013) 39-44.

[203] J.A. Sebben, J. da Silveira Espindola, L. Ranzan, N. Fernandes de Moura, L.F. Trierweiler, J.O. Trierweiler, *Development of a quantitative approach using Raman spectroscopy for carotenoids determination in processed sweet potato*, Food Chemistry, 245 (2018) 1224-1231.

[204] T. De Nardo, C. Shiroma-Kian, Y. Halim, D. Francis, L.E. Rodriguez-Saona, *Rapid and Simultaneous Determination of Lycopene and β-Carotene Contents in Tomato Juice by Infrared Spectroscopy*, Journal of Agricultural and Food Chemistry, 57 (2009) 1105-1112.

[205] P. Rungpichayapichet, B. Mahayothee, P. Khuwijitjaru, M. Nagle, J. Müller, *Non-destructive determination of β-carotene content in mango by near-infrared spectroscopy compared with colorimetric measurements*, Journal of Food Composition and Analysis, 38 (2015) 32-41.

[206] R. van Crevel, B. Alisjahbana, M. de Lange W. C, F. Borst, H. Danusantoso, M. van der Meer J. W, D. Burger, H. Nelwan R. H, *Low plasma concentrations of rifampicin in tuberculosis patients in Indonesia*, The International Journal of Tuberculosis and Lung Disease, 6 (2002) 497-502.

[207] K.H. Hee, J.J. Seo, L.S. Lee, *Development and validation of liquid chromatography tandem mass spectrometry method for simultaneous quantification of first line tuberculosis drugs and metabolites in human plasma and its application in clinical*

study, Journal of Pharmaceutical and Biomedical Analysis, 102 (2015) 253-260.

[208] E. Mattila, P. Arkkila, P.S. Mattila, E. Tarkka, P. Tissari, V.J. Anttila, *Rifaximin in the treatment of recurrent Clostridium difficile infection*, Alimentary Pharmacology & Therapeutics, 37 (2013) 122-128.

[209] A.C. Kogawa, H.R.N. Salgado, *Spectrophotometry in infrared region: A new, low cost and green way to analyze tablets of rifaximin*, Current Pharmaceutical Analysis, 14 (2018) 108-115.

[210] V. Brbaklic, A.C. Kogawa, H.R.N. Salgado, *Quantification of rifaximin in tablets by an environmentally friendly visible spectrophotometric method*, Current Pharmaceutical Analysis, 13 (2017) 532-537.

[211] N. Swamy, K. Basavaiah, *Spectrophotometric Determination of Rifampicin in Bulk Drug and Pharmaceutical Formulations Based on Redox and Complexation Reactions*, Journal of Applied Spectroscopy, 84 (2017) 694-703.

[212] S. Gao, Z. Wang, X. Xie, C. You, Y. Yang, Y. Xi, W. Chen, *Rapid and sensitive method for simultaneous determination of first-line anti-tuberculosis drugs in human plasma by HPLC-MS/MS: Application to therapeutic drug monitoring*, Tuberculosis, 109 (2018) 28-34.

[213] B. Louveau, C. Fernandez, N. Zahr, H. Sauvageon-Martre, P. Maslanka, P. Faure, S. Mourah, L. Goldwirt, *Determination of rifampicin in human plasma by high-performance liquid chromatography coupled with ultraviolet detection after automatized solid–liquid extraction*, Biomedical Chromatography, 30 (2016) 2009-2015.

[214] X. Zhang, R. Wang, H. Xie, Z. Jia, W. Li, J. Zhang, Y. Wang, *Determination of rifampicin in rat plasma by modified large-volume direct injection RAM-HPLC and its application to a pharmcokinetic study*, Biomedical Chromatography, 29 (2015) 475-480.

[215] P.R. Oliveira, A.F. Schibelbain, E.G.C. Neiva, A.J.G. Zarbin, L.H. Marcolino, M.F. Bergamini, *Nickel hexacyanoferrate supported at nickel nanoparticles for voltammetric determination of rifampicin*, Sensors and Actuators, B: Chemical, 260 (2018) 816-823.

[216] P.R. Chellini, T.O. Mendes, P.H.C. Franco, B.L.S. Porto, V.K. Tippavajhala, I.C. César, M.A.L. Oliveira, G.A. Pianetti, *Simultaneous determination of rifampicin, isoniazid, pyrazinamide and ethambutol in 4-FDC tablet by Raman spectroscopy associated to chemometric approach*, Vibrational Spectroscopy, 90 (2017) 14-20.

[217] D.J. Reed, J.R. Babson, P.W. Beatty, A.E. Brodie, W.W. Ellis, D.W. Potter, *High-performance liquid chromatography analysis of nanomole levels of glutathione, glutathione disulfide, and related thiols and disulfides*, Analytical Biochemistry, 106 (1980) 55-62.

[218] X. Guan, B. Hoffman, C. Dwivedi, D.P. Matthees, *A simultaneous liquid chromatography/mass spectrometric assay of glutathione, cysteine, homocysteine and their disulfides in biological samples*, Journal of Pharmaceutical and Biomedical Analysis, 31 (2003) 251-261.

[219] R. Gatti, R. Morigi, *1,4-Anthraquinone: A new useful pre-column reagent for the determination of N-acetylcysteine and*

captopril in pharmaceuticals by high performance liquid chromatography, Journal of Pharmaceutical and Biomedical Analysis, 143 (2017) 299-304.

[220] M. Verschraagen, M. Bosma, T.H.U. Zwiers, E. Torun, W.J.F. van der Vijgh, *Quantification of mesna and total mesna in kidney tissue by high-performance liquid chromatography with electrochemical detection*, Journal of Chromatography B, 783 (2003) 33-42.

[221] K.S. Lee, T.K. Kim, J.H. Lee, H.J. Kim, J.I. Hong, *Fluorescence turn-on probe for homocysteine and cysteine in water*, Chemical Communications, 0 (2008) 6173-6175.

[222] S. Huang, Q. Xiao, R. Li, H.-L. Guan, J. Liu, X.-R. Liu, Z.-K. He, Y. Liu, *A simple and sensitive method for l-cysteine detection based on the fluorescence intensity increment of quantum dots*, Analytica Chimica Acta, 645 (2009) 73-78.

[223] X. Chen, Y. Zhou, X. Peng, J. Yoon, *Fluorescent and colorimetric probes for detection of thiols*, Chemical Society Reviews, 39 (2010) 2120-2135.

[224] A.M. El-Didamony, *Spectrofluorimetric determination of the hypertensive drug captopril based on its oxidation with cerium (IV)*, Journal of the Chinese Chemical Society, 56 (2009) 755-762.

Anexos

Anexos

Anexo A: Contribuciones científicas derivadas de esta Memoria

1. Publicaciones científicas

En este Anexo se recogen los nueve artículos desarrollados por la autora de la presente Memoria. Todos ellos han sido publicados en revistas científicas internacionales especializadas en las áreas de Química Analítica y Tecnología de los alimentos.

Los artículos incluidos en la Memoria son los siguientes:

1. "*Multi-commutated fluorometric optosensor for the determination of citrinin in rice and red yeast rice supplements"*, Food Additives & Contaminants: Part A, 31 (2014) 1744-1750.
2. *"Determination of clothianidin in food products by using an automated system with photochemically induced fluorescence detection"*, Journal of Food Composition and Analysis, 49 (2016) 49–56.

3. *"Automated determination of Rifamycins making use of MPA–CdTe quantum dots"*, Journal of Luminescence, 175 (2016) 158–164.

4. *"Development of a semi-automatic and sensitive photochemically induced fluorescence sensor for the determination of thiamethoxam in vegetables"*, Talanta, 149 (2016) 149–155.

5. *"New perspectives of quantum dots in the food field: determination of β-carotene in tropical fruit juices and food supplements"*, Food Analytical Methods, 10 (2017) 2412–2421.

6. "*A photochemically induced fluorescence based flow-through optosensor for screening of nitenpyram residues in cruciferous vegetables"*, Food Additives & Contaminants: Part A, 35 (2018) 1-9.

7. *"Multicommutated flow system for the determination of glyphosate based on its quenching effect on CdTe-quantum dots fluorescence"*, Food Analytical Methods, 11 (2018) 1840–1848.

8. *"Sensitive photochemically induced fluorescence sensor for the determination of nitenpyram and pyraclostrobin in grapes and wines"*, Food Analytical Methods, (2018) Pendiente de publicación.

9. *"Exploiting the fluorescence resonance energy transfer (FRET) between CdTe quantum dots and Au nanoparticles for the determination of bioactive thiols"*,

Spectrochimica Acta Part A, (2018) Pendiente de publicación.

2. Comunicaciones a congresos

1. *"Multicommutated flow-through optosensor for the fluorometric determination of Citrinin"*, 18th ICFIA International Conference on Flow Injection Analysis, Porto (Portugal), 15-20 Septiembre 2013.

2. *"Implementation of flow-through solid phase spectroscopic transduction with photochemically induced fluorescence detection: Determination of clothianidin"*, XXIV Reunión Nacional de Espectroscopia-VIII Congreso Ibérico de Espectroscopía, Logroño (España), 9-11 Julio 2014.

3. *"Determination of thiamethoxam by a multicommutated flow-through optosensor based on photochemically induced fluorescence"*, XXIV Reunión Nacional de Espectroscopia-VIII Congreso Ibérico de Espectroscopía, Logroño (España), 9-11 Julio 2014.

4. *"Análisis de pesticidas en la industria alimentaria empleando optosensores multiconmutados"*, VII Jornadas de Jóvenes Investigadores en Física Atómica y Molecular, Jaén (España), 18-20 Marzo 2015.

5. *"Determinación fluorimétrica de rifampicin y rifaximin basada en el efecto quenching producido sobre Quantum Dots"*, VII Jornadas de Jóvenes Investigadores en Física Atómica y Molecular, Jaén (España), 18-20 Marzo 2015.

6. *"MPA-CdTe quantum dots: novel and automated fluorimetric method for the analysis of Rifamicins"*, 2015 Doctoral Conference for Young Researchers at the University of Jaén, Jaén (España), 23-27 Noviembre 2015.

7. *"New perspectives of quantum dots in the food field"*, 1st International Congress on Multidisciplinary Health Research, Jaén (España), 14-15 Abril 2016.

8. *"Nuevas perspectivas del uso de nanopartículas en el campo agroalimentario"*, XV Reunión del Grupo Regional Andaluz de la Sociedad Española de Química Analítica, Almería (España), 30 Junio-1 Julio 2016.

9. *"Desarrollo de un método fluorimétrico automatizado para el análisis de rifamicinas en fármacos y orina haciendo uso de quantum dots"*, XV Reunión del Grupo Regional Andaluz de la Sociedad Española de Química Analítica, Almería (España), 30 Junio-1 Julio 2016.

10. *"Evaluation of analytical potential of fluorescence resonance energy transfer (FRET) sensing combining CdTe quantum dots and Au nanoparticles for chemical analysis"*, 20th International Conference in Flow Injection Analysis and Related Techniques, Palma de Mallorca (España), 2-7 Octubre 2016.

11. *"A novel and simple screening method for the determination of Nitenpyram residues by using a Multicommutated Flow Injection System"*, 20th International Conference in Flow Injection Analysis and Related Techniques, Palma de Mallorca (España), 2-7 Octubre 2016.

12. *"Application of a potential fluorescence resonance energy transfer (FRET) method sensing combining CdTe quantum dots and Au nanoparticles for the determination of relevant analytes"*, 14th International Conference on Nanomaterials and Nanotechnology, Madrid (España), 30-31 Marzo 2017.

13. *"A new approach for the determination of nitenpyram and pyraclostrobin in food samples through a sensitive photochemically induced fluorescence sensor"*, 4th European Chemistry Congress, Barcelona (España), 11-13 Mayo 2017.

14. *"Implementation of photochemically induced fluorescence in flow-through optosensors for the determination of pesticides in food"*, 9º Congreso Internacional de Química de la ANQUE, San Pedro del Pinatar, Murcia (España), 17-20 Junio 2018.

15. *"Desarrollo de un sistema en flujo multiconmutado para el análisis de glifosato basado en el efecto quenching producido en la fluorescencia de quantum dots"*, XVI Reunión del Grupo Regional Andaluz de la Sociedad Española de Química Analítica, Granada (España), 4-5 Octubre 2018.

3. Divulgación científica

A raíz de la publicación del artículo "Development of an semi-automatic and sensitive photochemically induced fluorescence sensor for the determination of thiamethoxam in vegetables", diversos medios de comunicación contactaron con los autores del artículo (entre los que me incluyo como autora principal) para realizarnos diversas entrevistas y su publicación tanto en medios web y revistas como en radio y TV. Entre los medios que contactaron con nosotros se incluyen Canal Sur Televisión, Canal Sur Radio, Fundación Descubre, Modern Farmer (revista de carácter agroalimentario internacional),…

Anexo B: Otras contribuciones científicas

A continuación se relacionan otras contribuciones científicas adicionales que se han llevado a cabo durante la realización del presente trabajo de investigación:

1. Publicaciones científicas

1. *"Sequential Injection Analysis of Ciclopirox Olamine Using Lanthanide-Sensitized Luminescence Detection"*, Analytical Letters, 46 (2013) 1816–1825.

2. *"Quantitation of Hydroxytyrosol in food products using a Sequential Injection Analysis (SIA) fluorescence optosensor"*, Journal of Food Composition and Analysis, 32 (2013) 99-104.

3. *"Rosa rubiginosa and Fraxinus oxycarpa herbal teas: characterization of phytochemical profiles by liquid chromatography-mass spectrometry, and evaluation of the antioxidant activity"*, New Journal of Chemistry, 41 (2017) 7681-7688.

4. *"Phytochemical profile and antioxidant activity of caper berries (Capparis spinose L.): evaluation of the influence of the fermentation process"*, Food Chemistry, 250 (2018) 54-59.

2. Comunicaciones a congresos

1. *"Sequential Injection Analysis of Ciclopirox Using Lanthanide- Sensitized Luminescence Detection"*, 12th International Conference on Flow Analysis, Thessaloniki (Grecia), 23-28 Septiembre 2012.

2. *"Sequential Injection Analysis (SIA) optosensor for the determination of Hydroxytyrosol in food"*, 12th International Conference on Flow Analysis, Thessaloniki (Grecia), 23-28 Septiembre 2012.

3. *"Rosa rubiginosa and Fraxinus oxycarpa herbal teas: study of their phytochemical profiles and antioxidant activities"*, 4th European Chemistry Congress, Barcelona (España), 11-13 Mayo 2017.

4. *"Caper berries (Capparis Spinosa L.): Characterization of photochemical profiles and evaluation of the antioxidant activity along the fermentation process"*, 9º Congreso Internacional de Química de la ANQUE, San Pedro del Pinatar, Murcia (España), 17-20 Junio 2018.

5. *"Estudio del perfil fitoquímico y la actividad antioxidante en infusiones de las especies Rosa rubiginosa Y Fraxinus oxycarpa"*, XVI Reunión del

Grupo Regional Andaluz de la Sociedad Española de Química Analítica, Granada (España), 4-5 Octubre 2018.

6. *"Perfil fitoquímico y actividad antioxidante de los alcaparrones (Capparis spinosa L.): Evaluación de la influencia del proceso de fermentación"*, XVI Reunión del Grupo Regional Andaluz de la Sociedad Española de Química Analítica, Granada (España), 4-5 Octubre 2018.